

https://dspace.org/

A once daily multi-unit system for the site-specific delivery of multiple drug regimens

Cooppan, Shivaan

2011-10-19
http://hdl.handle.net/10539/10584

Downloaded from a DSpace repository. https://dspace.org/

A ONCE DAILY MULTI-UNIT SYSTEM FOR THE SITE-SPECIFIC DELIVERY OF MULTIPLE DRUG REGIMENS

SHIVAAN COOPPAN

A dissertation submitted to the Faculty of Health Sciences, University of the Witwatersrand, in fulfilment of the requirements for the degree of Master of Pharmacy

Supervisor:

Professor Viness Pillay

Department of Pharmacy and Pharmacology, University of the Witwatersrand, South Africa

Co-Supervisor:

Dr Yahya Essop Choonara

Department of Pharmacy and Pharmacology, University of the Witwatersrand, South Africa

Johannesburg, 2010

DECLARATION

I, Shivaan Cooppan, declare that this dissertation is my own work. It has being submitted for the degree of Master of Pharmacy in the Faculty of Health Sciences in the University of the Witwatersrand, Johannesburg. It has not been submitted before for any degree or examination at this or any other University.

…….....

This 19th day of December 2010

RESEARCH OUTPUTS

Conference Posters

Thermal, rheological and mechanical characterization of a crosslinked multi-polymeric membranous system

Shivaan Cooppan, Viness Pillay*, Yahya E. Choonara and Lisa C. du Toit

American Association of Pharmaceutical Scientists Annual Meeting and Exposition Los Angeles 2009

Crosslinking of polymethacrylates for controlled drug release in the small intestine

Shivaan Cooppan, Viness Pillay*, Yahya E. Choonara and Lisa C. du Toit

Pharmaceutical Society of South Africa, 2009

Thermo-physical characterization of a crosslinked multi-polymeric membranous system

Shivaan Cooppan, Viness Pillay*, Yahya E. Choonara and Lisa C. du Toit

Faculty Research Day, University of the Witwatersrand, South Africa 2008

Drug release studies and release mechanisms of a novel multiparticulate methacrylate delivery system

Shivaan Cooppan, Viness Pillay*, Yahya E. Choonara and Lisa C. du Toit

Conference of the Academy of Pharmaceutical Sciences, Johannesburg, South Africa, 2008

Physico-mechanical properties of a polymethacrylate membrane based on the exclusion of triethyl citrate

Dipesh Daya, Shivaan Cooppan, Viness Pillay*, Yahya E. Choonara and Lisa C. du Toit

Conference of the Academy of Pharmaceutical Sciences, Johannesburg, South Africa, 2008

Physical characterization of a novel membranous system for potential drug delivery

Shivaan Cooppan, Viness Pillay*, Yahya E. Choonara, Lisa C. du Toit, Valence Ndesendo

American Association of Pharmaceutical Scientists Annual Meeting and Exposition Atlanta Georgia, 2008

Double crosslinking of polymethacrylates for controlled drug release in the small intestine

Shivaan Cooppan, Viness Pillay* and Yahya E. Choonara

Conference of the Academy of Pharmaceutical Sciences, Cape Town, South Africa, 2007

Podium Presentations

A once daily multi-unit system for the site-specific delivery of multiple drug regimens

Shivaan Cooppan, Viness Pillay*, Yahya E. Choonara and Lisa C. du Toit

School Research Day, University of the Witwatersrand, 2009

Runner up for best podium presentation

SpheriXite® : Providing enhanced drug delivery solutions, today!

Shivaan Cooppan, Viness Pillay*, Yahya E. Choonara and Lisa C. du Toit

Bio2Biz SA, Small Business Competition, International Convention Centre, Durban, South Africa, 2009

Top 8 National Finalists

Publications

Rationalizing fixed dose combinations for tuberculosis and acquired immunodeficiency syndrome therapy

Shivaan Cooppan, Viness Pillay*, Yahya E. Choonara and Lisa C. du Toit

Int. J. Of Biotechnology 2010 – Vol. 11, No.3/4 pp. 284 – 304

A novel pH dependant and crosslinked polymethacrylate based multiparticulate drug delivery system for intestinal drug delivery

Shivaan Cooppan, Viness Pillay*, Yahya E. Choonara, Lisa C. du Toit, Valence M.K. Ndesendo, Nthato Chirwa and Pradeep Kumar

Scheduled for submission October 2010

Thermal, physico-mechanical and rheological characterization of a novel gastric release, polymethacrylate based membranous system

Shivaan Cooppan, Viness Pillay*, Yahya E. Choonara, Lisa C. du Toit, Valence M.K. Ndesendo, Nthato Chirwa and Pradeep Kumar

Scheduled for submission October 2010

A review of multi-responsive membranous systems for rate-modulated drug delivery

Rubina P. Shaikh, Viness Pillay, Yahya E. Choonara, Lisa C. du Toit, Valence M. K. Ndesendo, Priya Bawa and Shivaan Cooppan

Biomedical and Life Sciences, AAPS Pharmscitech, Volume 11

PATENTS

A heterogeneously configured multiparticulate gastrointestinal drug delivery system

Viness Pillay, Yahya Essop Choonara, Lisa Claire du Toit, Michael Paul Danckwerts and Shivaan Cooppan.

Publication date: 07/15/2010

Patent application number: 20100179170

(See Appendix B)

ABSTRACT

Complex medication regimens have major implications on patient therapy. When we consider that these regimen therapies can also be further convoluted by co-morbidity, it is then seen as an essential opportunity to research possible solutions to alleviate such complications. Globally identified conditions such as the Human Immuno-deficiency Virus (HIV) and Tuberculosis (TB) are known to have such complications within their respective regimens. In many cases, the regimental therapies themselves are overbearing with high pill burdens having to be taken in segregated manners throughout the day. Within a standard TB regimen, isoniazid and rifampicin are seen to have a deleterious drug-drug interaction in which the bioavailability is compromised through formation of an insoluble complex. Despite this interaction, the 2 active drugs must be taken concurrently for successful TB therapy. No true solution exists as fixed dose combinations of isoniazid and rifampicin (Rifinah®) are still in production despite the detrimental interaction that impedes successful bioavailability. The once daily multi-unit drug delivery system (ODMUS) has the benefits of superseding the described problems and aiding in therapeutic outcomes.

Preliminary studies utilized preliminary testing to ascertain the science surrounding the 2 components of the ODMUS, the memblet and the multiparticulate components. pH-sensitive polymers (Eudragit® L100-55 and E 100) were of critical importance to the success of the system and were individually manipulated for each component to produce a novel memblet and multiparticulate system through a unique salting out approach.

Primary studies focused on drug release testing and drug entrapment for the multiparticulate component. Testing of the memblet system addressed dissolution and thermal analysis. Utilizing this data, a series of process variables were used to achieve an optimized formulation through a Box-Behnken statistical design.

Optimized formulations used response testing to establish the optimal characteristics of both components. Multiparticulates achieved controlled release for 12 hours with an enhanced 71% drug entrapment efficiency. Memblet release profiles were confirmed over 2 hours with a maximal T_g of 56℃. Molecular modeling corroborated release understanding for both components. Surface area and porosity analysis, surface morphology, fourier transform infrared spectroscopy as well as thermal, rheological and mechanical analysis were additional tests undertaken on the optimized formulations.

In vivo analysis was the final testing to verify validity of the ODMUS components and utilized a pig model for the investigation. UPLC blood analysis revealed increase blood levels of INH (C_{max}INH= 0.0138ng/mL) and RIF (C_{max}RIF= 0.052ng/mL) in relation to conventional dosage forms validating segregated site-specific release and increased bioavailability.

Ideally, a segregated means of drug delivery throughout the gastrointestinal tract was achieved such that an enhanced bioavailability, a more controlled release and a simplified medication regimen was produced. This study aimed to achieve said goals through novel technique analysis, innovation and globally approved science to critically assess the success of the ODMUS as a potential means to reduce the complexities of medication regimen therapy.

ACKNOWLEDGEMENTS

I can only start acknowledgements with my parents, Rajen and Jyothi Cooppan who have supported and loved me since the beginning. Their tireless sacrifice and unconditional love has been more than part of the reason for my success in life up to this point.

To my Supervisor and Professor, Viness Pillay, who from the start has required nothing less than excellence, hard work, and commitment, thank you for instilling these qualities in me and I hope this dissertation is a reflection of your support, guidance and dedication to the field of pharmaceutics.

My Co-Supervisor Yahya Choonara, whose knowledge of all things is truly astounding. Thank you for answering all questions, including the ones that disturbed you.

I would like to sincerely thank Lisa Claire du Toit. Far more than a mentor, you have been an incredible friend as well. No matter the time or day, you have continually guided me through my research far more than required. I wish you all the success in life and future endeavours.

My mentors and friends, Valence Ndesendo and Oluwatoyin A. Kolawole. Since beginning my masters, the two of you have been the older brother and sister I have never had. Your guidance and knowledge in this field played critical importance in me completing this degree. Thank you.

To my friends and family, Avinash Nayiager, Yashodan Naidoo, Sambarthan Cooppan, Priyen Naidu, Rynae Grewen, Natanya Moodley, Kovanya Moodley, Kavitha Nundkwar, Firdaus Nabeemeeah, Chantal Koomcaran, Janine Carim and Narushka Pillay, thank you all for supporting and aiding me throughout this endeavour.

To my Sai family from Sandton Sai Centre, thank you for being a nexus of energy and support when my research seemed to complicate my life. The centre has provided a haven for me many a time.

The Central Animal Service staff needs to receive special acknowledgement for the amount of work, drama and difficulty we have brought to their doorstep. The *in vivo* portion of our work was draining on everyone but thanks to your undeniable assistance and hard work we persevered and overcame.

To my colleagues on the Eighth floor, Bongani Sibeko, Samantha Pillay, Sheri-Lee Harilal, Pradeep Kumar, Yasien Docrat, Sajida Suliman, Priya Bawa, Deshika Reddy, Zaheeda Khan, Caragh Murphy, Rubina Shaikh, Yusuf Dawood, Claire Dott, Ameena Wadee, Derusha Frank, Tong-sheng Tsai, Thiresan Govender, Ndidi Ngwuluka, Pius Fusinu, Steven Mufamad and Nthato Chirwa, keep up the hard work and thanks for all the lessons.

To the Wits staff, Mrs Shirona Naidoo, Mr David Bayever, Mrs Nompumelelo Damane, Mr Kleinbooi Mohlabi, Mr Bafana Themba, Miss Sibongile Sibambo, Professor Sandy Van Vuuren, Mrs Neelaveni Padayachee, Professor Paul Danckwerts, Miss Deanne Hazle and Mrs Neha Singh thanks for all the advice and help you have provided.

DEDICATION



I dedicate this dissertation at the lotus feet of Sri Sathya Sai Baba.
Thank you for guiding and blessing me throughout this endeavour.
Aum Sai Ram

TABLE OF CONTENTS

CHAPTER 1

AN OVERVIEW OF DRUG REGIMEN THERAPY AND CONCURRENT ORAL DELIVERY SYSTEMS

1.1 Introduction 1

1.2 Rationale and Motivation for Study 5

1.3 Aim and Objectives of this Study 7

1.4 Novelty of this Study 8

1.5 Overview of the Dissertation 8

CHAPTER 2

STRATEGIES IMPLEMENTED IN DRUG REGIMEN THERAPY AND THE ASSOCIATED LIMITATIONS

2.1 Introduction 10

2.2 HIV/AIDS and Concomitant Strategies Utilizing Drug Regimental Therapy 11

2.2.1 HIV/AIDS and fixed dose combinations 11

2.2.2 Opportunistic infections with HIV/AIDS 15

2.2.3 Interactions between ketoconazole and didanosine 16

2.3 Tuberculosis Regimen Treatment Schemes 18

2.3.1 Tuberculosis and fixed dose combination liposomal therapy 18

2.3.2 Tuberculosis and osmotically regulated drug delivery systems 23

2.3.3 The interaction between isoniazid and rifampicin 24

2.4 Regimen Strategies for the Asthma Management 26

2.4.1 Asthma and fixed dose combination drug delivery systems 26

2.5 The Role of a Dualistic Oral Drug Delivery System Encompassing both Multiparticulate and Membranous Technology for Drug Regimen Therapy 29

2.6 Concluding Remarks 33

CHAPTER 3

PRELIMINARY STUDIES FOR THE DEVELOPMENT AND DESIGN OF THE ONCE DAILY MULTI-UNIT SYSTEM

3.1 Introduction 34

3.2 Selection of Polymeric Material for the Individual Oral Delivery Systems 35

3.2.1 Rationale for the selection of polymers for the once daily multi-unit system 35

3.2.2 Rational selection of polymers and materials for the multiparticulate portion of the once daily multi-unit system 37

3.2.3 Rational selection of polymers and materials for a polyethylene glycol crosslinked novel tablet like polymeric oral membranous system 39

3.2.4 Method development of novel multiparticulates and a novel memblet drug delivery system 40

3.2.5 Ionotropic gelation and polyelectrolyte complexation 42

3.3 Materials and Methods 44

3.3.1 Materials 44

3.3.2 Multiparticulate method development: preparation of a 50mL Eudragit® L 100-55 latex 44

3.3.3 Multiparticulate method development: polymethyl methacrylate multiparticulate formation through an ionotropic gelation double crosslinking procedure 46

3.3.4 Memblet method development: formulation of a Eudragit® E 100 latex 47

3.4 Testing Procedures for the Once Daily Multi-Unit System 48

3.4.1 Construction of a calibration curves for spectrophotometric quantification of drug entrapment efficiency and *in vitro* analysis 48

3.4.2 Drug entrapment efficiency evaluation of double crosslinked drug saturated polymethacrylate multiparticulates and an overview of superficial morphological structure 48

3.4.3 Preliminary i*n vitro* drug release of double crosslinked drug saturated polymethacrylate multiparticulates 49

3.4.4 Preliminary *in vitro* drug release of polyethylene glycol crosslinked polymethacrylate based memblet system 49

3.4.5 Thermal analytical method development and subsequent thermal profiling of polyethylene glycol crosslinked polymethacrylate based memblet systems 50

3.5 Results and Discussion: Analysis of Preliminary Testing 50

3.5.1 Calibration curves for isoniazid and rifampicin to evaluate drug entrapment efficiency and *in vitro* drug release profiling 50

3.5.2 Drug entrapment efficiency of double crosslinked drug saturated polymethacrylate multiparticulates and superficial morphological structure scrutiny 51

3.5.3 *In vitro* drug release patterns of multiparticulates with varying crosslinking agents 55

3.5.4 Preliminary *in vitro* drug release results of polyethylene glycol crosslinked polymethacrylate based memblet system 57

3.5.5 Thermal analytical method implementation and analysis of thermal profiles of polyethylene glycol crosslinked polymethacrylate based memblet systems 58

3.5.5.1 Critical theoretical concepts 58

3.5.5.2 Pre-formulation differential scanning calorimetry thermal profiling on memblet systems 64

3.6 Concluding Remarks 69

CHAPTER 4
FORMULATION AND OPTIMIZATION OF ISONIAZID-LOADED MULTIPARTICULATES AND A RIFAMPICIN-LOADED ORAL MEMBRANOUS SYSTEM

4.1 Introduction 70

4.2 Optimization Utilizing a Box-Behnken Factorial Design 71

4.2.1 Selection of suitable independent variables to elucidate positive responses for the once daily multi-unit System 71

4.2.2 Generation of a design of experiments through a box-behnken design and subsequent testing 73

4.2.3 Comparative analysis of actual experimental and fitted response values calculated for the optimization of both components of the once daily multi-unit system 77

4.2.4 Graphical response data analysis 78

4.2.4.1 Response inspection of the once daily multi-unit system via 3 dimensional plotting 79

4.2.4.2 Analysis of the box-behnken design through residual plots for optimization and subsequent response optimization of the once daily multi-unit system 82

4.3 Concluding Remarks 90

CHAPTER 5
FORMULATION AND INVESTIGATION OF AN OPTIMIZED RIFAMPICIN-LOADED ORAL MEMBRANOUS SYSTEM FOR TARGETED DRUG DELIVERY TO THE STOMACH

5.1 Introduction 91

5.2 Materials and Methods 92

5.2.1 Materials 92

5.2.2 Fabrication of the optimized crosslinked memblet for gastric drug release 92

5.2.3.1 Rheological principles for the assessment of a novel semisolid Eudragit® E 100 based memblet system 92

5.2.3.2 Rheological testing of crosslinked hydrogels prior to drying 97

5.2.4 Assessment of the surface morphology and inter- and intra-polymeric interactions of the memblet 98

5.2.5 Mechanical evaluation of the memblet system 98

5.2.6 Thermal analysis of crosslinked polymethacrylate based memblet*s* 99

5.2.7 *In vitro* drug release of a polyethylene glycol 4000 crosslinked polymethacrylate based memblet system 99

5.3 Results and Discussion 100

5.3.1 Rheological analysis of crosslinked hydrogels prior to desiccation and memblet formation 100

5.3.1.1 Determination of the critical yield point for a polymethacrylate based latex and novel crosslinked interpolyelectrolyte complex hydrogels 100

5.3.1.2 Viscoelastic evaluation through stress sweep curves of novel crosslinked polyelectrolyte-complex hydrogels 103

5.3.1.3 Determination of the storage and loss modulus of novel crosslinked polyelectrolyte-complex hydrogels 103

5.3.2 Assessment of the inter- and intra-polymeric interactions of the memblet..... 104

5.3.3 Assessment of the surface morphology of the optimized crosslinked memblet 106

5.3.4 Mechanical evaluation and validation of structural integrity of the memblet system 109

5.3.5 Thermal analysis of an optimized crosslinked polymethacrylate based memblet 110

5.3.6 Construction of a calibration curve for rifampicin to interpolate *in vitro* analysis 116

5.3.7 *In vitro* drug release results of polyethylene glycol crosslinked polymethacrylate based optimized memblet system 116

5.4 Concluding Remarks 119

CHAPTER 6

FORMULATION AND INVESTIGATION OF AN OPTIMIZED ISONIAZID-LOADED MULTIPARTICULATE SYSTEM FOR TARGETED DRUG DELIVERY TO THE SMALL INTESTINE

6.1 Introduction 120

6.2 Materials and Methods 120

6.2.1 Materials 120

6.2.2 Preparation of the polymethacrylate based latex prior to double crosslinking 121

6.2.3 Polymethyl methacrylate polysphere formation through a double crosslinking process 121

6.2.4 Assessment of the surface morphology and inter- and intra-polymeric interactions of the optimized multiparticulate system 122

6.2.5 Validation of the enhancement of drug entrapment efficiency for optimized multiparticulates 122

6.2.6 Examination of surface area and investigation into porosity analysis for multiparticulates 123

6.2.7 Chemometric and molecular modelling to deduce the mechanism of crosslinking for the formation polyspheres and the drug release pattern thereof 124

6.2.8 Molecular modelling of a novel multi-crosslinked Eudragit® L 100-55 based multiparticulate system 124

6.2.9 *In vitro* drug release studies on the polyspheres 125

6.3 Results and Discussion 125

6.3.1 Assessment of the surface morphology and inter- and intra-polymeric interactions of the polyspheres 125

6.3.2 Evaluation of the augmentation of drug entrapment efficiencies of novel isoniazid loaded Eudragit® L 100-55 based multiparticulates 128

6.3.3 Inspection of surface area and corollary porosity data for optimized multiparticulates 129

6.3.4 Chemometric and molecular modelling deducing the mechanism of crosslinking for the formation polyspheres and the drug release pattern thereof 132

6.3.5 Molecular modelling of a novel multi-crosslinked Eudragit® L 100-55 based multiparticulate system 133

6.3.6 *In vitro* drug release profiles for a novel Eudragit® E L100-55 based double crosslinked multiparticulate system for site-specific delivery of isoniazid to the small intestine 136

6.4 Concluding Remarks 140

CHAPTER 7

THE *IN VIVO* INVESTIGATION INTO THE DUALISTIC DRUG BEHAVIOUR PATTERNS OF A COMBINATION OF RIFAMPICIN AND ISONIAZID LOADED ORAL SYSTEMS

7.1 Introduction 141

7.2 *In Vivo* Analytical Methodology for the Once Daily Multi-Unit System 142

7.2.1 Development of a blood sample retrieval protocol for the accurate analysis of plasma samples through the marginal ear vein 142

7.2.2 Development of a blood sample retrieval protocol for the accurate analysis of plasma samples through the insertion of a chronic catheter 143

7.3 Materials and Methods 146

7.3.1 Materials 146

7.3.2 Surgery and implantation of a permanent jugular catheter 147

7.3.3 Administration of the once daily multi-unit system 147

7.3.4 Blood sampling protocol for the once daily multi-unit system 148

7.3.5 Ultra performance lipid chromatography for the *in vivo* determination of drug content 148

7.3.5.1 Preparation of calibration curves for the *in vitro* analysis of isoniazid and rifampicin from a conventional dosage form 149

7.3.5.2 Development of a method for the concomitant *in vitro* analysis of isoniazid and rifampicin with subsequent analysis thereof 149

7.3.5.3 Plasma calibration curve development for the simultaneous evaluation of isoniazid and rifampicin concentrations 150

7.3.5.4 Plasma sample analysis for the simultaneous evaluation of the once daily multi-unit system in a female white pig 152

7.4 Results and Discussion 153

7.4.1 Validation of a method for the concomitant *in vitro* analysis of isoniazid and rifampicin with subsequent analysis thereof 153

7.4.2 Plasma calibration curves for the simultaneous evaluation of isoniazid and rifampicin concentrations 156

7.4.3 Plasma sample analysis for the evaluation of the once daily multi-unit system drug release in a female white pig 157

7.5 Concluding Remarks 162

CHAPTER 8

CONCLUSIONS AND RECOMENDATIONS

8.1 Conclusions..... 163

8.2 Recommendations..... 165

REFERENCES 166

APPENDICES 193

LIST OF FIGURES

Figure 2.1 Estimated worldwide prevalence of tuberculosis 19

Figure 2.2 Estimated worldwide mortality from tuberculosis 19

Figure 2.3 Chemical structure of polyethylene glycol 21

Figure 2.4 A schematic depiction of superficial polyethylene glycol segments on a microparticulate imparting the stealth function 22

Figure 2.5 Schematic representing the various liposomes 23

Figure 2.6 Schematic of an asymmetric membrane capsule 24

Figure 2.7 The pathway of the decomposition of rifampicin due to the presence of isoniazid. 25

Figure 2.8 Illustration depicting the complimentary effect of corticosteroids and long-acting β-agonists in a single fixed dose combination 27

Figure 2.9 Sub-classes of membranous systems 31

Figure 2.10 Schematic representation of the functional Once Daily Multi-Unit System 32

Figure 3.1 The molecular structure of Eudragit® 36

Figure 3.2 Site-specific release of grades of Eudragit® throughout the gastrointestinal tract 37

Figure 3.3 Molecular structure of Eudragit® L 100-55 38

Figure 3.4 Eudragit® E 100 molecular structure where R= $CH_3C_4H_9$ 40

Figure 3.5 Comparison between a novel Once Daily Multi-Unit System multiparticulate and a traditionally coated multiparticulate via cross-sectional examination 42

Figure 3.6 Formation of a polyelectrolyte complex through electrostatic attraction between 2 polymeric macromers 44

Figure 3.7 Eduragit® L 100-55 latex (50mL) preparation 45

Figure 3.8 The formation of multiparticulates through the crosslinking of the Eudragit® L 100-55 latex within a variable cationic solution 47

Figure 3.9 Formulation procedures implemented in the formulation of the memblet system..... 48

Figure 3.10 Calibration curves for a) isoniazid and b) rifampicin with corresponding regression co-efficient and y values 51

Figure 3.11 Photographic depiction of inter-sample variance due to formulation parameters for formulations 1-7..... 55

Figure 3.12 Preliminary *in vitro* release profiles for the multiparticulates 57

Figure 3.13 *In vitro* release patterns of the memblets..... 58

Figure 3.14 Rifampicin loaded, polyethylene glycol 4000 crosslinked novel memblet system..... 58

Figure 3.15 Differential Scanning Calorimetry thermogram of Eudragit® E 100 identifying the larger endset glass transition temperature in comparison to literature findings..... 65

Figure 3.16 Differential Scanning Calorimetry thermogram of polyethylene glycol 4000 corresponding to literature findings..... 66

Figure 3.17 Preliminary Differential Scanning Calorimetry thermogram of a novel memblet system..... 67

Figure 3.18 Thermal decomposition of the memblet system once passing 300℃ establishing upper testing limits 68

Figure 3.19 A second Differential Scanning Calorimetry run validating the upper limits of the temperature range for subsequent analysis 68

Figure 4.1 Release profiles for the multiparticulates design of experiments where a) represents formulations 1-4, b) represents formulations 5-8, c) represents formulations 9- 12and d) represents formulations 13-15 76

Figure 4.2 Release profiles for the memblet design of experiments where a) represents formulations 1-4, b) represents formulations 5-8, c) represents formulations 9-12 and d) represents formulations 13-15 77

Figure 4.3 Regression plots for a) memblet mean dissolution time b) memblet glass transition c) multiparticulate drug entrapment efficiency and d) multiparticulate mean dissolution time to ascertain R^2 values to verify the correlation between fitted and actual values for the formulation responses 78

Figure 4.4 Illustration of the relationship between independent variables and the response of a) mean dissolution time (MDT) and b) glass transition temperature (T_g) through 3-D surface plots for the memblet system 80

Figure 4.5 Illustration of the relationship between independent variables and the response of a) drug entrapment efficiency (DEE) and b) mean dissolution time (MDT) through 3-D surface plots for the multiparticulate system 82

Figure 4.6 Residual plots of a) mean dissolution time (MDT) and b) glass transition (T_g) of the memblet system 84

Figure 4.7 Optimization plots of the memblet system indicating optimal factors and factor levels and desirability 86

Figure 4.8 Residual plots of a) drug entrapment efficiency (DEE) and b) mean dissolution time (MDT) of the multiparticulate system. 87

Figure 4.9 Optimization plots of the multiparticulate system indicating optimal factors and factor levels and desirability 89

Figure 5.1 Thermohaake rheometer used in the analyses of rheometric parameters for the memblet 95

Figure 5.2 Inter-relations of storage modulus (G'), loss modulus (G''), complex modulus (G*) and the phase shift through the Pythagorean Theorem..... 97

Figure 5.3 Yield stress curves for a) hydrogel A b) hydrogel B and c) the latex prior to crosslinking to indicate the critical yield point (Pa)..... 102

Figure 5.4 Viscoelastic regions of hydrogel B (- 0) and hydrogel A (- X)..... 103

Figure 5.5 Dynamic oscillation curves depicting storage (G' depicted by x) and loss (G" depicted by o) moduli of: a) hydrogel A; and b) hydrogel B 104

Figure 5.6 Fourier Transmission Infrared Spectroscopy analysis in which a) represents the optimized memblet and the bonding of functional groups from polyethylene glycol 4000 and Eudragit® E 100 functional groups; and b) represents formulation A and B overlaid for which A is represented by the dotted line and B by the solid line emphasizing the peak sharpness of A 106

Figure 5.7 Scanning electron micrographs of a) control formulation and b) optimized memblet illustrating the increase in polymeric and formulation debris in the control memblet 108

Figure 5.8 Force/Distance profiles depicting matrix resilience, memblet flexibility and membrane deformation energy: a) control formulation; and b) optimized memblet 110

Figure 5.9 Differential Scanning Calorimetric thermograms of a) control memblet and b) optimized memblet 113

Figure 5.10 Alternating Differential Scanning Calorimetry thermal profiles of a) control memblet and b) optimized memblet 115

Figure 5.11 Calibration curve for rifampicin with corresponding regression co-efficients and y values 116

Figure 5.12 Concurrent release profiles of the optimized memblet and the control sample generated in simulated gastric fluid illustrating enhanced controlled release of the optimized memblet 117

Figure 6.1 Optimized crosslinked polymethyl-methacrylate based polyspheres 127

Figure 6.2 Scanning electron microscopy taken at a) 650X magnification and b) 100X magnification for the optimized double crosslinked multiparticulates to examine the surface morphology of optimized multiparticulates 127

Figure 6.3 Fourier Transmission Infrared Spectroscopy spectrum of crosslinked Eudragit® L 100-55 based multiparticulates 127

Figure 6.4 Surface area and porosity analysis of polyspheres with regards to: a) isothermal linear plots for optimized batch; b) Isothermal linear plot for control batch; c) T-plot micropore isotherm for batch A; d) T-plot micropore isotherm for batch B; e) BJH adsorption cumulative pore volume for batch A; and f) BJH adsorption cumulative pore volume for batch B 130

Figure 6.5 Polysphere formation process depicting: a) polymethacrylate latex with non-chemically crosslinked polymeric outer wall with load (isoniazid) in the polymethacrylate cavity; b) polymethacrylate latex with chemically crosslinked polymeric outer wall with load (isoniazid) in the polymethacrylate cavity 133

Figure 6.6 Visualization of geometrical preferences of Eudragit® E L100-55 molecule in complexation with divalent and trivalent cations after molecular simulation in a solvated system. Color codes: C (cyan), O (red), H (white), Al (yellow), Ba^{2+} (violet) and Mg^{2+} (brown) 136

Figure 6.7 Limited isoniazid release from optimized multiparticulates within simulated gastric fluid at pH 1.2 138

Figure 6.8 Percent drug release indicating the superior controlled drug release for an optimized multiparticulate system in relation to a control sample 139

Figure 7.1 Placement of the female white pig in a handling cage and blood sampling via the catheterized marginal ear vein 143

Figure 7.2 Dosing protocol employed to anaesthetize, monitor vitals, intubate and insert formulations 145

Figure 7.3 Schematic outline of the optimized blood sampling protocol for conventional and Once Daily Multi-Unit Systems 146

Figure 7.4 Formation of 3 immiscible layers via centrifugation of spiked plasma samples 151

Figure 7.5 *In vitro* calibration curves for a) isoniazid and b) rifampicin to elucidate the conventional dosage form's (Rifinah®) drug release profiles 154

Figure 7.6 Determination of release patterns of isoniazid and rifampicin from the conventional Rifinah® tablet within simulated gastric fluid (pH 1.2) 155

Figure 7.7 Ultra performance lipid chromatography chromatogram identifying isoniazid, rifampicin, methylparaben and the corresponding metabolites of rifampicin 156

Figure 7.8 *In vivo* calibration curves for a) isoniazid and b) rifampicin 157

Figure 7.9 Ultra performance lipid chromatography method development for the concomitant plasma drug content evaluation of isoniazid and rifampicin with separation of the undesirable degradation product using blank plasma 158

Figure 7.10 3-D modelling of a typical plasma chromatogram for isoniazid, rifampicin and furosemide indicating the respective range of absorption 159

Figure 7.11 24 hour investigation into the divergence of drug blood content between isoniazid and rifampicin from a conventional dosage form (S.D≤0.33) for which N= 5 for all samples 160

Figure 7.12 24 hour investigation into the divergence of drug blood content between isoniazid and rifampicin from the novel Once Daily Multi-Unit System (S.D≤0.33) for which N= 5 for all formulations..... 161

LIST OF TABLES

Table 1.1 Methods for managing regimen therapy, benefits and issues 2

Table 1.2 Potential drug regimens to be incorporated into the Once Daily Multi-Unit System 7

Table 2.1 Paediatric treatment guidelines for HIV/AIDS 14

Table 2.2 Frequency of opportunistic infections amongst paediatric patients 15

Table 2.3 Typical therapy for oral candidiasis 16

Table 2.4 Discrepancies between didanosine and ketoconazole 18

Table 2.5 Typical drugs employed in asthma treatment regimens 28

Table 3.1 Grades of Eudragit® and their properties 36

Table 3.2 Potential crosslinkers for the multiparticulate segment of the Once Daily Multi-Unit System 39

Table 3.3 Redispersion procedures for Eudragit® L 100-55 and Eudragit® E 100 41

Table 3.4 Parameters used for the formulation of preliminary multiparticulates 46

Table 3.5 Preliminary formulation parameters with subsequent drug entrapment efficiencies 52

Table 3.6 Initial observational data of cured spheres 54

Table 3.7 Thermal information on constituent polymers 64

Table 3.8 Method development criteria 64

Table 4.1 Listing of formulation variables with appropriate responses and objectives 72

Table 4.2 Listing of formulation variables with responses and objectives for the memblet 72

Table 4.3 Factors and levels of independent variables generated by the 3^3 Box- Behnken design for isoniazid-loaded, double crosslinked, polymethacrylate based multiparticulates 73

Table 4.4 Factors and levels of independent variables generated by the 3^3 Box- Behnken design for rifampicin-loaded, polyethylene glycol 4000 crosslinked, Eudragit® E 100 memblet systems 74

Table 4.5 Measured responses of the experimental run for the optimization of multiparticulates 75

Table 4.6 ANOVA analysis indicating factors for responses mean dissolution and glass transition and corresponding factor p values for the memblet system 84

Table 4.7 ANOVA analysis indicating factors for responses drug entrapment efficiency and mean dissolution time and the corresponding factor p values for the multiparticulate component of the Once Daily Multi-Unit System 88

Table 5.1 Method parameters for yield test, stress sweep and frequency sweep tests 98

Table 5.2 Parameters for flexibility, deformation energy and resilience testing 99

Table 5.3 Textural analysis results for the memblet system 109

Table 5.4 The relationship between optimization predicted and experimental values for responses mean dissolution time and glass transition 118

Table 6.1 Variant properties of the degassing and analysis procedures for surface area and porosity analysis 123

Table 6.2 Drug entrapment efficiencies for 100mg of polyspheres from optimized and control batches of multiparticulates 128

Table 6.3 Surface area of control and optimized polyspheres 129

Table 6.4 Calculated energy parameters (kcal/mol) of the complexes between Eudragit® L 100-55 and divalent and/or trivalent cation 135

Table 6.5 Correlation between predicted and experimental responses of mean dissolution and drug entrapment efficiency for the optimized multiparticulates 139

Table 7.1 Method parameters for the simultaneous determination of isoniazid and rifampicin concentrations 150

Table 7.2 Plasma method parameters for dual analysis of rifampicin and isoniazid 152

LIST OF EQUATIONS

Equation 3.1 Drug entrapment efficiency 49

Equation 3.2 Specific heat capacity 59

Equation 3.3 Average sample temperature 62

Equation 3.4 Total heat flow..... 62

Equation 3.5 Complex heat capacity..... 62

Equation 3.6 Complex heat capacity furthered..... 63

Equation 3.7 Cp in phase..... 63

Equation 3.8 Cp out phase..... 63

Equation 4.1 Mean dissolution time regression equation..... 85

Equation4.2 Glass transition temperature regression equation 85

Equation 4.3 Mean dissolution time regression equation..... 88

Equation 4.4 Drug entrapment regression equation 88

Equation 5.1 Law of viscometry 93

Equation 5.2 Shear stress..... 93

Equation 5.3 Shear rate 94

Equation 5.4 Shear rate between cone and stationary plate 94

Equation 5.5 Shear stress on cone 94

Equation 5.6 Time dependant strain 95

Equation 5.7 Stress equation 96

Equation 5.8 Complex modulus 96

Equation 5.9 Storage modulus 97

Equation 5.10 Loss modulus 97

Equation 5.11 Heat capacity 112

Equation 5.12 Complex heat capacity 112

Equation 6.1 Drug entrapment efficiency 123

Equation 7.1 Van Deemter equation 148

CHAPTER 1
AN OVERVIEW OF DRUG REGIMEN THERAPY AND CONCURRENT ORAL DELIVERY SYSTEMS

1.1 Introduction

The complexities of medication regimens are pertinent and influential to therapy with both health care professionals and patients. Co-morbidity along with multiple drug regimens in conditions such as tuberculosis (TB), Human Immunodeficiency Virus (HIV), Malaria, as well as regimens of antibiotic and antiepileptic medication, provides an inexorable task for patients to adhere to on a daily basis to successfully complete the prescribed regimen. A major cause of treatment failure is due to poor patient compliance as a result of elaborate regimens (Townsend *et al*., 2003), but this is not the sole problem associated within regimen therapy. Deleterious drug-drug interactions exist even within prescribed regimens, and often lead to sub-therapeutic drug levels. The consequences of such prescribing can potentially lead to drug resistance and treatment failure. Such deleterious interactions are noted between isoniazid and rifampicin used in the management of TB, in which the bioavailability of both drugs is impaired due to the insoluble complex formed between the 2 actives, a reaction which is accelerated through the acidic pH of gastric fluid (Shishoo *et al*., 2001). Both drugs are an essential component of TB therapy and cannot be substituted, and therefore each drug should be taken for a time apart from each other. These pharmacological actives are taken as a fixed dose combination, such as Rifafour e-275® (Aventis) and Rifinah® (Aventis), with little regard as to the detrimental interaction that does occur. Certain regimens contain excessive intolerable side effects that inhibit a patient's continuation with their regimens. Antiepileptic regimens induce a large number of side effects such as excess weight gain from valproate and cognitive impairment from topiramate (Bourgeois, 2002).

Non-pharmacological methods have been implemented over the course of many years to bolster patient compliance and aid in regimental therapy. Table 1.1 proposes non pharmacological means of treatment.

Methods, as shown in Table 1.1, have existed for many years for managing drug regimen therapy, a novel drug delivery system could possibly be a more practical approach. Well defined oral drug delivery systems, whilst being a singular solution to the issue of regimen therapy, could also be used in a synergistic program along with the methods described above.

Table 1.1 Methods for managing regimen therapy, benefits and issues

Proposed methods	Positive outcomes	Negative outcomes
Adaptive control	Produces a highly individualised regimen by producing pharmacokinetic and pharmacodynamic models	Creating precise pharmacokinetic and pharmacodynamic models, choosing the correct one and statistical issues such as the use of assay error patterns
Bayesian method	Produces individualised regimens from parametric population modelling in which standard deviations and mean values are implemented for the population parameter values	Requires numerous data points which are not always provided through routine clinical data
Therapeutic drug monitoring	Involves a monitoring of serum levels of drug and classification of concentrations into sub-therapeutic, therapeutic and toxic levels and adjusting regimens accordingly	Focuses on toxic concentrations indefinitely and excludes patients clinical behaviour as a factor for adjusting drug regimens
Motivational interviews	An individualised counselling method adapting techniques such as reflection and issue reframing	Require a highly specialised and trained councillor for successful impact on drug regimens
Nurse based interventions	Due to high contact rate with patients, nurses are ideally placed to implement usual adherence based interventions	Relies solely on the consistent availability of nurses to maintain

Adapted from Jelliffe et al., 1994

Multiparticulate drug delivery systems may address the challenges found within regimen therapy. An advantage of adopting a multiparticulate system involves the ability to specifically control drug release and consequently eliminate dose dumping and reduce side effects (Haslam *et al*., 1998). Recently, many approaches have been adopted for achieving controlled site-specific drug delivery using multiparticulate systems.

Due to the size range of multiparticulates (nm-mm), the system has previously been incorporated into the treatment of respiratory conditions, such as asthma, as an inhaled formulation as described by Corrigan and co-workers (2006).

In the aforementioned study, chitosan was formulated into chitosan-salbutamol-sulphate multiparticulates for local delivery to the lungs. However, the system focused on delivery of a single drug rather than multiple drugs in a regimen.

Success of many patented devices, show the impact of multiparticulates, as expressed in a product developed by Paul and co-workers (2004). A multiparticulate bisoprolol formulation for once-daily oral administration was developed, in which each particle comprised a core of bisoprolol surrounded by a polymeric coating. The polymeric coating was effective in achieving an initial lag of bisoprolol release *in vivo* of at least 4-6 hours following administration and thereafter maintaining therapeutic concentrations of bisoprolol for the remainder of the 24 hour period. Exploitation of the oral route of administration and prolonged drug delivery are both evident in contrast to the investigation provided by Corrigan and co-workers (2006). However, limitations are evident as the production sequence is lengthy and intricate knowledge is required in producing the multiparticulates and coating of them with fillers, plasticizers and copolymers in separate steps, which further convolutes the disadvantage of the system. Numerous production steps are not optimal for scale up manufacturing and this method does not guarantee highly reproducible particles in a single processing step.

Formulation approaches may dictate the positive and negative attributes of a multiparticulate drug delivery system. In a system developed by Liu and co-workers (2007), O-carboxymethylchitosan (OCMC) multiparticulates containing pazufloxacin mesilate were developed. The multiparticulates were prepared via an emulsion crosslinking method, which released drug over both the gastric and intestinal regions making the system pH independent. The O-hydroxyl group of each OCMC monomer substituted by a carboxymethylic group through ether bond formation, conferred its swelling properties and pH independent controlled drug release. Though this system employs a novel polymer and release system, the formulation approach however, was through a duplicated emulsion crosslinking method. Crosslinked multiparticulates were prepared by dissolving OCMC in distilled water, and varying quantities of pazufloxacin mesilate were added to the above to complete swelling of OCMC. The polymer solution containing pazufloxacin mesilate was added drop wise into liquid paraffin containing a surfactant resulting in the formation of a W/O emulsion. Various quantities of 25% glutaraldehyde solution were added depending upon the crosslinking density required using a hypodermic syringe.

It is apparent that such a method includes an undesirable and extensive formulation process. Furthermore, pazufloxacin mesilate remains the only drug to be delivered and the usage of multiparticulates for the treatment of drug regimens was not addressed. A recent study conducted by du Toit and co-workers (2007), focused on exploring modes of multiparticulate formulations. In the study, 3 approaches of multiparticulate production were investigated. These included the air-suspension method, a solvent evaporation emulsification method and a novel phase separation or salting-out approach. The air suspension method was a lengthy

formulation process with the only known flexible polymer to be included, a methacrylic acid copolymer derivative. The solvent evaporation-emulsification method depended largely on variables such as the type of solvent employed, temperature and mechanical agitation. Through comparative analysis of production of multiparticulates, using all 3 methods, it was concluded that phase separation was simple for any operational scale.

A second novel system that can be of benefit to regimen therapy is that of an oral membranous drug delivery system. Hydrogel formation is not a new technique and has been developed extensively throughout the years (Hideaki *et al*., 2008; Akihiro *et al*., 2009; Chen *et al*., 2009). Hydrogels are porous polymeric networks that retain and entrap large volumes of water within the matrices (Rajagopal and Schneider, 2004; Nair and Laurencin, 2006; Lee and Yuk, 2007). Selected drug molecules (mostly hydrophilic in nature) can be directly encapsulated within the network by triggering self-assembly in the presence of the drug (Branco and Schneider, 2009). Crosslinked polymeric hydrogels exhibit both structural and functional advantages in pharmaceutical research. The authenticity of the hydrogel and the subsequently desiccated membrane, with regards to drug delivery, is highly dependent on the reproducibility of drug release, novelty of design and well defined physico-chemical and physico-mechanical properties (Lin and Metters, 2006). Controlled and sustained release from polymeric matrices, ensure the delivery of drugs in a predictable manner so as to match physiological needs. However, hydrogels exhibit weak mechanical strength and in certain cases, rapid erosion and drug release from the internal matrix (Ruel-Gariepy and Leroux, 2004).

Membranous systems have been utilized for implants due to their ability to retard drug release in a highly site-specific manner. Implants through these systems have been noted to bypass regular side effects associated with other suturable devices such as inflammation and infection (Cabañas *et al*., 2009). A membrane is an inter-phase between 2 adjacent phases acting as a selective barrier and modulating the exchange of substances between the 2 compartments. One of the crucial advantages of membranes includes the transport selectivity of the membrane itself. Up-scaling and downscaling of membrane formulation processes are relatively easy when compared to other methodologies (Dongming *et al*, 2009).

A major disadvantage of a membrane produced system includes even weaker mechanical properties and manipulation of the formulation process needs to be considered if targeted and controlled drug release is to be achieved. Membranous systems derived from hydrogels also exhibit these weaker mechanical properties often producing a brittle formulation. The

use of membranous systems very rarely strays from the implant protocol, due to its high success rate in this field.

Chitosan has been the preferred polymer in membranous technology due to its non toxic, biocompatible and biodegradable properties (Wong *et al*., 1992; Francis and Matthew, 2000). This highly abundant polysaccharide does however pose some limitations particularly with regards to low acidic solubility and an inherent brittleness and stiffness (de Oliveira *et al*., 2009). When considering gastric oral drug delivery, these are unwanted characteristics for a polymer to possess and if optimal gastric delivery is required, the delivery system must avoid the same limitations of chitosan. Additionally, novelty is hard to achieve with a polymer that has been so extensively manipulated.

Consequently, the drug delivery system proposed in this dissertation intends to develop a Once Daily Multi-Unit System (ODMUS) for the site-specific delivery of a multiple drug regimen, developing firstly a multiparticulate system from a modified salting-out approach adapted from du Toit and co-workers (2007). Additionally, a novel membranous oral delivery system shall be developed such that concurrent delivery of at least 2 pharmacological actives can be achieved simultaneously with the multiparticulates, while subsequently providing segregated drug delivery within the gastrointestinal tract and eliminating the deleterious drug-drug interactions that occur amongst certain actives within a regimen. The novelty of the ODMUS is purported by its advantages of decreasing the amount of tablets a patient needs to consume in regimen therapy, the avoidance of deleterious drug interactions within regimens, reduction in dosing frequency and reducing intolerable side effects by providing a segregated and sustained drug release.

1.2 Rationale and Motivation for Study

The proposed ODMUS offers positive outcomes in relation to patient compliance, the negation of deleterious drug-drug interactions and a decrease in frequency of dosing when compared to standard regimen therapy. Currently, oral drug delivery systems do not allow for the delivery of a multiple drug regimen as a single formulation using multiparticulates. The ODMUS will be able to decrease the amount of tablets required by the patient on a daily schedule and reduce daily dosing frequency. Conditions such as TB, HIV, Malaria and infections requiring numerous antibiotics, will be most suited for incorporation into the ODMUS, as regimen quantity is decreased.

In epilepsy treatment, a common trend includes an increase in the regimen quantity as the disease progresses. Subsequent increases in the amount of tablets within a regimen can

ultimately lead to an out of control situation (dose dumping), revolving around an increase in intolerable side effects and decreased compliance (Haslam *et al*., 1998; Bourgeois, 2002). These situations will be easily negated by the ODMUS through its multiparticulate delivery of drug regimens in a single dosage form, at separate locations in the gastrointestinal tract (GIT) in a controlled manner. The controlled delivery of drug at site-specific regions in the GIT allows for a greater bioavailability and therefore should remove any need to increase the dose which was previously rendered insufficient.

The novel formulation approach of the ODMUS is a further advantage. The method to be employed involves a salting-out or phase separation approach as adapted from du Toit and co-workers (2007). The phase separation method offers numerous advantages over preparations described previously. The method employs an environmentally inert latex rather than an organic solution of the polymer. This polymeric solution is traditionally used as a coating agent to protect formulations from the acidic environment of the stomach. Consequently, as the polymeric matrix of the multiparticulates are comprised of this polymer, the coating process required by other delivery systems is bypassed and is replaced by a single process step without the use of potentially toxic solvent vapours. Furthermore, the salting out approach does not use organic solvents for dissolution of the polymer and allows for highly reproducible particles. The entire process of drug loaded multiparticulate production can then be described as a simple method of assembly.

The delivery of drug to various regions in the GIT highlights another positive application of the ODMUS. A novel tablet like membranous system has been developed to be co-administered with the drug loaded multiparticulates and promoting the release of the contained drug upon coming into contact with the gastric fluids. As such the membranous system shall contain a drug intended for drug delivery into the stomach and the multiparticulate system shall contain a drug intended for the small intestine. The overall effect of drug delivery in such a manner is that harmful deleterious drug interactions between drugs within the same regimen can be negated with both drugs being given as a single dose of 2 delivery systems. Furthermore, dose dumping can be reduced as the system provides controlled site-specific release of both drugs in the GIT. Crosslinking agents chosen were based on research concluded and discovery throughout the lab design. The crosslinking agents played a vital role in determining the release patterns of both drugs. The following Table 1.2 shows potential therapies to benefit from the ODMUS.

Table 1.2 Potential drug regimens to be incorporated into the Once Daily Multi-Unit System

Drug A	Drug B	Therapy	Problem
Rifampicin	Isoniazid	Tuberculosis	Deleterious drug interactions in which, in an acidic pH, isoniazid converts Rifampicin into an insoluble complex
Carbamazepine	Lamotrigene	Epilepsy	Deleterious drug interaction resulting in decreased seizure control. Poor compliance. Increase in tablet amount leading to intolerable side effects
Ketoconazole	Didanosine	HIV and Co-morbid fungal infections	Didanosine reduces the acidic environment of the stomach and inhibits the absorption of ketoconazole

Adapted from the South African Medicines Formulary, 2005

1.3 Aim and Objectives of this Study

The aim of this study was to develop an ODMUS able to overcome multiple daily dosing for chronic conditions that require adherence to long term therapy. Secondly, the system also aimed to prevent deleterious drug interactions between 2 or more drugs utilizing 2 novel drug delivery systems and furthermore decrease dosing frequency. The following objectives were outlined to achieve the aims of the study.

1) To select appropriate polymers and crosslinking reagents to formulate 2 delivery systems i.e. a multiparticulate system and a membrane like system, both with pH dependant solubility profiles.
2) To develop drug loaded multiparticulates based on a novel salting out/phase separation technique.
3) To develop a novel membrane tablet like system for concurrent oral delivery with multiparticulates.
4) To perform *in vitro* release studies in order to determine the drug release behaviour for both systems.
5) To develop a stability indication study for the novel membranous tablet like system to assess integrity.
6) To perform *in vivo* animal studies to assess the release behaviour and establish pharmacokinetic parameters of the system.

1.4 Novelty of this Study

The novelty of this study includes the formulation of a combination of 2 oral drug delivery systems, which allow for the concurrent administration of 2 pharmacological actives to achieve segregated drug delivery of the actives along the gastrointestinal tract. A single process step is utilized in the formulation of both systems as well as the novel use of Eudragit® polymers as pH-sensitive matrices which impart controlled release patterns for the respective drugs from each system at the individual pH of the stomach (pH1.2) and small intestine (pH6.8). Deleterious drug interactions that can potentially occur between the actives, can be negated due to segregated delivery of each compound along the gastrointestinal tract and an enhanced bioavailability can be achieved.

1.5 Overview of the Dissertation

Chapter One introduces the problem of medication regimens and emphasizes the rationale for the study. A background inspection on medication regimens is provided while indicating the aims and objectives of this research project.

Chapter Two contains an in depth review of drug regimen therapy strategies, the associated conditions and the limitations of said strategies. Deleterious drug interactions within regimens are highlighted followed by an in depth look into technologies utilized to manage complex regimen therapy. Furthermore, an explanation of the 2 technologies (membrane and multiparticulate) is provided which would comprise the Once Daily Multi-Unit System (ODMUS).

Chapter Three establishes the specific polymeric Eudragit® material, crosslinkers and other constituents for each formulation and the subsequent method development implemented in producing a novel rifampicin loaded memblet for gastric drug release and a novel isoniazid loaded multiparticulate system for intestinal drug delivery. Preliminary analysis focused on producing the upper and lower limits for formulation variables of each system which were to be inserted into a Box-Behnken factorial design. Upper and lower limits were emulated through dissolution testing, drug entrapment efficiency and differential scanning calorimetry.

Chapter Four describes the formulation of a design of experiments determined from the Box-Behnken factorial design. Fifteen formulations from both the multiparticulate and memblet system were subjected to response testing in order to achieve data to derive a candidate formulation.

Chapter Five provides an in depth characterization of an optimized memblet system intended for gastric delivery of rifampicin. Rheological, thermal, mechanical, morphological and structural characterizations were thoroughly investigated. Thermal and drug release profiles were established as correlating with the predicated data generated through statistical designs.

Chapter Six reviews the molecular and internal structure of an optimized multiparticulate system with corroborating surface area and morphological analysis. Drug entrapment and drug release profiles generated were validated as corroborating with predicted data derived in statistical designs for the system intended for isoniazid release in the small intestine.

Chapter Seven includes an in depth development of an *in vivo* analysis protocol for the combined ODMUS system relative to a conventional dosage form. Selection of an animal model is verified and development of surgical implantation procedure for the pig model is described. The protocol of blood sampling, storage and blood drug analysis via ultra performance lipid chromatography is described. The superiority of the ODMUS over a conventional dosage form is provided through the simultaneous analysis of plasma from both systems.

Chapter Eight presents the conclusions and recommendations of future work.

CHAPTER 2
STRATEGIES IMPLEMENTED IN DRUG REGIMEN THERAPY AND THE ASSOCIATED LIMITATIONS

2.1 Introduction

Health care cannot be simply defined as diagnosis and treatment and in clinical practice, due to many complications, treatment failure often occurs. When considering chronic therapy, we cannot assume that treatment can follow a simple therapeutic guideline. Chronic conditions may consist of extensive medication regimens in which the patient takes multiple drugs, frequently throughout the day and for prolonged periods (Richter *et al*., 2003). These compounded factors lead to poor patient compliance, treatment failure and drug resistance. To relieve such problems, fixed dose regimens are considered vital for severe chronic conditions. Additionally, above stated regimens may have detrimental interactions among the actives of the dosing regimen requiring direct monitoring and segregation of dosing on a daily basis.

Human Immunodeficiency Virus (HIV) is a worldwide pandemic characterised by extensive morbidity and mortality and is growing in severity in many countries. The development of the highly active antiretroviral therapy (HAART) regimens has significantly reduced associated morbidity and mortality (Mugavero and Hicks, 2004) and such a protocol shows the direct impact fixed dose regimens have on HIV therapy. Complications arise when opportunistic infections occur and further pharmacological actives are added to the already substantial quantity (Van Dyke, 1995; Manosuthi *et al*., 2007). Asthma is another chronic condition requiring fixed dose regimens for therapy and these regimens have been designed to optimize the physical well being of patients. As asthma is largely a self management condition, fixed dose regimens that simplify therapy, are of importance (Hyland and Elisabeth, 2004).

Tuberculosis (TB) has made major impact on a global scale for its highly contagious quality and its high level of mortality, especially amongst the economically challenged countries and regions (du Toit *et al*., 2006). TB treatment consists of several regimens which include both induction and continuation phases. In an effort to make regimental therapy compliance standard and to combat multi-drug resistant TB, the directly observed therapy (DOTS) protocol has been established (Gleeson and Decker, 2006).

Endocrine disorders see fixed dose regimens as crucial parts of therapy. Diabetes, growth hormone deficiencies, and hormonal replacement therapies include the use of fixed dose regimental therapy to combat symptoms associated with the disorders and on a regular basis, attempts have been made toward novel and innovative ways to deliver such regimens (Belland and Wyne, 2006; Out *et al*., 2006).

In all examples, the commonality lies in the extensive regimens that cannot be substituted. A rational approach for optimization of treatment would be to develop novel oral delivery systems for such regimens. Drug delivery systems for regimental management have been approached and studied for many years. Development of such systems, are crucial towards successful management of chronic conditions that leave patients feeling debilitated with not only their condition but their extensive drug consumption. Efficacious drug delivery systems will not only address non-adherence issues, but also cost issues and emergence of resistance towards these chronic conditions.

2.2 HIV/AIDS and Concomitant Strategies Utilizing Drug Regimental Therapy

2.2.1 HIV/AIDS and fixed dose combinations

When looking specifically at HIV/AIDS therapy, regimental therapy is a necessity when considering the host of drug-drug interactions that are likely to occur. The HIV virus has a highly accelerated means of viral replication or viral turnover regardless of immune response. Also noted is the fact that during the transcription process of the virus, mutations occur. The combination of mutation and accelerated viral replication results in a seriously debilitating condition (Gupta and Pillay, 2007).

Consequently, HIV/AIDS is treated via regimental therapy in order to address the issues of vast replication rates and mutation of the virus, while carefully selecting the drugs in the regimen that minimize the possibility of drug-drug interactions. When extensive anti-retroviral (ARV) therapy is considered, it is noted that administration of regimens is inefficient. The issuing of regimens without further comprehensive strategies may propagate poor adherence, which can culminate to detrimental drug resistance, disease progression, incomplete viral suppression and, in extreme cases, death (Bangsberg *et al*., 2003). This failure to adhere is commonly instigated by the complex regimens and debilitating side effects (Fogarty *et al*., 2002). Furthermore, as with TB chemotherapy, patients have to consume an excessive number of tablets, which is a common cause for non-compliance. Non-adherence by HIV-infected patients has been associated with incomplete viral suppression, the development of drug resistance, disease progression, and mortality (Nicca *et al.,* 2007).

With such factors in mind, regimen treatment needs to be designed in such a manner that minimizes the physical number of tablets a patient is required to take and/or reduce the dosage frequency while maintaining therapeutic levels. Currently, most viral strains lack resistance to more than one type of ARV and it is generally accepted that regimen therapy is an efficient way to treat highly advanced viruses. Ideal regimens for maximal efficacy should contain 3 different drugs from 2 separate classes, with the objective of suppression of the viral load to allow for an improvement in the immune system and to abstain from any resistance.

To aid health care professionals in the dispensing of HIV anti-retrovirals (ARV's), the highly active anti-retroviral therapy (HAART) program was designed. This categorized ARV's into 4 main subtypes: non-nucleoside reverse transcriptase inhibitors (NNRTI's), nucleoside reverse transcriptase inhibitors (NRTI's), protease inhibitors (PI's) and fusion inhibitors (Boguszewski *et al*., 2005). NRTI's in being nucleoside analogues function as false substrates for reverse transcriptase. In doing so, termination of the DNA chain occurs. NNRTI's inhibit reverse transcriptase directly and as such potently suppress HIV replication. PI's are potent suppressors of HIV replication and are mostly used in combination therapy. They inhibit the protease enzyme which prevents cleavage of viral polyproteins and results in poorly formed and non infectious HIV particles (Tibotec HIV information and living with HIV medications, 2010).The following fixed regimens are recommended for therapy:

1) NNRTI-based regimen: Efavirenz + Lamivudine or Emtricitabine + Zidovudine or Tenofovir
2) PI-based regimen: Kaletra® (lopinavir/ritonavir) + Lamivudine or Emtricitabine + Zidovudine

Alternative Regimens include one of the following NNRTI-based regimens:

1) Efavirnez + Lamivudine or Emtricitabine + Abacavir or Didanosine or Stavudine
2) Nevirapine + Lamivudine or Emtricitabine + Zidovudine or Stavudine or Didanosine or Abacavir or Tenofovir

One of the following PI-based regimens may also be instituted:

1) Atazanavir + 2 NRTIs
2) Fosamprenavir + 2 NRTIs
3) Fosamprenavir + Ritonavir + 2 NRTIs
4) Indinavir + Ritonavir + 2 NRTIs
5) Indinavir + Ritonavir (Kaletra®) + Lamivudine or Emtricitabine + 1 NRTI other than Zidovudine
6) Nelfinavir + 2 NRTIs
7) Saquinavir sgc or Saquinavir hgc + Ritonavir + 2 NRTIs

Adapted from Temesgen et al., 2006

With such complicated regimens, the need for a delivery system to manage the issue was urgent. An attempted solution was the fixed dose combination (FDC). The FDC means of drug delivery offers a relief from complex regimens and aimed to rectify compliance. With an FDC, 2 or 3 ARV's can be incorporated into a single pill or tablet. The implications of such a delivery system can be clearly outlined in terms of lowered costs and simplified dosing. The outcome of such implications is the limiting of monotherapy, which is a problem in resource poor countries. However, a problem faced with FDC design is that not all regimens can be formulated into a single pill and not all FDC's have been approved (US Department of Health and Human Services Food and Drug Administration, 2006).

One of the most frequently prescribed regimens used in Africa includes the regimen of nevirapine, lamivudine and stavudine. A study by Laurent and co-workers (2004) chose to assess the efficacy and safety of creating an FDC with the above mentioned ARV's. A valid point to take note of in economically impaired countries is the lack of resources and an established infrastructure to meet the demands of the HAART program. The cost for the average HIV infected individual in such regions is quite high especially when taking into account that the person has to purchase individual drugs. The cost for an FDC is much lower than independently priced drugs and additionally improves compliance through simply taking fewer tablets. 60 patients were each given 1 tablet of the fixed dose combination twice a day. The researchers concluded that such a system was in fact reliable and efficacious with an adherence rate of 99%. With such a positive outcome from this study, it was concluded that further exploration into FDC's is warranted.

The benefits of better adherence and reverting from monotherapy highlights only more efficient drug therapy especially in resource poor environments where compliance and erratic supply of individual drugs are problematic. Despite the positive appearance of FDC's, there are not enough studies underway for safety, efficacy and tolerability. More emphasis needs

to be placed on such studies so that more interest and development can be placed on FDC's. Current examples of FDC's include Combivir® and Trizivir® (GlaxoSmithKline, Research Triangle Park, NC, 27709). Combivir® is an FDC comprising of Lamivudine and Zidovudine. Both actives are synthetic nucleoside analogues and fall under the category of nucleotide reverse transcriptase inhibitors. The use of such an FDC must be in a beneficial manner with other ARV's. Studies show that use of Combivir® and a non-nucleoside reverse transcriptase inhibitor or a protease inhibitor decreases the likelihood of viral resistance (AIDS treatment data network, 2006). Trizivir® comprises Abacavir, Lamivudine and Zidovudine with dosage being a single tablet twice daily (TreatHIV.com, 2010).

One of the main benefactors of FDC's are developing countries in Africa. Malawi is one such country, suffering from more than 85000 deaths per year and numerous patients are receiving insufficient and inadequate ARV therapy (The Malawi Paediatric Antiretroviral Treatment Group, 2007). Poor economic growth and lack of capital are trademarks for many poverty stricken African countries and it is these countries which are affected most drastically by HIV/AIDS. Focus, until quite recently, remained on adults in Malawi, but in an article by the The Malawi Paediatric Anti-retroviral Treatment Group, emphasis for treatment was placed on children. The first line treatment for HIV in Malawi is Triomune®, an FDC including stavudine, lamivudine and nevirapine (Cipla Ltd, Mumbai Central, Mumbai, India). Adult therapy includes 1 tablet twice daily of Triomune-30® for patients weighing less than 60kg. For patients above 60kg, 1 tablet of Triomune-40® is prescribed daily (United Pharmacies, 2010). Children require a separate dosing schedule guidelines were stipulated for FDC therapy as shown in Table 2.1. The consensus of the treatment group included a positive outlook on the development of more FDC's especially in developing countries. Positive outcomes were seen in the groups used for the study, with viral loads decreasing.

Table 2.1 Paediatric treatment guidelines for HIV/AIDS

Weight of the child (kg)	Dose in the morning[a]	Dose in the evening[a]
<8	¼ tablet	None
8-11	¼ tablet	¼ tablet
12-17	½ tablet	¼ tablet
18-21	½ tablet	½ tablet
22-27	¾ tablet	½ tablet
28-31	¾ tablet	¾ tablet
32-37	1 tablet	¾ tablet
>38	1 tablet	1 tablet

[a]*Dose of Triomune® tablet having the composition: 40mg stavudine,150mg lamivudine and 200mg nevirapine* (*adapted from The Malawi Paediatric Antiretroviral Treatment Group, 2007)*

FDC's are an intricate part of ARV therapy, especially in developing countries. The benefits from using such a delivery system cannot be ignored. FDC's offer one of the cheapest

means of ARV treatment without losing any efficacy. Whilst such a treatment is beneficial so far as cost is concerned, the availability of combination products is limited to major cities and developed countries (Meldrum J, 2003). Pressure must be placed on governments to establish a means of procurement and distribution of basic FDC's to resource poor communities. Patenting and intellectual property rights directly affect the distribution of FDC's according to Warren Kaplan (2010) in his critique describing the need for FDC's (Kaplan, 2010). The recommendations from this critique include, making intellectual property information more freely available, the integration of intellectual property/ legal issues regarding FDC's of both HIV and TB and to incentivize private sector development of FDC's. Whilst FDC's address compliance issues, detrimental drug interactions that occur amongst ARV's and actives used in opportunistic infections are not controlled.

2.2.2 Opportunistic infections with HIV/AIDS

Opportunistic infections are critical complications for an HIV/AIDS patient. Treatment often means compounding already extreme regimens and potential interactions. According to Table 2.2, oesophageal or pulmonary candidiasis, had a 19% frequency as an opportunistic infection amongst children (taken from a pool of 771 patients) and is described as the most frequent mucocutaneous disease in HIV/AIDS paediatric patient (Van Dyke, 1995).

Table 2.2 Frequency of opportunistic infections amongst paediatric patients

Opportunistic infection	% Frequency amongst paediatric patients (pool of 771 patients)
***Pneumocystis carinii* pneumonia**	31
Lymphoid interstitial pneumonitis	20
Candidiasis, oesophageal or pulmonary	19
Failure to thrive	16
HIV encephalopathy	15
Multiple/recurrent bacterial infections	13
Cytomegalovirus	9
Nontuberculous mycobacteria	5
Herpes simplex virus	4
Cryptosporidiosis	3
Tuberculosis, disseminated	1
CNS toxoplasmosis	1
Lymphoma	1

Adapted from Van Dyke, 1995

Oral candidiasis, is a common infection amongst HIV/AIDS patients and can occur in 3 forms individually or may even present concurrently. *Pseudomembranous Candidiasis* or thrush is presented as a loosely held creamy and yellowish plaque which is inflamed and resembling milk curds. These elevated lesions are prominent on any mucosal surface. Ulceration may be a complication and the lesions have been known to spread to most areas of the mouth. *Erythematous Candidiasis* similarly occurs on any mucous membrane but often occurs in the region where the tongue touches the palate and the lesions present as red patches. *Angular*

Chelitis presents with cracks and fissures at the commissures and lesions are present bilaterally (Greenspan, 1994; Hoepelman and Dupont, 1996). Treatment for oral candidiasis comprises topical formulations (usually requiring a minimal half an hour contact time) using nystatin, amphotericin B and the azole derivatives resulting in clearing of the lesions. However deep seated infections such as oesophageal candidiasis requires systemic treatment in the form of the azole compound ketoconazole or the triazole compounds itraconazole and fluconazole (Greenspan, 1994; Hoepelman and Dupont, 1996; Farah *et al.,* 2000).

Table 2.3 Typical therapy for oral candidiasis

Active	Form	Dosage
Nystatin$_T$	Cream	100 000 units/g to be applied 2-4 times daily
Nystatin$_T$	Ointment	100 000 units/g to be applied 2-4 times daily
Clotrimazole$_T$	Cream 1%	10mg/ g (1%) to be applied 2-3 times daily for 2-4 weeks
Ketoconazole$_T$	Cream 2%	20mg/g (2%)to be applied twice daily until a few days after symptoms have disappeared
Ketoconazole$_S$	Tablet 200mg	200mg to be taken once daily with food
Fluconazole$_S$	Capsules 50mg, 100mg and 200mg	50-100mg daily for 7-14 days
Itraconazole$_S$	Capsules 100mg or oral solution 10mg/mL	200mg daily for 1-2 weeks
Amphotericin B	IV infusion	0.6mg/kg/day for 2 weeks

$_T$ represents a topical formulation and $_S$ a systemic formulation (adapted from The South African Medicines Formulary, 2005 and Greenspan, 1994)

Treatment of candidiasis follows set guidelines but complications do arise with co-morbidities such as HIV/AIDS. The issues surrounding treatment of the 2 conditions simultaneously has been under scrutiny for many years, (Sangeorzan *et al.,* 1994; Silverman *et al.,* 1996; Migliorat *et al.,* 2004), but focus for the purpose of this dissertation shall be on the direct interaction that occurs between ketoconazole and didaosine.

2.2.3 Interactions between ketoconazole and didanosine

Ketoconazole is an antifungal agent belonging to the imidazole group that has been successfully used since the 1980's (Maertens, 2004). It is chemically referred to as a (α)*cis*-1-acetyl-4-[*p*-[[2-(2,4dichlorophenyl)-2-imidazol-1-ylmethyl) 1,3-dioxolan-4-yl]methoxy]phenyl] piperazine and is insoluble in water. The mechanism of action for ketoconazole has various proposals including being a cytochrome P450 inhibitor, interference with ergosterol synthesis, interrupting drug metabolism through blocking the activation of the nuclear

receptors and mobilization of Ca^{2+} in renal tubular cells (Jan and Tseng, 2000; Moody *et al.,* 2004; Ko-Long *et al.,* 2009; Huang *et al.,* 2007).

Therapeutically, it is used for mycotic infections, antifungal therapy and is used often for opportunistic infections in immune-compromised patients (Córdoba-Díaz, 2001; Karasulu *et al.,* 2004). Ketoconazole has very distinct advantages as an antifungal in that it can be given as a single dose and be used for systemic and topical infections (Patton *et al.,* 2001).

Didanosine is an anti-retroviral nucleoside reverse transcriptase inhibitor. This synthetic nucleoside analogue is referred to chemically as 2',3'-dideoxyinosine and structurally, didanosine follows a similar structure to adenosine but for the presence of hydrogen at the 3' position on the ribose ring in place of the hydroxyl group. Additionally, a substituted primary amine on the nucleoside moiety is present. Dideoxyadenosine 5'-triphosphate is the active metabolite formed intracellularly by cellular enzymes. HIV-1 reverse transcriptase is inhibited from its natural substrate deoxyadenosine 5'triphosphate by dideoxyadenosine 5'-triphosphate and furthermore, the active metabolite of didanosine assimilates itself into the viral DNA consequently leading to termination of DNA chain elongation (Videx package insert, 2010; World Health Organisation Didanosine guidelines, 2005; Acosta and Fletcher, 1995).

One of the challenges in didanosine therapy is its instability in an acidic environment resulting in its degradation to hypoxanthine with bioavailability as low as 20%. In many cases and studies bioavailability often fluctuates but at a low level (Sinko *et al*., 1994; Acosta and Fletcher, 1995). Increasing the dose can even lead to a decrease in bioavailability in a study conducted by Knupp and co-workers (1991). The presence of food also promotes an increase in gastric acidity and gastric retention further propagating the detrimental effect on didanosine (Crevoisier *et al*., 2003; Schubert and Peura, 2008). The addition of buffers to the formulation or the concomitant usage of antacid allows bioavailability to reach up to $^{+}/-$ 40% but this low bioavailability can still be attributed to the acidic environment of the stomach and first pass metabolism even with the presence of a buffer (Blum *et al.,* 1988; Bramer *et al.,* 1993; Moreno *et al*., 1993; Acosta and Fletcher, 1995; Taburet Singlas, 1996; Aungst, 1999; Videx package insert, 2010).

The interaction between didanosine and ketoconazole is referred to as an absorption interaction (Gupta *et al*., 1999). Ketoconazole requires an acidic environment for favourable absorption and the concurrent administration with food enhances an acidic environment. Didanosine is converted into the non-active hypoxanthine compound reducing the absorption and availability of didanosine. The co-administration of the 2 actives can be seen to lead to

the reduction in didanosine absorption and possibly treatment failure. Medication should therefore be separated by at least 2 hours with ketoconazole taken at meals and didanosine 2 hours after (Acosta and Fletcher, 1995; Dykeman *et al*., 1996; Gupta *et al*, 1999).

Table 2.4 Discrepancies between didanosine and ketoconazole

Actives	Required pH	Time Taken	Bioavailability at an acidic pH
Didanosine	Basic	After meals	Low/Impaired
Ketoconazole	Acidic	During meals	Good

Adapted from Acosta and Fletcher, 1995; Dykeman et al., 1996; Gupta et al., 1999

2.3 Tuberculosis Regimen Treatment Schemes

2.3.1 Tuberculosis and fixed dose combination liposomal therapy

TB has been a worldwide crisis for many years. The severity of TB can be attributed directly to it being contracted like the common cold (an airborne contaminant), with only a small portion required to be inhaled for infection to commence. According to the World Health Organization (WHO):

- Someone in the world is newly infected with TB bacilli every second.
- Overall, one-third of the world's population is currently infected with the TB bacillus.
- 5-10% of people who are infected with TB bacilli (but who are not infected with HIV) become sick or infectious at some time during their life. People with HIV and TB infection are much more likely to develop TB (World Health Organisation Tuberculosis fact sheet, 2010).

The WHO has been vigilant on the current escalation of TB and derived the following statistics, as reported in Figure 1 which highlights prevalence and mortality of tuberculosis. TB therapy cannot be defined as a simple drug treatment plan. Therapy consists of regimental therapy in conjunction with Directly Observed Therapy (DOT). TB therapy is a standardized treatment protocol. A 2 months induction period is the first approach and includes isoniazid, rifampicin, pyrazinamide and ethambutol. This is then followed by a 4 month continuation phase of isoniazid and rifampicin (Gleeson and Decker, 2006). TB if left untreated or if inadequately treated can lead to further dissemination of TB in the individual, spread towards others and multiple drug resistance. The implementation of the DOT protocol was aimed at ensuring compliance and efficacious treatment. The program was initiated more than 40 years ago and remains today one of the most successful and well studied adherence programs to date. Thus the WHO has been ever vigilant on the current escalation

of TB and derived the following statistics, as reported in Figure 2.1 and Figure 2.2:

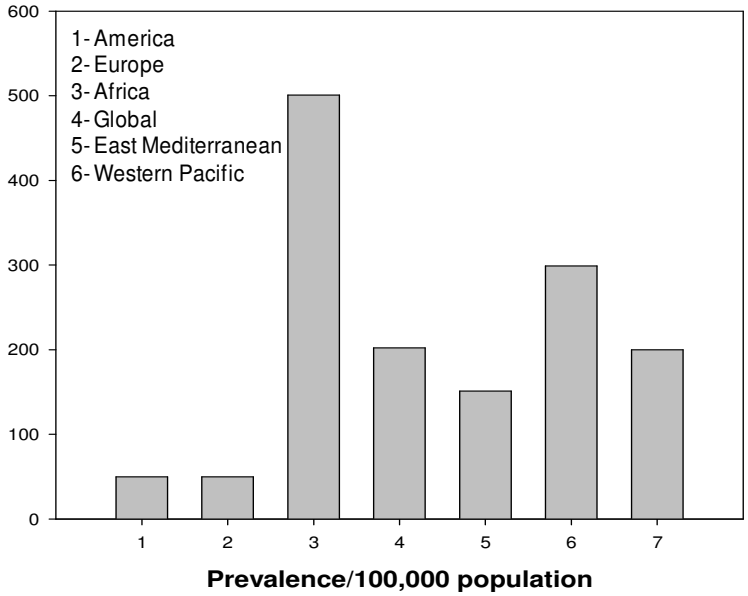


Figure 2.1 Estimated worldwide prevalence of tuberculosis *(adapted from the World Health Organisation Tuberculosis facts sheet, 2010*)

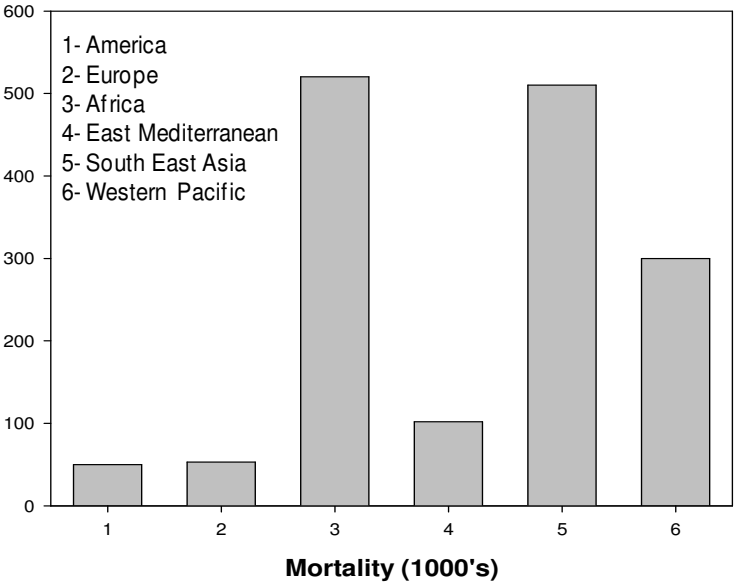


Figure 2.2 Estimated worldwide mortality from tuberculosis *(adapted from the World Health Organisation Tuberculosis facts sheet, 2010*)

DOT's for TB is usually carried out with once-daily administration of 4 anti-TB drugs (isoniazid, rifampicin, pyrazinamide, and ethambutol), usually 5 days per week for 2 months, followed by once-daily treatment with isoniazid and rifampicin, 3–5 days per week, for a total of 6–9 months of therapy (Migliori *et al*., 1999; Friedland *et al*., 2004).

Whilst DOTS is an effective means of treatment, a more reliable means of drug delivery is

required for adequate therapy to ensue. TB therapy must also be observed with a distinct complication. This prevalent, common complication is that of resistance to treatment. Multidrug-resistant tuberculosis (MDR-TB) and the more recent Extensively-resistant TB (XDR-TB) is rife in heavily populated areas with poor infrastructure and ill equipped health care services. Drug resistance can be attributed to direct causal aspects such as non adherence or failure to complete courses and the tendency of some strains of mycobacterium to undergo mutation and co-morbidity with conditions such as HIV/AIDS (Rad *et al*., 2003; Shah *et al*., 2007).

The severity of such resistance can be seen in areas incapable of upholding a reliable DOTS program. The DOTS program requires a dynamic and committed effort from both private and public sectors of health care and consequently, developing countries are affected by both MDR and XDR TB with an increasing affinity (Pepper *et al*., 2007). MDR TB can be defined as TB resistant to initial TB therapy (isoniazid and rifampicin) whilst XDR TB can be defined as being resistant to isoniazid and rifampicin and to any of the fluoroquinolones and to at least one of the following injectable drugs: capreomycin, kanamycin, and amikacin. This problem can be seen to extend to developed countries as resistant strains can easily spread from region to region through a host of travel mediums such as commercialized flights and trade routes through both sea and air transport agents and even travel holidays (Aziz *et al*., 2001; Dowdall *et al*., 2006; Martinez *et al*., 2007).

Drug delivery systems that have the potential to negate the challenges associated with TB therapy include liposomal drug delivery, developed more than 25 years ago. Brenda Ryman in the 1970's, proposed the idea of targeted drug delivery using liposomes and described the use of the technology in anticancer and antimicrobial therapy (Gregoriadis, 1995). Applications of liposomes are seen in a range of daily uses from cosmetic applications to drug delivery (Lasic and Papahadjopoulos, 1998). Liposomal design and theory has been well defined in the past as micro- to nanoscale, spherical vesicles formed through the hydration of phospholipids (Bangham, 1968). Anticancer and antibiotic therapies are most often associated with liposomal therapy and reveal much success (Bao *et al*., 2006). The formation of liposomal vesicles is due to hydration of phospholipids. The advantages of liposomes include the ability to encapsulate a large volume of drug and the functionalization of the liposome composition (Lasic, 1993). Liposomes can be categorized as conventional, long circulating, cationic or targeted liposomes. In order for liposomes to have a desired function, they must bypass the mononuclear phagocyte system to decrease the rate of uptake by phagocytes. To counter this, long circulating or stealth liposomes have been developed by attaching polyethylene glycol (PEG) via coupling PEG to phosphatidylethanolamine in the liposome bi-layer. Uptake into the reticular endothelial

system and opsonization are prevented as the PEG provides a layer of steric hindrance (Crommelin *et al*., 2002). PEG has seen many applications where block copolymers are formed with the process of PEGylation in which PEG is added to a particular polymer. The addition of PEG is a process that has been incorporated into numerous drug delivery systems, the copolymers of which have many beneficial functions. Functionally, PEGylation can offer an improvement in solubility of proteins, a protection from immune response and a decrease in antigenicity (Pierce the protein people, 2008).

Monomeric repeating units of ethylene glycol comprise a single molecule of water soluble PEG and has a formula of $H(OCH_2CH_2)_nOH$, with 'n' as the average number of repeating ethylene oxide groups as depicted in Figure 2.3. The conventional uses of PEG include a thickening agent and when chemically reacted with fatty acids results in detergents having both thickening and foam stabilizing characteristics. Further utilization can be seen in the cosmetic, ceramics and textile industry revealing the versatility of PEG. Grading of PEG is greatly dependent upon the average molecular mass of the molecule in which higher molecular masses results in a decrease in water solubility and solubility in certain solvents. Due to these properties it is evident that PEG is extensively used in the development of drug delivery systems even by forming co-polymers in the process of PEGylation (Quellen, 2003, Khandare; Minko, 2006). When PEGylation occurs the PEG molecule is incorporated onto the surface of the molecule providing the entire system a physical shielding against the body's immune system. This concept of a stealth system has been furthered in more than just liposomes and has seen expression in microparticle drug delivery as depicted in Figure 2.4 (Dorati *et al*., 2007). The injectable microparticle system is effectively shielded from the immune system due to the presence of PEG in a similar manner to the liposome delivery system (Panoyan *et al*., 2003).

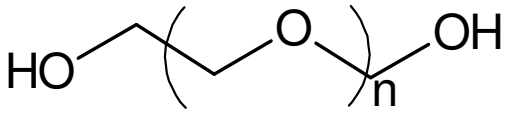


Figure 2.3 Chemical structure of polyethylene glyco*l) (Quellen, 2003)*

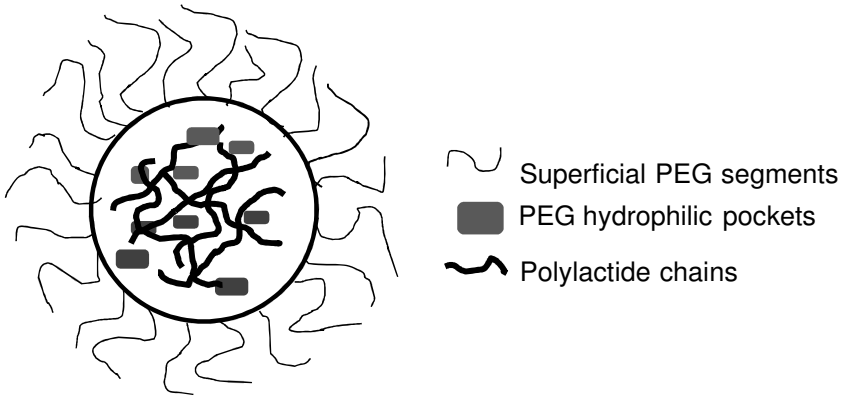


Figure 2.4 A schematic depiction of superficial polyethylene glycol segments on a microparticulate imparting the stealth function *(adapted from Dorati et al., 2007)*

When considering the management of TB using regimental therapy, liposomal drug delivery was implemented in a recent study by Khuller and co-workers (2004), where isoniazid and rifampicin were incorporated into intravenously administered stealth liposomes. Preparation of the liposomes included the use of probe sonication and the addition of O-stearylamylopectin, which provided an increased affinity of the liposomes to lung tissue. It was found that the liposomal therapy was more effective than administering free drug. The liposomal delivery system provided sustained drug release and was considerably stable, less toxic and exhibited a greater efficacy in clearance of mycobacterial infections compared to the drugs administered individually. The use of stealth liposomes was concluded to be an effective carrier of both the antimycobacterial drugs isoniazid and rifampicin. Numerous studies have also shown that drug concentration is more vital in the alveolar macrophages than the systemic circulation as the mycobacterium accumulates in these specific cells (Suarez *et al*., 2001). Therefore, emphasis has been placed on the development of more site-specific drug delivery to the lung alveolar macrophages, as opposed to conventional systemic delivery. Liposomes may also act as drug reservoirs to provide slow and sustained drug release and their nanoscale size has applicability in the targeting of the alveolar macrophages. This approach would not only be advantageous in reducing the cost of TB treatment but also have the potential to shorten the duration of the treatment. Liposomal technology has been in existence for many years but has not been fully exploited. Particular interest can be shown for pulmonary delivery due to the nano-size and the diversion from invasive injectable administration. Sustained drug release can be achieved for chronic conditions such as TB, asthma and even diabetes using liposomal technology (Liu *et al.,* 1993; Huang and Wang, 2006). Liposomes as a mode of FDC administration should be explored with reference to other chronic conditions such as hypertension, asthma, and diabetes that require multi-drug therapy, in view of the highly controlled and sustained drug release and the decrease in total therapeutic doses required.

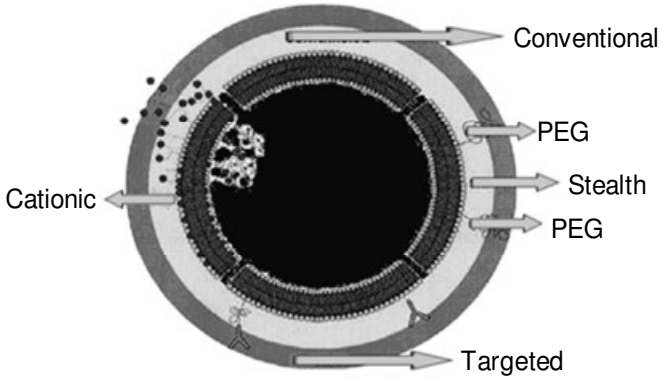


Figure 2.5 Schematic representing the various liposomes *(adapted from Khuller et al., 2004)*

Further exploration of TB treatment has been shown with drug-loaded polymeric nanosystems. du Toit and colleagues (2008) developed nanosystems using an emulsion-based-salting-out approach. The foremost challenge with site-specific drug delivery for pulmonary pathologies is the anatomical barrier in which most particles are prevented from reaching the terminal ends of the pulmonary system. Nanosystems can effectively bypass this barrier and offer a flexible yet rate controlled release of the selected drug. Nanosystems are an emerging technology, in particular for regimen therapy but an oral delivery system is still the preferred medium to date.

2.3.2. Tuberculosis and osmotically regulated drug delivery systems

Osmotically regulated multi-drug delivery systems have been introduced for the management of TB and have been considered to be an oral system catering to regimental concerns. As the name describes, the system offers an oral drug delivery system and the simultaneous delivery of more than one type of drug in a single delivery system. Prabakaran and co-workers (2004) demonstrated the use of an osmotic drug delivery system for the concurrent administration of rifampicin and isoniazid for the treatment of TB in which asymmetric membranes were utilized. Asymmetric membrane capsules are osmotic delivery systems used for precisely controlled drug delivery (Figure 2.6).

Asymmetric membrane coatings for tablets were developed to further increase coating permeability. The coating consists of a porous substrate with a thin outer layer or skin. Drugs that have poor solubility or a higher dose can be delivered osmotically and at a more controlled and higher release rate compared to conventional osmotic systems. This approach of osmotic delivery is due directly to the high water flux provided by the asymmetric membrane coatings. The basic framework of an asymmetric membrane capsule is that of a single-core osmotic delivery system comprising a drug-loaded core surrounded by the asymmetric membrane. The advantages of the delivery system include the selection of membrane permeability by altercation of the membrane structure which in turn may modify

the drug release profiles. In addition, the porosity of the outer layer or skin can be manipulated and thereafter minimize the lag time prior to the commencement of drug release. This feature allows drug to be released from a large number of delivery ports. The technology can be applied to both multiparticulate and capsular delivery systems (Herbig *et al*., 1995; Thombre *et al*., 1999; Lin and Ho, 2003). The study performed by Prabakaran and colleagues (2004) utilized a variety of materials for designing the asymmetric membrane. The capsule shell that modulates the drug release from the delivery system usually comprises a water soluble polymer such as cellulose acetate. Normal capsular systems are composed of gelatin but with the substitution of cellulose acetate, sustained release of the chosen drug from the system may be achievable. Cellulose acetate is defined as an adaptable polymer. Due to its extreme versatility, cellulose acetate can be easily bonded with heat, pressure and plasticizers. The wide range of applications, found in numerous methodologies, is directly related to the solubility of cellulose acetate in a host of solvents. Furthermore it is biocompatible and therefore is often used for the design of drug delivery systems (Audoin, 2003).

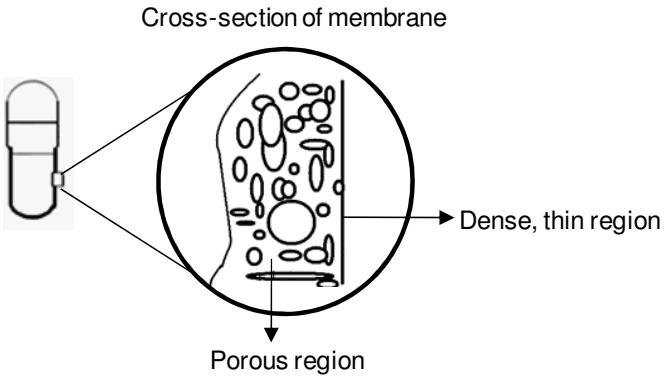


Figure 2.6 Schematic of an asymmetric membrane capsule *(adapted from Prabakaran et al., 2004)*

2.3.3 The interaction between isoniazid and rifampicin

In 1994, the World Health Organization (WHO) and the International Union against Tuberculosis and Lung Disease (IUATLD) cautioned the use of FDC's which included simultaneous use of rifampicin and isoniazid. The use would only be permitted should the bioavailability of rifampicin prove adequate (World Health Organization Communicable Diseases Cluster, 1999). A recent study by Shishoo and co-workers (2001) demonstrated the low bioavailability of rifampicin when co-administered with isoniazid in an FDC. It has been postulated that the presence of isoniazid enhances the degradation of rifampicin in the stomach (Seifart *et al*., 1991).

A recent study by Mariappan and co-workers (2000) discovered a new peak (due to the formation of isonicotinyl hydrazone) that coincided with the degradation of rifampicin in the presence of isoniazid. It is proposed that once 3-formylrifamycin is formed within the acidic conditions of the stomach, there is a direct interaction with isoniazid to form isonicotinyl hydrazone, through a fast second-order reaction.

The isonicotinyl hydrazone is unstable in an acidic environment and consequently regenerates isoniazid and the insoluble 3-formylrifamycin by a pseudo first-order reaction. As the second-order forward reaction is faster than the preceding (rifampicin to 3-formylrifamycin) and the following (hydrazone to 3-formylrifamycin and isoniazid) first order reactions, the overall reaction is favoured towards the formation of isonicotinyl hydrazone as rifampicin is degraded to 3- formylrifamycin (Singh *et al*., 2001). Figure 2.7 shows the chemical pathway leading to the degradation of rifampicin.

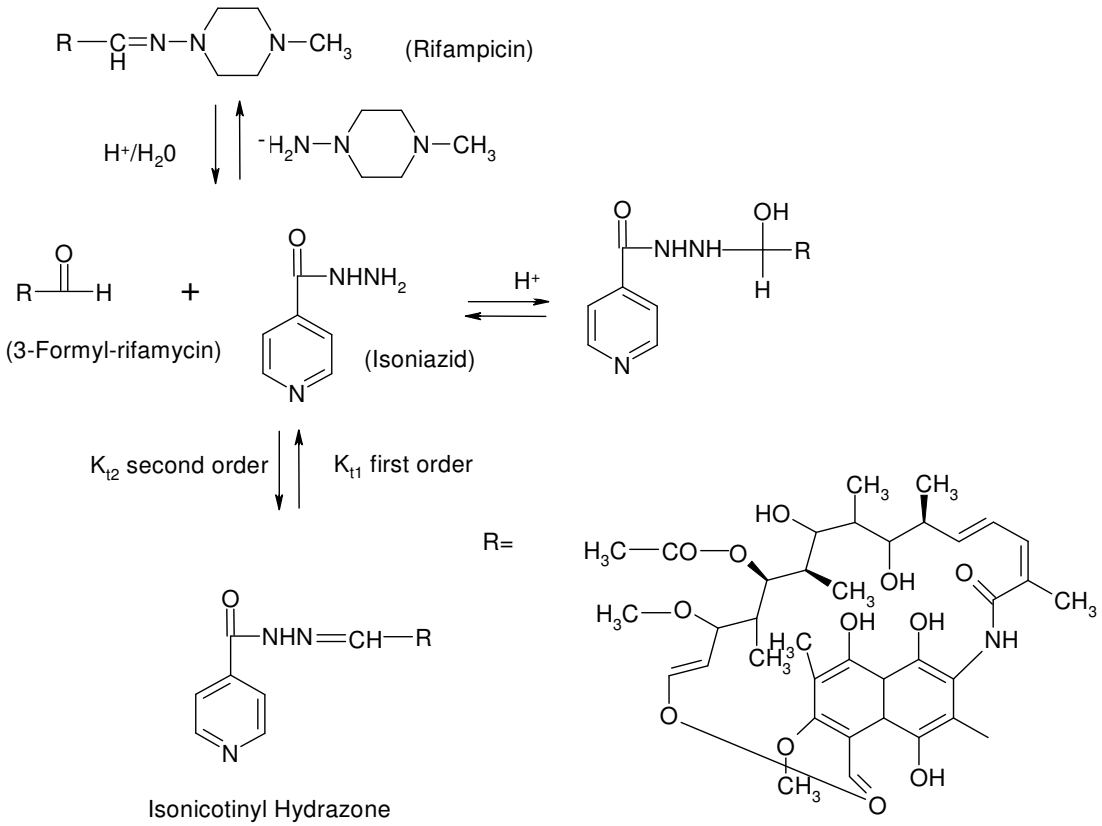


Figure 2.7 The pathway of the decomposition of rifampicin due to the presence of isoniazid *(adapted from Singh et al., 2001)*

2.4 Regimen Strategies for the Asthma Management

2.4.1 Asthma and fixed dose combination drug delivery systems

Currently asthma is another regimentally treated condition affecting individuals on a daily basis with more than 300 million people affected worldwide. If inappropriately managed, asthma can become a debilitating condition to any patient in many circumstances. As a general definition, asthma is a chronic respiratory condition marked by inflammation of the lung tissue, though there is no generally accepted accurate definition of asthma. Airway obstruction, hyper-responsiveness and remodelling are also noted to occur (Diamant *et al*., 2007). The actual occurrence of asthma may in fact be much higher due to the fact that asthma does not have a precise definition and in many case misdiagnosis is a frequent occurrence (GINA science and executive committee Global Strategy for Asthma Management and Prevention, 2009). The debilitating nature of asthma can affect a patient's daily routine through a host of stimulating factors. Simple activities such as walking, running climbing stairs or participating in sports are factors than can elicit an asthmatic attack. Allergens can elicit both early and late asthmatic responses and act through an IgE-mast cell-triggered immune response, resulting in the typical inflammatory action associated with an acute attack (Boulet *et al.,* 2007).

Certain patients exhibit asthmatic attacks due to drugs such as aspirin. Bronchoconstriction occurs as leukotrienes are released by eosiniphils due to aspirin degradation in aspirin sensitive patients (Nasser *et al.,* 1996). More emphasis needs to be placed on studies relating to clinical proof of concept so that exact causative factors of asthma can be understood. Too much uncertainty surrounds the aetiology of asthma and in particular what may elicit an asthmatic attack. Functional and relative testing should be explored further such that current regimens with asthma therapy can be evaluated for efficacy and the quality of treatment (Diamant *et al.,* 2008). Most cases of patient therapy reveal an unmet treatment plan due to: 1) patient non-compliance, 2) poor understanding of treatment plans 3) poor patient-practitioner communication and 4) unmet treatment needs. Whilst treatment regimens for asthma are designed to optimize therapy, they fail to take into consideration a patient's daily functions and lifestyle. It is therefore quite understandable that the most frequent complaint from most patients is maintaining vigilance with drug administration (Hyland and Hi, 2004). Asthmatic therapy can be expressed as short-term relief and long-term management. Acute onsets or attacks are treated with selective short-term drugs and long-term drugs are crucial for the sufficient control over asthma. The combination of drugs into a single FDC may pose a few challenges with the treatment of asthma. The combination of 2 or more drugs should not result in a deleterious interaction between the 2 drugs. Specifically, 3 types of interactions that are likely to occur include interactions between the drugs, the

drugs and the carriers and the drug and the device (Sanders, 2003). However, despite these potential drawbacks on manufacturing and cost, the patient's benefits outweigh the failure rate. Various inhalation devices have been developed for the purpose of acknowledging patients needs with regards to complex asthma regimens.

Advair Diskus® is an inhaler drug delivery system utilizing a FDC. The system comprises 2 drugs, fluticasone proprionate (a corticosteroid) and salmeterol (a long-acting β-agonist) (Nelson, 2001). The combination of the 2 drugs offers benefits in that there are now 2 distinct and separate mechanisms of actions occurring in a single drug delivery system. A study by Baraniuk and co-workers (1997) showed that therapeutic doses of glucocorticoids can increase the number of β-receptors functionally depicting the 2 drugs simultaneously (Figure 2.8). Furthermore β-agonists such as salmeterol initiate ligand independent activation of glucocorticoid receptors (Eickelberg *et al.,* 1999). This approach therefore offers superior function and efficacy, an economical treatment option as opposed to purchasing the individual drugs separately and improved patient compliance (Nelson, 2001).

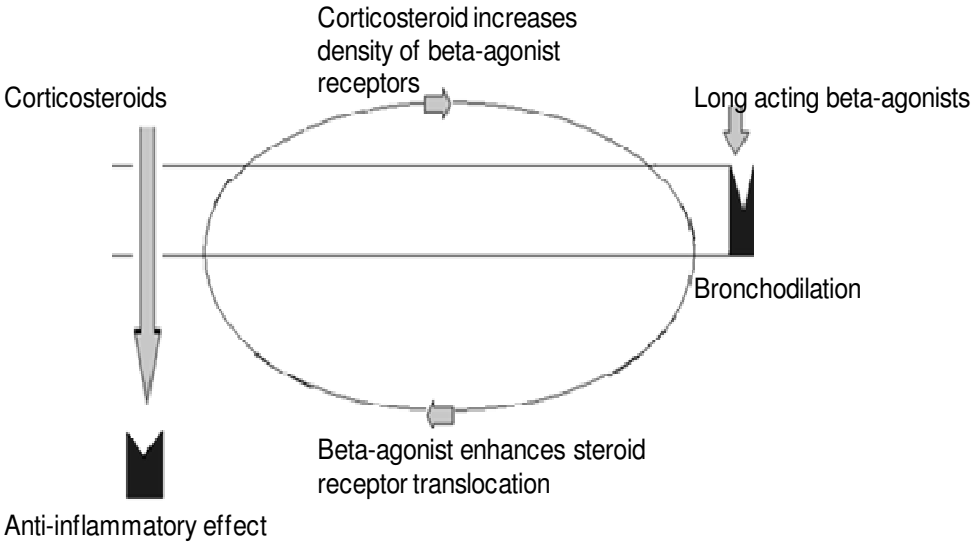


Figure 2.8 Illustration depicting the complimentary effect of corticosteroids and long-acting β-agonists in a single fixed dose combination *(adapted from Baraniuk et al., 1997)*

Table 2.5 Typical drugs employed in asthma treatment regimens

Type of drug	Short/long-term therapy	Mechanism of action
β-Agonists	Short	Bronchodilators responsible for smooth muscle relaxation
Corticosteroids	Short	Anti-inflammatory used in conjunction with short acting β-agonists for acute attacks
Anticholinergics	Short	Reduction in vagal tone of airways via antagonistic effect on muscurinic receptors
Methylxanthines	Long	Mild-moderate bronchodilator used in combination with inhaled corticosteroids
Immunomodulators	Long	Monoclonal antibody preventing IgE mediated inflammation
Leukotriene modifiers	Long	Leukotriene receptor antagonist and a 5-lipoxygenase inhibitor
Cromolyn sodium and Nedocromil	Long	Interferes with chloride channels function and stabilizes mast cells
Corticosteroids	Long	Anti-inflammatory
β-agonists	Long	Bronchodilators with a duration of action up to 12 hours

Adapted from the National Heart Lung and Blood Institute, 2010

Furthermore, the drug eformoterol has been formulated with budesonide in a single drug delivery system known commercially as Symbicort®. This delivery system is also a metered dose inhaler and similarly to Advair® comprises both a corticosteroid and a long-acting β-agonist. The delivery system offers the same advantages of combination therapy such as reducing the drug quantity, enhancing efficacy and an instantaneous bronchodilating effect with the use of eformoterol (Palmqvist *et al.,* 1999). Use of an inhaled corticosteroid in conjunction with a long-acting β-agonist in a FDC inhaler is noted as beneficial to patients with regards to efficacy, convenience and the decrease in systemic side-effects (Currie *et al.,* 2005).

As detailed in this chapter, 3 relevant and prominent conditions and the associative regimen therapies have been detailed as well as the pertinent drug delivery systems. The ODMUS shall cater for these and any other therapies requiring regimen therapy but shall not utilize the delivery systems discussed in Chapter 2.

In retrospect, all aforementioned systems have drawbacks and a different approach to formulating a novel delivery system was sought after taking into account:

- Novelty
- A simplified formulation method
- Cost effectiveness
- Scale up
- Oral delivery
- And site-specific controlled delivery of 2 different pharmacological actives

2.5 The Role of a Dualistic Oral Drug Delivery System Encompassing both Multiparticulate and Membranous Technology for Drug Regimen Therapy

Multiparticulate carrier systems have vast positive implications for advanced drug delivery. In particular multiparticulates or hydrogel beads have been shown increasing interest due to their small size, which allows the particulates to easily pass through the upper gastrointestinal tract (GIT) (Meyer *et al.,* 1985). This has an advantage over larger drug delivery systems such as tablets or capsules due to their size, which allows an even or more uniform dispersion of drug throughout the GIT, more reliable and accurate drug absorption with less intra and inter-patient variability (Zhang *et al.,* 2002) and the overall delivery of drug is independent of the nutritional state of the patient (Kramer and Blume, 1994; Schmidt and Bodmeier, 2001). This is specifically beneficial for the simultaneous treatment of candidiasis and HIV in which didanosine is taken after meals and ketoconazole during meals as stated in Table 2.4 in Chapter 2.2.3. Furthermore it has long been established that multiparticulates have the potential to be retained in the colon for longer durations thus making them suitable in instances where one of the drugs within a FDC is required for local or site-specific treatment within the colon (Wilson and Wood, 1958). Therefore, multiparticulates are an ideal delivery system to be used in the ODMUS.

One of the most reliable factors of multiparticulates includes the ability to deliver reliable quantities of drug. This can be explained in that the loss of a single particulate does not translate to failure of the entire delivery system. Most multiparticulate systems undergo a spray congealing process which allows for further entrapment of drug, so as to be used for regimental drug therapy in order to obtain a pulsatile effect or release rate. The core of the particulate comprising of a suitable water soluble/swellable polymer is encapsulated by an insoluble polymer. Upon contact with gastric/colonic fluid, the swellable layer expands and ruptures the outer layer allowing for the pulsatile drug release that is required (Dashevsky and Mohamad, 2006). A study by Lamprecht and co-workers (2000) showed the use of multiparticulates in delivering FDC's. Sulfasalazine and betamethasone were entrapped within the multiparticulates and microencapsulation was performed by a solvent evaporation/extraction technique. Selection of the technique is determined by the solubility of the drug and polymer in various solvent systems (Alex and Bodmeier, 1990; Nihant *et al.*,

1994) and allowing for encapsulation of either water soluble or insoluble drugs (Bodmeier *et al.,* 1994). For the purposes of the ODMUS however, a simplified method was developed avoiding the intricate process of microencapsulation. In addition, polymers used for the design of drug regimen therapies have to be carefully selected, as the type of polymer dictates the site-specific release capabilities of the system.

Previously described in Chapter 1, hydrogels are intricate porous polymeric networks that retain and entrap large volumes of water (Rajagopal and Schneider, 2004; Nair and Laurencin, 2006; Lee and Yuk, 2007). Functionally, a hydrogel has the ability to swell in an aqueous environment and entrap large volumes of water while maintaining its 3-dimensional network (Qiu *et al*., 2003). Membranous systems formulated from the described hydrogels offer an attractive solution for regimen therapy, in particular biodegradability and biocompatibility (Gong *et al*., 2009) and can be used in conjunction with multiparticulates. The versatility of membranous systems can be seen through its extensive use with artificial organs, tissue regeneration, diagnostic devices and drug delivery (Stamatialis *et al.,* 2008). In terms of drug delivery, membranes have utilized various delivery systems to achieve controlled drug release illustrated in Figure 2.9. Most often, membranes find expression in osmotic membrane systems, which is composed of a semi-permeable membrane allowing water to diffuse in and the concentrated drug to leave its reservoir in a modulated manner (Kuethe *et al.,* 1992). Fick's Law of diffusion governs the release mechanism for diffusion controlled membrane systems in which membranes can be porous, non-porous and biodegradable. A popular formulation method for membranous systems is that of phase inversion. A homogenous solution of solvent, polymer and various constituents (including drug), undergoes phase separation due to the solvent evaporating into the atmosphere or by a solvent-nonsolvent exchange in a quench bath resulting in membrane formation (McHugh 2005; Ma and McHugh, 2007).

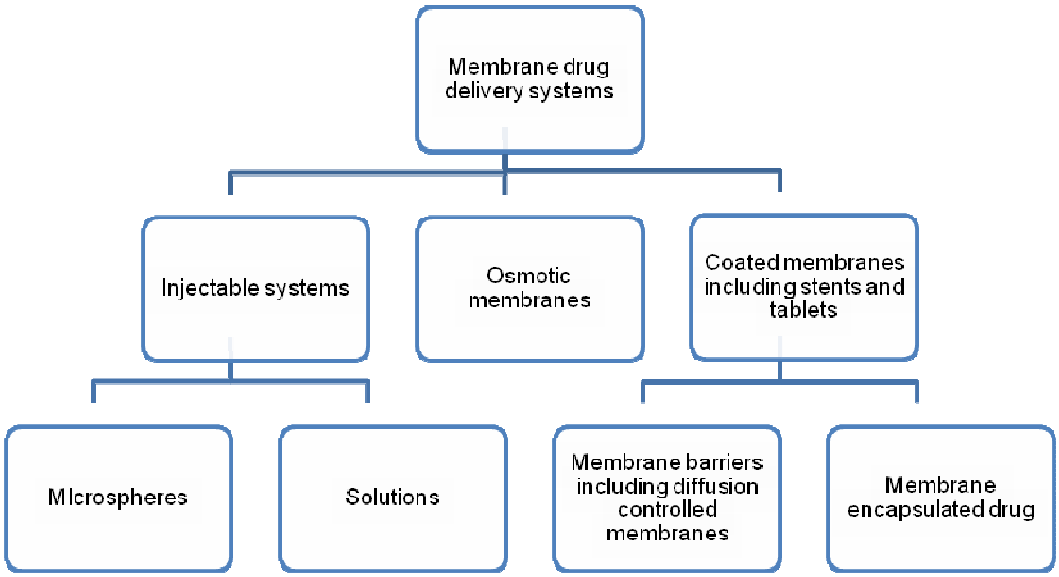


Figure 2.9 Sub-classes of membranous systems *(adapted from McHugh, 2005)*

Other systems utilizing membranous technology include pills, implants and patches clearly identifying the versatility of membranes (Stamatialis *et al., 2008)*. The core release mechanisms for synthesized polymeric membranes include dissolution, diffusion and erosion. The complexity of these release mechanisms is that they can be exhibited concurrently within the same membrane obscuring a desired controlled release (Temtem *et al.,* 2009). Additionally, methodology, chemical and physical properties and drug content effects release patterns incidentally demanding arduous development of membrane systems (Siepmann and Siepmann, 2008). In summary, membranes offer an attractive candidate as an oral delivery system with the primary advantages being biocompatibility and biodegradability. Efficacy is however compromised due to potentially erratic and influenced drug release patterns.

The delivery of drug to various regions within the GIT highlights a positive application of such a delivery system. A combination of the multiparticulate system and a novel tablet-like membranous system is shown in Figure 2.10 and this was the framework upon which the ODMUS was designed. Drug release in this manner was pH-dependant, based on the polymeric material selected for each component within the multiparticulate and membranous system. The multiparticulate system contained a polymeric material rendering the beads impervious to the acid like conditions of the stomach. Consequently no leeching of drug occurred in the stomach region.

The tablet like membranous system or 'memblet*',* released its active at an acidic pH due to its polymeric constituents. The system may offer outcomes in relation to patient compliance,

deleterious drug-drug interactions and controlled release of the respective actives. Currently oral drug delivery systems do not allow for the delivery of a multiple drug regimens within a combination of systems including multiparticulates and a membranous system in unison and therefore the ODMUS will be able to decrease the quantity of tablets required for the patient to consume on a daily basis. Illnesses such as TB, HIV/AIDS, asthma and infections requiring multiple drugs may be most suited for incorporation into the ODMUS.

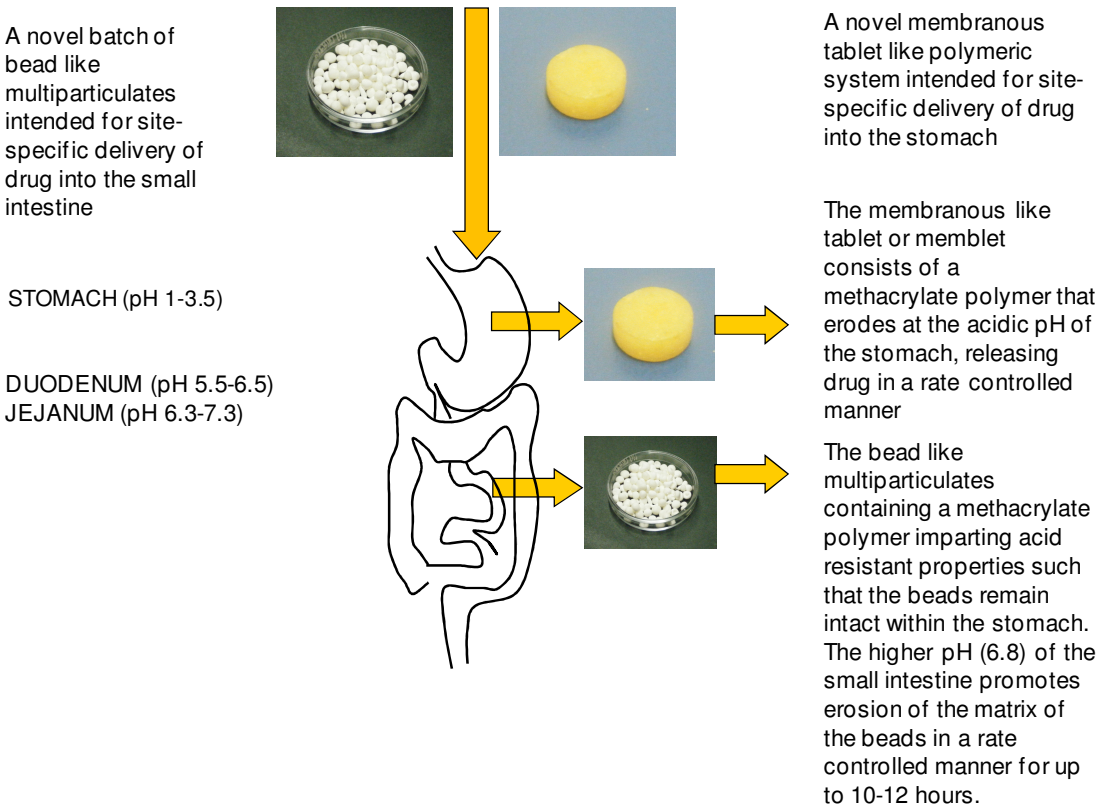


Figure 2.10 Schematic representation of the functional Once Daily Multi-Unit System

2.6 Concluding Remarks

This Chapter sought to address the modern therapies requiring regimental treatment and a brief synopsis was provided for HIV/AIDS, tuberculosis and asthma. The challenges including drug-drug interactions were highlighted and reviewed with particular emphasis on ketoconazole-didanosine in HIV/AIDS treatment and rifampicin-isoniazid in tuberculosis management. Novel approaches towards regimental therapies were viewed in relation to asthma, HIV/AIDS and tuberculosis. Novel delivery systems were discussed to highlight a need for development and research with respect to regimen therapy. The necessity for a novel delivery system to be developed was enforced. Finally, the selection of membranous and multiparticulate technology was introduced and discussed to be incorporated into a once daily multiple unit delivery system for the management of regimen therapies to negate drug-drug interactions, maintain controlled release and improve patient compliance through reducing pill quantities.

CHAPTER 3
PRELIMINARY STUDIES FOR THE DEVELOPMENT AND DESIGN OF THE ONCE DAILY MULTI-UNIT SYSTEM

3.1 Introduction

In this Chapter, method development and preliminary testing of the ODMUS was the primordial focus. A rudimentary understanding of the mechanistic release patterns and behaviour of each component of the ODMUS was prerequisite for optimization studies. When considering method development, method simplicity and scale up for bulk manufacturing were critical points. The methods were not exclusively similar for each respective delivery system, but retained the attributes stated above.

Multiparticulate desired properties included a robust quality, relatively aesthetic appearance, as accurately as possible a spherical shape and uniformity in shape and size. The multiparticulates were to avoid being produced as brittle and ideally not be influenced, with regards to bead integrity, by various factors whilst under storage conditions. A generally acceptable appearance would circumvent aesthetic coating of the beads and therefore a bypassed procedure simplifying bulk manufacturing and formulation procedures. In terms of the means of delivery, the multiparticulates had to achieve site-specific drug delivery in the small intestine and simultaneously retard any release of drug within the stomach to avoid deleterious drug-drug interactions with the chosen drug loaded on the memblet system.

Memblet development followed a parallel study of controlled drug release and characterization studies, which required the development of individualized methods. Characterization of said memblet*s* influenced methodology in relation to drying time, shape, stability and drug loading techniques, bearing in mind that scale up, method simplicity and reproducibility were similarly linked to characterization parameters.

Polymeric material was scrutinized to select a polymer of which the inherent properties would be imparted to the spheres and the memblet system, such that a functional coating process would be negated. An in depth study of Eudragit® polymers was undertaken for both systems, taking into account the individual requirements of each respective system in that spheres and memblet*s* were to release drug at a higher pH of 6.8 and at a pH of 1.3 respectively.

3.2 Selection of Polymeric Material for the Individual Oral Delivery Systems

3.2.1 Rationale for the selection of polymers for the once daily multi-unit system

Polymer selection was vital to the success of the ODMUS as the polymeric material indicated for each system would influence drug release patterns, release location along the GIT and susceptibility of the system towards pH. Novelty was another key factor in polymer selection to allow for an innovative means of using the polymeric compound.

Polymethyl methacrylates (PMMA's), a subclass of the acrylates, have seen extensive use as bone cements in orthopaedic surgery (Mestiri *et al*., 1993) and shatter proof replacements for glass. The more conventional use includes surface coating agents for tablets, capsules and other dosage forms (El-Malah and Nazzal, 2008; Fini *et al*., 2008; Ma *et al*., 2008). With regards to pharmaceutical drug delivery systems, Eudragit® products, PMMA's, are traditionally utilized as coating agents. Much exploitation of these polymers has occurred over the years as polymethacrylates are excreted unchanged (pharmacologically inert), require small amounts for coating and are biologically compatible polymers (Degussa Eudragit®, AG Pharma Polymers, Darmatadt, Germany, 2007). Chemical stability and good compactability makes these products very relevant and effective choices for novel drug delivery research (Ceballos *et al*., 2005). Figure 3.1 depicts the molecular structure of Eudragit® and Table 3.1 categorizes the classes of Eudragit® based on the R functional group which ascertains the selective applications and highlights the diverse properties of these polymers. The extensive variety of Eudragit® polymers has been directly linked to the site-specific release of each polymer and a graphical depiction of individual pH dependant release at various points of the GIT, is provided in Figure 3.2.

The use of the Eudragit® PMMA products, whilst extensive, is very limited to spray drying from its aqueous dispersion (Rattes and Oliveira, 2007; Al-Zoubi *et al.,* 2008; Oosegi *et al.,* 2008) to form a surface coating and based on the grade chosen, elucidate an effect within the GIT or to provide taste masking in formulations which have undesirable tastes. Very few studies have been conducted to use any Eudragit® PMMA products as the primary polymers for formulating the dosage form and loading drug into the said delivery system, (Pignatello *et al.,* 2002; Fujimori *et al.,* 2005; Elgindy and Samy, 2009), and as such, very few attempts have been made to use any Eudragit® products in a novel way. Cui and co-workers (2007) demonstrated a different use of Eudragit® E 100 by using the taste masking polymer as a drug carrier and an emulsifying agent in the formulation of a novel redispersible dry emulsion. The study successfully produced a novel dry emulsion through incorporation of Eudragit® E 100.

It was deduced for the purposes of this study that Eudragit® polymers would constitute the core of both components of the ODMUS. Due to the extensive range of Eudragit® polymers, range is a further look into the various grades in addition to their function was warranted.

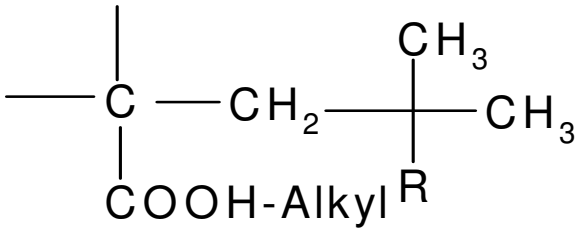


Figure 3.1 The molecular structure of Eudragit® *(adapted from the Degussa Eudragit® manual, AG Pharma Polymers, Darmatadt, Germany, 2007)*

Table 3.1 Grades of Eudragit® and their properties

Eudragit® Grade	Type of copolymer	Functional group (From Figure 3.1 R=)	Solubility	Applications
L 100	Methacrylic	COOH	Gastroresistant and enterosoluble	Resistance to gastric fluid, release in the colon
L 100-55	Methacrylic	COOH	Gastroresistant and enterosoluble	Resistance to gastric fluid, release in the colon
L 30D-55	Methacrylic	COOH	Gastroresistant and enterosoluble	Resistance to gastric fluid, release in the colon
E 100	Aminoalkyl Methacrylate	$COOH_2CH_2N(CH3)_2$	Gastrosoluble	Taste and odour masking, protection against moisture
E PO	Aminoalkyl Methacrylate	$COOH_2CH_2N(CH3)_2$	Gastrosoluble	Taste and odour masking, protection against moisture
NE 30D/NE 40D	Methacrylate	$COOCH_3$	Insoluble, permeable, pH-independent	Sustained drug release
RL PO/RS PO	Ammonioalkyl Methacrylate	$COOCH_2CH_2N^+(CH_3)3Cl^-$	Insoluble, permeable or dispersible, pH-independent	Sustained drug release
RL 30D/RS 30D	Ammonioalkyl Methacrylate	$COOCH_2CH_2N^+(CH_3)3Cl^-$	Insoluble, permeable or dispersible, pH-independent	Sustained drug release

Adapted from the Degussa Eudragit® manual, AG Pharma Polymers, Darmatadt, Germany, 2007

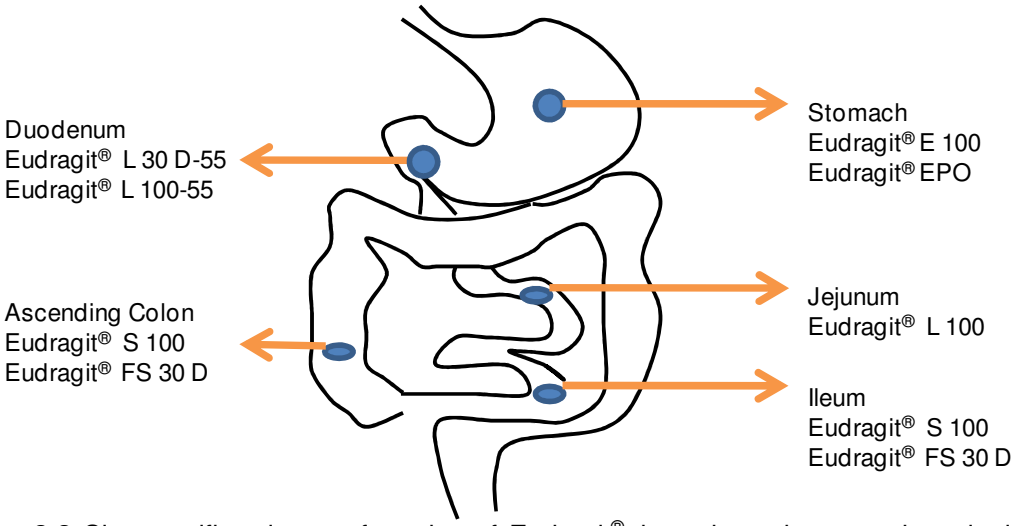


Figure 3.2 Site-specific release of grades of Eudragit® throughout the gastrointestinal tract *(adapted from the Degussa Eudragit® manual, AG Pharma Polymers, Darmatadt, Germany, 2007)*

3.2.2 Rational selection of polymers and materials for the multiparticulate portion of the once daily multi-unit system

Figure 2.10, illustrated in Chapter 2.5, graphically summarized the functional application of the ODMUS. The multiparticulate delivery system is intended for intestinal drug release whilst simultaneously negating the erosion-like effects of the acidic environment of the stomach. From Table 3.1, 3 polymers showed functional capability including Eudragit® L 100, Eudragit® L 100-55 and, Eudragit® 30D-55. Eudragit® L 100-55, an anionic copolymer of methacrylic acid and ethyl acrylate with a carboxylic acid functional group (Figure 3.3), was selected due to its gastroresistant and enterosoluble characteristics coupled with its solubility at a pH of 6.8 allowing for site-specific delivery of drug to the small intestine. This polymer has been traditionally used as an enteric coating agent initially formulated as a latex before being applied as a coating (Abbaspour *et al.*, 2008; Oosegi *et al.*, 2008). Additionally, Eudragit® L 100-55 contains surfactants sodium lauryl sulphate and polysorbate 80, which aid in prevention of aggregation or clumping of polymeric material. As the compound contains the above stated surfactants, the burden of physically adding the surfactants is bypassed in the formulation method.

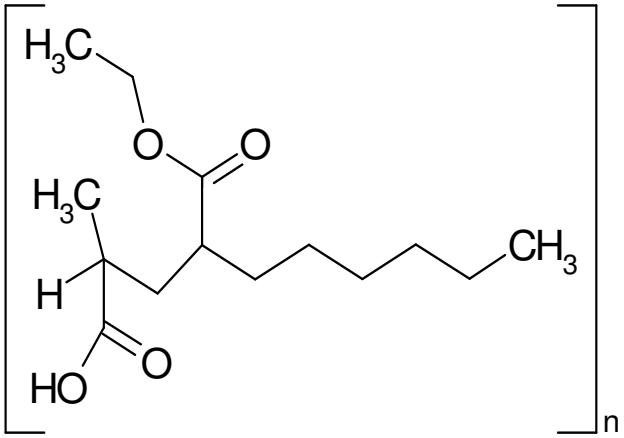


Figure 3.3 Molecular structure of Eudragit® L 100-55 *(adapted from the Degussa Eudragit® manual, AG Pharma Polymers, Darmatadt, Germany, 2007)*

Prolonged controlled release was a key factor during preliminary studies of the ODMUS. A gastroprotectant sphere was inadequate if the sphere exhibited a burst release once reaching the proximal portion of the small intestine. Ethyl cellulose has been widely used to achieve sustained drug delivery due to its hydrophobic properties (Chambin *et al.,* 2004; Desaia *et al*., 2006). Coating, tablet binding, incorporation into microspheres and microcapsules are some of the ways in which ethyl cellulose is used (Babar and Muhammad, 2002). Therefore, ethyl cellulose was a prime candidate based on these qualities as well as its non toxic and relatively stable properties (Crowley *et al*., 2004).

Pankaj and co-workers (2005) utilized ethyl cellulose as a coating agent for multiparticulates to achieve controlled release of chlorpheniramine maleate. For the purposes of the OMDUS, the avoidance of a spraying process was mandatory and an alternate means of incorporating ethyl cellulose into the ODMUS was used to achieve the same effect.

Crosslinking agent selection was highly dependent on achieving sustained and controlled release and consequently a range of cationic crosslinking agents were chosen from Table 3.2 to achieve the desired effects. Additionally, crosslinking time and concentration were factors to consider during method formulation. Potential crosslinking agents were identified based on the anionic copolymer Eudragit® L 100-55 molecule.

Table 3.2 Potential crosslinkers for the multiparticulate segment of the Once Daily Multi-Unit System

Monovalent ions	Divalent ions	Trivalent ions
Na^+	Zn^{2+}	Al^{3+}
K^+	Mg^{2+}	-
-	Ba^{2+}	-
-	Ca^{2+}	-

3.2.3 Rational selection of polymers and materials for a polyethylene glycol crosslinked novel tablet like polymeric oral membranous system

Eudragit® E 100 is a methacrylic copolymer (-Butylmethacrylat-(2-Dimethylamioethyl) methacrylat-Methylethacrylate) with the monomer ratio of 1:2:1 respectively. This is a water-soluble polymer consisting of hydrophilic groups, fitting hydrophobic groups and a low viscosity as shown in Figure 3.4. Said cationic polymers exhibit solubility from a pH of 1.2-5 making the polymer suitably soluble in gastric acid (pH 1.2) (Kohri *et al*., 1989), a preferred selection in relation to chitosan when trying to elucidate gastric release of drug. Table 3.1 in Chapter 3.2.1 identifies Eudragit® E 100 as a gastro-soluble polymer conventionally used for taste masking. Very few studies have been undertaken to utilise Eudragit® E 100 beyond its conventional use as a coating and taste masking agent (Moustafine *et al*., 2005; Quinteros *et al*., 2008).

Goddeeris *et al*. (2008) utilized Eudragit®'s gastro-protectant capability by using Eudragit® E 100 and a surfactant to develop a novel ternary solid dispersion to deliver the poorly soluble UC-781 (an anti-HIV drug) to enhance its dissolution.

Eudragit® E 100 also shows the potential for use in sustained drug delivery, due to it being minimally impacted by changes in environmental pH (Kabanova *et al*., 2006). Specifically, the Eudragit® E 100 polymer requires half an hour to completely dissolve in an acidic environment making the polymer ideal for gastric drug delivery as gastric transit time can vary between 3 and 4 hours. The disadvantage of incorporating this polymer for drug delivery is that total release will occur within 30 minutes and this is not a guaranteed controlled release mechanism.

The cationic properties of Eudragit®, due to its tertiary amine group have been useful in the stabilization of other polymers both natural and synthetic. This property has influenced its use as an excipient in pharmaceutical products and in drug-in-adhesive transdermal systems where it also serves the purpose of prevention of crystallization of the active drug (Ausar *et al*., 2003).

Polyethylene glycol (PEG) has been used as early as the mid 90's as a means of covalent attachment to various compounds (Zalipsky, 1995). Use of PEG has even been expressed in terms of demulcents or soothing agents, used as laxatives and as food additives (Karlsson *et al., 2005)*.

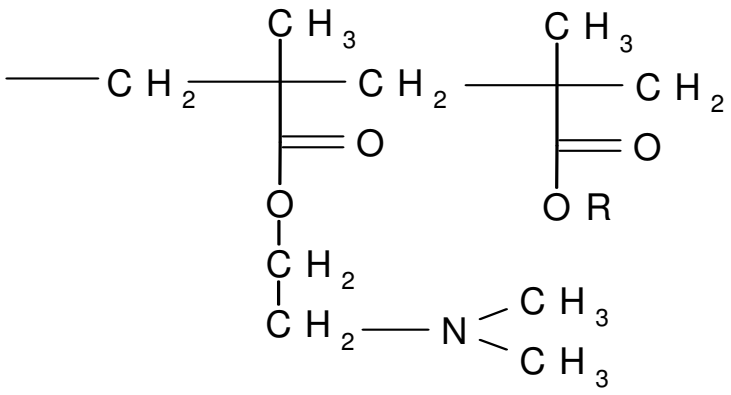


Figure 3.4 Eudragit® E 100 molecular structure where R= $CH_3C_4H_9$ *(adapted from Moustafine et al., 2005)*

With regards to manipulating PEG into an oral dosage form, this amphiphilic polymer exhibits ideal characteristics such as low toxicity and good solubility in water (Zalipsky, 1995; Sun and Chu, 2006) and has even been used to improve biocompatibility and in other formulations (Chung *et al*., 2003). Incorporation of PEG into the memblet system was based on the extensive work PEG has been used for (Hossainy and Hubbell, 1994; West and Hubbell, 1995; Park *et al.,* 2004; Sun and Chu, 2006). As an anionic crosslinker, it was postulated that PEG would retard drug release from the polymeric memblet while incorporating the benefits stated above. Additionally PEG has plasticizing effects which can drastically affect thermal properties (Feldstein *et al.,* 2000; Cao *et al*., 2009).

3.2.4 Method development of novel multiparticulates and a novel memblet drug delivery system

Eudragit® polymeric materials have a primary function as coating agents and are developed with advantages such as an improved chemical stability, better compliance and enhanced therapeutic efficacy (the Degussa Eudragit® manual, AG Pharma Polymers, Darmatadt, Germany, 2007). The application benefits of the polymethacrylates make them ideal polymeric materials to be incorporated into the ODMUS. Application benefits of Eudragit® coatings include:

- pH-dependent drug release
- protection of actives against the acidic gastric environment
- protection of gastric mucosa from aggressive actives
- improvement on drug effectiveness
- acceptable storage stability
- controlled release of active

As explained in Figure 3.2 of Chapter 3.2.1, Eudragit® polymers have been extensively used as coating agents in pH dependant or site-specific drug delivery, but the coating process is an additional formulation step. The ODMUS shall aim to bypass all coating procedures and utilize the Eudragit® polymers by incorporating the polymer into the matrix of the multiparticulate and ultimately simplifying formulation procedures.

Figure 3.5 depicts cross-sectioned multiparticulates in which Figure 3.5a represents a novel ODMUS multiparticulate incorporating Eudragit® L 100-55 within the internal matrix and the outer layer in a single process step, whilst Figure 3.5b represents a multiparticulate comprised of another polymeric material comprising the core of the sphere and coated with Eudragit®.

Additionally, Eudragit® E 100 was formulated into a novel tablet like system diverting from its role as a traditional coating agent. Formation of a Eudragit® E 100 based hydrogel with subsequent membrane formation led to the preliminary memblet formation. Degussa products follow set guidelines for re-dispersion and the procedures for Eudragit® L 100-55 and Eudragit® E 100 are displayed in Table 3.3.

Table 3.3 Redispersion procedures for Eudragit® L 100-55 and Eudragit® E 100

Eudragit® Grade	Constituents
Eudragit® L 100-55	NaOH 10%, Water-60%, Solid Content- 30%
Eudragit® E 100	Acetone/Isopropyl alcohol- 85%, Water 5% Solid content-10%

Adapted from the Degussa Eudragit® manual, AG Pharma Polymers, Darmatadt, Germany, 2007

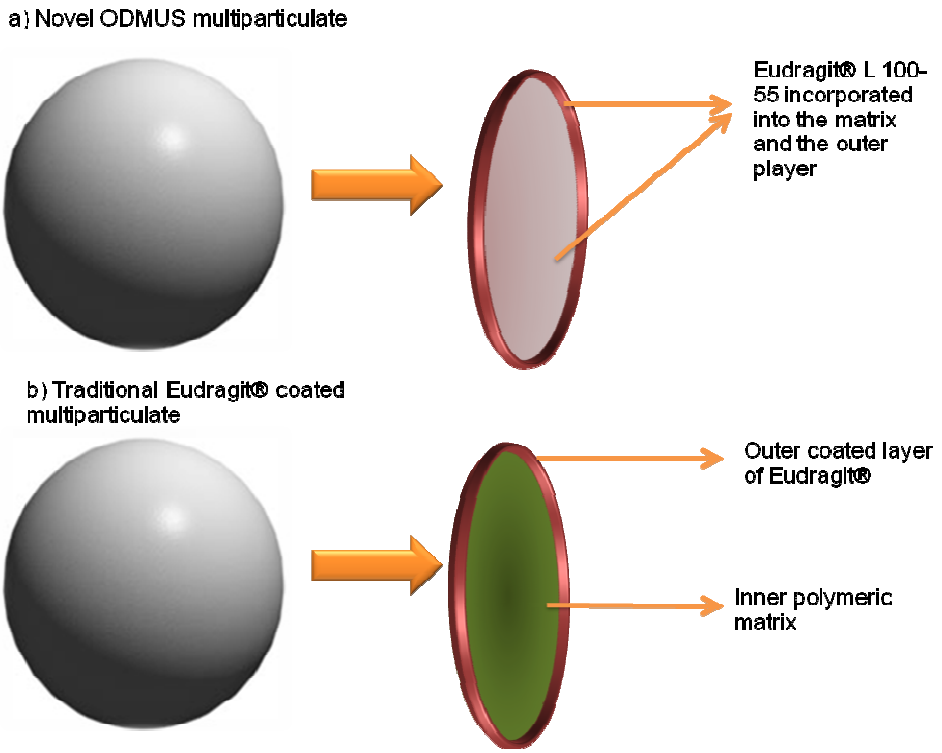


Figure 3.5 Comparison between a novel Once Daily Multi-Unit System multiparticulate and a traditionally coated multiparticulate via cross-sectional examination

3.2.5 Ionotropic gelation and polyelectrolyte complexation

Ionotropic gelation, due to method authenticity and efficacious drug delivery in the past, provides success as a delivery system (Sadeghi *et al.,* 2008; Sriamornsak *et al.*, 2008; Ma and Liu, 2010). Specifically, ionotropic gelation is described as the ability of poly-electrolytes to ionically crosslink (non-covalently) with counter ions to form a hydrogel complex in a spontaneous manner (Patil *et al.*, 2010). Poly-electrolytes are defined as polymers with ionizable groups. In the case of the Eudragit® polymers utilized in this study, each polymeric structure has natural anionic/cationic moieties and can subsequently form intermolecular meshworks amongst their respective counter ions/polymers. Poly-electrolyte complexes with closely related ion to cation ratios are insoluble in water (Holappa, 2005). As the ionic bond is based on electrostatic attractions, the ionic strength of the crosslinking solution plays an integral role in the formation of the poly-electrolyte complex. When crosslinking occurs in an aqueous environment, the crosslinkers present potentiate ionic remodeling of bonds shifting equilibrium to thermodynamic stability such that the degree of complexation is controlled by the ratio of polymer to crosslinker (Zintchenko *et al.,* 2003). The ratio is critical to solubility resulting in either a readily soluble or an insoluble complex essential for controlled drug release.

In the case of Eudragit® L 100-55, functional moieties are anionic and dropping the latex into a cationic solution results in ionic attraction. Cationic poly-electrolytes diffuse into the latex droplet and form a 3-dimensional lattice of ionically crosslinked groups. Attraction between cationic metals and the anionic polymer are based on the concentration of metal ions at the polymeric surface functional groups. Specifically, complexation occurs between polyvalent metal ions and the halogenide salt (Holappa, 2005). Attraction follows 2 distinct pathways namely, territorially and directly to functional groups. Territorially refers to ions that are thermodynamically bound but move via electrostatic attraction within the poly-electrolyte domain (Radeva , 2001). Direct binding of ions to the functional group are referred to as sight bound and can be described as ion pairs, multidentate complexes and chelate complexes (Radeva, 2001). However, the multiparticulate system utilizes a combination of polyvalent cations to achieve double crosslinking and retard release and this Chapter aimed to limit the combinations that could be used with the goal of optimizing to a rudimentary pair of metal ions.

Eudragit® E 100 readily produces a polyelectrolyte membrane when expelled into a crosslinking solution under constant agitation. As such, 2 types of polyelectrolyte membranes can be produced, namely ones that contains a polyelectrolyte and a low molecular weight ion with an opposite charge or membranes that contain 2 polyelectrolyte polymers that have opposite charges with the latter referred to as the more stable of the 2 methodologies (Zhu, 2006). The memblet system adopted the more stable double poly-electrolyte complex system. A recent study by de Vasconcelos *et al.* (2006) illustrated the concept of polyelectrolyte complexation, between a polymethacrylic acid (anionic functional groups) and chitosan (cationic functional groups) through a drop wise expulsion of the methacrylate latex into a 2%$^{w}/_{v}$ chitosan solution in a similar formulation procedure to the ODMUS memblet. Figure 3.6 highlights the ionic attraction between the 2 polymeric constituents.

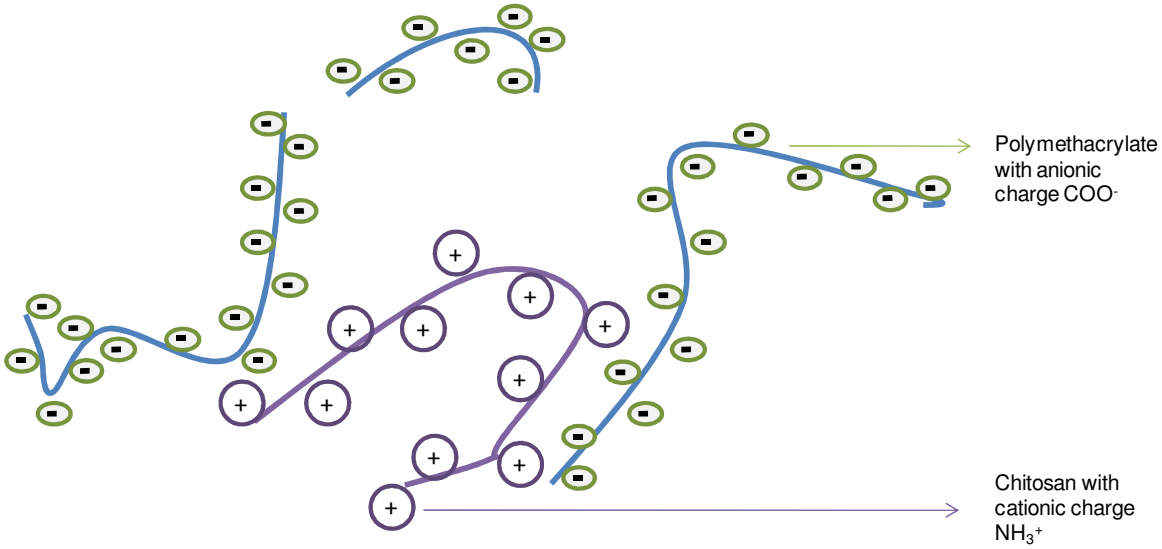


Figure 3.6 Formation of a polyelectrolyte complex through electrostatic attraction between 2 polymeric macromers *(adapted from de Vasconcelos et al., 2006)*

3.3 Materials and Methods

3.3.1 Materials

Eudragit® L100-55 was donated by Degussa AG, Pharma polymers, RÖhm GmbH (Germany). Triethyl Citrate (TEC), isoniazid (INH) and ethylcellulose (EC) were of analytical grade and purchased from Sigma Aldrich (Pty) Ltd. (St Louis, MO, USA). All electrolytes identified in Table 3.2 of Chapter 3.2.2 for crosslinking were of analytical grade and purchased from Merck Chemicals (Halfway House, Gauteng, South Africa). Sodium Hydroxide pellets were purchased from Rochelle Chemicals (Johannesburg, South Africa). Silicone was obtained from Merck Chemicals (Halfway House, Gauteng, South Africa). All chemicals and raw materials were used as received without further processing. Water was purified by a MilliQ Millipore water purification system (Milli-Q, Millipore, Billerica, MA, USA).

Eudragit® E 100 was kindly supplied by Evonik Degussa Africa (Pty) Ltd. (Midrand, Gauteng, South Africa) and polyethylene glycol 4000 (PEG 4000) was purchased from Merck chemicals (Halfway House, Gauteng, South Africa). Acetone, triethyl citrate (TEC), isopropyl alcohol, sodium lauryl sulphate (SLS) and tween 80 were all of analytical grade. Water was purified by a MilliQ Millipore water purification system (Milli-Q, Millipore, Billerica, MA, USA). Rifampicin (RIF) was of analytical grade and donated by Sigma Aldrich.Inc (South Africa).

3.3.2 Multiparticulate method development: preparation of a 50mL Eudragit® L 100-55 latex

An aqueous solution of 30%$^{w}/_{v}$ Eudragit® L 100-55 was prepared. The PMMA polymer was added gradually to the aqueous phase (deionized) under constant agitation using a magnetic

stirrer over a period of 5 minutes to avoid agglomeration and sedimentation. To prevent foaming, 0.4mL of silicone was added to the latex and the solution was left to stir for 45 minutes referred to as 45_{t1} in Figure 3.7 During 45_{t1}, 2 solutions of 4%$^{w}/_{v}$ NaOH and 20%$^{w}/_{v}$ Ethylcellulose (EC) were dissolved. EC was added gradually to 50mL of Ethanol till complete dissolution was achieved. At 45_{t1}'s conclusion, 5mL of the NaOH solution was drawn up with a 20mL syringe and added to the latex within 5 minutes in a drop wise manner for neutralization of the carboxyl functional groups of the PMMA.

The latex was left to stir for a further 45 minutes, referred to as 45_{t2}, to ensure proper dispersion and neutralization of the latex. Following 45_{t2}, 3g of INH and 5mL of TEC was introduced to the latex and left for a final 45 minutes under constant agitation, 45_{t3}.

Ethyl Cellulose was incorporated into the latex in preliminary designs in an attempt to improve drug release in the small intestine from between 10-12 hours. A 5%$^{w}/_{v}$ solution of EC solution was drawn up using a 20mL syringe and gradually added to the latex during 45_{t3} prior to homogenization (Polytron Kinematica, Switzerland) for a full 15 minutes. As homogenization generated substantial heat, the latex was then left on the stirrer to cool for 10 minutes prior to crosslinking. Potential crosslinking agents detailed in Table 3.2 of Chapter 3.2.2 were then selected for crosslinking.

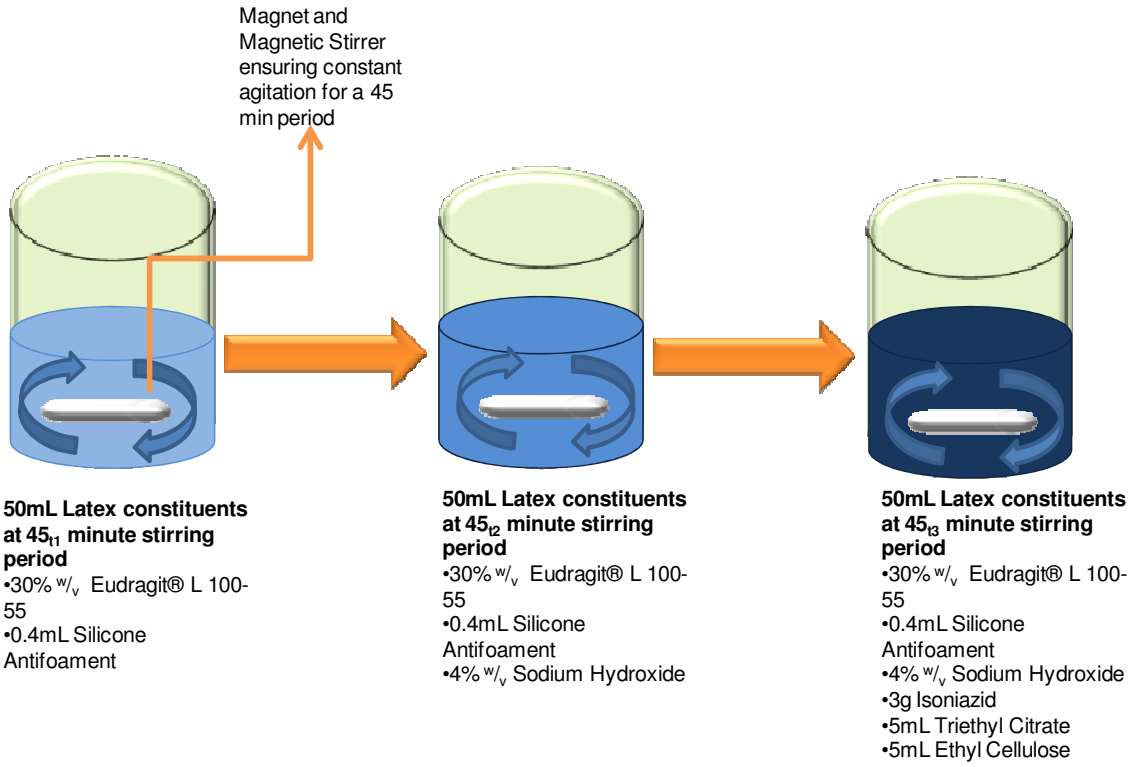


Figure 3.7 Eudragit® L 100-55 latex (50mL) preparation

3.3.3 Multiparticulate method development: polymethyl methacrylate multiparticulate formation through an ionotropic gelation double crosslinking procedure

Batches of multiparticulates were formulated and crosslinked initially in electrolyte combinations as shown in Table 3.4.The crosslinking solution was kept on a magnetic stirrer for the duration of crosslinking to keep the formed polyspheres in constant motion to prevent unwanted agglomeration. In batches 3-5, first and second electrolyte solutions were saturated with 3g of INH in an attempt to improve on drug entrapment efficiency. A measured 10mL of the 50mL PMMA latex was drawn up with a syringe and the latex was expelled in a drop wise manner into the first electrolyte solution for crosslinking. The above process is graphically depicted in Figure 3.8. After complete expulsion of the latex, the multiparticulates were left to cure for 20 minutes in a dark cupboard. The polyspheres were washed twice in 500mL double deionized water and placed in a second crosslinking solution and left to cure in a dark cupboard for a further 20 minutes. The double cured and drug saturated multiparticulates were then washed with 500mL deionized water and left to air dry under an extractor for 12 hours at room temperature. Batches of spheres were then weighed and placed in glass containers until testing.

Table 3.4 Parameters used for the formulation of preliminary multiparticulates

Batch Number	Combinations of Crosslinking Agents	Duration of curing in both solutions (minutes)	Contained Ethyl Cellulose	Saturated with INH
1	$MgSO_4$[a] (15%$^w/_v$) + $ZnSO_4$[b](25%$^w/_v$)	20	No	No
2	$CaCl_2$ [a](25%$^w/_v$) + $AlCl_3$[b](25%$^w/_v$)	40	No	No
3	$MgCl_2$[a](30%$^w/_v$) + $AlCl_3$[b](25%$^w/_v$)	20	Yes	Yes
4	$BaCl_2$ [a](15%$^w/_v$) + $AlCl_3$[b](25%$^w/_v$)	20	Yes	Yes
5	$BaCl_2$ [a](25%$^w/_v$) + $AlCl_3$[b](25%$^w/_v$)	20	Yes	Yes
6	$K_2S_2O_8$ [a](25%$^w/_v$) + $AlCl_3$(25%$^w/_v$)[b]	20	No	No
7	NaCl [a](25%$^w/_v$) + $AlCl_3$[b](25%$^w/_v$)	20	No	No

[a] and [b] represent the first and second crosslinking solutions respectively

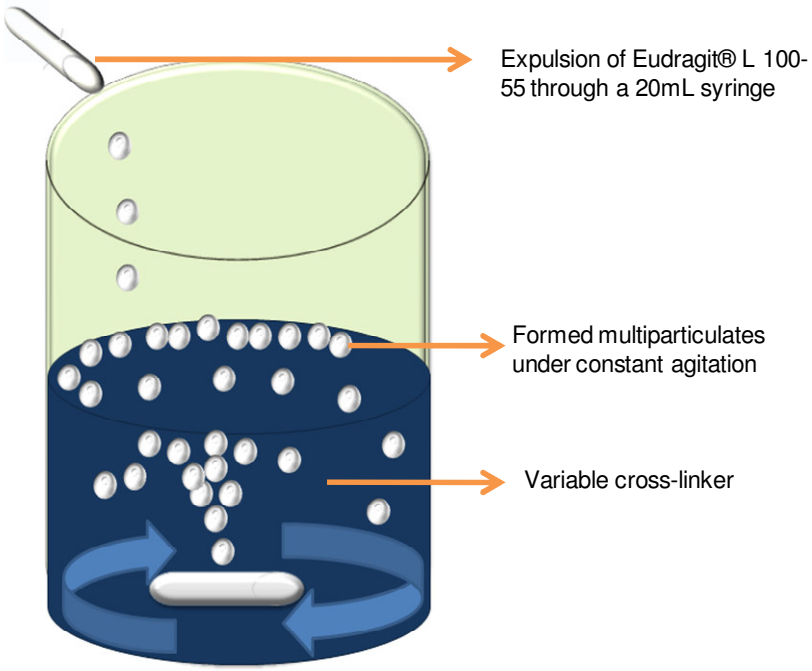


Figure 3.8 The formation of multiparticulates through the crosslinking of the Eudragit® L 100-55 latex within a variable cationic solution

3.3.4 Memblet method development: formulation of a Eudragit® E 100 latex

Method development required the manipulation of a standard Eudragit® E 100 re-dispersion procedure in a similar manner to the multiparticulate method as indicated in Table 3.3 of Chapter 3.3.1. Amounts of 34%$^{v}/_{v}$ of acetone, 46.9%$^{v}/_{v}$ of isopropyl alcohol and 1.8%$^{v}/_{v}$ of de-ionized water were measured and added to a 200mL beaker. A measured 13.6%$^{w}/_{v}$ of the Eudragit® E 100 polymer was gradually added to the aforementioned latex with constant agitation employing a magnetic stirrer at room temperature (21°C) for 1 hour.

This preliminary latex was left under agitation until complete dissolution of the Eudragit® E 100 beads. TEC and the remaining constituents (Tween 80 and SLS) were gradually added to the latex and left to stir for approximately an hour. Simultaneously, 30%$^{w}/_{v}$ and 60%$^{w}/_{v}$ PEG 4000 solutions were produced. A measured 5mL of the Eudragit® E 100 latex was drawn up and expelled through a syringe into each solution. Crosslinking resulted in hydrogels A (60%$^{w}/_{v}$ PEG 4000) and B (30%$^{w}/_{v}$ PEG 4000), which were subsequently left to cure in their respective solutions for twenty minutes. Following the curing, samples were washed 3 times in 500mL de-ionized water before storage in a desiccant jar (using silica crystals) for 10 days of drying time. The dried membranes were then ground using a standard coffee grinder and the powder obtained was mixed with 150mg of RIF and subsequently compressed into a tablet like structure or memblet (memblets A and B).

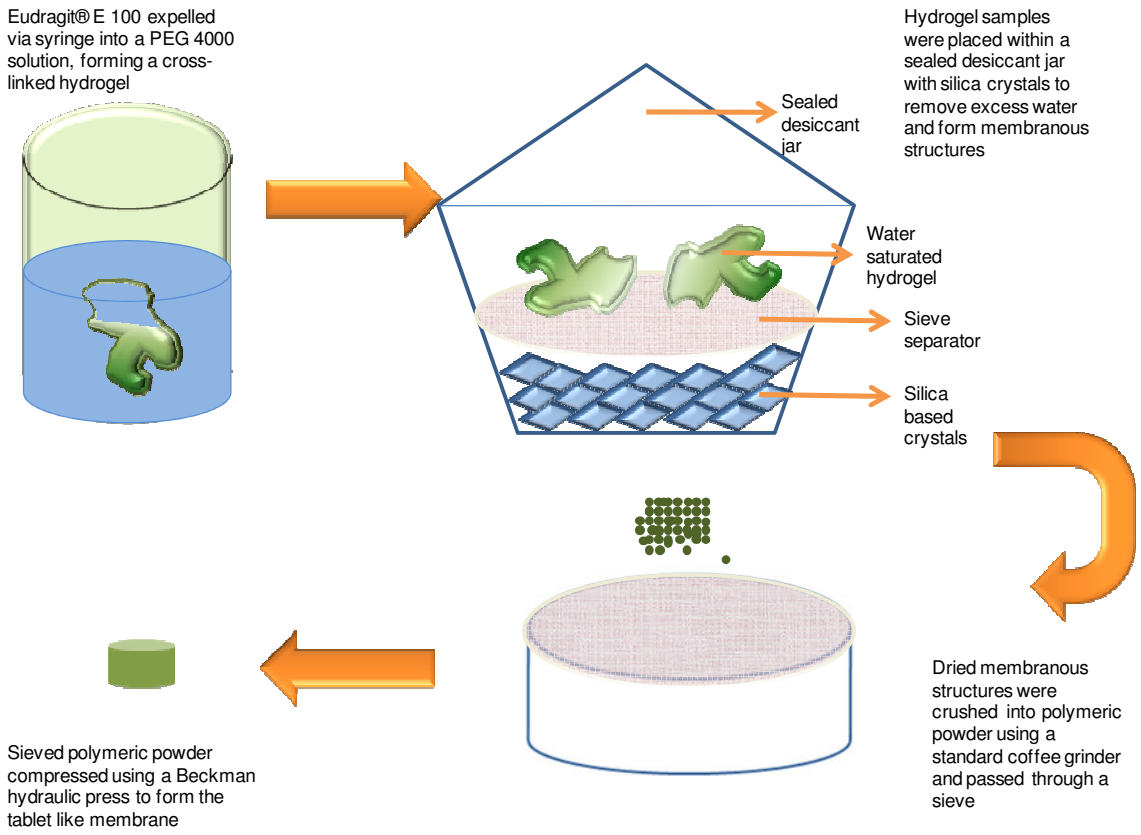


Figure 3.9 Formulation procedures implemented in the formulation of the memblet system

3.4 Testing Procedures for the Once Daily Multi-Unit System

3.4.1 Construction of a calibration curves for spectrophotometric quantification of drug entrapment efficiency and *in vitro* analysis

A calibration curve for INH was plotted using a known series of dilutions of INH (using an initial 0.1mg/mL) dissolved in the same medium to be used for entrapment efficiency testing and *in vitro* analysis (phosphate buffer solution pH 6.8). A linear curve was plotted to determine the R^2 value using Sigma Plot Version 10.0 Systat Software, Inc, GmBH, Germany.

3.4.2 Drug entrapment efficiency evaluation of double crosslinked drug saturated polymethacrylate multiparticulates and an overview of superficial morphological structure

Solutions of 200mL phosphate buffer solution (PBS), pH 6.8, were prepared and used for drug entrapment efficiencies. Polyspheres of weight 100mg, from respective batches, were weighed out in triplicate (N= 3) and placed within 200mL of PBS and left to achieve complete dissolution overnight with aided agitation from a stirrer at room temperature. UV analysis

through a spectrophotometer (Cecil CE 3021, Cambridge, CB24 6AZ, England) was conducted and drug entrapment was evaluated through the following equation:

$$DEE \quad \% = \frac{D_a}{D_t} \times \frac{100}{1} \qquad \textit{(Equation 3.1)}$$

Where, DEE % represents drug entrapment efficiency, Da represents the actual amount of drug within the multiparticulates and Dt represents the theoretical amount of drug within the multiparticulates.

Surface morphology, in the case of oral delivery systems, is required to be of an aesthetic quality for compliance purposes. Additionally, the surface characteristics of batches would give an educated guess as to the release patterns based on solid structure, the presence of highly porous areas, colour and genuine spherical shape.

3.4.3 Preliminary *in vitro* drug release of double crosslinked drug saturated polymethacrylate multiparticulates

Drug release studies were conducted following the USP 33 apparatus II (ERWEKA DT 700 GmbH Germany), in which 100mg of spheres were weighed out in triplicate from each batch and placed within the vessel under a stainless steel ring mesh assembly, to prevent the paddle inflicting physical/mechanical damage to the spheres and alter release profiles as well as to prevent erratic fluctuation due to unstable hydrodynamics (Pillay and Fassihi, 2000).

Each vessel was filled with 900mL PBS and heated to a temperature of 37℃ prior to the addition of the multiparticulates and the stainless steel ring mesh assembly. The rotating paddle method was selected at a rotational speed of 50rpm and the machine was calibrated for a 12 hour run with samples taken at hourly intervals. Sampling involved the drawing of 5mL of now drug incorporated solution from the dissolution vessel with subsequent refilling of removed buffer to maintain sink conditions. Samples were then subject to UV spectroscopy using a spectrophotometer (Cecil CE 3021, Cambridge, CB24 6AZ, England).

3.4.4 Preliminary *in vitro* drug release of polyethylene glycol crosslinked polymethacrylate based memblet system

Drug release studies were conducted following the USP 33 apparatus II (ERWEKA DT 700 GmbH Germany), in which a single memblet in triplicate was placed within the vessel under a stainless steel ring mesh assembly, to prevent the paddle inflicting physical/mechanical damage to the spheres and alter release profiles as well as to prevent erratic fluctuation due to unstable hydrodynamics (Pillay and Fassihi, 2000). Each vessel was filled with 900mL simulated gastric fluid (SGF) and heated to a temperature of 37℃ prior to the addition of the

memblet and the stainless steel ring mesh assembly. The rotating paddle method was selected at a rotational speed of 50rpm and the machine was calibrated for a 2 hour run with samples taken at half hourly intervals. Sampling involved the drawing of 5mL of now drug incorporated solution from the dissolution vessel with subsequent refilling of removed buffer to maintain sink conditions. Samples were then subject to UV spectroscopy using a spectrophotometer (Cecil CE 3021, Cambridge, CB24 6AZ, England).

3.4.5 Thermal analytical method development and subsequent thermal profiling of polyethylene glycol crosslinked polymethacrylate based memblet systems

Thermal analysis was conducted on a *DSC1* STAR^e system (Mettler Toledo DSC1 STAR^e System, Switzerland). Testing of memblet*s* required method development of both differential scanning calorimetry (DSC) and alternating differential scanning calorimetry (ADSC) prior to analysis. All samples were prepared in 40µl aluminum crucibles. DSC was conducted using a temperature range of 0-200 ℃ and ramped at 10℃ per minute. ADSC was carried out with an underlying heating rate of 1℃ per minute and a modulated temperature of 0.1℃ per 0.8 minutes. All samples were run in duplicate to remove thermal history.

3.5 Results and Discussion: Analysis of Preliminary Testing

3.5.1 Calibration curves for isoniazid and rifampicin to evaluate drug entrapment efficiency and *in vitro* drug release profiling

Calibration curves for INH and RIF were plotted to determine DEE and *in vitro* results and can be seen in the following Figure:

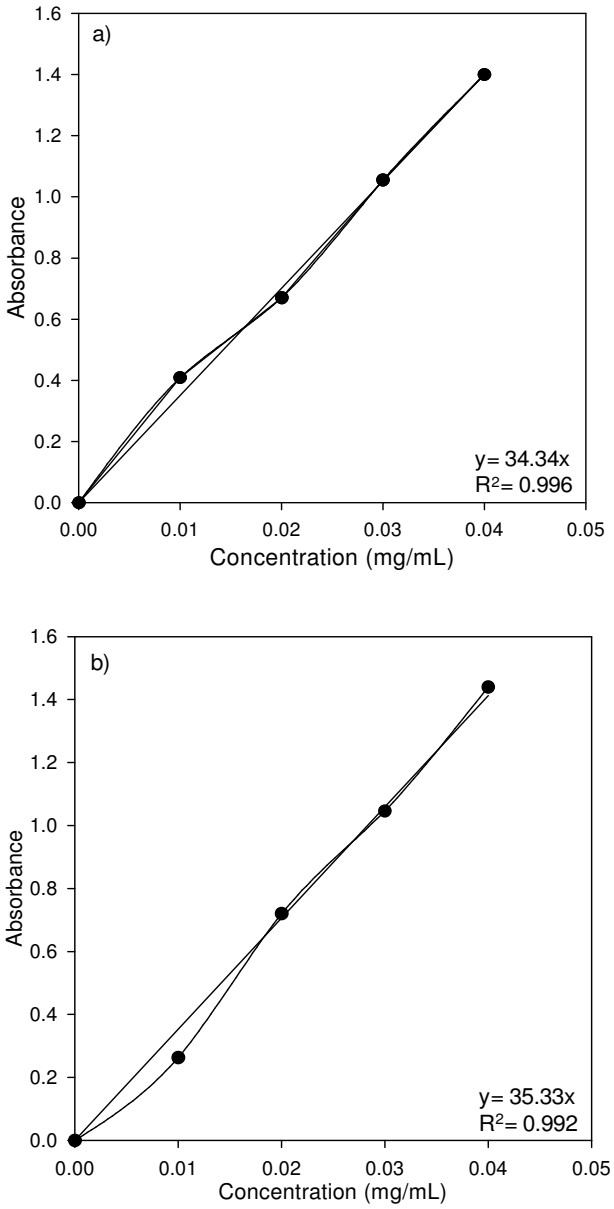


Figure 3.10 Calibration curves for a) isoniazid and b) rifampicin with corresponding regression co-efficient and y values

3.5.2 Drug entrapment efficiency of double crosslinked drug saturated polymethacrylate multiparticulates and superficial morphological structure scrutiny

Early assessment of samples revealed uniformly low entrapment efficiencies with the exception of batch 3 and batch 5, identified in Table 3.5. Poor drug loading within multiparticulates was attributed to compounding factors. Primarily, the presence of 2 cationic molecules competing for positioning along the PMMA polymeric backbone prevented INH from having a higher loading tendency. Furthermore, the double curing procedure within 2 separate solutions at 20 minute intervals provided an abundant crosslinker saturation resulting in a reduced distribution of INH within the multiparticulates. In the case of batch 2, a 40 minute curing time in each solution vastly depleted drug loading, identifying a maximum

20 minute curing period. The aqueous medium of the above mentioned crosslinkers provided a diffusion gradient for already entrapped drug to leech into, a common problem encountered during crosslinking (Pongjanyakul and Rongthong, 2010). As INH is readily soluble in water, drug passively diffused through the concentration gradient from the internal matrix into the crosslinking solution.

A contrary DEE was in evidence for batch 3 and 5 of preliminary results. Almost double the entrapment was achieved for 50% and 61% respectively, validating the proposal of saturating INH within crosslinking solutions. It was postulated that a drug saturated aqueous environment created a reverse concentration gradient and effectively minimized the leeching process. What is important to note is that a higher entrapment occurs whilst in the presence of an additional polymeric component (ethyl cellulose). The addition EC to modulate release profiles would always be contradictory to DEE values, but on the contrary, the incorporation of this additional component demonstrated a 61% DEE. These preliminary studies corroborated 2 method parameters to improve DEE including a maximum 20 minute duration of curing and the saturation of crosslinking solutions with INH. Of particular interest were the influence of Mg^{2+} and Ba^{2+} ions with higher concentrations (between 25%$^{w}/_{v}$ and 30%$^{w}/_{v}$) and the inclusion of EC. A synergistic effect between the 2 parameters, rather than the expected antagonistic inadequate DEE results, displayed an improved DEE and controlled release indicated with the release studies in Chapter 3.5.3 Figure 3.12.

Table 3.5 Preliminary formulation parameters with subsequent drug entrapment efficiencies

Batch Number	Combinations of Crosslinking Agents	Duration of curing in both solutions (minutes)	Contained EC	Saturated with INH	DEE (%)
1	$MgSO_4$ [a] (15%$^{w}/_{v}$) + $ZnSO_4$ [b](25%$^{w}/_{v}$)	20	No	No	32
2	$CaCl_2$ [a](25%$^{w}/_{v}$) + $AlCl_3$ [b](25%$^{w}/_{v}$)	40	No	No	10
3	$MgCl_2$[a](30%$^{w}/_{v}$) + $AlCl_3$ [b](25%$^{w}/_{v}$)	20	Yes	Yes	50
4	$BaCl_2$ [a](15%$^{w}/_{v}$) + $AlCl_3$ [b](25%$^{w}/_{v}$)	20	Yes	Yes	42
5	$BaCl_2$ [a](25%$^{w}/_{v}$) + $AlCl_3$ [b](25%$^{w}/_{v}$)	20	Yes	Yes	61
6	$K_2S_2O_8$ [a](25%$^{w}/_{v}$) + $AlCl_3$(25%$^{w}/_{v}$) [b]	20	No	No	33
7	NaCl [a](25%$^{w}/_{v}$) + $AlCl_3$ [b](25%$^{w}/_{v}$)	20	No	No	35

[a] and [b] represent the first and second crosslinking solutions respectively

Through general observation, and without the initial use of powerful tools such as scanning electron microscopy for this part of the study, an array of data and theoretical concepts were derived. Batches 6 and 7 were aesthetically, the worst formed spheres. Both displayed compromised physical integrity and were brittle to the touch which could be postulated to reveal a poor drug release profile. Physical stability of these formulations was undesirable. The yellow discoloration of batch 7 was attributed to a residual deposit of INH agglomerating superficially, a potential indicator of poor entrapment which was verified through entrapment results of 33% shown in Table 3.5. $K_2S_2O_8$ was determined to be an unsuccessful crosslinker due to its formation of irregularly shaped particulates and brittle nature. The highly porous nature viewed in Figure 3.11 for batch 6, eluded to a mostly hollow internal structure as the crosslinking process between Na^+ and Al^{3+} was not sufficient to form a solid spheroid multiparticulate.

The physical content of these spheres were at a minimum to the extent that some spheres were completely hollow for both batches 6 and 7. Coupled with the brittle quality, it was considered realistic to assume these spheres would provide as poor a release pattern as the DEE (33% and 35% for batches 6 and 7 respectively as indicated in Table 3.5).

The aesthetic success of batch 5 in relation to DEE (61%) and release profiles cannot be overlooked. Spheres displayed unique characteristics such as a smooth spherical shape, a sturdy texture and a glossy white exterior. This glossy even exterior was obtained without the additional process step of active coating which is seen as a beneficial and sought after characteristic of this batch of spheres. The presence of the Eudragit® L 100-55 is not limited to the exterior however (illustrated in Figure 3.5 of Chapter 3.2.4) and it is this specific characteristic that makes this system unique.

Saturation of crosslinking solutions with INH drastically increased DEE % to 50%, 42% and 61% in batches 3, 4 and 5 respectively through the reversal of the INH concentration gradient, despite the inclusion of EC and 2 crosslinking solutions. Similarly to batch 5, batches 3 and 4 yielded spheres of solid texture, colour and multiparticulate integrity.

In an attempt to improve release profiles, multiparticulate curing time was extended for a 40 minute duration in batch 2. The spheres produced were aesthetic relative to the qualities desired, but were stained a yellow colour. The extended curing period promoted drug surface agglomeration rather than matrix incorporation and a drastically reduced DEE (10%), which was further propagated by the absence of INH in the crosslinking solutions. Preliminary studies concluded that 20 minutes was an optimal crosslinking time to achieve maximal ionic interaction and drug loading.

To reduce formulation variables during optimization, the secondary crosslinker was identified during preliminary studies as $AlCl_3$. Batch 1 relative to other formulations, did not achieve the physical and aesthetic success of the other batches which used $AlCl_3$.

Table 3.6 Initial observational data of cured spheres

Batch Number	Physical Texture	Visual Porosity	Spherical Shape	Coloration
1 $MgSO_4$[a](15%$^w/_v$) +$ZnSO_4$[b](25%$^w/_v$)	Weakly formed with an uneven texture	None	Irregularly shaped	White
2 $CaCl_2$[a](25%$^w/_v$) +$AlCl_3$[b](25%$^w/_v$)	Sturdy with a smooth texture	None	Roughly spherical	Yellowish tinge
3 $MgCl_2$[a](30%$^w/_v$) + $AlCl_3$[b](25%$^w/_v$)	Sturdy and large with a smooth texture	None	Roughly spherical	Glossy white colour
4 $BaCl_2$[a](15%$^w/_v$) + $AlCl_3$[b](25%$^w/_v$)	Sturdy and large with a smooth texture	None	Roughly spherical	Glossy white colour
5 $BaCl_2$[a](25%$^w/_v$) + $AlCl_3$[b](25%$^w/_v$)	Sturdy and large with a smooth texture	None	Roughly spherical	Glossy white colour
6 $K_2S_2O_8$[a](25%$^w/_v$) + $AlCl_3$(25%$^w/_v$)[b]	Weakly formed with an uneven texture	Large pores evident	Tailed hollow spheres	White
7 NaCl[a](25%$^w/_v$) + $AlCl_3$[b](25%$^w/_v$)	Weakly formed with an uneven texture	Large pores evident	Irregularly drop shaped	Yellowish tinge

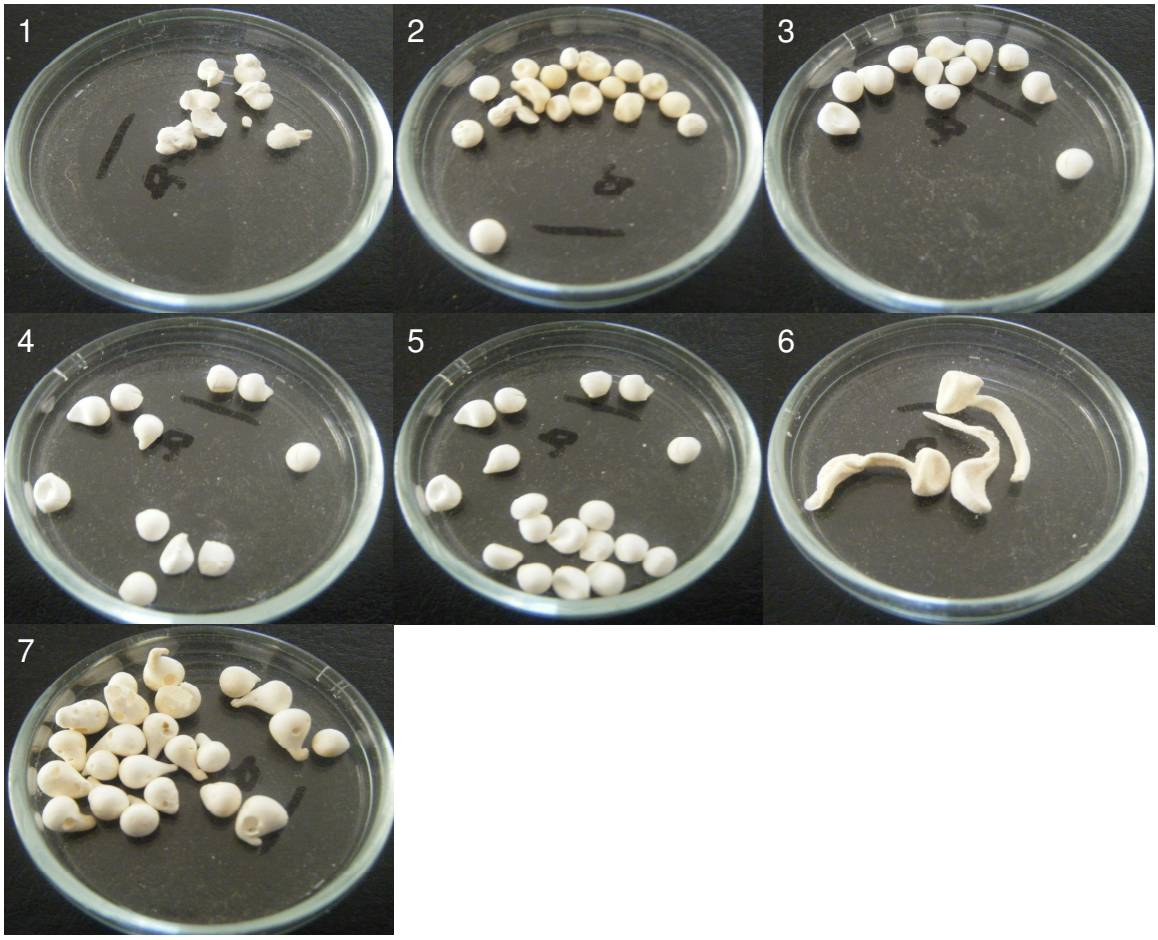


Figure 3.11 Photographic depiction of inter-sample variance due to formulation parameters for formulations 1-7

3.5.3 *In vitro* drug release patterns of multiparticulates with varying crosslinking agents

As per the objectives stated in Chapter 1.3, the release profiles for the multiparticulates were explored through dissolution testing. Contrasting release profiles were attributed to the variant formulation parameters and constituents of the latex. The general pattern emerging was an initial burst release seen in Figure 3.12 for batches 1, 6 and 7. More than 80% of INH was released within an hour of testing. This was expected in the case of batches 6 and 7 with poorly formed spheres. Similarly, a burst effect was seen for the release profile of batch 1, even though relatively aesthetic spheres were formed. Batch 4, though saturated with INH, displayed a higher burst release compounded with erratic release thereafter due to the minimized concentration of the secondary crosslinker (Ba^{2+} 15%$^{w}/_{v}$).

Relative to the above mentioned batches, batch 2 displayed a more controlled means of release. A similar burst release occurred at 2 hours, but this was moderated to 48%, substantially less than previous batches. Thereafter, a release until 12 hours was achieved but the profile generated was erratic and deviating from zero-order release.

A more controlled and desirable release pattern was shown with batches 3 and 5 Figure 3.12c and Figure 3.12e). The typical burst release with an hour of testing was drastically reduced, with an effective continual release pattern thereafter up to a period of 12 hours. In these profiles, the initial burst effect was limited to 30%$^{w}/_{v}$ and 25%$^{w}/_{v}$ for batches 3 and 5 respectively with subsequent data points indicating a relatively controlled release pattern. Such results were attributed to the incorporation of EC and the higher crosslinking concentration.

Further manipulation of formulation parameters were required to achieve as close to zero-order release as possible whilst maintaining a high DEE with a concurrent aesthetic looking multiparticulate. From preliminary release profiles data, it was evident that double cross-linking with the inclusion of the EC as an acid protectant polymer and the saturation of the crosslinking solutions with INH were imperative to achieve controlled release of INH for extended hours and to significantly improve DEE.

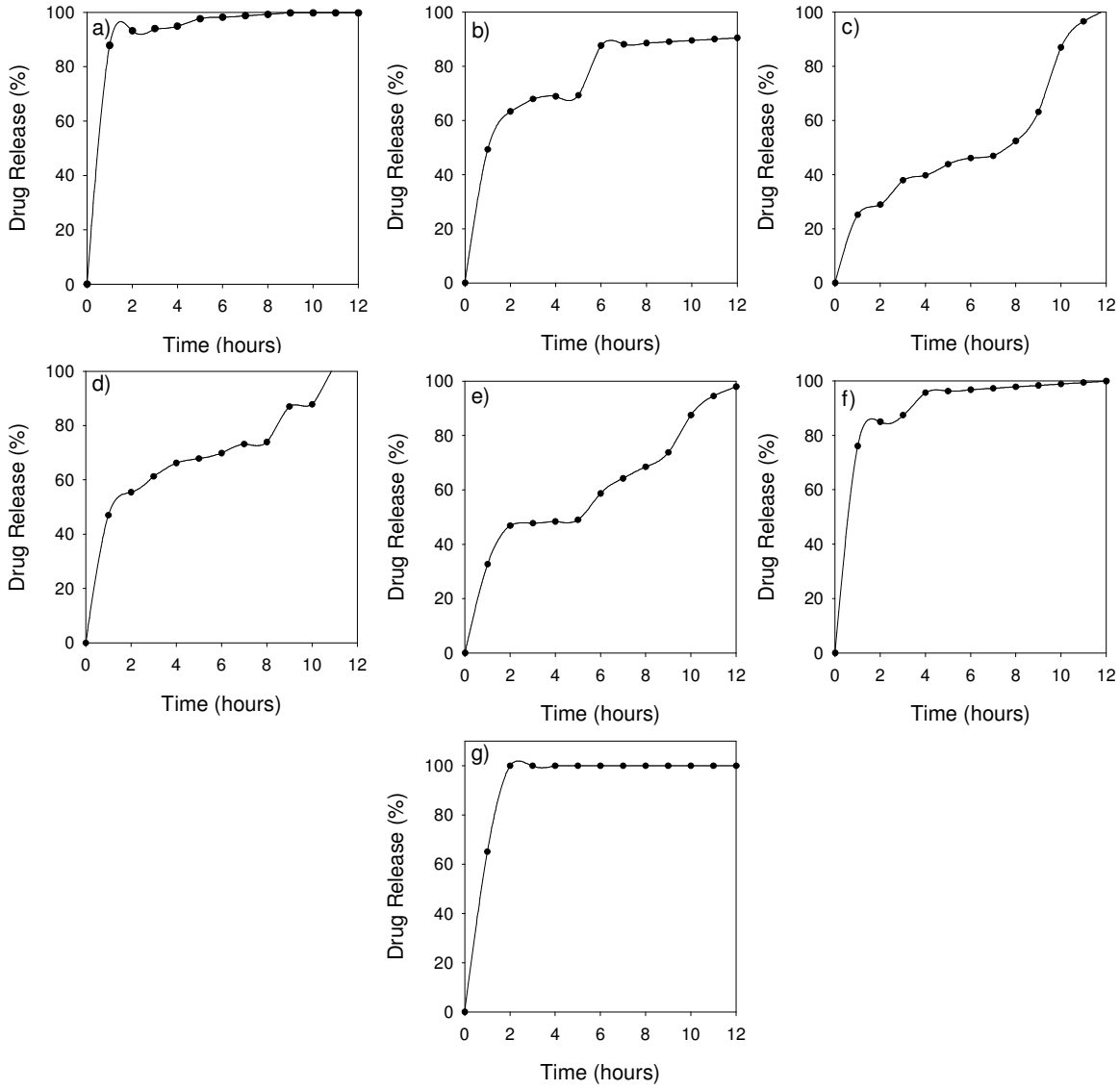


Figure 3.12 Preliminary *in vitro* release profiles for a) $MgSO_4$ 15%$^{w}/_{v}$ + $ZnSO_4$ 25%$^{w}/_{v}$ b) $CaCl_2$ 25%$^{w}/_{v}$ + $AlCl_3$ 25%$^{w}/_{v}$ c) $MgCl_2$ 30%$^{w}/_{v}$ + $AlCl_3$ 25%$^{w}/_{v}$ d) $BaCl_2$ 15%$^{w}/_{v}$ + $AlCl_3$ 25%$^{w}/_{v}$ e) $BaCl_2$ 25%$^{w}/_{v}$ + $AlCl_3$ 25%$^{w}/_{v}$ f) $K_2S_2O_5$ 25%$^{w}/_{v}$ + $AlCl_3$ 25%$^{w}/_{v}$ and g) NaCl 25%$^{w}/_{v}$ + $AlCl_3$ 25%$^{w}/_{v}$; where N= 3 and SD < 1.4 in all cases

3.5.4 Preliminary *in vitro* drug release results of polyethylene glycol crosslinked polymethacrylate based memblet system

In contrast to multiparticulate studies, memblet samples had to release within 2 hours but analogous relative zero-order drug release was required. For the purposes of this study, complete dissolution within 2 hours was warranted to ensure a total release of RIF prior to gastric emptying which was successfully achieved as illustrated in Figure 3.13.

Of importance to note, is the difference in release patterns. A lower crosslinker concentration (30%$^{w}/_{v}$) benefited release comparatively to a burst effect with more than 60% released within 30 minutes and complete release at 1.6 hours as in memblet *A (*60%$^{w}/_{v}$*)*. The potential

of a lower crosslinker concentration is seen with both the release pattern and the extended duration of release (2 hours).

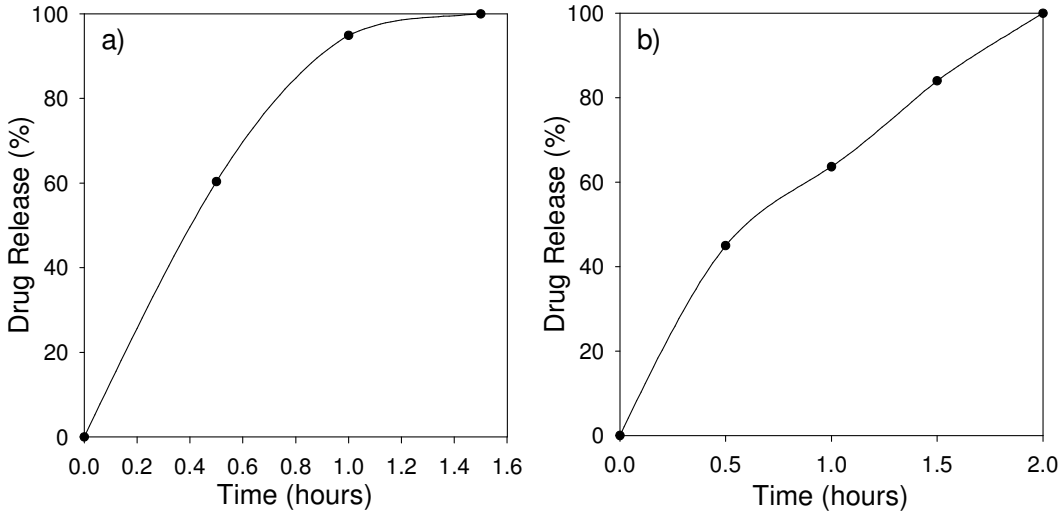


Figure 3.13 *In vitro* release patterns of a) memblet A and b) memblet B with varying crosslinker concentrations of 30%$^{w}/_{v}$ and 60%$^{w}/_{v}$ respectively; where N= 3 and S.D <1 in all cases



Figure 3.14 Rifampicin loaded, polyethylene glycol 4000 crosslinked novel memblet system

3.5.5 Thermal analytical method implementation and analysis of thermal profiles of polyethylene glycol crosslinked polymethacrylate based memblet systems

3.5.5.1 Critical theoretical concepts

Calorimetry is defined as the measurement of heat and such analysis plays a critical role in characterization studies for drug delivery systems. This particular thermal analysis tool has been used to evaluate the unknown thermal properties of the memblet to provide a full thermal characterization.

To measure heat an instrument must exchange heat and this exchanged heat causes a temperature change in the body/mass (in this case, the memblet system) and this ultimately induces the heat change or measurement of heat. Another explanation is that through the exchange of heat, a heat flow is created and this heat flow causes local temperature changes in the mass/body which can be used to measure the heat flow.

Differential Scanning Calorimetry (DSC) has the ability to measure heat/heat flow within the memblet*'s* matrix and the rate of heat flow (power). Furthermore, this analytical technique was adopted to ascertain thermal transitions or even chemical reactions that may occur due to the influence of heat on the memblet system. DSC can be defined as the measurement of the change of the difference in the heat flow rate to the sample and to a reference sample while they are subjected to a controlled temperature program (Celej *et al.*, 2006).

DSC utilized 40µL aluminium crucibles (a blank reference and a sample) to analyze slivers of the memblet. The sample and reference crucibles were subjected to an identical heat induction, but due to weight differences, a greater energy input for the sample crucible was required to ensure an equal temperature increase between sample and reference crucibles to validate data. For the purposes of thermal analysis, the excess heat required to keep the rates even constitute thermal data.

The amount of heat required to elucidate a certain temperature increase is called the heat capacity, or Cp. Cp is better defined as the amount of energy required to raise the temperature of 1g of memblet sample by 1K under a constant pressure (Mettler Toledo Usercom 7, 1998; Xua *et al.*, 2000). Usually, Cp is not measured during first order transitions (such as melting and cold crystallization) as the values are infinitely large. The heat capacity is calculated by dividing this heat supplied by the resulting temperature increase or change in temperature. Heat capacity can best be described in saying that it is the heat flow (HF) divided by the heating rate (HR) as shown in Equation 3.2:

$$C_p = \frac{HF}{HR} \qquad \textit{(Equation 3.2)}$$

By subjecting the memblet system to the aforementioned theory, we can evaluate the Cp for the memblet, but further thermal information can be evaluated when heating pass this point.

Upon further heating of the polymeric memblet beyond the Cp value, an increase in the heat flow would be observed and an alteration to the thermogram would be noted. This also means that the Cp value of the memblet has increased concurrently. This phenomenon

occurs as the polymer has reached the glass transition temperature or T_g. This T_g is a temperature at which change of physical state occurs and is a phenomenon that occurs within many polymers (Edwards, 1994; Fujimori *et al.*, 2005). Below the T_g, polymers are hard and brittle just like glass, but above it they are rubbery and elastic and may exhibit flow properties. Polymers tend to have a higher heat capacity above their T_g than below it. The change in heat capacity does not occur instantaneously but over a range of temperature, such that the T_g is taken at the midpoint of the peak.

A glass transition always requires the presence of a certain amount of disorder in the molecular structure of the sample. It is very sensitive to changes in molecular interactions. Measurement of the glass transition can thus be used to determine and characterize structural differences between memblet samples or changes within the memblet polymeric backbone. In many cases, the T_g is dependent on the degree of saturation of crosslinking which is an important factor to evaluate within the memblet studies (Maes *et al.,* 1995).

With regards to the actual thermogram, the glass transition is not displayed as a peak or trough in the curve as this is neither an endothermic or exothermic reaction as heat is neither taken nor given off by the polymer molecules during the glass transition. As there is a change in the heat capacity but no latent heat given off or absorbed, this phenomenon is a second order transition. The transitions of crystallization and melting are first order transitions.

Above the T_g, the polymers molecules are highly mobile and align themselves in a highly ordered manner in the form of crystals. The formation of these crystals is an exothermic process and as such gives off heat. Consequently, the machine has heat added to it and it does need to use its own heating system to increase heat flow and is depicted in thermograms as a peak.

The temperature at the highest point in the peak is the T_c or the polymers crystallization temperature. The area within the peak indicates the latent energy of the crystals whilst the peak itself indicates that the polymer can or has undergone crystallization. This exothermic type of thermal transition is one type of transition that can occur due to heat.

Melting Temperature or T_m is another type of thermal transition that can occur when heating continues past the T_c. The aligned polymer chains (in the form of crystals) begin to lose their uniform distribution and melting begins. For melting to occur, polymers must absorb heat and doing so forces the DSC machine to put in additional heat to maintain equal rates and as such the heat flow curve increases to form a trough. This transitional process is an

endothermic one. The latent heat of melting can be determined by calculating the area under this peak. The temperature at the apex of the peak is the T_m (Mettler Toledo Usercom 11, 1998; The University of Southern Mississippi, Differential Scanning Calorimetry, 2005; Silicon Far East, 2005).

Alternating Differential Scanning Calorimetry (ADSC) provides the same qualitative and quantitative information about physical and chemical changes as conventional DSC, and it also provides unique thermochemical data that is unavailable with conventional DSC. The effects of baseline slope and curvature are reduced, increasing the sensitivity of the system. Overlapping events such as molecular relaxation and glass transitions can be separated. Heat capacity can be measured directly with ADSC in a minimum number of experiments.

Both ADSC and DSC measure the difference in heat flow to a sample and to an inert reference. The sample and reference cells are identical. However, ADSC uses a different heating profile. DSC measures heat flow as a function of a constant rate of change in temperature and in comparison ADSC superimposes a sinusoidal temperature modulation on this rate. The sinusoidal change in temperature permits the measurement of heat-capacity effects simultaneously with the kinetic effect. Typical experimental procedure for an initial ADSC experiment include a heating rate from isothermal to 5℃/min and a modulation amplitude from 0.01 to 10℃. The modulation period can vary from 10 to 100 seconds or expressed as a frequency from 10 to 100MHz.

The advantages of ADSC include improved resolution and sensitivity, in addition to being able to separate overlapping phenomena. Comparatively, when we use standard DSC and a high heating rate, we get large peaks but relatively low resolution. In the case of lower heating rates, we get small peaks which are well separated. ADSC utilizes the periodic temperature program which provides both large peaks and good separation (high resolution). The temperature program of ADSC comprises a periodic succession of short, linear heating and cooling phases. The heating or cooling rates lie between 2 and 5K/min. For a heating measurement the final temperature of the cooling phase is higher than that of the start temperature of the previous heating phase by a small amount thus leading to the low, average rate. ADSC uses the heat flux DSC instrument design and configuration to measure the differential heat flow between the memblet sample and an inert reference material as a function of time whilst at the same time superimposing a sinusoidal temperature flux. The temperature programme derived is such that the average sample temperature varies continuously in a typical sinusoidal manner. The modulation of the sinusoidal temperature includes alterations to the amplitude (AT) and the frequency ώ is expressed in Equation 3.3:

$$T = T_0 + q_0 t + A_T \sin(\omega t) \qquad \textit{(Equation 3.3)}$$

Where, T= the average sample temperature, T_o= the initial temperature, $q_o t$= the underlying linear heating rate, A_T= the amplitude of modulation and ω= 2pi/p (where p= the modulation period).

Total heat flow at any point in a DSC or ADSC experiment can be given by Equation 3.4:

$$\frac{dQ}{dt} = C_p \beta + f(T,t) \qquad \textit{(Equation 3.4)}$$

Where Q= heat (in Joules), t= time(s), Cp= sample heat capacity and f(T,t)= heat flow from kinetic processes which are absolute temperature and time dependent.

Conventional DSC only measures the total heat flow. ADSC by effectively applying 2 simultaneous temperature profiles to the sample can estimate the individual contributions to Equation 3.3. The heat capacity component of the total heat flow, $C_p\beta$, is generally referred to as the reversing heat flow. From an ADSC curve, information on the C_p complex, C_p in phase, C_p out phase, reversible heat flow, non reversible heat flow and total heat flow can be obtained.

Heat capacity for a standard DSC curve was previously defined as dividing HF by HR in Equation 3.2. Thus the complex heat capacity of the ADSC curve can be defined with Equation 3.5:

$$C_p \quad complex = \frac{AHF}{AHR} \qquad \textit{(Equation 3.5)}$$

Where, AHF= the amplitude of the heat flow modulation and AHR= the amplitude of the heating rate modulation.

The average value of heat flow, also called total heat flow, is very similar to the signal obtained by conventional DSC at the same heating rate.

A complex heat capacity can be further defined as:

$$C_p \quad complex = C_p - C_{p''} \qquad \textit{(Equation 3.6)}$$

Where, $C_{p'}$= the in phase heat capacity and $C_{p''}$= the out phase heat capacity.

As a result of the periodical temperature variation the heating rate, we get a periodic heat flow signal which is shifted by the phase angle (φ) with respect to the heating rate. Therefore, the phase angle is between the heating rate and the heat flow. The C_p in phase and C_p out phase heat capacities are represented by the Equation 3.7 and Equation 3.8 respectively:

$$C_{p'} = C_p \cos\varphi \qquad \textit{(Equation 3.7)}$$

$$C_{p''} = C_p \sin\varphi \qquad \textit{(Equation 3.8)}$$

Where, φ= the phase angle.

The phase angle occurs between the modulated heat flow and the heating rate. This phase shift occurs during the ADSC measurement due to the relaxation process. In the glass transition region, the phase angle is relatively small and the $C_{p'}$ is practically equal to the C_p complex. Any linear and time-invariant system follows the premise that if the system is subjected to a sinusoidal stimulus the output will also be sinusoidal with the same frequency, though with a different amplitude and a shifted phase.

Based on these theories, 3 types of heat flow can be derived from an ADSC study namely reversible heat flow, non reversible heat flow and total heat flow.

Total heat flow curves correspond to the heat flow that would be obtained with conventional DSC at the same heating rate. This curve shows thermal effects due to aging in the glass transition region. The glass transition value is based on the heating rate.

Reversible heat flow curves normally show the glass transitions and the endothermic melting peak. This does not show thermal information due to aging as compared to the total heat flow curve in the glass transition region. Glass transitions found in the reversible heat flow and total heat flow curves are not the same. A frequency dependant dynamic glass transition is measured. Normally effects such as cold crystallization are not observed but in some instances a small oscillation may be seen. Modulation of the heating rate gives us the reversing heat flow. This is not analogous with the term thermodynamically reversible.

The non reversing heat flow is defined as the total heat flow minus the reversible heat flow. Kinetic effects contribute mainly to the non reversing heat flow. Examples of kinetic effects are cold re-crystallization and enthalpic recovery (Flikkema *et al*., 1998; Carpentier *et al*., 2002; Yuji *et al*, 2007; Yanga *et al*., 2009).

3.5.5.2 Pre-formulation differential scanning calorimetry thermal profiling on memblet systems

The pre-formulation studies were conducted on memblet*s* A only, as this was method development and not comparative analysis. Samples were conducted in this manner to determine test parameters rather than ascertain credible results for comparison and analysis. After an initial training session from METTLER Toledo training staff, a suitable level of competency was achieved to begin basic DSC analysis on membrane samples. DSC analysis for membrane samples included testing individual polymeric constituents (Polyethylene Glycol 4000 and Eudragit® E 100). Successful DSC analysis depended on knowing information on test samples prior to analysis to allow accurate analysis of results. Table 3.7 displays prerequisite information for rudimentary DSC analysis.

Table 3.7 Thermal information on constituent polymers

Test samples	T_g	M_{pt}	T_c
PEG 4000	-	53-58℃	-
E 100	40℃	-	-

T_g= the glass transition temperature, M_{pt}= melting point of sample, T_c= crystallization temperature, PEG 4000= polyethylene glycol 4000 and E 100= Eudragit® E 100 (Polyethylene glycol general properties, 2000; Inc. Morflex, 2004)

With this information obtained, DSC temperature ranges can be narrowed during the testing phase. Testing consisted of a wide temperature range at a set ramping rate to determine the optimal testing of each individual polymer and to verify literature surveys for thermal information.

Table 3.8 Method development criteria

Test samples	Temperature range	Ramping rate	Crucibles used	Weight
PEG 4000	-30℃-150℃	10℃	40µL	18mg
E 100	-30℃-150℃	10℃	40µL	18mg

In comparison to literature surveys, a large discrepancy was found between E 100 tested samples and the information gathered. Glass transition temperatures were observed to have a larger value with the E 100 beads tested on the *DSC1 STAR*^{e} system as depicted in Figure 3.15. All samples were weighed to precisely 18mg and inserted into 40µL crucibles and the lids were punctured 3 times to account for pressure differentials. Thereafter, crucibles were

hermetically sealed using the sealant clamp. Samples were run in duplicate for accuracy and to remove thermal history from a sample and in all runs a glass transition endset of between 55℃-58℃ was evaluated for raw E 100 bead samples. PEG 4000 samples fell less out of range than the E 100 and out of the range of the melting points stated in literature (53-58℃) with, an endset temperature of 61.91℃ as shown in Figure 3.16.

From the individual polymeric testing it was deduced that a temperature range of between 0℃-200℃, ramped at 10℃ would be initially used until a precise temperature range could be determined for DSC membrane runs. A standard weight of 18mg would be used for all memblet samples for DSC measurements. All samples were prepared in 40µl aluminium crucibles. ADSC was carried out with an underlying heating rate of 1℃ per minute and a modulated temperature of 0.1℃ per 0.8 minutes. All samples were run in duplicate.

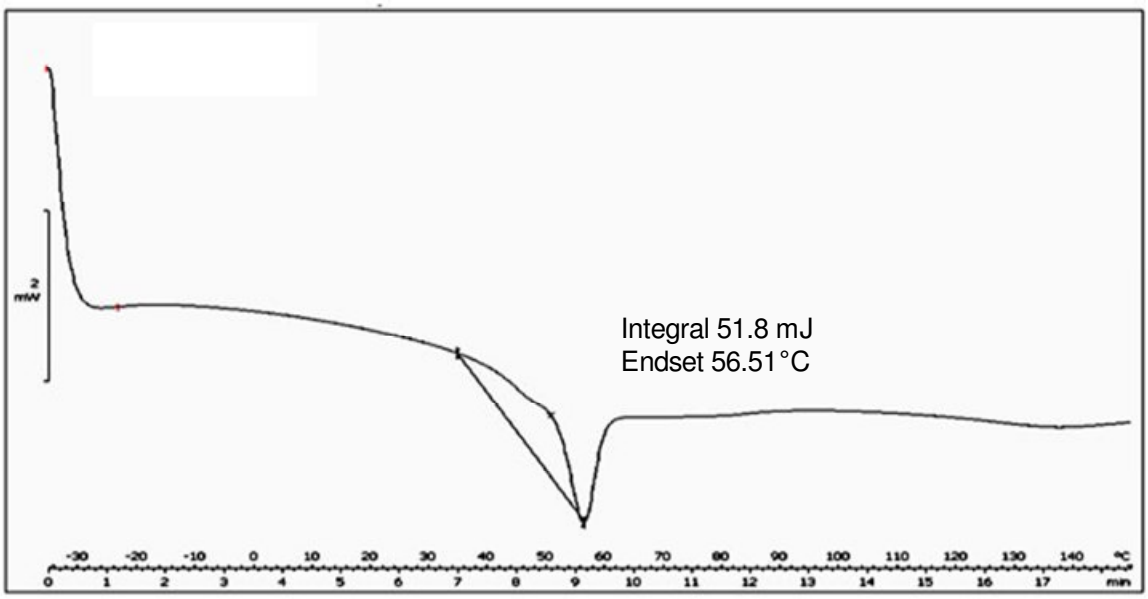


Figure 3.15 Differential Scanning Calorimetry thermogram of Eudragit® E 100 identifying the larger endset glass transition temperature in comparison to literature findings

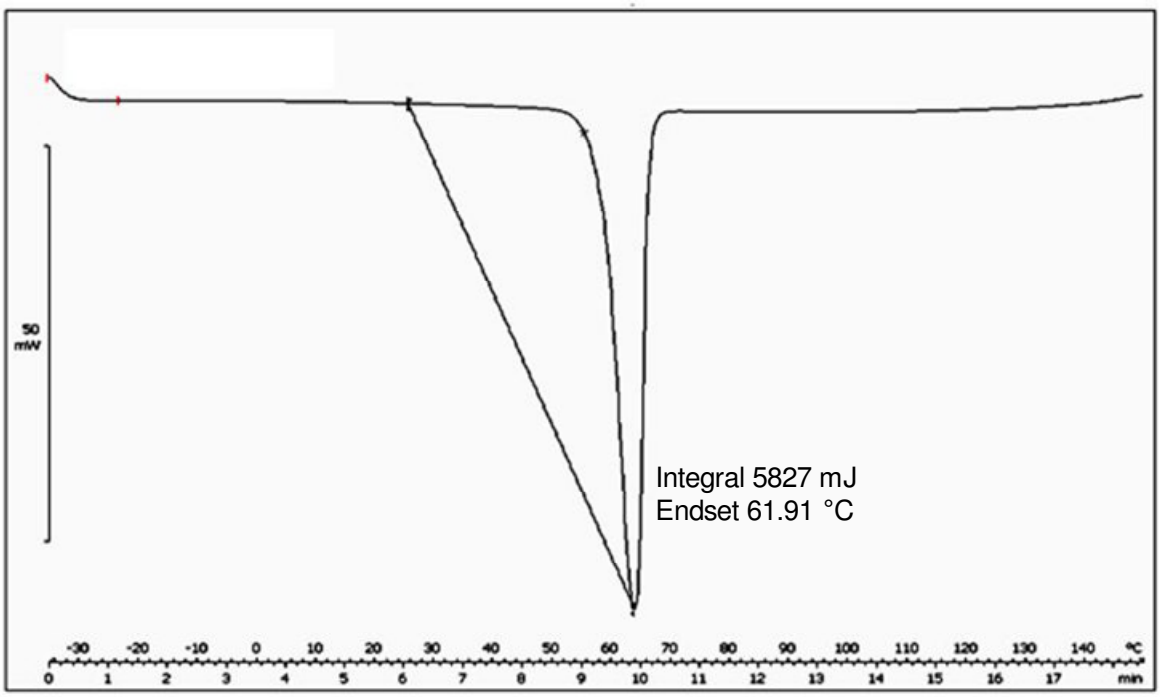


Figure 3.16 Differential scanning calorimetry thermogram of polyethylene glycol 4000 corresponding to literature findings

Figure 3.17 shows a definite thermal profile of the memblet system comprising of both Eudragit® E 100 and PEG 4000. The thermogram has a well defined trough which can display the melting point of the PEG 4000. The melting point shows a very similar value to the test conducted on the individual polymeric material having a melting point of 52.12℃. This value still however falls in the range of the tested Eudragit® E 100 beads and as such a distinction must be made as to whether the thermal event depicted is the glass transition temperature of the Eudragit® E 100 beads or the melting point of the PEG 4000. There were 2 factors that influenced the decision made. Firstly, the trough itself is not a gradual slope seen with a glass transition but is a sharp spike typically expressed with a melting point. The second factor indicating that the event is a melting point is the integral (or C_p) value of 712.67mJ. As previously explained in Chapter 3.5.5.1, melting is a first order endothermic energy transition requiring a considerable amount of energy in the form of heat to transpire. Relative to the integral value of the Eudragit® E 100 T_g, 51.86mJ, the memblet system requires a large amount of energy for an event to take place.

Though the event is classified as a melting point, it is known from preliminary studies that the Eudragit® E 100 polymeric component comprises of a T_g though the event is not seen on the thermogram. As the glass transition and melting point of Eudragit® E 100 and PEG 4000 respectively are close values, it is assumed that there was an overlapping of thermal events taking place. A solution offered was to decrease the ramping temperature from 10℃ to 5℃ at the detriment to resolution to separate the thermal events.

A more thorough and practical solution was opting for Alternating Differential Scanning Calorimetry (ADSC) to allow for individual analysis of events. The memblet sample showed an erratic behaviour towards the 300℃ temperature range which is indicative of either release of gas or thermal decomposition. The second run of the same crucible, shown in Figure 3.18, displayed an atypical curve which establishes that the event is in fact thermal decomposition. From this data, it is non-conducive to accurate results to keep this temperature range as the sample must follow the duplication procedure in analysis to remove any thermal history. The upper end range should therefore be within 260℃.

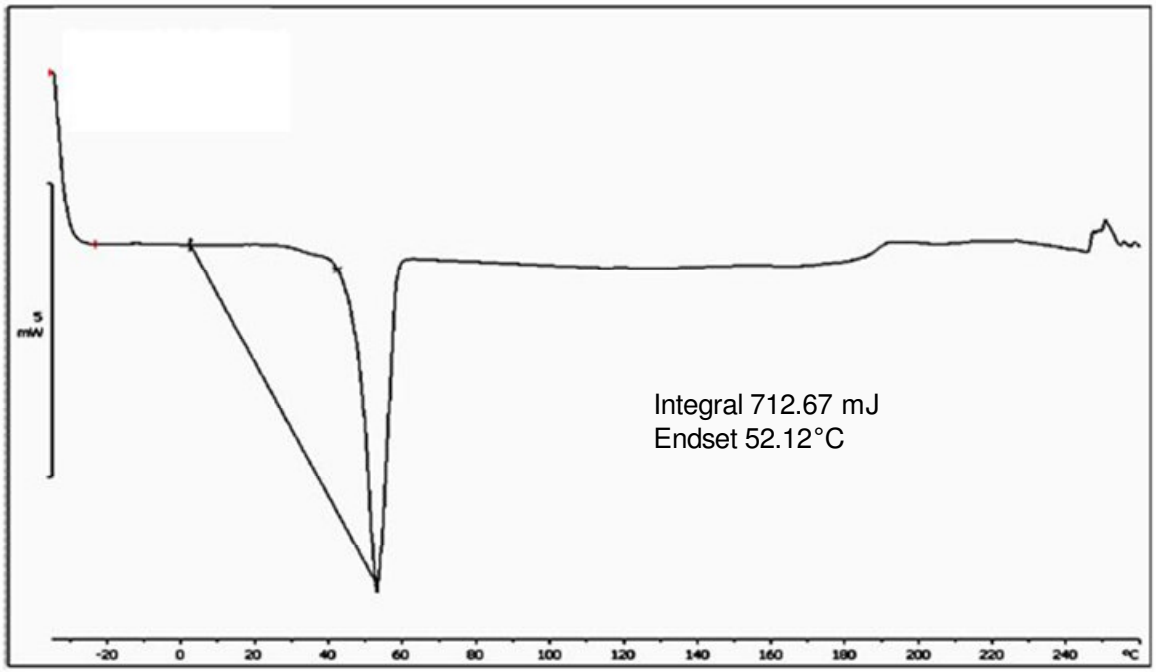


Figure 3.17 Preliminary Differential Scanning Calorimetry thermogram of a novel memblet system

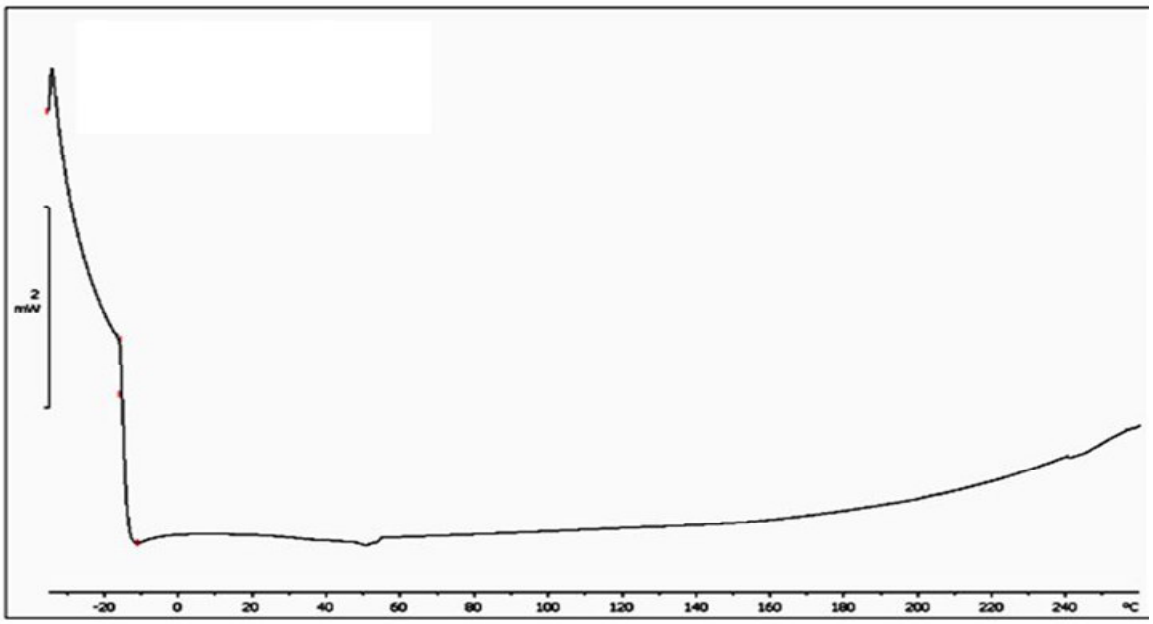


Figure 3.18 Thermal decomposition of the memblet system once passing 300℃ establishing upper testing limits

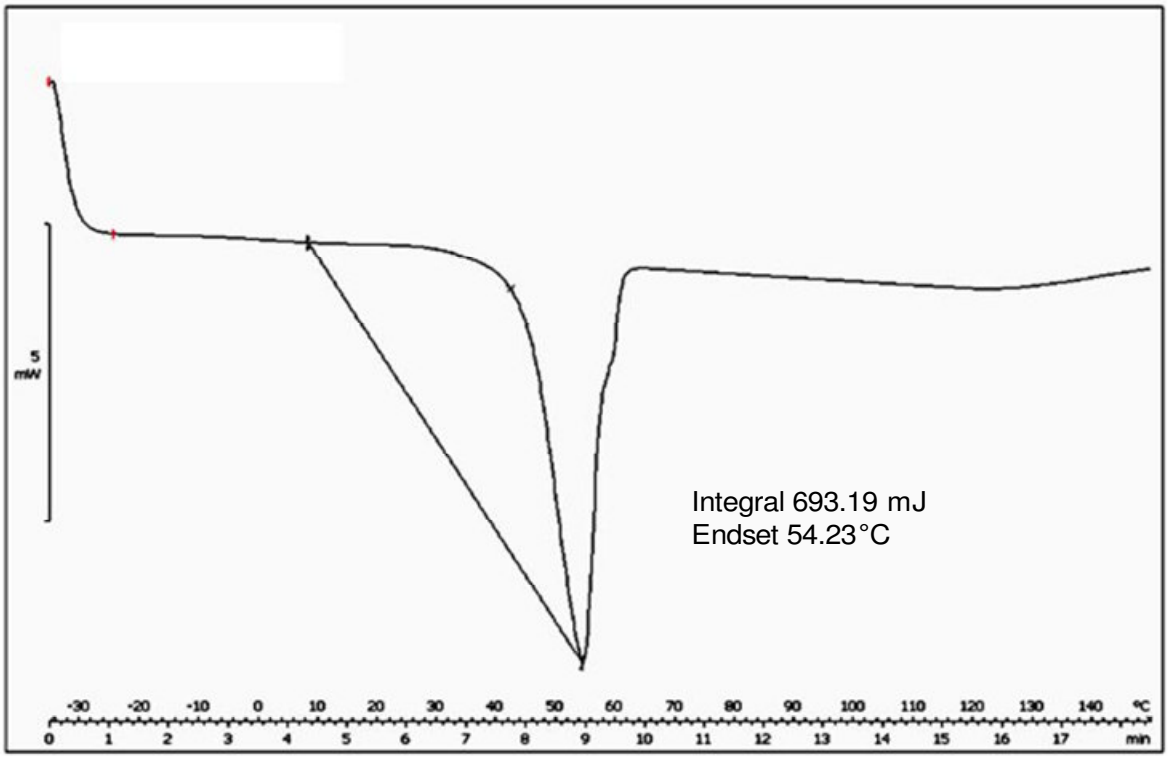


Figure 3.19 A second Differential Scanning Calorimetry run validating the upper limits of the temperature range for subsequent analysis

A remodelled test was conducted on the *DSC1 STAR*^{e} system with upper limit being at 150℃ in which the second run, depicted in Figure 3.19, yielded no thermal decomposition. An upper limit of 200℃ was verified for all DSC memblet samples.

3.6 Concluding Remarks

Preliminary studies provided a framework for formulation variables to be selected. Fixed formulation parameters were also decided, as variation in their incorporation into method development would drastically alter results.

The multiparticulate component of the ODMUS required an increase in DEE and a closer to zero-order release pattern for a period of between 10 and 12 hours at a pH of 6.8. Fixed method parameters included a 20 minute curing period for both crosslinker solutions in which the second crosslinker would be $AlCl_3$ for all formulations.

The inclusion of ethyl cellulose into the formulation was also a fixed formulation parameter as its influence positively influenced release profiles though the physical amount to be included was yet to be determined by optimization analysis detailed in Chapter 4 of this dissertation. Saturation of crosslinker solutions provided an acceptable DEE and subsequently an amount of 3g INH was to be saturated with the crosslinker solutions as the final fixed formulation parameter.

Memblet samples in preliminary studies showed an effective duration of release (under 2 hours) for the respective crosslinker concentrations (30%$^{w}/_{v}$ and 60%$^{w}/_{v}$). Thermal analysis methods were successfully developed for both DSC and ADSC for subsequent testing elaborated in Chapter 4 of this dissertation.

CHAPTER 4
FORMULATION AND OPTIMIZATION OF ISONIAZID-LOADED MULTIPARTICULATES AND A RIFAMPICIN-LOADED ORAL MEMBRANOUS SYSTEM

4.1 Introduction

Preliminary studies outlined in Chapter 3, were of critical importance for the optimization of the ODMUS. Through these studies upper and lower limits (formulation independent variables) for both multiparticulate and memblet systems were ascertained, as will be detailed in this Chapter. An individualised experimental design was employed through manipulation of the variables to determine measured responses as per component of the ODMUS. The multiparticulate system included independent variables that were both qualitative and quantitative in comparison to the memblet system's quantitative independent variables only. Based on these statistical results, an optimized formulation was formulated for both the multiparticulate and the memblet systems. These optimized versions of the ODMUS were then put through drug delivery testing and characterization prior to *in vivo* studies.

When implementing the design of experiments, a response surface methodology approach was selected to evaluate the best combination of formulation components to achieve an optimal ODMUS formulation. Functionally, this methodology was selected to optimize both components of the ODMUS utilizing statistical experimental designs, specifically a Box-Behnken design. Response surface methodology achieves its objective of optimization through:

- Formulating a design of experiments derived from the upper and lower limits of the formulation variables (independent variables)
- Conducting the physical tests on the design of experiments
- The manipulation of regression analysis techniques to evaluate the coefficients of a mathematical model
- Prediction of responses (dependent variables) and validation of the mathematical model resulting in optimization of that particular formulation (Raya *et al*., 2009; Raya *et al*., 2010).

4.2 Optimization Utilizing a Box-Behnken Factorial Design

4.2.1 Selection of suitable independent variables to elucidate positive responses for the once daily multi-unit System

Selection of factors and factor levels for the design of experiments was based on preliminary studies discussed in Chapter 3. Factors were selected for each component of the ODMUS such that individualised mathematical models were generated.

Of specific importance for the multiparticulates was the incorporation of ethylcellulose (EC) and the choice and concentration of the second crosslinker. Effectively, the independent variables constituted qualitative and quantitative variables relative to type of crosslinker and concentration of EC and crosslinker respectively. The *main effect,* or factor averaged above all other levels of factors relating to the largest magnitude of change in responses (Bolton, 1997), would be allocated to an individual factor or a combination of factors after responses were obtained through mathematical modelling.

With regards to the multiparticulate component, Figure 3.12e of Chapter 3.5.3 authenticated that relatively good release with a concurrently improved DEE of 61% was achieved with batch 3. A test amount of 5%$^{w}/_{v}$ (1g of EC) was used and subsequently, upper and lower limits of this numerical value were selected as shown in Table 4.1.

The type of secondary crosslinker was limited to 3 of the most proficient cationic electrolytes namely $BaCl_2$, $CaCl_2$ and $MgCl_2$ for the purposes of simplifying mathematical modelling. $ZnCl_2$ was excluded due to the poor release patterns relative to the other 3 metal ions. Successful release patterns shown for batch 3 could not be attributed to any single variable at that point. Concentrations of secondary crosslinkers were therefore subject to scrutiny in mathematical modelling with upper and lower limits of 20%$^{w}/_{v}$ and 40%$^{w}/_{v}$, respectively.

For the purposes of this study, responses in Table 4.1, mean dissolution time (MDT) and drug entrapment efficiency (DEE) were to be maximized in all situations to achieve an optimal formulation.

Table 4.1 Listing of formulation variables with appropriate responses and objectives

Independent variables	Upper limits	Lower limits	-
Type of crosslinker	$BaCl_2$, $CaCl_2$ or $MgCl_2$	$BaCl_2$, $CaCl_2$ or $MgCl_2$	-
Concentration of secondary crosslinker (%$^{w}/_{v}$)	40	20	-
Ethylcellulose content (g)	2.000	0.750	-
Response	**Upper limit**	**Lower Limit**	**Objective**
Drug Release (MDT)	65	45	Maximize
DEE (%)	65	45	Maximize

In a similar context, the memblet system would require a controlled release pattern, but conversely, a shorter duration of release. Rifampicin (RIF) would require a total release in the stomach within 2 hours prior to gastric emptying to avoid any associative release in the small intestine. It was already postulated that the *main effect* of independent variables on the dependent responses would be a synergistic influence through a combination of factors as polyethylene glycol (PEG) 4000 and triethyl citrate (TEC) had a similar plasticizing effect and would alter release patterns.

Furthermore, a high glass transition temperature (T_g) was imperative to ensure structural, functional and aesthetic integrity for the period prior to dosing. Specifically, the T_g of the memblet was required to be above 37℃ so as not to undergo premature degradation *in vivo*.

Independent variables numerical values were chosen based on the influence each had on the T_g, bearing in mind that both TEC and PEG 4000 had a compounding effect of lowering T_g as both are plasticizers. Table 4.2 depicts the upper and lower limits for the independent variables obtained through preliminary studies including desired responses based on said preliminary studies.

Table 4.2 Listing of formulation variables with responses and objectives for the memblet

Independent variables	Upper limits	Lower limits	-
Concentration of Polyethylene Glycol 4000 (%$^{w}/_{v}$)	70.0%$^{w}/_{v}$	30.0%$^{w}/_{v}$	-
Concentration of Triethyl Citrate (%$^{v}/_{v}$)	10.0%$^{v}/_{v}$	1.0%$^{v}/_{v}$	-
Concentration of Sodium Lauryl Sulphate (g)	2.0g	0.5g	-
Response	**Upper limit**	**Lower limit**	**Objective**
Drug Release (MDT)	200	100	Maximize
Glass Transition Temperature (℃)	65	35	Maximize

4.2.2 Generation of a design of experiments through a box-behnken design and subsequent testing

With the establishing of the independent variables, a design of experiments was formulated in the form of runs or trials. These experimental runs aimed to produce a minimum amount of runs that would ascertain maximum efficacy of information for prediction of responses. A Box-Behnken design was selected for this generation of runs requiring only 3 levels ie. upper, lower and central numerical values such that the use of an independent quadratic design resulted in 15 formulations as 3 independent factors were chosen for each formulation of the ODMUS (MINITAB®,V14, Minitab, USA). Table 4.3 and Table 4.4 demonstrates the experimental runs of double crosslinked, isoniazid-loaded polymethacrylate multiparticulates and PEG 4000 crosslinked Eudragit® E 100 memblet systems respectively, generated by a Box-Behnken design. Measured responses employed in the Box-Behnken design for the experimental runs, are similarly displayed in Table 4.5 for both multiparticulates and memblets. During the design of experiments stage, experimental responses are recorded for the runs of experiments carried out in a systematic way to develop a mathematical model.

Table 4.3 Factors and levels of independent variables generated by the 3^3 Box- Behnken design for isoniazid-loaded, double crosslinked, polymethacrylate based multiparticulates

Experimental Run	Independent factors		
	Ethyl Cellulose (g)	Crosslinking agent	Crosslinking solution concentration ($\%^{w}/_{v}$)
1	0.750	$MgCl_2$	40
2	2.000	$CaCl_2$	30
3	0.750	$CaCl_2$	30
4	1.375	$MgCl_2$	30
5	1.375	$BaCl_2$	40
6	2.000	$MgCl_2$	40
7	0.750	$BaCl_2$	30
8	1.375	$MgCl_2$	30
9	1.375	$BaCl_2$	20
10	2.000	$MgCl_2$	20
11	1.375	$CaCl_2$	20
12	1.375	$MgCl_2$	20
13	1.375	$CaCl_2$	40
14	0.750	$MgCl_2$	20
15	2.000	$BaCl_2$	30

Table 4.4 Factors and levels of independent variables generated by the 3^3 Box- Behnken design for rifampicin-loaded, polyethylene glycol 4000 crosslinked, Eudragit® E 100 memblet systems

Experimental Run	Independent factors		
	Triethyl citrate (mL)	Polyethylene glycol 4000 (%$^{w}/_{v}$)	Sodium lauryl sulphate (g)
1	1	70	1.25
2	10	50	2.00
3	1	50	2.00
4	5.5	50	1.25
5	5.5	70	0.50
6	10	70	1.25
7	1	50	0.50
8	5.5	50	1.25
9	5.5	30	0.50
10	10	30	1.25
11	5.5	30	2.00
12	5.5	50	1.25
13	5.5	70	2.00
14	1	30	1.25
15	10	50	0.50

Table 4.5 Measured responses of the experimental run for the optimization of multiparticulates

Multiparticulate component experimental run

Experimental Run	MDT	DEE(%)
1	68.663	49.39
2	71.273	40.13
3	69.793	60.40
4	66.345	46.94
5	66.877	45.69
6	70.166	44.49
7	59.854	43.76
8	68.352	46.40
9	60.757	48.39
10	70.841	40.45
11	67.355	63.66
12	71.911	50.09
13	59.176	48.62
14	49.646	49.14
15	69.115	63.76

Memblet component experimental run

Experimental Run	MDT	T_g (℃)
1	163.773	47.72
2	167.328	53.40
3	165.438	53.45
4	161.449	51.09
5	152.095	53.94
6	146.740	54.44
7	150.841	54.65
8	147.790	49.00
9	143.705	51.58
10	150.198	55.89
11	142.552	55.97
12	159.178	57.94
13	146.422	55.30
14	245.833	52.15
15	159.341	49.30

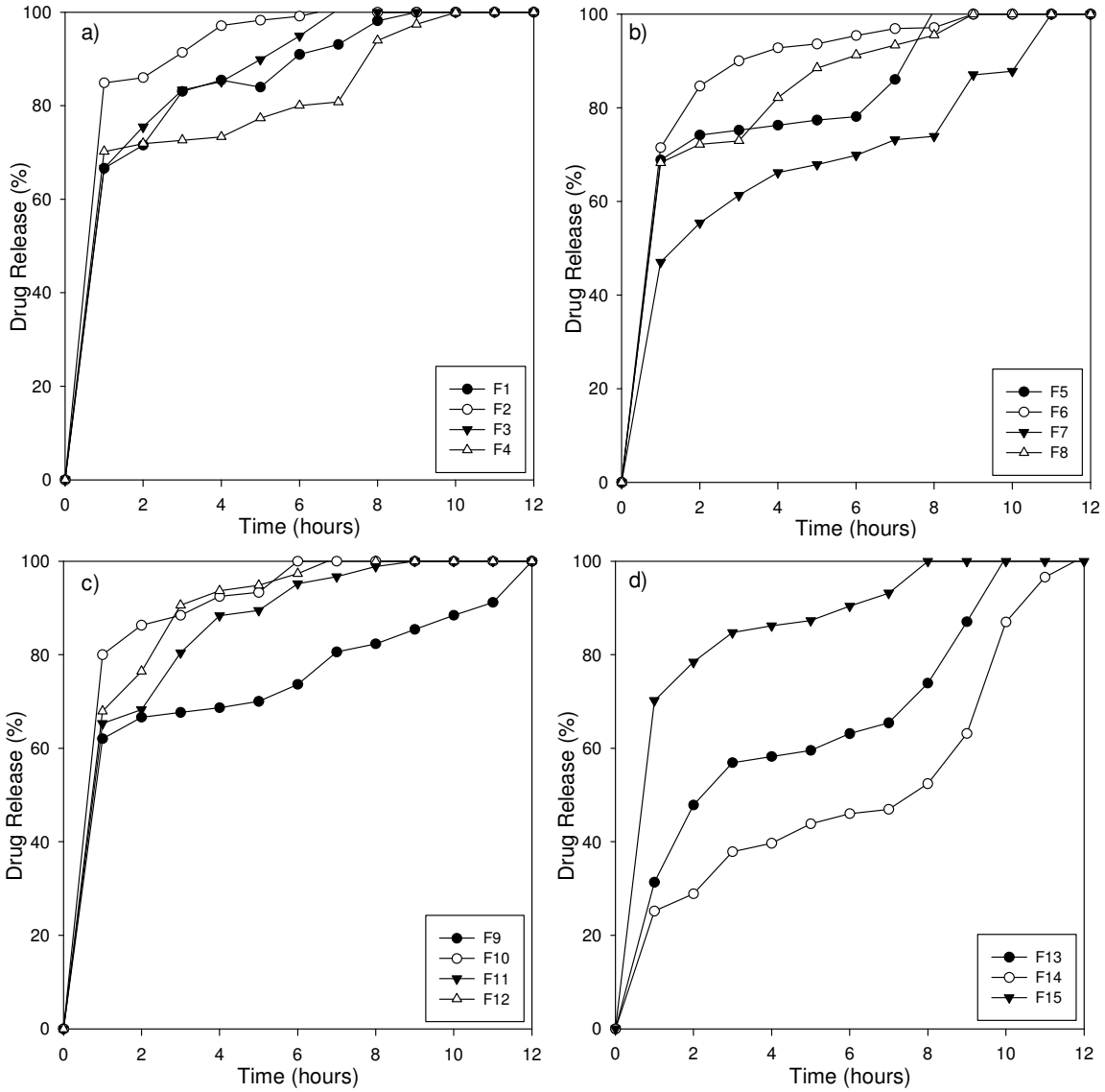


Figure 4.1 Release profiles for the multiparticulates design of experiments where a) represents formulations 1-4, b) represents formulations 5-8, c) represents formulations 9-12and d) represents formulations 13-15; where N= 3 and SD < 1.0 in all cases

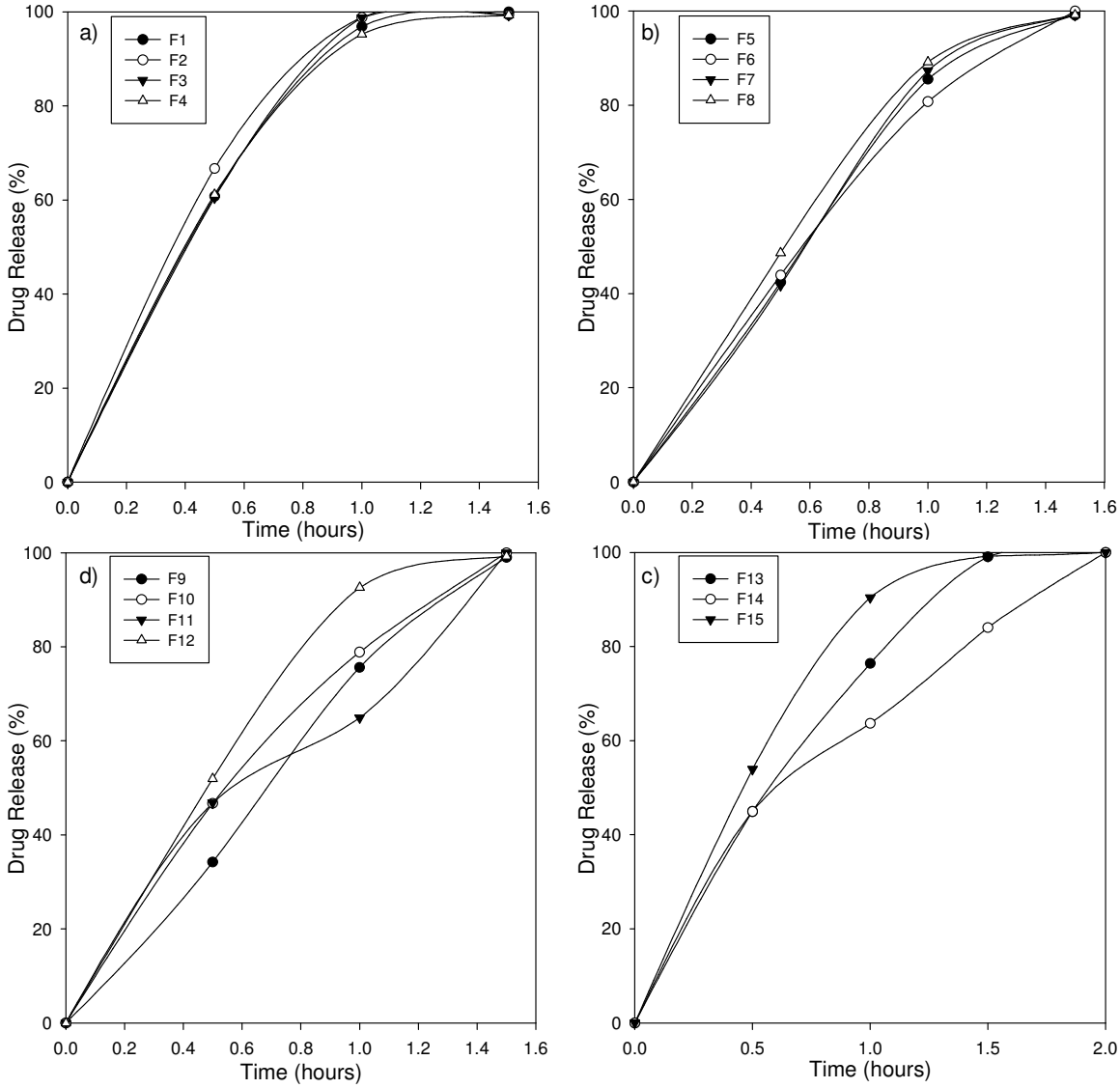


Figure 4.2 Release profiles for the memblet design of experiments where a) represents formulations 1-4, b) represents formulations 5-8, c) represents formulations 9-12 and d) represents formulations 13-15; where N= 3 and SD < 1.6 in all cases

4.2.3 Comparative analysis of actual experimental and fitted response values calculated for the optimization of both components of the once daily multi-unit system

Data collected from the design of experiments were comparatively plotted for a) memblet MDT b) memblet T_g c) multiparticulate DEE and d) multiparticulate MDT, against Fitted responses which resulted in R^2 values of 0.796, 0.535, 0.869 and 0.551 respectively. An acceptable correlation between the experimental and fitted responses was determined verifying the Box-Behnken design for the responses of MDT and T_g for the memblet system and MDT and DEE for the multiparticulate system.

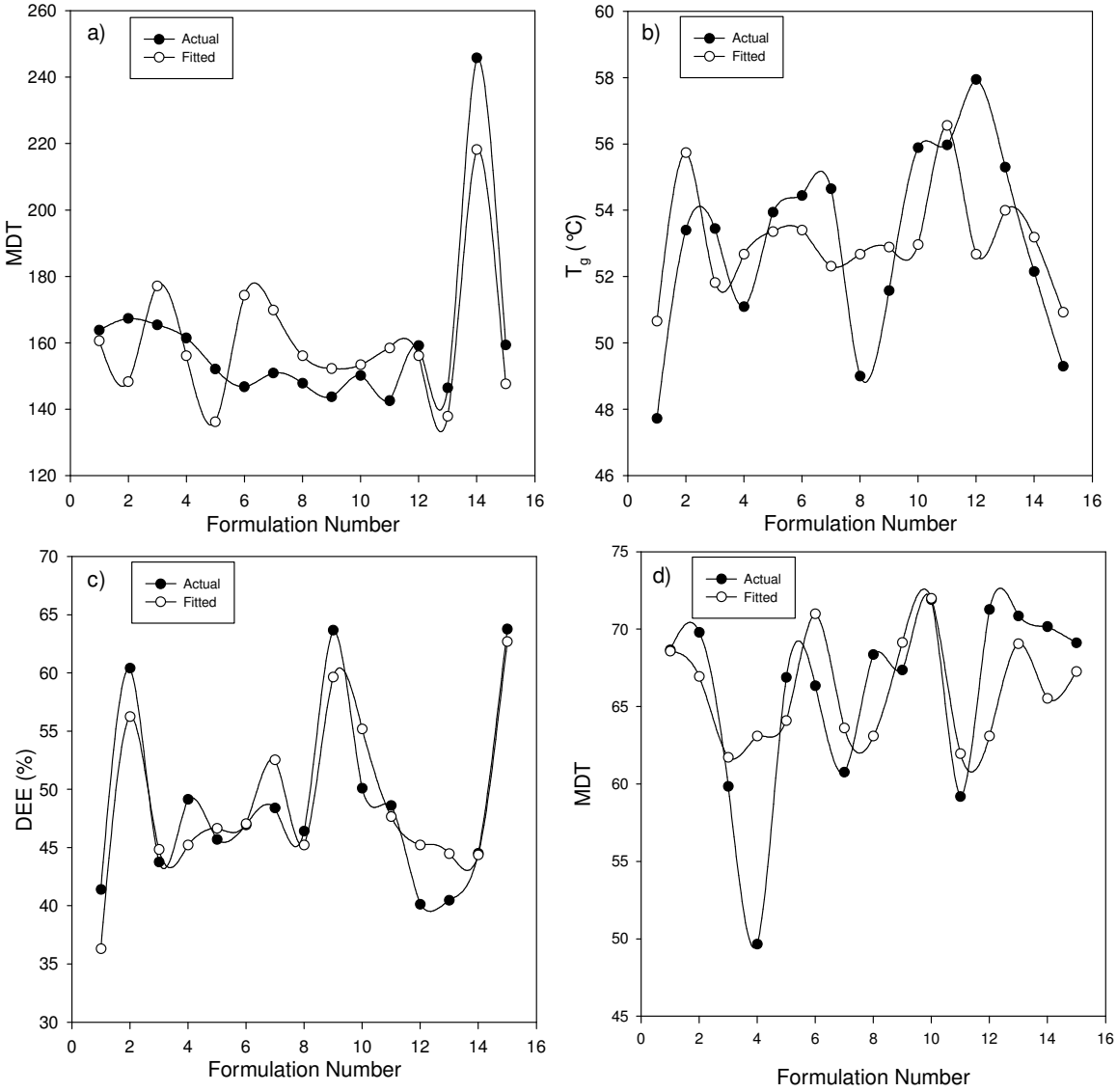


Figure 4.3 Regression plots for a) memblet mean dissolution time b) memblet glass transition c) multiparticulate drug entrapment efficiency and d) multiparticulate mean dissolution time to ascertain R^2 values to verify the correlation between fitted and actual values for the formulation responses

4.2.4 Graphical response data analysis

The data obtained from response surface methodology can be suitably modelled to produce mathematic relationships between the independent variables (*Factors*) and the dependent variables (*Responses)*. Graphically, these are depicted as 3-D models (*response surface plots)* representing the independent variables and the responses. Of critical importance is the interaction (if any) between the independent variables and the *effect* of these factors on the response, to give us a deeper look into the behaviour of the system. Additionally, residual plots such as Normal Probability Plot of the Residuals, Residuals Versus the Fitted Values, Histograms of the Residuals and Residuals Versus the Order of the Data are plotted for comparative purposes.

4.2.4.1 Response inspection of the once daily multi-unit system via 3-dimensional plotting

Mean dissolution time (MDT) and glass transition temperature (T_g) were the responses measured for the memblet system. Surface plot analysis validates the relationship between the independent variables PEG 4000 and TEC on the response of MDT in Figure 4.4a and Figure 4.4b. A direct linear relationship exists for these factors as a simultaneous decrease in PEG 4000 (between 30 and 45%$^w/_v$) and TEC (<5%$^w/_v$) elucidates a maximal MDT (>200) or a positive effect on response. The relationship between these factors can be termed as synergistic for the response of MDT. Conversely, sodium lauryl sulphate (SLS) influences a relatively negative response on MDT in comparison to the synergistic effect of PEG 4000 and TEC. A maximal amount (>1.8g) produced a maximum MDT response of only 180 in either case of increasing PEG 4000 (50%$^w/_v$) or TEC (6%$^w/_v$). For the purposes of optimizing the response of MDT, PEG 4000 and TEC have a more positive effect through synergistically decreasing levels to rate control release of rifampicin, as compared to any manipulation of SLS. T_g was required to be maximized, in particular to be well above 37°C (homeostatic body temperature). Surface responses (Figure 4.4) indicated a similar pattern as for the response of MDT for all factor levels (i.e. 45%$^w/_v$ PEG 4000, a slightly increased 5%$^w/_v$ TEC and a maximum 1.8g SLS) to achieve a T_g of >54°C.

Data analysis postulated that an effective MDT of >200 and a Maximum T_g value of >54°C for factor levels of PEG 4000 30-45%$^w/_v$, TEC 1-5%$^w/_v$ and SLS > 1.8g.

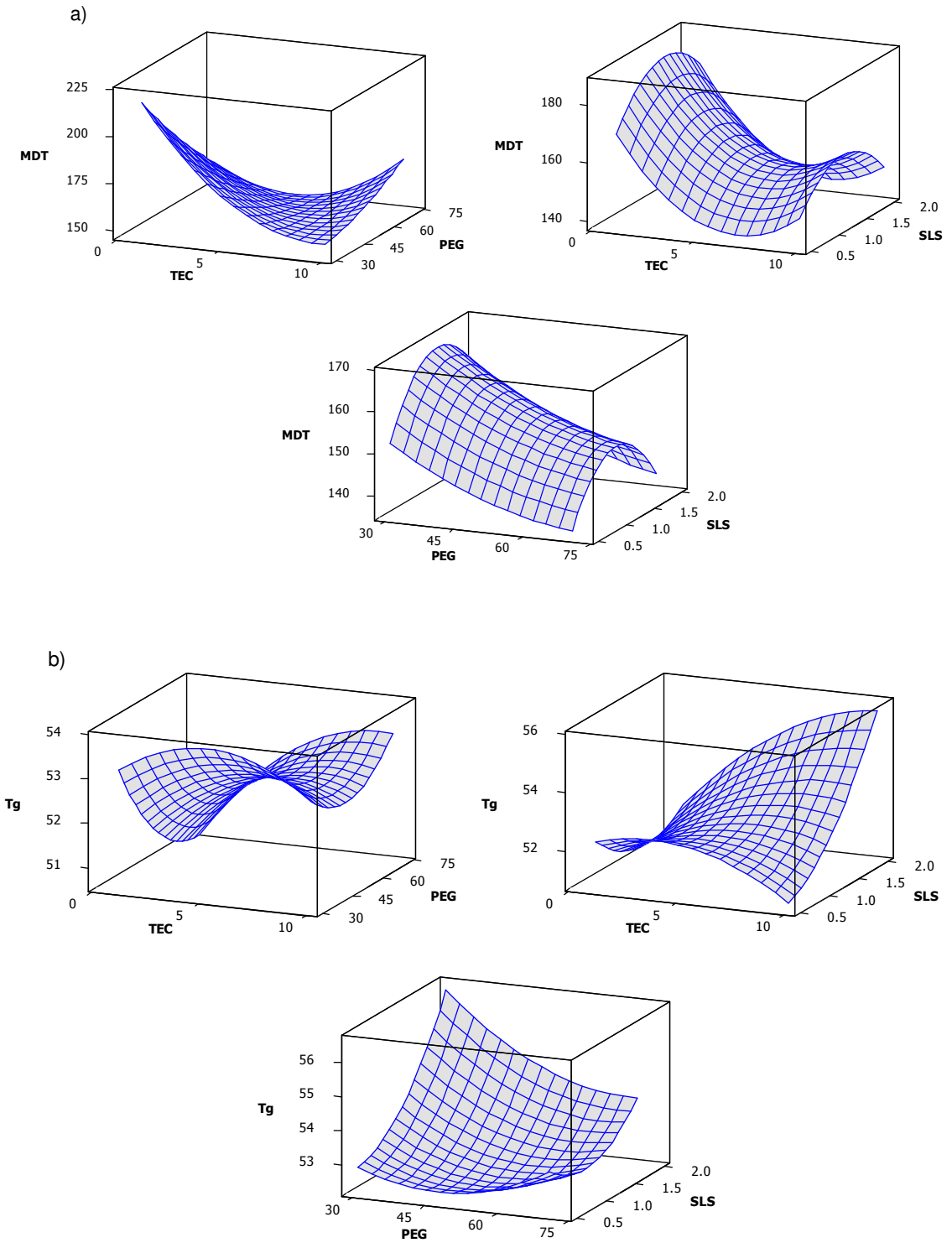


Figure 4.4 Illustration of the relationship between independent variables and the response of a) mean dissolution time (MDT) and b) glass transition temperature (T_g) through 3-D surface plots for the memblet system

Responses of MDT and DEE for the multiparticulate system were dependent upon the factors ethylcellulose, type of crosslinker (1= Ba^{2+}, 2= Mg^{2+} and 3= Ca^{2+}) and concentration of crosslinker shown in Figure 4.5a. As a function of DEE, when a maximum ethylcellulose

concentration (2g) is selected, a crosslinker concentration of (20%$^{w}/_{v}$) elucidates a 55% DEE. An indirect relationship exists between the factors as a decrease in crosslinker concentration with simultaneous increase in EC results in a positive effect on the response of DEE. TOC or type of crosslinker is displayed as 1 or Ba^{2+} for both an increase and decrease of EC and TOC respectively. From the collated data, a positive response of maximizing DEE is based on using Ba^{2+}, decreasing crosslinker concentration to 20%$^{w}/_{v}$ and increasing EC to 2g. Figure 4.5b revealed an optimal MDT value (>60) for crosslinker concentrations of between 20 and 30%$^{w}/_{v}$ and EC amounts of 2g revealing the indirect relationship between the factors. The effect on the MDT due to the TOC varied based on the co-factor i.e. Ca^{2+} when EC is 2g and Ba^{2+} when crosslinker concentration is between 20 and 30%$^{w}/_{v}$.

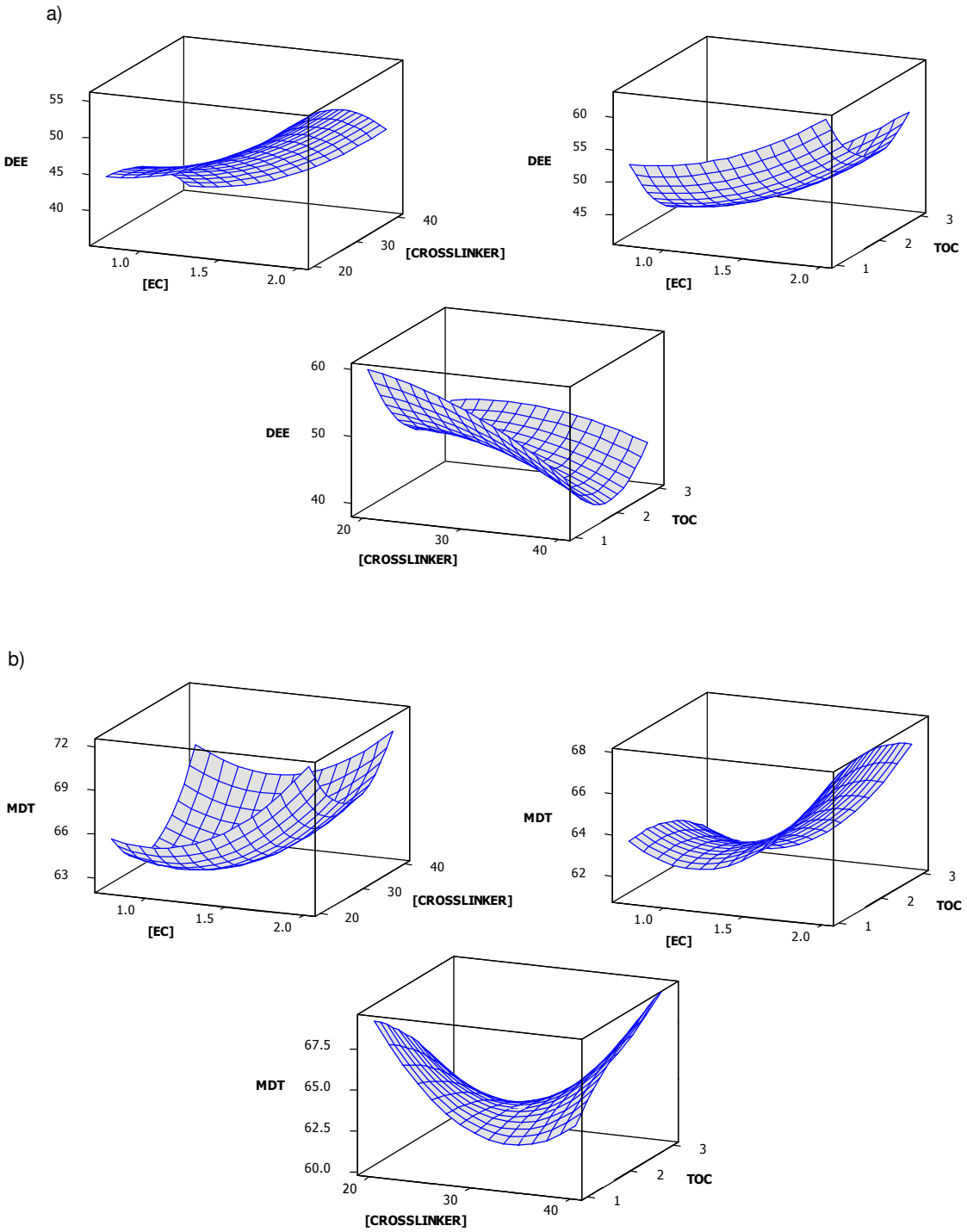


Figure 4.5 Illustration of the relationship between independent variables and the response of a) drug entrapment efficiency (DEE) and b) mean dissolution time (MDT) through 3-D surface plots for the multiparticulate system

4.2.4.2 Analysis of the box-behnken design through residual plots for optimization and subsequent response optimization of the once daily multi-unit system

Residual plots are model diagnostic plots which function to validate transformation of data (Singh *et al*., 2004). Specifically, 1 or more plots are used to investigate fit of the proposed model data to data collated and these plots are indicated in Figure 4.6 and Figure 4.8.

Residual analysis of data for the memblet system indicated an even distribution of data for T_g and MDT as illustrated in Figure 4.6a and Figure 4.6b respectively. The normal probability plots of the residuals showed a close distribution of data points along the medial line forming a linear curve. For the graph of residuals versus the fitted values, the plot tests the assumption of constant variance. Here desirable data points were obtained with a random and uniform scatter, with these data points close to the zero axis and validating the assumption of constant variance. Additionally, the histograms confirmed the assumption of constant variance and that the residuals had a normal distribution with zero mean. The plot of residuals versus the order of the data is a plot of residuals versus the order of the experimental runs. Traditionally, this graph is used to test for lurking variables that may have influenced responses and to identify non-random errors. The plots for both MDT and T_g showed a negative correlation through the alternating data points (alternating through positive and negative values), whilst the MDT plot indicated a concurrent positive correlation through clustering of formulations 6-11.

Through data capturing from selected experimental responses, an empirical mathematical model was formulated. This mathematical model functions to predict formulation responses based on independent variable input. Specifically, response surface modelling involves fitting the generated coefficients into the mathematical model equation of a particular response variable and mapping the response over the whole region of the experimental domain in the form of a surface (Singh *et al.*, 2004). ANOVA testing was adopted as a test of significance. The polynomial equation calculated the varying responses based on different variables used. A statistically significant effect is indicated by $p<0.001$ for any factor. The factor coefficients and their respective p values are depicted in Table 4.6 and the mathematical models generated for each component depicted in Equation 4.1 and Equation 4.2.

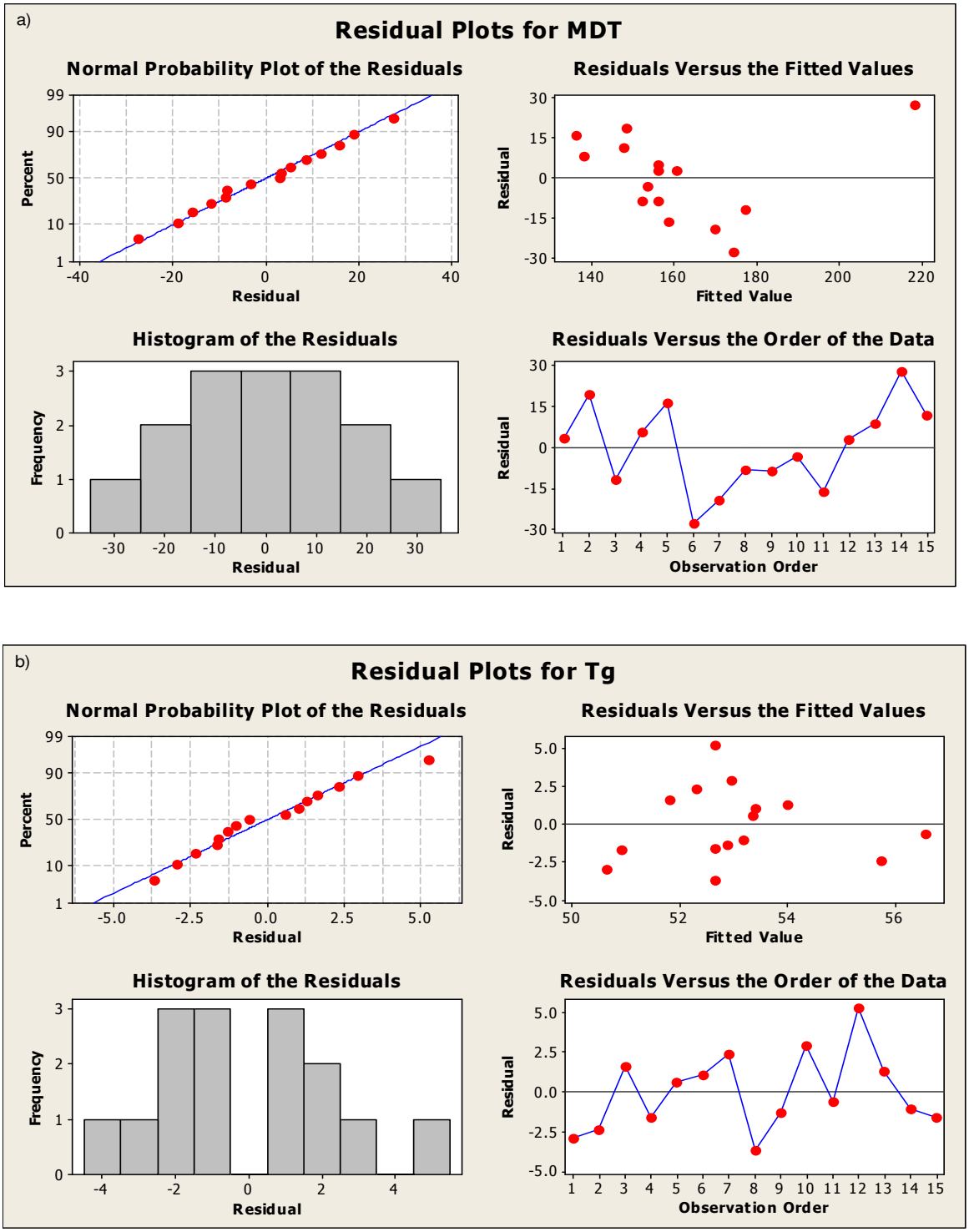


Figure 4.6 Residual plots of a) mean dissolution time (MDT) and b) glass transition (T_g) of the memblet system

Table 4.6 ANOVA analysis indicating factors for responses mean dissolution and glass transition and corresponding factor p values for the memblet system

Term	MDT factor coefficients	MDT factor *p* values	T_g factor coefficients	T_g factor *p* values
[TEC]	-12.785	0.218	+0.6325	0.680
[PEG]	-9.157	0.360	-0.5238	0.732
[SLS]	+1.970	0.837	+1.0813	0.488
[TEC]*[TEC]	+17.520	0.247	-0.8121	0.718
[PEG]* [PEG]	+2.977	0.833	+0.6854	0.760
[SLS]*[SLS]	-12.922	0.378	+0.8354	0.710
[TEC]*[PEG]	+19.651	0.187	+0.7450	0.730
[TEC]*[SLS]	-1.652	0.903	+1.3250	0.545
[PEG]*[SLS]	-1.130	0.933	-0.7575	0.726

[TEC]= triethyl citrate, [PEG]= polyethylene glycol, [SLS]= sodium lauryl sulphate, MDT= mean dissolution time and T_g= glass transition temperature

$$MDT = 156.140 - 12.785[TEC] - 9.157[PEG] + 1.970[SLS] + 17.520[TEC]^2 + 2.977[PEG]^2 - 12.922[SLS]^2 + 19.651[TEC \times PEG] - 1.652[TEC \times SLS] - 1.130[PEG \times SLS] \quad \textit{(Equation 4.1)}$$

$$T_g = 52.6767 + 0.6325[TEC] - 0.5238[PEG] + 1.0813[SLS] - 0.8121[TEC]^2 + 0.6854[PEG]^2 + 0.8354[SLS]^2 + 0.7450[TEC \times PEG] + 1.3250[TEC \times SLS] - 0.7575[PEG \times SLS] \quad \textit{(Equation 4.2)}$$

Regression Equation 4.1 and Equation 4.2 for the responses of mean dissolution time (MDT) and glass transition (T_g) for the memblet system.

Response optimization was finalized through MINITAB®, V14, Minitab, USA statistical software resulting in fixed levels for all factors to achieve optimal and desired responses. Response optimization sets of values (3), were achieved for the memblet system as seen in Figure 4.7 including a Hi, Lo and optimal set of factors. For the optimal set of factors, a desirability of 0.99848 was achieved indicating an optimal set of factor variables in which TEC= 1.6168mL, PEG= 30%$^{w}/_{v}$ and SLS= 1g. Predicted responses based on these optimal factor variables were:

MDT= 200.913 (Desirability= 1.00000)

T_g= 54.909℃ (Desirability= 0.99545)

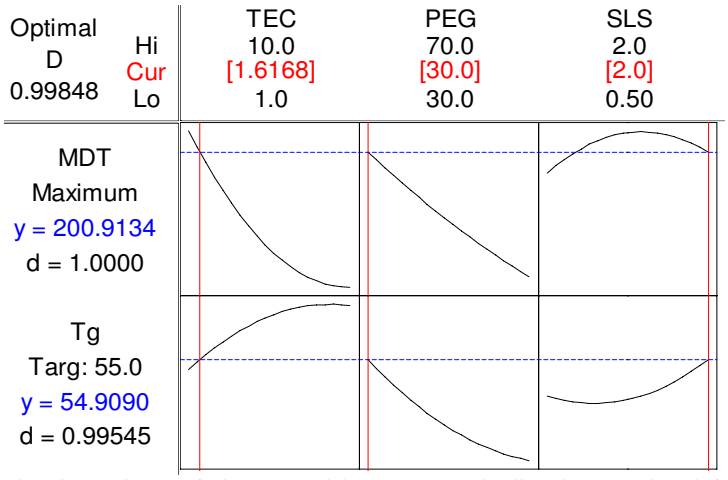


Figure 4.7 Optimization plots of the memblet system indicating optimal factors and factor levels and desirability

Residual analysis of data for the multiparticulate system revealed a similar even distribution of data for DEE and MDT illustrated in Figure 4.8a and Figure 4.8b respectively. The normal probability plots of the residuals showed a general close distribution of data points along the medial line with slight deviations indicating that the experimental values were analogous to predicted values. For the graph of residuals versus the fitted values, desirable data points were obtained with a random and uniform scatter with these data points close to the zero axis and validating the assumption of constant variance. The plots for both DEE and MDT showed a negative correlation through the alternating data points (alternating through positive and negative values). A statistically significant effect is indicated by $p<0.001$ for any factor. The factor coefficients and their respective p values are depicted in Table 4.7 and the mathematical models generated for MDT and DEE are shown in Equation 4.3 and Equation 4.4 respectively.

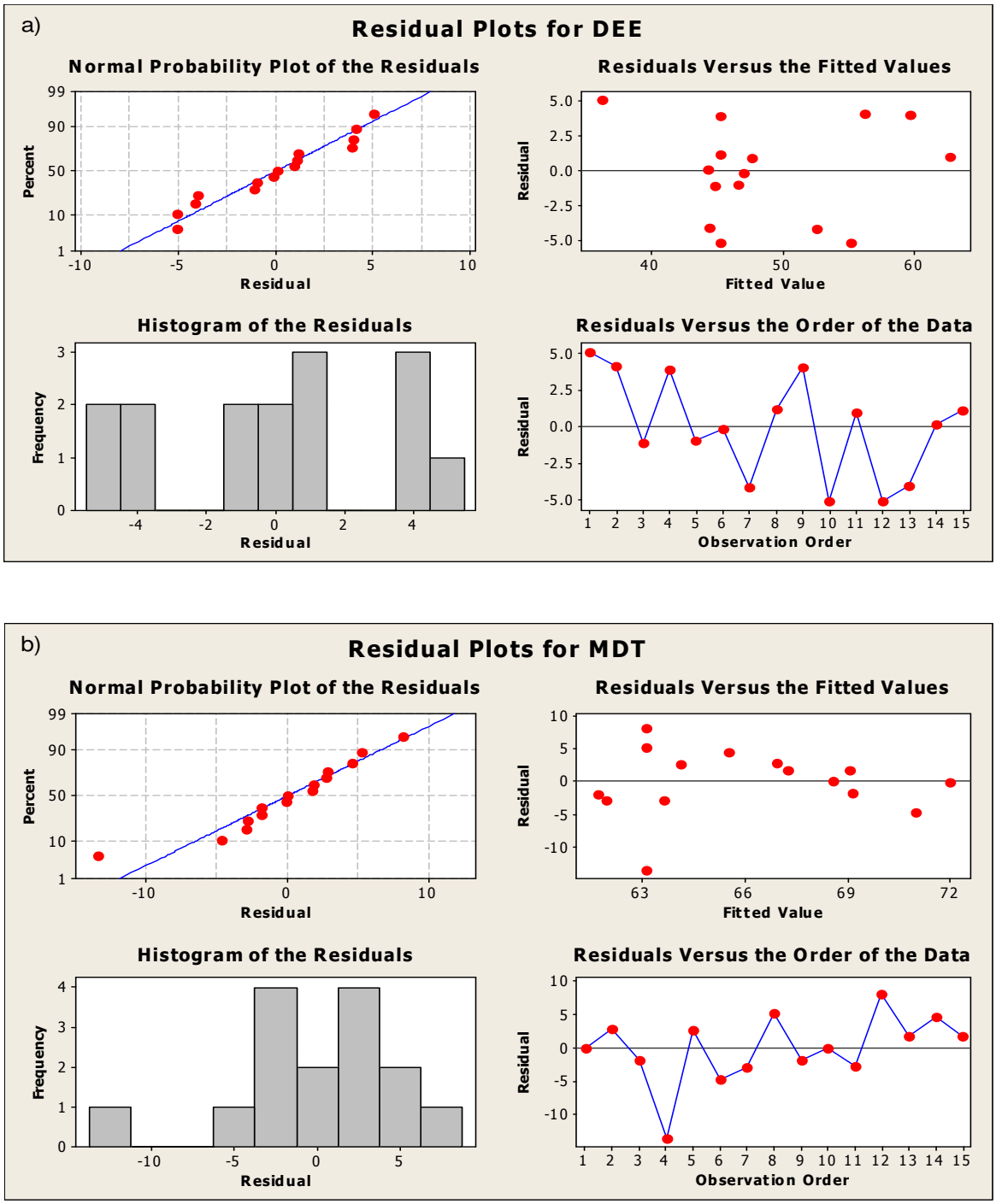


Figure 4.8 Residual plots of a) drug entrapment efficiency (DEE) and b) mean dissolution time (MDT) of the multiparticulate system

Table 4.7 ANOVA analysis indicating factors for responses drug entrapment efficiency and mean dissolution time and the corresponding factor p values for the multiparticulate component of the Once Daily Multi-Unit System

Term	DEE factor coefficients	DEE factor *p* values	MDT factor coefficients	MDT factor *p* values
[EC]	+5.3952	0.045	+2.2154	0.495
[CROSSLINKER]	-4.0495	0.103	+0.5148	0.871
[TOC]	-3.5343	0.143	-0.5550	0.861
[EC]*[EC]	+2.4897	0.444	+2.4993	0.598
[CROSSLINKER]* [CROSSLINKER]	-1.9836	0.537	+3.6817	0.445
[TOC]*[TOC]	+6.3679	0.087	-0.7095	0.879
[EC]*[CROSSLINKER]	-0.0141	0.996	-1.0155	0.821
[EC]*[TOC]	+0.3195	0.916	+0.3952	0.930
[CROSSLINKER]*[TOC]	+2.4526	0.433	+3.0357	0.508

[EC]= ethyl cellulose, [CROSSLINKER]= concentration of crosslinker, [TOC]= type of crosslinker, DEE= drug entrapment efficiency and MDT= mean dissolution time

$$MDT = 63.0908 + 2.2154[EC] + 0.5148[CROSSLINKER] - 0.5550[TOC] + 2.4993[EC]^2 + 3.6817[CROSSLINKER]^2 - 0.7095[TOC]^2 - 1.0155[EC \times CROSSLINKER] + 0.3952[EC \times TOC] + 3.0357[CROSSLINKER \times TOC] \quad \text{(Equation 4.3)}$$

$$DEE = 45.2214 + 5.3952[EC] - 4.0495[CROSSLINKER] - 3.5343[TOC] + 2.4897[EC]^2 - 1.9836[CROSSLINKER]^2 + 6.3679[TOC]^2 - 0.0141[EC \times CROSSLINKER] + 0.3195[EC \times TOC] + 2.4526[CROSSLINKER] \times [TOC] \quad \text{(Equation 4.4)}$$

Regression Equation 4.3 and Equation 4.4 for the responses of mean dissolution time and drug entrapment efficiency for the multiparticulate system.

Response optimization was achieved through MINITAB®, V14, Minitab, USA statistical software producing optimal levels for all factors to achieve optimal and desired responses of MDT and DEE. A total of 3 response optimization sets of values were achieved for the multiparticulate system as seen in Figure 4.9 including a Hi, Lo and optimal set of factors. For the optimal set of factors, a desirability of 1.0000 was achieved authenticating optimal factor levels for maximal responses. Predicted responses based on these optimal factor variables were:

DEE= 67.2216% (Desirability= 1.00000)

MDT= 74.4739 (Desirability= 1.00000)

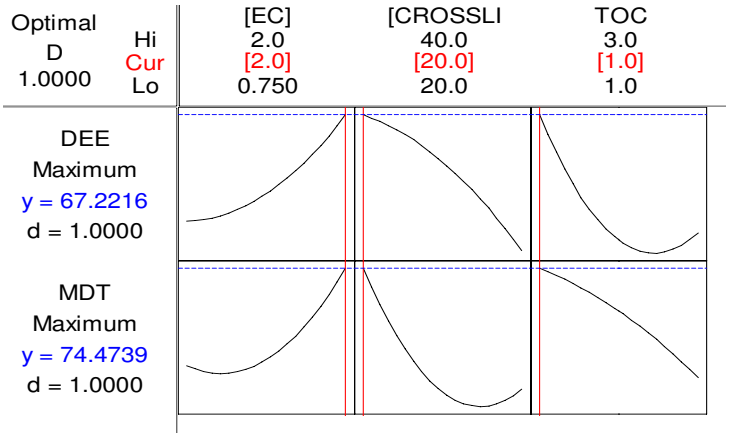


Figure 4.9 Optimization plots of the multiparticulate system indicating optimal factors and factor levels and desirability

4.3 Concluding Remarks

The purpose of Chapter 4 was to achieve an optimal set of formulation variables or independent factors for both the memblet and multiparticulate components of the ODMUS. A design of experiments proved to be an authentic methodology for the clarification of optimal formulation variables. Varying statistical analysis methods were chosen, employed and comparatively scrutinized to produce the variables and to ensure verification and validity of these produced factors in relation to the optimal responses.

The memblet system optimized formulation variables of TEC, PEG and SLS with a desirability of 0.99848 in which TEC= 1.6168mL, PEG= 30%$^{w}/_{v}$ and SLS= 1g. Predicted responses based on these optimal factor variables were an MDT= 200.913 (Desirability= 1.00000) and T_g= 54.909℃ (Desirability= 0.99545). During the optimization process, SLS was found to have very little impact on the formulation responses relative to the large effect produced on both MDT and T_g for both TEC and PEG.

A desirability of 1.00000 for the multiparticulate system expressed the confidence in the formulation variables [EC],[CROSSLINKER] and [TOC]. As indicated through testing, EC was to be maximized to achieve and optimal response for both DEE and MDT and the concentration of the crosslinker was between 20-30%$^{w}/_{v}$ for the same responses. The type of crosslinker varied on the response and consequently the most desired responses were achieved through EC= 2.0g, [CROSSLINKER]= 20%$^{w}/_{v}$ and [TOC]= Ba^{2+}. Predicted responses generated were an MDT= 74.4739 (Desirability= 1.00000) and DEE= 67.2216% (Desirability= 1.00000).

Both components achieved a high desirability for all levels of factors. The following Chapters shall delve into the full and relevant analytical testing as per component of the ODMUS.

CHAPTER 5
FORMULATION AND INVESTIGATION OF AN OPTIMIZED RIFAMPICIN-LOADED ORAL MEMBRANOUS SYSTEM FOR TARGETED DRUG DELIVERY TO THE STOMACH

5.1 Introduction

When considering non-invasive delivery systems, the oral route is generally preferable when considering site-specific drug release, patient compliance, ease of administration and patient acceptance (Sastry *et al*., 2000; Sangalli *et al*., 2001; Weidner, 2001). Past research has explored the oral dosage form in ardour to obtain a succinct design that amalgamates method simplicity and design efficacy. The tenuous balance between theses desired factors has always been difficult to achieve. Membranous/hydrogel delivery systems have been thoroughly investigated (Peppas *et al*., 2000; Lee and Mooney, 2001; Kim *et al*., 2007) and could potentially achieve this balance between formulation method simplicity and efficacy. In retrospect, many studies have achieved efficacy but are unable to yield basic method parameters and periodically involve complex procedures (Chun *et al.,* 2005; Lin and Metters, 2006; Bae *et al*., 2008; Huynh *et al*., 2008). Oral membranous systems however remain preferred delivery systems for therapeutic agents (Knuth *et al*., 1993; Lin *et al*., 2008; Ma and McHugh, 2008) with much success in their respective applications. Standard protocol implies that oral membranous/hydrogel systems should be biodegradable or biocompatible with impetus placed upon excluding toxicity (Mandal *et al*., 2009).

The memblet delivery system achieved equilibrium in both method simplification and site-specific, segregated drug delivery. The novelty of the system lies in the innovative manipulation of the taste masking agent Eudragit® E 100 by crosslinking the cationic methacrylate functional moiety with the anionic polyethylene glycol 4000 to produce a crosslinked hydrogel. This single process step provides an attractive methodology compared to its membranous predecessors fabrication procedures and significantly decreases formulation time. The dried, drug-loaded, compressed and optimized memblet was placed under investigation in this Chapter.

Previous Chapters focused on preliminary studies and a rudimentary understanding of the novel system and optimizing the fabrication of the system. This Chapter aimed to fully characterise the memblet through rheological, thermal, textural and surface morphological understanding. Scrutiny was placed on the memblet*'s* efficacy for drug release, elucidated through the acidic pH of the stomach through dissolution studies. An in depth molecular

examination was conducted to understand the role the molecular structure induced on the memblet.

5.2 Materials and Methods

5.2.1 Materials

Eudragit® E 100 was kindly supplied by Evonik Degussa Africa (Pty) Ltd (Evonik Degussa Africa (Pty) Ltd. (Midrand, Gauteng, South Africa) while polyethylene glycol 4000 (PEG 4000) was purchased from Merck chemicals (Merck chemicals, Halfway House, Gauteng, South Africa). Acetone, triethyl citrate (TEC), isopropyl alcohol, sodium lauryl sulphate (SLS) and tween 80 were all of analytical grade and employed as purchased. Water was purified by a MilliQ Millipore water purification system (Milli-Q, Millipore, Billerica, MA, USA). Rifampicin was of analytical quality Sigma Aldrich.Inc (Pty) Ltd. (St Louis, MO, USA).

5.2.2 Fabrication of the optimized crosslinked memblet for gastric drug release

For fabrication of a memblet, 34%$^{v}/_{v}$ of acetone, 46.9%$^{v}/_{v}$ of isopropyl alcohol and 1.8%$^{v}/_{v}$ of de-ionized water were measured and added to a 200mL beaker. Affectively, 13.6%$^{w}/_{v}$ of the Eudragit® E 100 polymer was gradually added to the aforementioned latex with constant agitation employing a magnetic stirrer at room temperature (21°C) for 1 hour. This was left under agitation until all the Eudragit® E 100 beads were completely dissolved. TEC (1.6168mL) and the remaining constituents [tween 80 (4g) and SLS (1g)] were gradually added to the latex and left to stir for approximately an hour. Simultaneously a 30%$^{w}/_{v}$ (the optimized formulation) and 60%$^{w}/_{v}$ (a control sample) PEG 4000 solutions were prepared. A measured 5mL of the Eudragit® E 100 latex was drawn up and expelled through a syringe into both solutions. Crosslinking resulted in hydrogel A (optimized) and B (control), which were subsequently left to cure in their respective solutions for 20 minutes. Following the curing, samples were washed 3 times in 500mL de-ionized water before storage in a desiccant jar (using silica crystals) for 10 days of drying time. The dried membranes were then ground using a standard coffee grinder and the powder obtained was mixed with 150mg of rifampicin. Subsequently, compression of the mixed powders resulted into the tablet like structure termed the memblet.

5.2.3.1 Rheological principles for the assessment of a novel semisolid Eudragit® E 100 based memblet system

The memblet system has the potential to undergo deformation and flow with the addition of heat, as was determined through the basic DSC preliminary analysis in Chapter 3.5.5.2 which conveyed a glass transition temperature below 100°C (52.12°C). Rheological analysis was crucial in determining deformation and flow due to a shear rate and a shear force. The

consistency of the memblet could potentially oscillate between solid and liquid based on a shear force and shear rate, due its semisolid nature complicating and impeding standard rheological characterization techniques. The viscoelastic nature of the memblet was to be evaluated and defined through the more powerful dynamic oscillatory testing.

Traditionally, a basic curve of viscosity (n) versus shear rate (*Y*) garners crucial information with regards to storage and optimizing method parameters in bulk manufacturing (Herh *et al*., 1998). Basic flow curves derived from these parameters include Newtonian Flow, Dilatant Flow, and Pseudoplastic Flow curves which have been employed to indicate how structure changes occur to comply with shear forces under storage conditions, processing and during the pharmaceutical products use. For characterization purposes of the memblet, further testing through more intricate and powerful analyses have been developed.

The basic Law of Viscometry described by Isaac Newton defines the ideal flow properties of a liquid as:

$$\tau = n.Y \qquad \textit{(Equation 5.1)}$$

Where, τ is expressed as shear stress, *n* as viscosity and *Y* as the shear rate (Schramm, 2004).

Shear force can be defined as a force applied tangentially to an area between the interface of the measuring plate and the sample tested (memblet*)*.

The following equation depicts shear stress or τ :

$$\tau = \frac{F}{A} \qquad \textit{(Equation 5.2)}$$

Where, *F*= force in Newton's and *A*= area in m^2 (Schramm, 2004).

As a shear force is applied to a system, a flow speed is concurrently associated with the sample. From the superficial layer of the sample, the flow rate begins to decreases the lower the layer due to the displaced tangential force. Laminar flow is described which states that infinitesimally thin liquid layers slide on top of each other. This decrease in velocity is termed the shear rate or *Y.* For the purposes of rheometric analysis *Y* is expressed as:

$$\dot{\gamma} = \frac{v_{max}}{y} \qquad \textit{(Equation 5.3)}$$

Where V_{max}= the velocity of flow at that particular layer of sample and y= the gap size between the measuring plate and the stationary lower plate (Schramm, 2004).

For the purposes of rotational rheometry with a *Thermohaake* Rheometer, a rotating cone or cylinder sensor system is utilized to generate the basic parameters of shear rate, shear force and viscosity. The shear stress applied allows the cone to only rotate at a particular speed or shear rate according to the applied shear force. This is inversely proportional to the viscosity of the sample. The individualized mathematical equations used to interpolate data points through the sensor from the sample between the cone and the stationary plate are depicted accordingly:

$$\dot{\gamma} = \frac{1}{\tan\alpha} \times \omega = M.\omega[s^{-1}] \qquad \textit{(Equation 5.4)}$$

Where $\dot{\gamma}$= shear rate, α= cone angle (C35/1° Ti cone), M= shear rate factor [1/rad], $M = \frac{1}{\tan\alpha} \approx \frac{1}{\alpha}$, $\omega = \frac{2\pi.n}{60}$, ω = angular velocity (rad/s) and n = rotor speed (rev.min^{-1})

$$T_c = [\frac{3}{2\pi R_c^3}] \times M_d = A.M_d \qquad \textit{(Equation 5.5)}$$

Where τ_c= shear stress on the cone, R_c= outer radius of the cone, M_d= Torque to be measured and A= shear stress factor (Schramm, 2004).

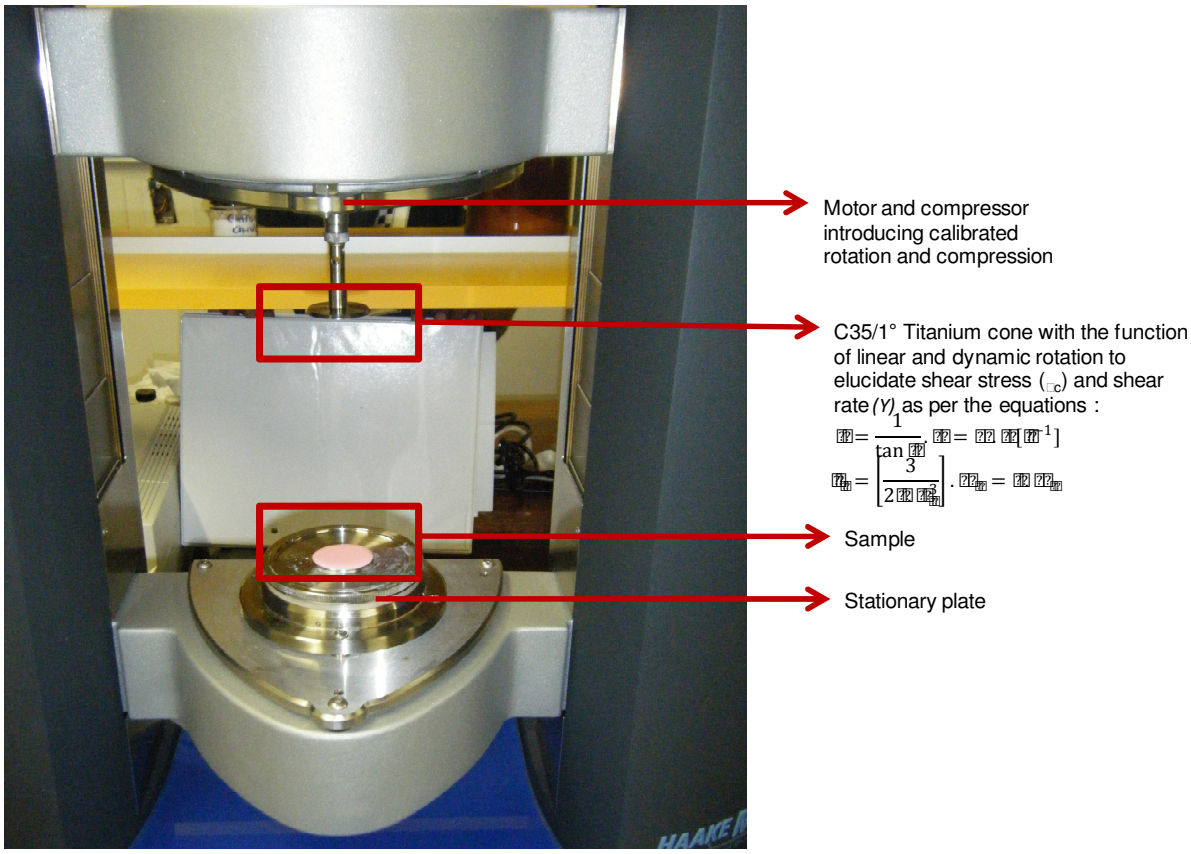


Figure 5.1 Thermohaake rheometer used in the analyses of rheometric parameters for the memblet

Yield stress (measured in Ƭ or Pa) is defined as the minimal shear force/stress required to induce deformation or flow. It is only an estimation of the force required as this is a time dependent test (Herh *et al.*, 1998), but the relevance for preliminary understanding of the memblet system is pertinent. Below the yield stress, deformation occurs in a linear manner with an increase in shear stress and the viscoelastic sample (in this case the memblet) is categorized as a solid. Above the critical yield value, the sample undergoes unlimited deformation and flows.

Dynamic oscillatory experiments subject the test sample to sinusoidal stress and this is a non-destructive test unlike the yield stress test. The term non-destructive implies that the internal structure of the sample will remain unchanged for the duration of the test. The cone rather than turning in a unidirectional manner, oscillates at a pre-determined frequency dependent sinusoidal time function which imparts the same sinusoidal shear strain on the sample in a non destructive manner producing a time dependent strain:

$$\tau = \tau_0 \sin(\omega.t) \qquad \textit{(Equation 5.6)}$$

Where, τ_0 = the amplitude of the stress, ω= angular velocity and *t*= time (Schramm, 2004). The amplitude of the resulting stress and the phase angle between the imposed stress and the strain are the data points derived. Benefits of this test can be correlated to the memblet as this specific test can gather information on material that cannot be sheared due to their 3-D structure, as in the case of hydrogels. As the experiment is running, the stress applied leads to a deformation. Due to the elastic and viscous properties of the sample, the amplitude of deformation is not reached at the same time as the stress amplitude. There is thus a phase shift between stress and deformation referred to as a phase shift angle or δ.

Pure elastic materials have a phase shift of 0° (stress and strain are in phase) and pure viscous samples exhibit a phase shift of 90° (a 90° out of phase stress). Viscoelastic materials exist between 0-90°. The following equation incorporates the above data into the stress equation used in dynamic oscillation studies:

$$\tau = \tau_0 \quad sin(\omega.t + \delta) \qquad \textit{(Equation 5.7)}$$

Where, τ = stress, τ_0 = amplitude of stress, ω= angular velocity, t= time and *δ*= phase shift.

ω= 2π.*f* where *f*= frequency of oscillation (Schramm, 2004).

Dynamic oscillation studies concurrently introduces the concept of the complex modulus or G* which indicates the total resistance of a testing material against the applied strain and is derived from the amplitude of stress (τ_0) and the amplitude of deformation (Y_0) depicted in Equation 5.8 *(*Schramm, 2004).

$$G^* = \frac{\tau_0}{Y_0} \qquad \textit{(Equation 5.8)}$$

Once a test material is subjected to sinusoidal oscillation, the sample can potentially undergo elastic energy storage (storage modulus or G'), viscous energy dissipation (loss modulus or G'') or more commonly, a combination of both. The storage modulus implies the stress energy stored in a transitory manner for the duration of an oscillatory test with the ability of recovery of said energy upon completion of the study. Conversely, the loss modulus describes energy used to induce flow and impart deformation and consequently irreversibly transforming into heat. Both, energy states are dependent upon the phase shift and the complex modulus. Utilizing the Theorem of Pythagoras in Figure 5.2, equations for both storage and loss moduli have been produced in Equation 5.9 and Equation 5.10:

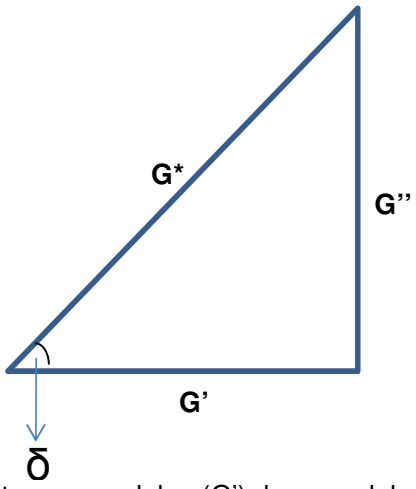


Figure 5.2 Inter-relations of storage modulus (G'), loss modulus (G''), complex modulus (G*) and the phase shift through the Pythagorean Theorem

$$G' = G^* \cos\delta \qquad \textit{(Equation 5.9)}$$

$$G'' = G^* \sin\delta \qquad \textit{(Equation 5.10)}$$

5.2.3.2 Rheological testing of crosslinked hydrogels prior to drying

Rheological measurements were performed on a MAARS Thermohaak Rheometer (THERMO HAAKE, modular advanced rheometer system, LASEC South Africa). A 1^{o} 35mm titanium cone was used for standard rotational studies (yield stress test) and dynamic oscillatory measurements (stress and frequency sweeps in which there is the constant application of sinusoidal shear stress). Samples tested included the Eudragit® E 100 latex prior to crosslinking and crosslinked hydrogels A and B prior to drying through a desiccant jar. The hydrogels (A and B) were used for no more than 2 tests before a fresh sample had to be prepared and all tests were conducted in triplicate (N= 3). Separate testing parameters were chosen for each of the samples (latex and hydrogel) as depicted in Table 5.1. Upon reaching full dispersion, the latex was poured directly onto the rheometer plate for analysis.

Sample preparation for the hydrogel involved a far more intricate method. Methods proposed in previous studies include the use of sand paper glued to the parallel plates with the gap size set 2mm to account for the thickness of the sample (Roger *et al*., 2008; Sozer, 2008).

The method was replicated but proved unsuccessful as the hydrogel was deformed by the sand paper and though slippage of the memblet was prevented, the required gap size of 0.051mm was not reached. A successful method was developed by using the cone of the rheometer to compress the sample thrice with ample recovery time between compressions,

until the sample was of a uniform surface area to reach the required gap size without detrimental deformation. Samples were coated with petroleum jelly to prevent excess water loss during the test.

Table 5.1 Method parameters for yield test, stress sweep and frequency sweep tests

Yield test	**E 100 Latex**	**Hydrogel A**	**Hydrogel B**
Temp (ºC)	20	20	20
Ƭ start (Pa)	0	0	0
Ƭ end(Pa)	5	100	400
Duration (s)	200	200	200
Stress Sweep	**-**	**Hydrogel A**	**Hydrogel B**
Temp (ºC)	-	20	20
Ƭ start (Pa)	-	0	0
Ƭ end (Pa)	-	100	100
Frequency (Hz)	-	1	0.1
Steps	-	20	20
Frequency Sweep	**-**	**Hydrogel A**	**Hydrogel B**
Temp (ºC)	-	20	20
Fixed Ƭ (Pa)	-	6.5	6.5
Start Freq (Hz)	-	1	1
End Freq (Hz)	-	0.01	0.01

5.2.4 Assessment of the surface morphology and inter- and intra-polymeric interactions of the memblet

Surface morphology was characterized by a FEI PHENOM integrated scanning electron microscope system (Hillsboro OR 97124-5793 USA). Samples were mounted onto a metal stub prior to analysis.

Fourier Transmission Infrared Spectroscopy (FTIR) was performed on the individual polymers being Eudragit® E100 and PEG 4000 prior to memblet analysis. Samples were analyzed with a Spectrum 2000 FTIR spectrometer with a MIRTGS detector (PerkinElmer Spectrum 100, Beaconsfield, UK). The spectrum was a ratio spectrum of 16 sample scans against 16 ranging from 4000-650cm^{-1}.

5.2.5 Mechanical evaluation of the memblet system

Textural profiling was conducted with a Texture Analyzer (TA.XT*plus,* Stable Microsystems, Surrey, UK) to evaluate memblet deformation energy, flexibility and resilience. For deformation energy and memblet flexibility, a flat steel probe was used to puncture the memblet matrix. A cylindrical probe, which applied surface pressure to the memblet, determined matrix resilience. Table 5.2 shows the parameters chosen for each study.

Table 5.2 Parameters for flexibility, deformation energy and resilience testing

Parameters	Flexibility (N.mm)	Deformation Energy (J)	Resilience (%)
Pre-test speed	1mm/sec	1mm/sec	1mm/sec
Test speed	0.5mm/sec	0.5mm/sec	0.5mm/sec
Post-test speed	1mm/sec	1mm/sec	1mm/sec
Compression Force	40N	40N	-
Trigger type	Auto	Auto	Auto
Trigger Force	0.05N	0.05N	0.05N
Load cell	5kg	5kg	5kg

5.2.6 Thermal analysis of crosslinked polymethacrylate based memblet*s*

Thermal analysis was conducted on a *DSC1* STAR^e system (Mettler Toledo DSC1, STAR$_e$ System, Switzerland).Testing of memblet*s* were conducted using both Differential Scanning Calorimetry (DSC) and Alternating Differential Scanning Calorimetry (ADSC). All samples were prepared in 40µl aluminum crucibles. DSC was conducted using a temperature range of 0-200℃ and ramped at 10℃ per minute. ADSC was carried out with an underlying heating rate of 1℃ per minute and a modulated temperature of 0.1℃ per 0.8 minutes. All samples were run in duplicate (N= 2).

5.2.7 *In vitro* drug release of a polyethylene glycol 4000 crosslinked polymethacrylate based memblet system

Drug release studies were conducted following the USP 33 apparatus II (ERWEKA DT 700 GmbH Germany), in which a single memblet in triplicate (N= 3) was placed within the vessel under a stainless steel ring mesh assembly, to prevent the paddle inflicting physical/mechanical damage to the spheres and alter release profiles as well as to prevent erratic fluctuation due to unstable hydrodynamics (Pillay and Fassihi, 2000). Each vessel was filled with 900mL simulated gastric fluid (SGF) and heated to a temperature of 37℃ prior to the addition of the memblet and the stainless steel ring mesh assembly. The rotating paddle method was selected at a rotational speed of 50rpm and the machine was calibrated for a 2 hour run with samples taken at half hourly intervals. Sampling involved the drawing of 5mL of now drug incorporated solution from the dissolution vessel with subsequent refilling of removed buffer to maintain sink conditions. Samples were then subject to UV spectroscopy using a spectrophotometer (Cecil CE 3021, Cambridge, CB24 6AZ, England).

5.3 Results and Discussion

5.3.1 Rheological analysis of crosslinked hydrogels prior to desiccation and memblet formation

5.3.1.1 Determination of the critical yield point for a polymethacrylate based latex and novel crosslinked interpolyelectrolyte complex hydrogels

Rheological evaluation was conducted on the Eudragit® E 100 latex prior to crosslinking to assess whether the latex was being produced in an accurate and reproducible manner. In previous studies an inconsistently formulated hydrogel matrix resulted in erratic membrane formation and non-reproducible results. Latex solutions of 10mL were crosslinked and cured in their respective crosslinking PEG solutions of 30%$^{w}/_{v}$ and 60%$^{w}/_{v}$ for hydrogel A (optimized) and B (control) respectively.

Yield stresses for all samples are plotted in Figure 5.3. Typical latex samples showed very similar critical yield points. Yield stress tests resulted in an average critical yield point of 0.36Pa that correlates to the viscous nature of the latex. The consistent yield point can be attributed to the astringent and meticulous method used for preparing the latex each time. Uniform dispersion was achieved through vigorous stirring protocols and through a gradual addition of constituents. It could be postulated that there were no major and highly altering physico-chemical interactions and that the distribution of the particles was isotropic. No mechanical alteration or damage to the latex was incurred. All samples had very similar deformation (Y) points at the 57.73Y region, indicating that this is the region at which the latex behaved in a very fluid-like manner.

For analysis of hydrogels, the critical yield point was determined to assess maximal crosslinking potential of the novel membranous system subsequent to the drying protocol. Critical yield points are dependent upon formulation parameters such as type of crosslinker, crosslinker concentration and temperature. Yield stress curves for hydrogels A and B varied in that hydrogel B achieved a greater critical yield point, 14.94Pa, than hydrogel A, 5.23Pa (Figure 5.3). This can be explained with an understanding of the properties of hydrogels. Hydrogels are defined as 3-dimensional, hydrophilic polymer networks, which when in their swollen state, have the capability to retain water and swell to a much larger size than their original state. Furthermore, hydrogels are insoluble in water due to chemical or physical crosslinking that has occurred. Physical ionic crosslinking has occurred between PEG's ether functional group (anionic) and Eudragit® E 100's dimethyl aminoethyl methacrylate functional group (cationic) resulting in an interpolyelectrolyte complex hydrogel. Hydrogel B consisted

of a higher degree of saturation of functional groups, with regards to crosslinking, and resulted in a dense accumulation of polyethylene glycol to produce a more rigid structure. In addition, there may have been fewer free functional groups along the polymeric backbone of hydrogel B (as compared to hydrogel A) due to the higher degree of crosslinking in the 60%$^{w}/_{v}$ PEG solution impeding the polymeric backbone's mobility. This dense accumulation of polymeric material rendered hydrogel B less flexible rheologically. Both factors resulted in retarded molecular mobility. Molecular movement described by a lower critical yield point of 5.23Pa, due to the fewer free functional groups, was improved in hydrogel A, indicating a more flexible and versatile formulation.

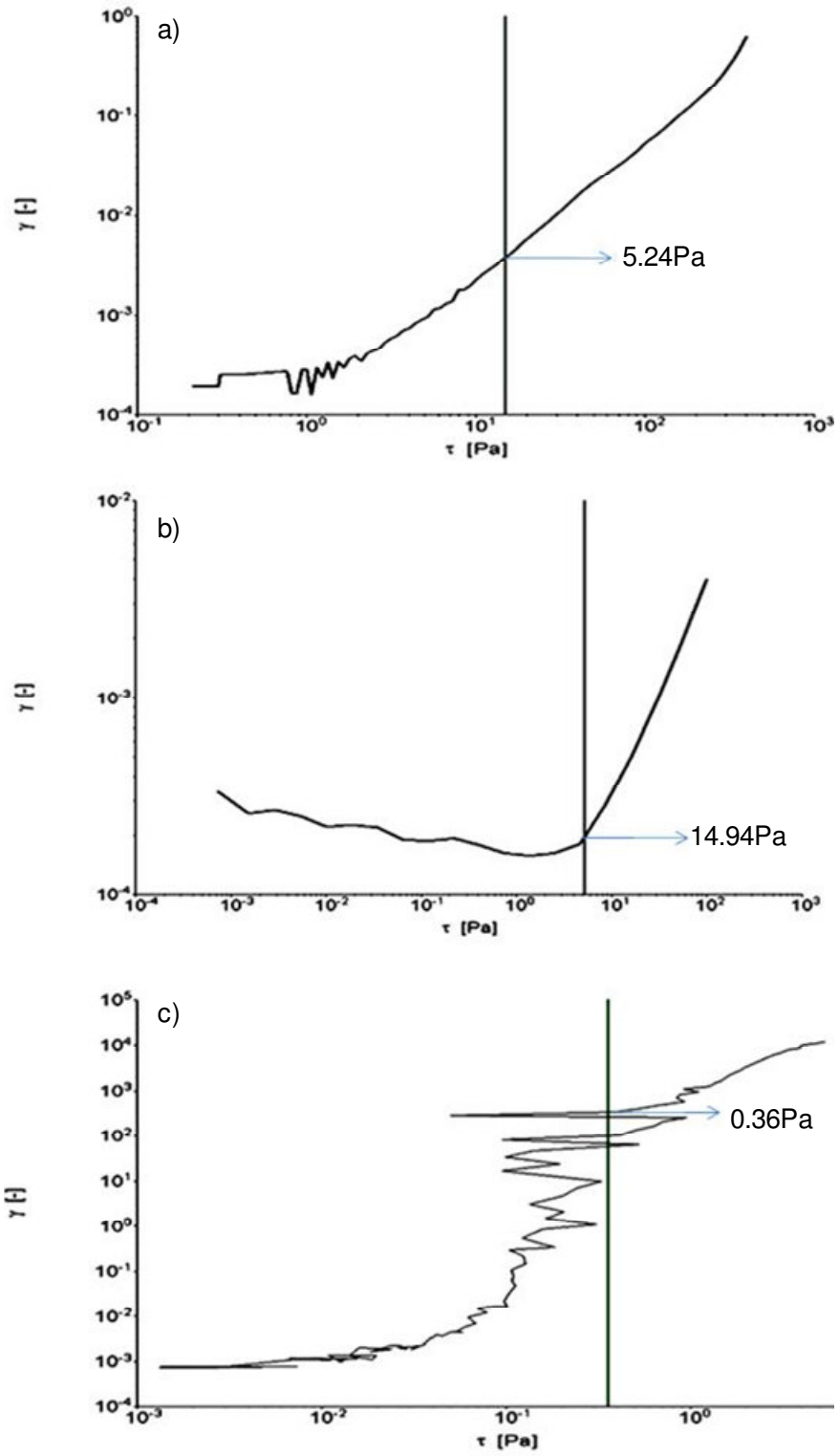


Figure 5.3 Yield stress curves for a) hydrogel A b) hydrogel B and c) the latex prior to crosslinking to indicate the critical yield point (Pa)

5.3.1.2 Viscoelastic evaluation through stress sweep curves of novel crosslinked polyelectrolyte-complex hydrogels

The viscoelastic region for each hydrogel was determined such that a value for input into the frequency sweep curves to generate values of G' (storage modulus) and G'' (loss modulus) could be obtained. The stress sweep curves illustrated the viscoelastic regions for hydrogels as shown in Figure 5.4. The presence of a viscoelastic region in both samples confirmed that the hydrogel was a viscoelastic or semisolid material displaying both solid and liquid properties. Such data is crucial in understanding the final memblet's stability as a drug delivery system. Hydrogel B demonstrated a viscoelastic region below 10.67Pa and hydrogel A below 2.542Pa, corroborating with the findings in yield stress that flexibility and versatility was improved with for the optimized formulation with a lowered crosslinker concentration (30%$^{w}/_{v}$).

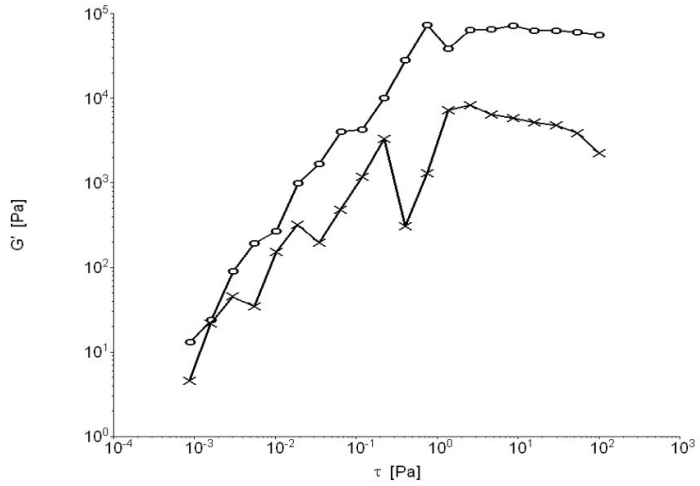


Figure 5.4 Viscoelastic regions of hydrogel B (- 0) and hydrogel A (- X)

5.3.1.3 Determination of the storage and loss modulus of novel crosslinked polyelectrolyte-complex hydrogels

The semi-solid hydrogels used in the testing were evaluated and found to encompass viscoelastic properties through the stress sweep curves. As such the hydrogels of samples A and B displayed both elastic (solid) and viscous (liquid) properties which can be determined simultaneously through frequency sweep tests. In testing both samples, frequency ranges of 1-0.01Hz and a τ value of 6.5Pa were chosen to assess the effect on loss and storage moduli for both samples at the same parameters. For a frequency sweep test, G' is a measure of the deformation energy stored within a sample during the shearing process. G' is therefore a measure of the elastic (solid) nature of the sample. G'' is a measure of deformation energy used in the sample during the shearing process and lost to the sample afterwards, making G'' a measure of the viscous (liquid) nature of the sample.

Figure 5.5 depicts very different rheological responses for hydrogels A and B with the same testing parameters. Hydrogel B has a continuous curve in which G' is constantly above G''. This is indicative of a solid, immobile and rigid structure for all of the frequency ranges and with no G' / G'' crossover. Within the testing parameters, the formulation remains rigid for all shear rates and shear forces. The accumulation and saturation of PEG 4000 results in a rigid membrane, which would require larger shear forces to achieve the desired mobility. Hydrogel A however can be described as having gel like properties (Lee and Anema, 2009). At the same testing parameters, hydrogel A displayed the converse of hydrogel B with G'' being above G' for all frequency ranges indicating highly mobile characteristics. Such a curve was obtained due to a lower saturation of free bonds in hydrogel A as compared to hydrogel B. The formation of bonds between functional groups of both Eudragit® E 100 and PEG 4000 were evenly distributed within the optimized hydrogel due to a lower crosslinker concentration of 30%$^{w}/_{v}$. This enhanced flexibility and improved rheological properties promote the use of a lower concentration of crosslinker in comparison to high crosslinker content.

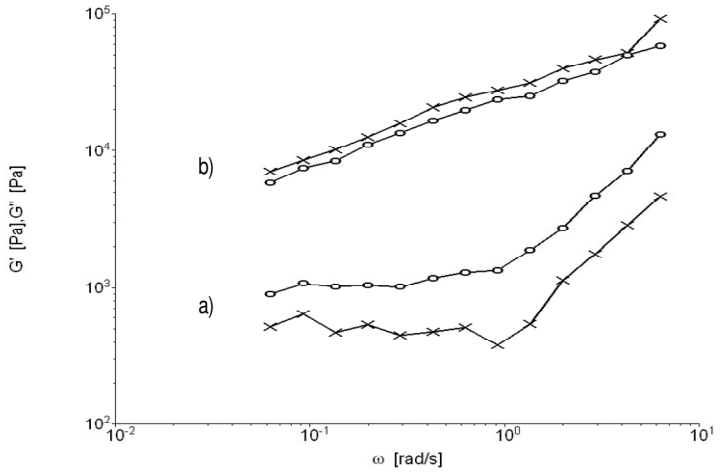


Figure 5.5 Dynamic oscillation curves depicting storage (G' depicted by x) and loss (G'' depicted by o) moduli of: a) hydrogel A; and b) hydrogel B

5.3.2 Assessment of the inter- and intra-polymeric interactions of the memblet

This assessment was conducted to evaluate any unforeseen chemical interactions between molecules, surface morphologies and the extent of crosslinking that occurred between the samples. In Figure 5.6, FTIR analysis showed that no unforeseen chemical bonding has occurred resulting in new functional bonding within the 2 structures. FTIR analysis of the memblet*s* were conducted and Figure 44a indicates the optimized memblet and emphasized an amine functional group for the Eudragit® E 100 polymer at a wavelength of 1143.45cm^{-1} and a primary alcohol group of wavelength of 1059.63cm^{-1} was determined for the PEG 4000 polymer.

These 2 functional groups allowed for the ionic crosslinking that occurred between the 2 polymers to result in the memblet structure. When comparing the memblet's A and B (Figure 44b), it was evident that formulation A displayed sharper and more defined peaks when compared to formulation B. Peak sharpness enforced an improved even distribution of PEG 4000 described as enhanced membrane flexibility in rheological studies. Peak sharpness is similarly observed when FTIR is conducted on a plain powder and then compared to its compressed form. In this case, the bonding between the primary alcohol and the amine group in formulation A is evidently more prominent and defined when compared to B which leads us to conclude that formulation A has greater membrane flexibility properties. This corroborates with statistical analysis in Chapter 4 which identifies a 30%$^{w}/_{v}$ crosslinker concentration of PEG 4000 as the optimal concentration for saturation of bonding between functional groups and that any higher concentrations can lead to weaker flexibility and compromised rheological properties.

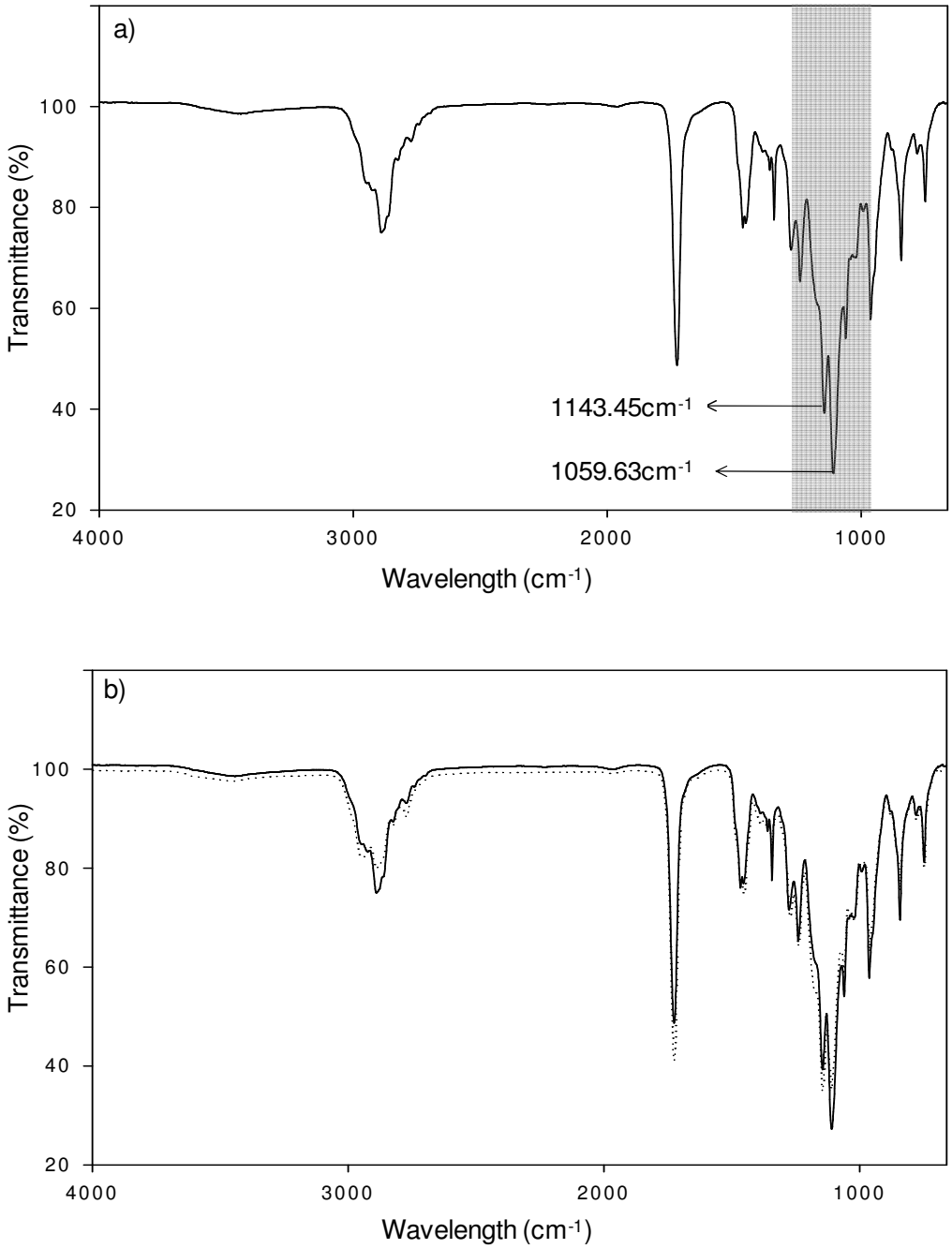


Figure 5.6 Fourier Transmission Infrared Spectroscopy analysis in which a) represents the optimized memblet and the bonding of functional groups from polyethylene glycol 4000 and Eudragit® E 100 functional groups; and b) represents formulation A and B overlaid for which A is represented by the dotted line and B by the solid line emphasizing the peak sharpness of A

5.3.3 Assessment of the surface morphology of the optimized crosslinked memblet

Scanning Electron Microscopy (SEM) was utilized to evaluate the surface morphology of the optimized memblet formulation. This evaluation was used to substantiate the results obtained in FTIR analysis which indicated that the optimized formulation had superior mechanical properties. The SEM for the optimized memblet (Figure 5.7a) revealed a consistently even

surface with limited crevices, cracks or large pores. A scattering of white powder like debris could be seen and this was attributed to the sodium lauryl sulphate which may have been in excess. The uniformity of structure and surface morphology gives an indication of the solid structural integrity of the formulation.

With regards to the control formulation, a notable difference in surface morphology was seen. A greater amount of surface debris was found compared to the optimized memblet (Figure 5.7b). This could be attributed to an aggregation of polymeric material of non crosslinked PEG 4000 and sodium lauryl sulphate which were viewed as congested white areas. This could be deduced as having a detrimental effect on thermal and mechanical properties due to the amount of non crosslinked polymer segments. The memblet itself had a large amount of cracks and pores relative to the optimized formulation and this could further influence structural integrity. Uniformity was not seen clearly throughout the imaging. Certain areas had surface structure similar to the optimized memblet, whilst other areas showed the aggregation of this polymeric material. It is postulated that in areas with this build up, dumping of PEG 4000 rather than a consistent crosslinking had occurred. The dumping prevented an optimal saturated crosslinking to occur leaving a weaker inter-polymeric structure. This was further investigated through textural and thermal analysis.

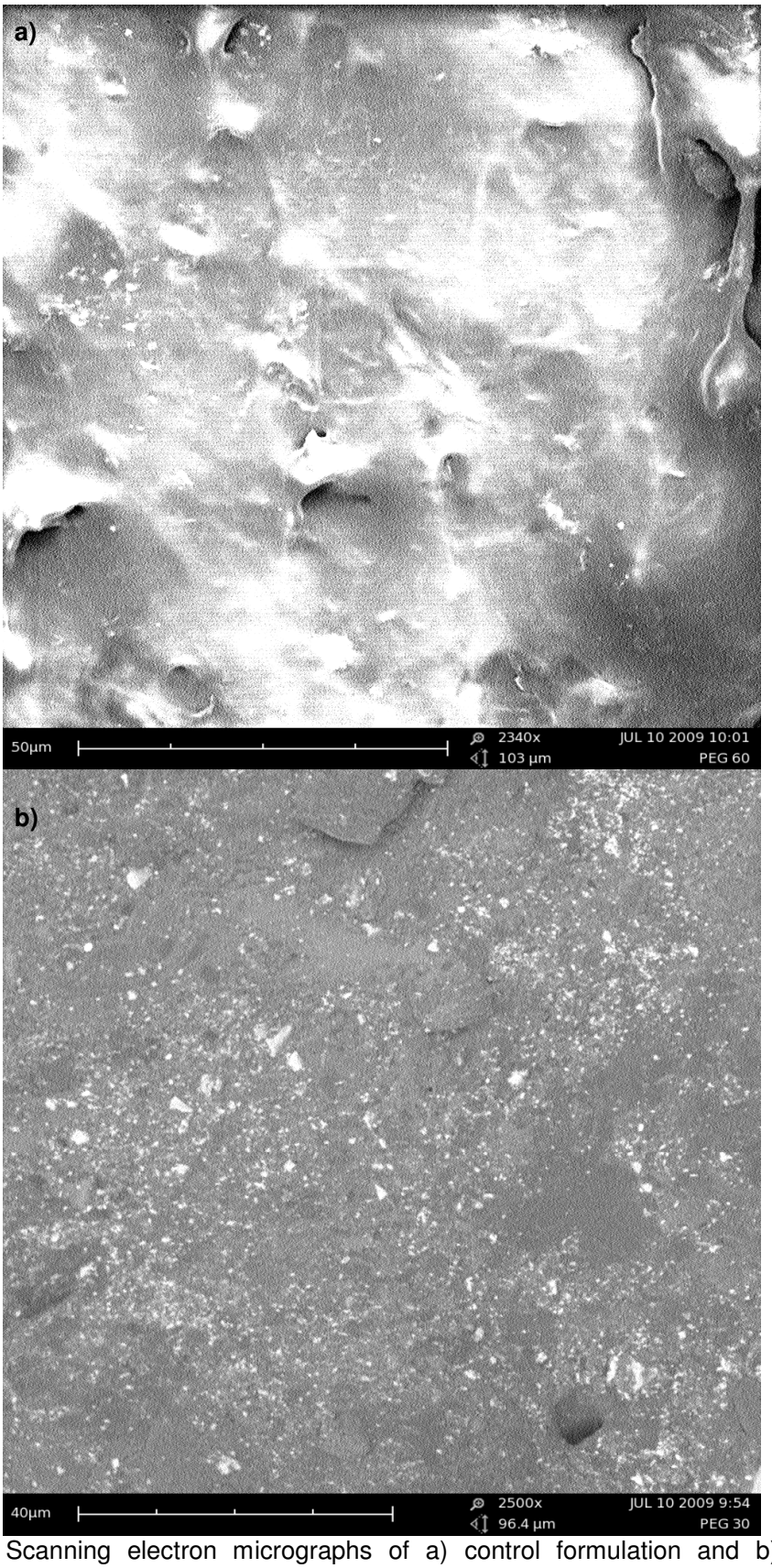


Figure 5.7 Scanning electron micrographs of a) control formulation and b) optimized memblet illustrating the increase in polymeric and formulation debris in the control memblet

5.3.4 Mechanical evaluation and validation of structural integrity of the memblet system

Mechanical evaluation of memblet systems was conducted in triplicate (N= 3). For both formulations (optimized and control), a typical force/distance profile was generated to evaluate both deformation energy and rigidity (Figure 5.8a and Figure 5.8b). In the textural analysis profile, the gradient represents the memblet flexibility while the area under the curve depicts the deformation energy for each sample. The results displayed in Table 5.3 highly convince that the optimized formulation has superior mechanical properties. Almost identical values were obtained for both memblet resilience and deformation energy (Table 5.3). Notably both memblets allowed for high memblet resilience. As described earlier, this is attributed to the high crosslinking concentration in both systems allowing for saturated ionic bonds to be formed. The memblet flexibility results were however quite different. Formulation A, with lower crosslinker concentration, displayed a greater membrane flexibility of 7.173N.mm against 6.293N.mm for formulation B (Table 5.3). This highlights the optimized formulation's superior flexibility whilst the control sample retains a rigid and hard nature. Furthermore, this analysis indicates that there is a maximal crosslinker concentration around the 30%$^{w}/_{v}$ region. Extremely high concentrations (e.g. 60%$^{w}/_{v}$) have no drastic positive influences to improve memblet flexibility.

Table 5.3 Textural analysis results for the memblet system

Formulation	Resilience (%)	Flexibility (N.mm)	Deformation Energy (J)
Control	17.6	6.293	0.062
Optimized	17.6	7.173	0.060

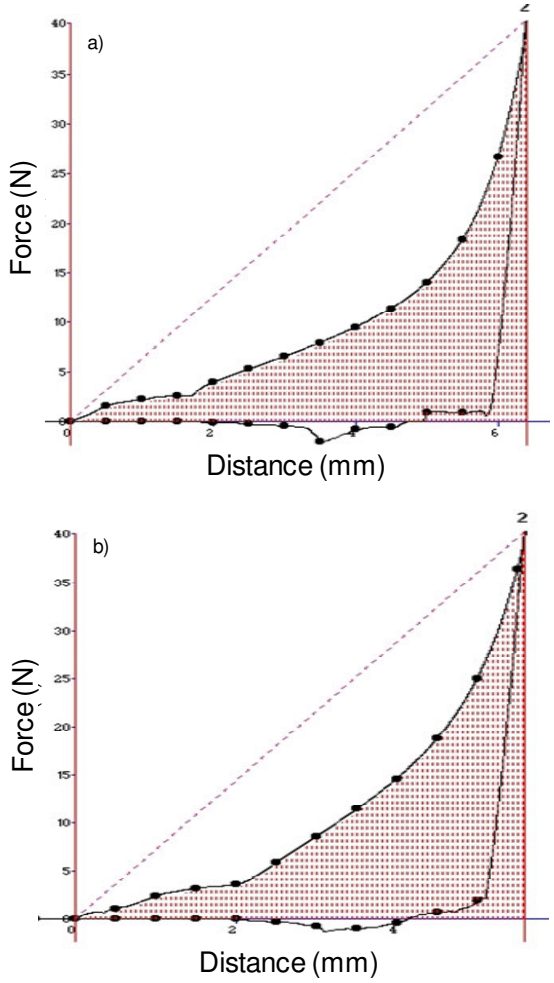


Figure 5.8 Force/Distance profiles depicting matrix resilience, memblet flexibility and membrane deformation energy: a) control formulation; and b) optimized memblet

5.3.5 Thermal analysis of an optimized crosslinked polymethacrylate based memblet

Thermal characterization was conducted in duplicate (N= 2) to identify any abnormalities or detrimental changes to the sample after the crosslinking process and to identify the thermal stability of the potential drug delivery system. The crosslinking of both the optimized memblet A and control memblet B with PEG 4000 and the incorporation of TEC allowed for a synergistic plasticizing effect. This is of significant importance as plasticizers, whilst causing a reduction in polymer-polymer chain secondary bonding by forming secondary bonds with the polymer chains, decrease the glass transition temperatures (T_g), increase flexibility and elongation at break and decrease Young's modulus (Feldstein *et* al., 2001; Lee and Anema, 2009). Plasticizers increase the free volume between polymer chains and in this case, Eudragit® E 100's polymer chains. The absence of plasticizers would lead to a highly solid but brittle product unsuitable for any avenue of oral drug delivery.

PEG compounds consist of polar hydroxyl functional groups and it is the hydrogen bonds formed from these hydroxyl groups which replace the polymer-polymer bonds within the

Eudragit® E 100 chains and thus provide the plasticizing effect (Gal and Nussinovitch, 2009). Additionally, PEG serves as a crosslinking agent for the Eudragit® E 100 molecule allowing for the increase in resistance to acidic gastric degradation (through hydrolytic cleavage) of the Eudragit® E 100 molecule. Due to the considerable length of PEG crosslinks creating a space between the Eudragit® E 100 chains, the network formed has enhanced free volume leading to the plasticizer effect. TEC serves as a better plasticizer than PEG due to its low volatility and its high miscibility with Eudragit® E 100.

The optimized and control memblet were tested under the same formulation parameters for both DSC and ADSC. DSC results were very similar for both formulations and a drastic improvement in the glass transition can be seen in both formulations as compared to Eudragit® E 100's thermograms (T_g= 40°C) from Table 3.7 of Chapter 3.5.5.2. DSC was run twice utilizing the same temperature programmes. The second run was selected for analytical purposes (as thermal information was deemed more accurate in a second run to remove any thermal history). The optimized memblet displays a larger relaxation peak when compared to the control memblet as seen in Figure 5.9. This is defined by the lower integral value of -14.01mJ of the control compared to the higher -137.95mJ of the optimal memblet indicating that more energy was required from the heating system (for the optimized) to allow for a first order energy transition (melting) to occur.

The thermograms revealed curves that were not the definite peaks, melting points or the gradual curve of a glass transition but rather a hybridization as can be seen in Figure 5.9.

As PEG 4000 and Eudragit® E 100 have very similar melting and glass transition points (both within the range of between 40-60°C) and have their glass transition and melting point fairly close, ADSC was used to separate the curves overlapping thermal events. A more intricate look into the memblet*s* thermal characteristics was obtained through the Cp-Complex, reversible and total heat flow curves. The heat capacity in a DSC curve can be calculated by dividing the heat supplied by the resulting temperature increase or change in temperature and gives us an indication of the amount of energy or heat required to increase the samples temperature by a certain amount. Heat capacity can best be described in saying that it is the heat flow (HF) divided by the heating rate (HR) as shown in Equation 5.11. Complex heat capacity of the ADSC curve can be defined as the amplitude of the heat flow (AHF) modulation divided by the amplitude of the heating rate modulation (AHR) as seen in Equation 5.12.

$$C_p = \frac{HF}{HR} \qquad \textit{(Equation 5.11)}$$

$$C_p \quad complex = \frac{AHF}{AHR} \qquad \textit{(Equation 5.12)}$$

Where, HF is the heat flow, HR is the heating rate, AHF is the amplitude of the heat flow and AHR amplitude of the heating rate modulation.

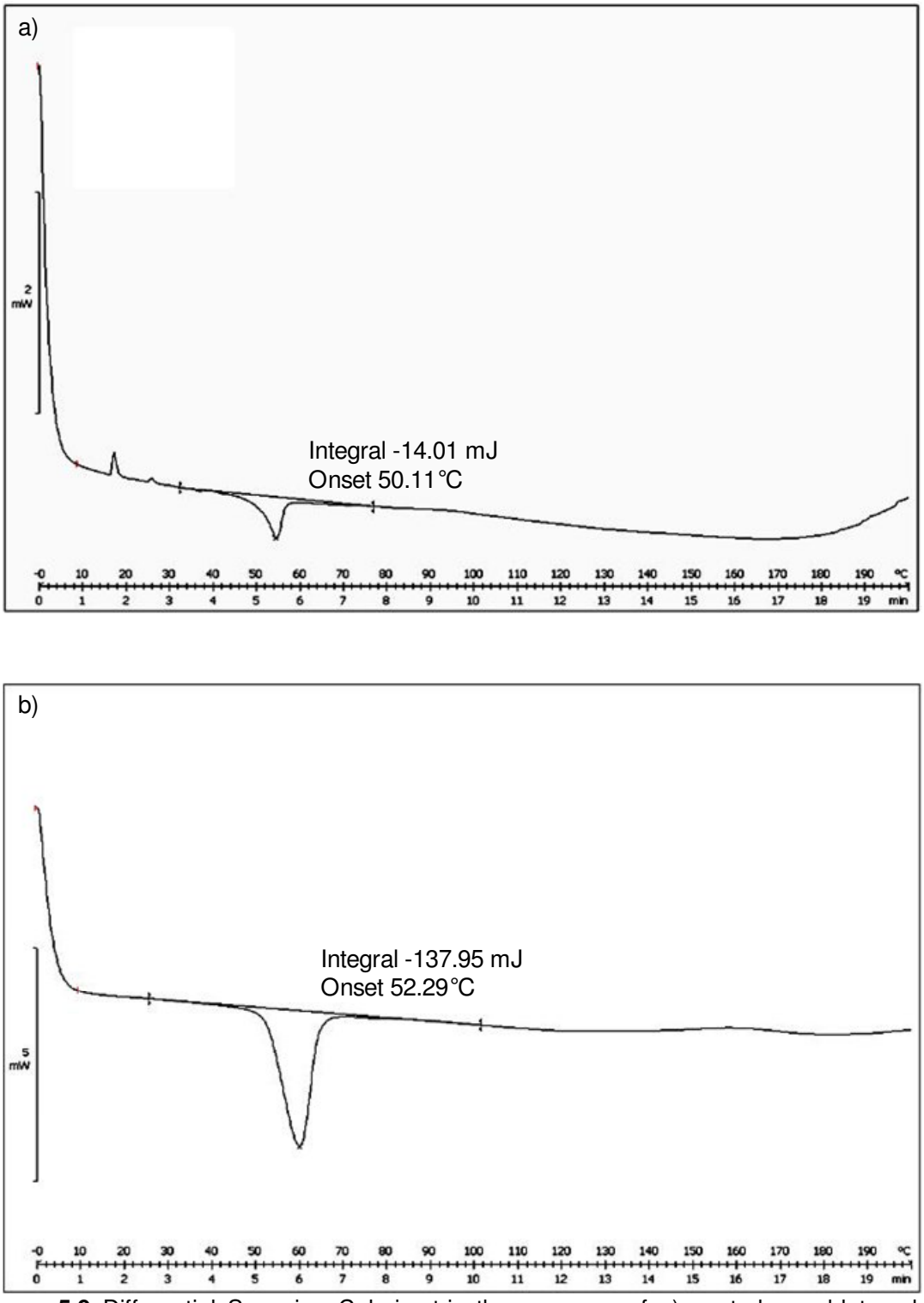
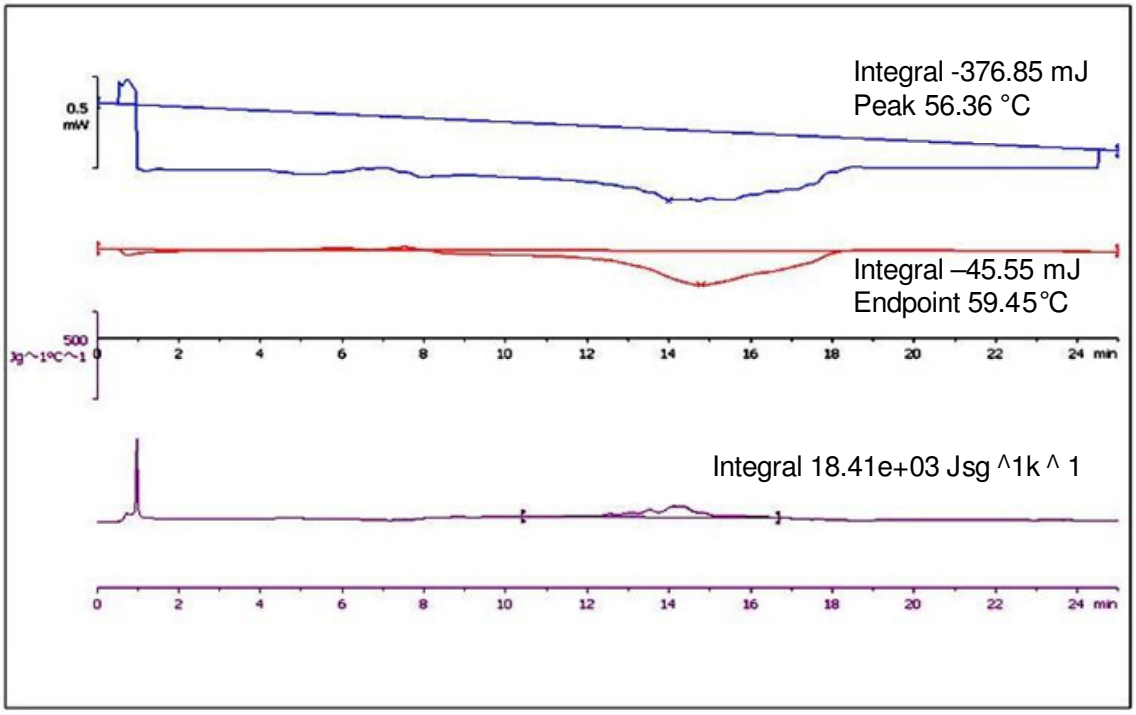


Figure 5.9 Differential Scanning Calorimetric thermograms of a) control memblet and b) optimized memblet

Figure 5.10 identifies the glass transition and the melting point as successfully separated thermal events which are plotted on the reversible heat flow and total heat flow curves respectively. Melting point remains the same for both formulations at 59°C as was expected indicating no major molecular alteration, results which are in congruence with the FTIR

analysis. Slight variance can be noted in the glass transition. As previously described, PEG 4000 and TEC have a compounded effect of lowering glass transition. The control formulation with a higher PEG 4000 concentration (60%$^{w}/_{v}$) when compared to the optimized memblet (30%$^{w}/_{v}$), displayed a marginally lowered glass transition of 55℃ and 56℃ respectively, which verifies the predicted values from the optimization studies indicated in Table 5.4 of Chapter 5.3.7. The Cp complex (also seen in Figure 5.10), indicated that the control memblet utilizes slightly less energy (endothermically) than the optimal memblet for the melting point to be reached, giving an indication that the optimized formulation displayed slightly improved mobility. The optimal crosslinking concentration of 30%$^{w}/_{v}$ PEG 4000 determined through optimization studies has been validated. Coupled with FTIR analysis and textural analysis, this further authenticates the utilization of 30%$^{w}/_{v}$ PEG as an optimal formulation and gives a better indication towards the relative strength of the bond through slightly improved thermal characteristics and rheologically superior characteristics.



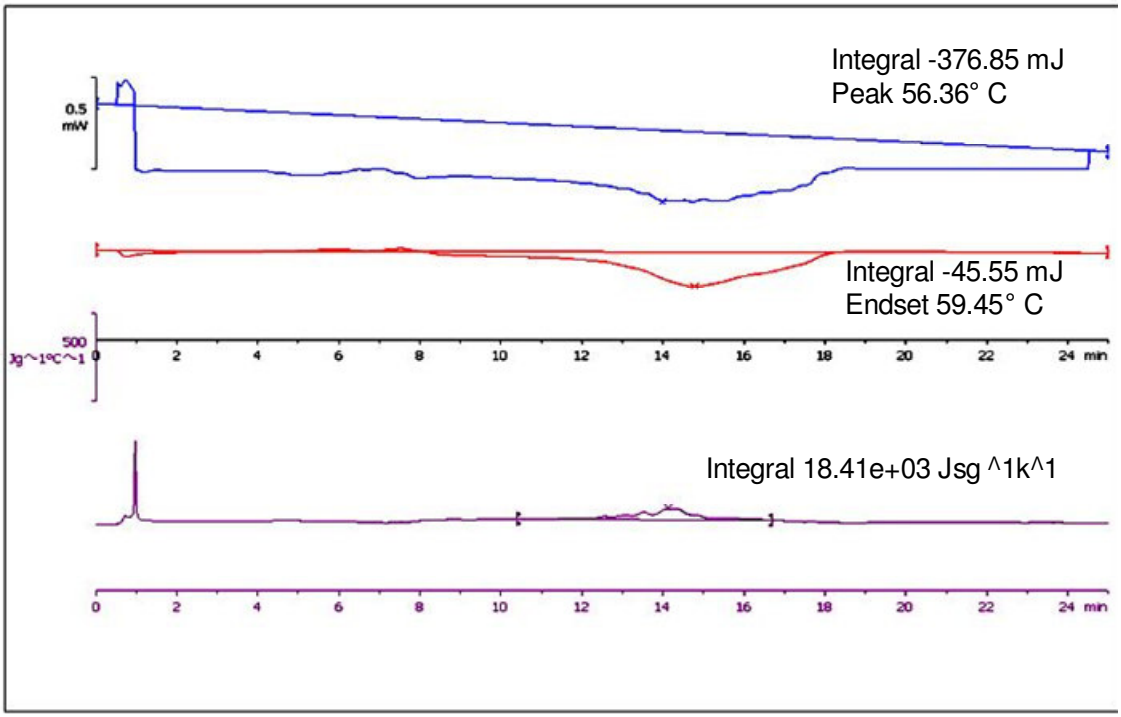


Figure 5.10 Alternating Differential Scanning Calorimetry thermal profiles of a) control memblet and b) optimized memblet

5.3.6 Construction of a calibration curve for rifampicin to interpolate *in vitro* analysis

Calibration curves formed were the same identified in Chapter 3.5.1 for preliminary analysis.

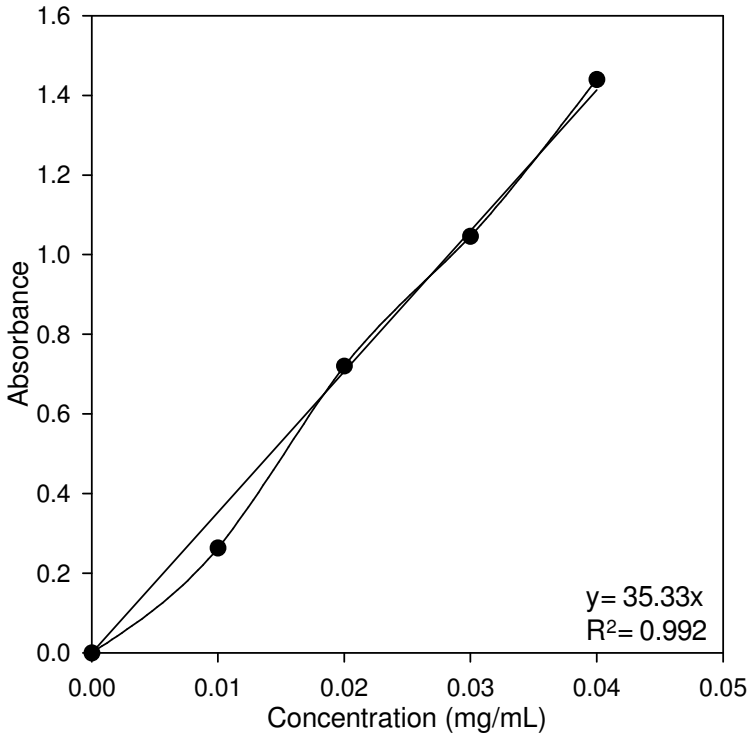


Figure 5.11 Calibration curve for rifampicin with corresponding regression co-efficients and y values

5.3.7 *In vitro* drug release results of polyethylene glycol crosslinked polymethacrylate based optimized memblet system

Release characteristics for the memblet component of the ODMUS system had to be highly specific for the gastric environment. *In vitro* testing aimed to achieve as close to zero-order drug release as possible within a 2 hour threshold. Complete release of rifampicin needed to be accomplished such that the majority of rifampicin would achieve gastric absorption and a fractional quantity would be concurrently released with isoniazid in the small intestine. A 79% MDT response desirability conveyed in Table 5.4, demonstrated the accuracy of the release profile generated in Figure 5.12 for the optimized formulation. At 0.5 hours, both formulations display a general burst effect. The optimized memblet has restricted the release to 40% of total drug in comparison to 70% in the control sample. It is postulated that the limited rheological properties of the viscoelastic optimized memblet, provided the slight burst effect as the SGF and mechanical rotation of the spindle (to mimic gastric churning) accelerated the conversion of the memblet to a more viscous state compounding erosion. Despite this, burst release of drug is still limited in comparison to the control memblet.

From 0.5 to 2 hours, a far more controlled means of release is in evidence. Retardation of drug release is attributed to the improved thermal, mechanical and intermolecular characteristics of the memblet. The improved molecular bonding through a lowered crosslinker concentration (30%$^{w}/_{v}$ PEG) enforces a more rigid intermolecular bond than the overcompensated control memblet crosslinker content (60%$^{w}/_{v}$ PEG). Enhanced structural integrity, thermal rigidity and intermolecular attraction has been achieved and detailed in mechanical, thermal and FTIR analysis within this Chapter. The thermal strength allows the memblet system to erode at a slower rate as per the elevated glass transition temperature (50℃), which requires greater energy to undergo a phase transition and begin erosion thus controlling drug release. This regulated release pattern is compounded by the improved intermolecular bonding indicated through FTIR and textural analysis. Furthermore, the maximal crosslinking concentration of 30%$^{w}/_{v}$ PEG does not induce a dumping of sodium lauryl sulphate as debris, in comparison to the control sample as seen in Figure 5.7 of Chapter 5.3.3 with SEM imaging. The SLS plays a role as a surfactant within the formulation matrix rather than act as debris and interfere with release patterns or complex with the excess PEG 4000 as in the control sample. The compounded effect is in producing a robust delivery system that can withstand the simulated gastric environment and display a more controlled release pattern. Release can be described as deliberately controlled from 0.5-2hours through the erosion of the memblet.

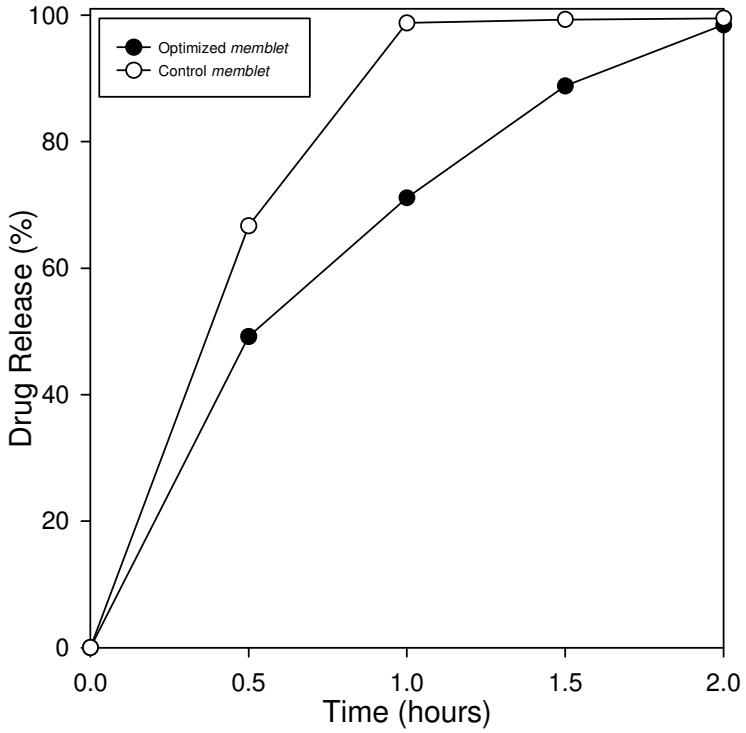


Figure 5.12 Concurrent release profiles of the optimized memblet and the control sample generated in simulated gastric fluid illustrating enhanced controlled release of the optimized memblet; where N= 3 and SD< 0.222 in all cases

Table 5.4 The relationship between optimization predicted and experimental values for responses mean dissolution time and glass transition

Responses	Predicted values	Experimental run values	Desirability
T_g	54.9090℃	56℃	100%
MDT	200.9134	253.9557	79%

T_g= glass transition and MDT= mean dissolution time

5.4 Concluding Remarks

The memblet component of the ODMUS indicated desired properties for pH mediated release within the stomach. Experimental and predicted values (generated in optimization studies) are near super imposable achieving the accuracy and efficacy required for the optimization process. Thermal stability was displayed through calorimetric analysis which emphasized the optimized and slightly improved glass transition of an optimized memblet. Rheologically speaking, the optimized hydrogel proved to have superior qualities to the control sample with regards to flexibility and mobility. The internal integrity and functional intermolecular bonding of the fully desiccated memblet are vastly superior to the control sample. Surface morphology also implemented the debris concept and highlighted the significance of using a lowered 30%$^{w}/_{v}$ PEG to ensure a relatively clear surface area to enhance controlled release. These factors synergistically improved drug release of rifampicin and the obligatory complete release of drug within 2 hours at the site-specific location of the stomach. Furthermore, this was accomplished in a rate controlled manner.

CHAPTER 6
FORMULATION AND INVESTIGATION OF AN OPTIMIZED ISONIAZID-LOADED MULTIPARTICULATE SYSTEM FOR TARGETED DRUG DELIVERY TO THE SMALL INTESTINE

6.1 Introduction

Multiparticulate drug delivery systems have been used increasingly in recent times (Ensslin *et al*., 2009; McConnell *et al*., 2009; Muschert *et al.,* 2009*;* Glaessl *et al*., 2010; Pund *et al., 2010)*. The advantages of multiple unit delivery systems have been well established in the past (Bodmeier and Paeratakul, 1994) and these include more precise bioavailability, decreased intra- and inter-individual variability, accurate uniformity of dispersion and reliable formulation processes (Zhang *et al*., 2002). In the case of single unit systems, the loaded drug can potentially lose its efficacy through premature release or dose dumping (Streubel *et al*., 2002). Conversely, the loss of a single multiparticulate does not mean complete failure for the rest of the system. The reproducibility of uniform distribution of the multiparticulates within their environment potentiates controlled release and decreases variability. The small size aides in passage and transfer time through the gastrointestinal tract limiting erroneous site-specific drug delivery. The nutritional state of the stomach can influence drug release and absorbance and therefore impart complex dosing intervals while multiparticulate dosing is independent upon such food states (Schmidt and Bodmeier, 2001).

This study focused on producing multiparticulates that are pH dependent, elucidate site-specific release and maintain controlled release. Multiparticulates have been implemented for site-specific delivery through regions of the gastrointestinal tract (Lamprecht *et al*., 2000; Markus *et al*., 2001). Optimized multiparticulates were formed through the single process step of crosslinking Eudragit® L 100-55 with trivalent (Al^{3+}) and bivalent (Ba^{2+}) cations. The use of Eudragit® L 100-55 imparted gastric resistance and enabled the system to deliver INH in a rate controlled manner due to the higher pH of the small intestine. This Chapter describes the release and entrapment studies of the optimized formulation with concurrent analyses of the porosity of the system and intermolecular network of the multiparticulates.

6.2 Materials and Methods

6.2.1 Materials

Eudragit® L 100-55 was donated by Degussa AG, Pharma polymers, RÖhm GmbH (Midrand Gauteng, South Africa). Triethyl Citrate (TEC), isoniazid (INH) and ethylcellulose (EC) were

of analytical grade and purchased from Sigma Aldrich.Inc (St. Louis, Missouri USA). All electrolytes used for crosslinking were of analytical grade and purchased from Merck Chemicals (Halfway House, Gauteng, South Africa). Sodium hydroxide pellets and potassium dihydrogen (phosphate reagent) were purchased from Rochelle Chemicals (Johannesburg, Gauteng, South Africa). Silicone was obtained from Merck Chemicals (Halfway House, Gauteng, South Africa). All chemicals and raw materials were used as received without further processing. Water was purified by a MilliQ Millipore water purification system (Milli-Q, Millipore, Billerica, MA, USA).

6.2.2 Preparation of the polymethacrylate based latex prior to double crosslinking

An aqueous solution of 30%$^{w}/_{v}$ Eudragit® L 100-55 was prepared with deionized water. The PMMA polymer was added gradually to the aqueous phase under agitation using a magnetic stirrer, over a period of 5 minutes to avoid agglomeration and sedimentation. Silicone (0.4mL) (antifoament) was added to the latex and the solution was left to stir for 45 minutes. During the 45 minute stirring process 2 solutions were dissolved. The first solution was a 4%$^{w}/_{v}$ NaOH solution, which was left to stir until complete dissolution of pellets was achieved. The second solution was a 20%$^{w}/_{v}$ ethylcellulose (EC) solution. EC was added gradually to 50mL of ethanol, and left to stir. Upon completion of the 45 minutes stirring period, 5mL of the NaOH solution was drawn up with a 20mL syringe and added to the latex within 5 minutes in a drop wise manner for neutralization of the carboxyl functional groups of the PMMA. The latex was left to stir for a further 45 minutes to ensure proper dispersion and neutralization of the latex.

After the second 45 minute stirring period, 3g of INH was then added to the latex and left for 30 minutes to stir. The TEC was added to the latex and left to stir for 15 minutes. EC solution (3.75mL) was drawn up using a 20mL syringe and gradually added to the latex prior to homogenization (Polytron, Kinematica, Lucerne Switzerland) for 15 minutes. As homogenization generates a lot of heat, the latex was then left on the stirrer to cool for 10 minutes prior to crosslinking. Thereafter, 2 batches of spheres were then formulated with varying crosslinking agents to produce an optimized batch of multiparticulates and a control sample.

6.2.3 Polymethyl methacrylate polysphere formation through a double crosslinking process

Initially, 2 batches of polyspheres were formulated and crosslinked in a 25%$^{w}/_{v}$ electrolyte solution of $AlCl_3$. A control formulation of spheres was left to cure in a second solution of $MgCl_2$ and the optimized multiparticulate system was similarly was left to cure in a solution of $BaCl_2$ in which both electrolyte solutions were of 20%$^{w}/_{v}$ concentration. The crosslinking

solution was kept on a magnetic stirrer for the duration of crosslinking to prevent unwanted agglomeration. The first electrolyte solution (25%$^{w}/_{v}$ $AlCl_3$ saturated with 3g INH) was prepared and left on a magnetic stirrer. A measured 10mL of the 50mL PMMA latex was drawn up with a syringe and the latex was expelled in a drop wise manner into the first electrolyte solution for crosslinking. Once all the latex had been expelled, the polyspheres were left to cure for 20 minutes in a dark cupboard. The control polyspheres were washed twice in 500mL double deionized water and placed in the second crosslinking solution of $MgCl_2$ and left to cure in a dark cupboard for 20mins. Optimized multiparticulates were left to cure in the $BaCl_2$ solution following the same procedures. All secondary crosslinkers were saturated with 3g of INH to enhance drug entrapment efficiency. Both batches were then washed twice with double deionized water and then left to air dry under an extractor for 12 hours at room temperature.

6.2.4 Assessment of the surface morphology and inter- and intra-polymeric interactions of the optimized multiparticulate system

Surface morphology was characterized by Scanning Electron Microscopy (SEM), (JEOL, JEM 840, Tokyo, Japan) at an accelerating voltage of 19kV. Multiparticulates were mounted on an aluminium stub. Samples were sputter-coated with carbon or gold and photomicrographs were then taken at various magnifications.

FTIR spectroscopy was performed on the individual polymers, INH, constituents and dried polyspheres. Samples were analyzed with a Spectrum 2000 FTIR spectrometer with a MIRTGS detector (PerkinElmer Spectrum 100, Llantrisant, Wales, UK). The spectrum was a ratio spectrum of 16 samples against 16 background scans with a resolution of 4cm^{-1}. Samples were analyzed at wavenumbers ranging from 4000-400cm^{-1}.

6.2.5 Validation of the enhancement of drug entrapment efficiency for optimized multiparticulates

Solutions of 200mL phosphate buffer saline (PBS), (pH 6.8, 37^{o}C) were prepared and used for drug entrapment efficiencies. A fixed amount of 100mg of polyspheres from batch A and B were weighed out and placed within 200mL of PBS and left to completely dissolve overnight with aided agitation from a stirrer at room temperature. UV analysis through a spectrophotometer (Cecil CE 3021, Cambridge, CB24 6AZ, England) was conducted and drug entrapment was calculated through Equation 6.1:

$$DEE \quad \% = \frac{D_a}{D_t} \times \frac{100}{1} \qquad \textit{(Equation 6.1)}$$

Where, DEE %= drug entrapment efficiency of polyspheres, D_a= the actual amount of drug contained within multiparticulates and D_t= the theoretical amount of drug required.

6.2.6 Examination of surface area and investigation into porosity analysis for multiparticulates

Surface area and porosity studies were conducted using a micromeritics ASAP analyzer (Micromeritics ASAP 2020, GA, USA). Samples were first degassed prior to analysis and 0.3g of polyspheres were weighed out and placed in a glass holding tube. This glass tube was inserted into the degassing vacuum system for complete degassing of the sample prior to analysis. Degassing conditions include both evacuation phase and heating phase parameters and adsorptive properties for analysis conditions as depicted in Table 6.1.

Table 6.1 Variant properties of the degassing and analysis procedures for surface area and porosity analysis

Evacuation phase parameters during the degassing process	
Evacuation phase parameters	
Temperature Ramp Rate	10℃/min
Target Temperature	90℃
Evacuation Rate	50.0 mmHg/s
Unrestricted evacuation	30.0 mmHg
Vacuum Set Point	500 µmHg
Evacuation Time	60 min
Heating phase parameters during the degassing process	
Temperature Ramp Rate	10℃/min
Hold Temperature	120℃
Hold Time	900 min
Adsorptive properties during the analysis process	
Adsorptive gas	Nitrogen
Maximum manifold pressure	925.00 mmHg
Non-ideality factor	0.0000620
Density conversion factor	0.0015468
Hard sphere diameter	3.860Å
Molecular cross-sectional area	0.162nm^2

6.2.7 Chemometric and molecular modelling to deduce the mechanism of crosslinking for the formation polyspheres and the drug release pattern thereof

Chemometric and molecular modelling were performed to deduce the transient mechanisms, interaction of ions and entities and sol-gel inter-conversion of the polymethacrylate based latex when crosslinked with $AlCl_3$, $BaCl_2$ and $MgCl_2$ to form polyspheres.

This approach allowed for a provision to make predictive findings solely based on the chemical concepts underlying the crosslinking of the polymethacrylate based latex into polyspheres through double crosslinking process. Models and graphics based on the step-wise molecular mechanism of gel formation, sol gel inter-conversion, permanent gelation and erosion with respect to the conceived energy profile as envisioned by the chemical behavior and stability were generated on ACD/I-Lab, Version 5.11 (Add-on) software (Advanced Chemistry Development Inc., Toronto, Ontario, Canada, 2000).

All models were based on the evident molecular changes rather than on any calculation or predictions from the software. The critical minimum concentration of the polymethacrylate based latex was assessed for maximizing the sol-gel transition as a function of the concentration of the polymethacrylate based latex and crosslinkers employed (i.e. $AlCl_3$, $BaCl_2$ and $MgCl_2$). The energy distribution curves generated assumed an initial population of mono-dispersed polymethacrylate based latex monomers, a spatially uniform distribution of crosslinkers in the system, and an irreversible double crosslinking process.

6.2.8 Molecular modelling of a novel multi-crosslinked Eudragit® L 100-55 based multiparticulate system

Molecular Mechanics (MM) Computations in solvated system with water as solvent were performed using the HyperChem™ 8.0.8 Molecular Modeling System (Hypercube Inc., Gainesville, Florida, USA) and ChemBio3D Ultra 11.0 (CambridgeSoft Corporation, Cambridge, UK) on an HP Pavilion dv5 Pentium Dual CPU T3200 workstation. The nonamer of polymethyl-methacrylate copolymer (Eudragit® L 100-55) was generated from standard bond lengths and angles employing polymer builder tools using ChemBio3D Ultra in their syndiotactic stereochemistry as 3D model. The Eudragit® L 100-55 model was initially energy-minimized using MM+ force field and the resulting structure was again energy-minimized using the Amber 3 (Assisted Model Building and Energy Refinements) force field. The conformer having the lowest energy was used to create the polymer-cation complexes. All MM simulations were performed for cubic periodic boxes with a side length of 16.52Ås containing one centered Eudragit® L 100-55 fragment, 9 surrounding cations molecules at the edges and the centre of the cubic box and the remaining free space filled with water molecules and the same procedure of energy-minimization was repeated to generate the

final models: EUD-Al^{3+}, EUD-Ba^{2+}, EUD-Mg^{2+}, EUD-Al^{3+}-Ba^{2+} and EUD-Al^{3+}-Mg^{2+}. Full geometry optimizations were carried out in solvated system employing the Polak–Ribiere conjugate gradient method until an RMS gradient of 0.001kcal/mol was reached. Force field options in the AMBER (with explicit solvent) were extended to incorporate cutoffs to Inner and Outer options with the nearest-image periodic boundary conditions. The outer cutoff was set to 8.26Å and the inner cutoff was set to 4.26Å to ensure that there were no discontinuities in the potential surface.

6.2.9 *In vitro* drug release studies on the polyspheres

Drug release studies were conducted following the USP 33 Apparatus II (ERWEKA DT 700 GmbH Germany), in which 100mg of spheres were weighed out in duplicate from each sample and placed within the vessel under stainless steel ring meshes assembly to prevent the paddle inflicting physical/mechanical damage to the spheres and alter release profiles as well as to prevent erratic fluctuation due to unstable hydrodynamics (Pillay and Fassihi, 2000). Each vessel was filled with 900mL PBS and heated to a temperature of 37°C prior to the addition of the multiparticulates and the stainless steel ring mesh assembly. The rotating paddle method was selected at a rotational speed of 50rpm and the machine was calibrated for a 12 hour run with samples taken at hourly intervals. Sampling involved the drawing of 5mL of PBS from the dissolution vessel with subsequent refilling of removed buffer to maintain sink conditions. Samples were then subject to UV spectroscopy in the same manner as entrapment studies to generate release profiles.

6.3 Results and Discussion

6.3.1 Assessment of the surface morphology and inter- and intra-polymeric interactions of the polyspheres

Optimized multiparticulates formed were spherical in shape, glossy in appearance, robust and devoid of any brittleness as observed in Figure 6.1. SEM studies revealed a solid and non porous surface morphology for the optimized batch (Figure 6.2). This is accentuated by the fact that porosity studies revealed a low pore volume. Larger crystal-like structures were identified on the surface of the polyspheres and postulated to be ethyl-cellulose crystals. The crystals were largely distributed on the peripheral surface of the multiparticulates. An inconsistent PMMA latex preparation could be the reason for the high quantity of irregularly placed surface crystals as well as the effects of the non homogenous latex solution when EC was added to the latex. These surface crystals would have been expected to have an impact on drug delivery by facilitating controlled delivery but due to the random accumulation of the EC, an inconsistent type of drug release was expected.

However, the drug release (indicated in Figure 6.8 of Chapter 6.3.6), was relatively controlled highlighting an acceptable incorporation of crystals into the matrix of the spheres. In both control and optimized formulations, both superficial layering and internal constitution of the matrix core in the EC content were not factors that portrayed comparative data as to the significant secondary crosslinker.

However, EC did impart improvement on drug release for both formulations. The images also portrayed few localized pores within the system identified via of cracks and fissures (Figure 6.2a). The presence of these pores could be associated with the varying environmental or manufacturing factors. The most likely combination of factors that determine the size and volume of pores include the non-homogenicity in the latex prior to crosslinking as well as prolonged exposure during the drying phase. Since these factors could carefully be monitored, pore size and volume were minimized so as not to drastically affect drug release. However, this could only be found in a few localized areas of the spheres substantiating the results obtained in the porosity studies in which there was a low volume of pores.

An FTIR spectroscopy of the optimized formulation is plotted in Figure 6.3. Al^{3+} can be described as a hard electrophile according to Pearson's HSAB scale. The ionic bond formed with carboxyl groups is an electrostatic, columbic type bond (Fleming, 1996). Al^{3+} therefore induced a strong negative charge at the carboxyl functional groups and therefore not altering the carbonyl/carboxyl stretching bands at $1600cm^{-1}$. Due to the double crosslinking with Ba^{2+} or Mg^{2+} for polyspheres from the optimized and control multiparticulates respectively, their characteristic bands were shifted to $1726.42cm^{-1}$ as demonstrated in Figure 6.3.

When compared to Al^{3+}, Ca^{2+} and Ba^{2+} are referred to as "soft" electrophiles which accept electrons from the carboxyl functional groups. Covalent co-ordinate bonds are formed with the subsequent loss of the negative charge of the carboxyl functional groups which ultimately causes the stretching of the carbonyl band (Williams and Fleming, 1997). Both formulations displayed no other changes in structure and no other interactions were seen amongst the constituents.



Figure 6.1 Optimized crosslinked polymethyl-methacrylate based polyspheres

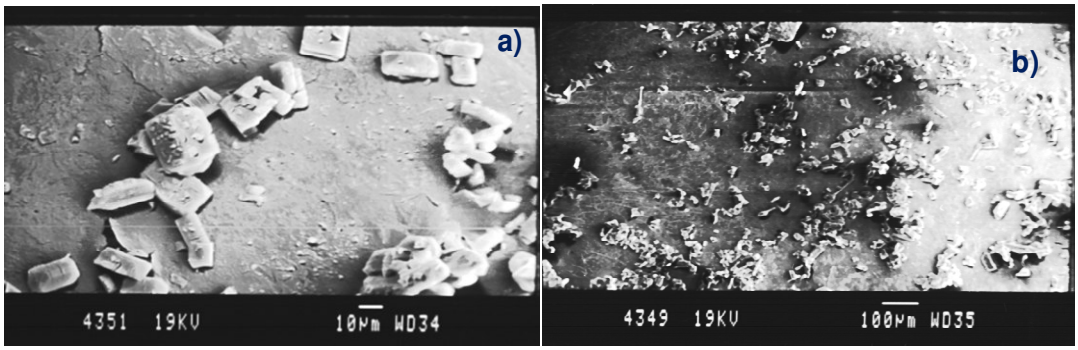


Figure 6.2 Scanning electron microscopy taken at a) 650X magnification and b) 100X magnification for the optimized double crosslinked multiparticulates to examine the surface morphology of optimized multiparticulates

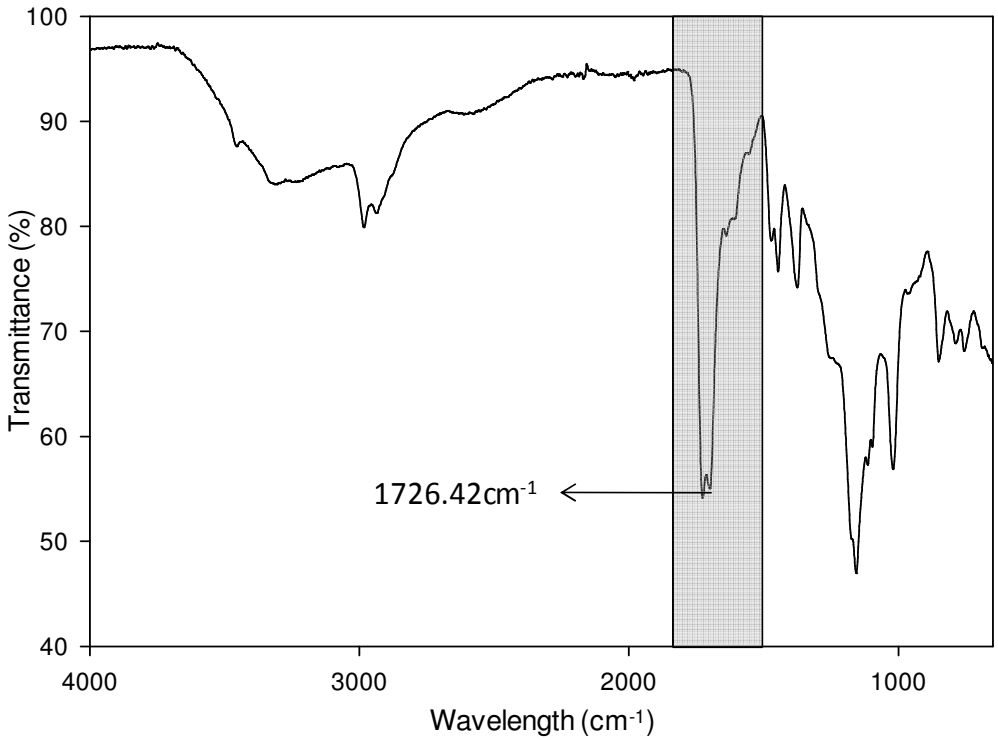


Figure 6.3 Fourier Transmission Infrared Spectroscopy spectrum of crosslinked Eudragit® L 100-55 based multiparticulates

6.3.2 Evaluation of the augmentation of drug entrapment efficiencies of novel isoniazid loaded Eudragit® L 100-55 based multiparticulates

Drug entrapment is always of primary importance during development of a drug delivery system. The manufacturing procedure that involved a 20 minute double crosslinking process and the high quantity of polymeric material employed, both contributed to the observed low entrapment efficiency. Polyspheres from the control sample reflect a lower drug entrapment of 50% relative to the 71% of optimized spheres portrayed in Table 6.2. This attributed Mg^{2+} as a crosslinker. It is evident from Table 6.4 and Figure 6.6 of Chapter 6.3.5 that the hydrophobic van der Waals energies are directly correlated to the size of the cation where Ba^{2+}, having the largest atomic radius, represented highest van der Waals energy followed by Mg^{2+} and Al^{3+}. This predisposes the polymeric backbone to reduced entrapment efficiency due to destabilization of the backbone in comparison to the optimized Ba^{2+} cations which promote enhanced stability and intermolecular forces and ultimately an enhanced DEE.

The greater the bombardment of ionic molecules to free carboxyl groups, which results in a higher saturation of ionic bonding than drug incorporation, the less the drug to be included into the matrix of the sphere. This is furthered by the initial crosslinking of $AlCl_3$ for double crosslinking, compounding the filling of molecular space. The crosslinking time influenced drug entrapment and release in an indirectly proportional manner. Extended crosslinking time would improve drug release but significantly decrease drug entrapment as drug would be given more time to leech out of the matrix and into the solution. Duration of 20 minutes crosslinking time was selected to achieve a balance between entrapment and saturated crosslinking for controlled release. The crosslinking solutions (both primary and secondary crosslinkers) were saturated with INH to negate the diffusion of drug into the electrolyte solution during the 20 minute period. The inclusion of EC has affected the amount of drug that can be loaded, because the greater the number of polymeric constituents results in lower drug entrapment within the control sample. However, EC is not a detrimental factor in the optimized formulation. Therefore, EC is an independent factor in drug entrapment efficiency which is based primarily on type of cationic molecule. The correlation between predicted and experimental DEE achieved 100% desirability as depicted in Chapter 6.3.6 Table 6.5.

Table 6.2 Drug entrapment efficiencies for 100mg of polyspheres from optimized and control batches of multiparticulates

Batch	Yield (mg)	Drug content in Yield (mg)	Entrapment Efficiency (%)
Optimized	4400	428.76	71.5
Control	4222	300.42	50.0

6.3.3 Inspection of surface area and corollary porosity data for optimized multiparticulates

The conducted studies were used to analyze the total surface area exposed by optimal multiparticulates as well as the volume of distribution of pores and pore size. The multiparticulates were subject to analysis following the Barret, Joyner and Halenda method (BJH) and the t-plot of Lippins, Linsen and de Boer. Table 6.3 shows the surface area for both adsorption and desorption isotherms, in which polyspheres both the optimal and control formulations, depicted similar low exposed surface areas after adsorption and desorption of nitrogen. Successful degassing was achieved for both formulations and illustrated in Figure 6.4a and Figure 6.4b for both formulation batches. Both figures depict an isothermal linear plot which depicts the layering of liquid nitrogen in the adsorptive phase (the adsorption isotherm) and the removal of the liquid nitrogen in the desorptive phase (desorption isotherm). The isotherms depicted a closure of adsorption and desorption curves at the start and end points, proving that successful degassing had occurred with the removal of all liquid, gas and solid impurities. The low surface area can be attributed to the shape and size of the multiparticulates because all spheres had a uniform spherical shape. The surface area determined from each formulation however was sufficient for further evaluation of pore size and pore volume.

Table 6.3 Surface area of control and optimized polyspheres

Batch	BJH Adsorption$_A$	BJH Desorption$_A$
Control	3.5910	3.8777
Optimized	3.4890	3.8777

A: cumulative surface area of pores between 17.000Å and 3000.000Å diameter (m^2/g)

Pore Volume and Size of polyspheres

Formulation	t-Plot (cm^3/g)	BJH Adsorption for Pore Volume$_1$	BJH Desorption for Pore Volume$_1$	Pore Size: BJH Adsorption (Å)	Pore Size BJH Desorption (Å)
Control	-0.000892	0.028310	0.020460	315.314	292.000
Optimized	-0.001076	0.020460	0.020411	234.603	210.545

1: cumulative surface area of pores between 17.000Å and 3000.000Å diameter (m^2/g)

T-plot isotherms were generated to determine the presence of micropores (pores with a diameter of 2nm or 20Å) within the formulation. For t-plot isotherms, the quantity of nitrogen adsorbed (V_a) is plotted against the thickness (t) of the adsorbed layer. Extrapolation of the linear isotherm to the adsorption y axis will give the micropore volume if the intercept value is a positive one. As seen in Table 6.3, T-plot volumes were -0.000892cm^3/g and -0.001076cm^3/g for polyspheres from control and optimized batches respectively and a linear representation can be seen in illustrating a negative intercept on the adsorption y axis indicating the lack of micropores in the system. This is illustrated in Figure 6.4a and Figure

6.4b), in which extrapolation of the linear curves resulted into a negative intercept that was observed in both formulations.

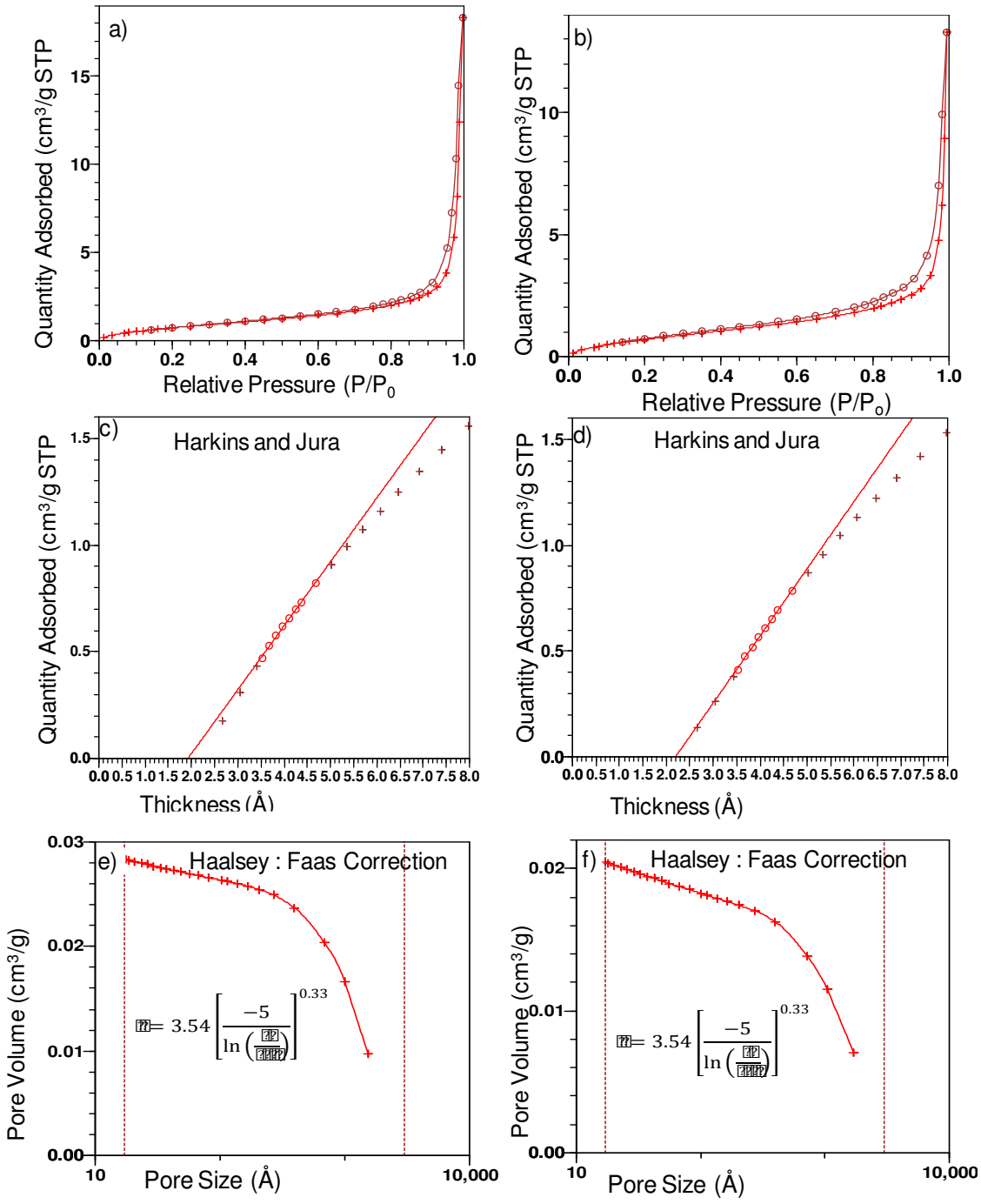


Figure 6.4 Surface area and porosity analysis of polyspheres with regards to: a) isothermal linear plots for optimized batch; b) Isothermal linear plot for control batch; c) T-plot micropore isotherm for batch A; d) T-plot micropore isotherm for batch B; e) BJH adsorption cumulative pore volume for batch A; and f) BJH adsorption cumulative pore volume for batch B

Pore volume in both formulations showed relatively small values when compared to the surface areas. Figure 6.4a and Figure 6.4b depict the BJH adsorption cumulative pore

volume for control and optimized formulations respectively. The Halsey: Faas correction equation was used for both Figure 6.4a and Figure 6.4b as this equation assumes an adsorbed liquid monolayer with the same density and packing as the normal liquid (Webb and Orr, 1997). In both cases, a significant decrease in pore volume is noted with subsequent increases in pore diameter. Control polyspheres showed a larger cumulative volume of pores in the 200-300Å region when compared to the optimized batch and had significantly larger pores in comparison. A detailed an average pore size of 315.314Å and 292.000Å for adsorption and desorption isotherms respectively were documented for control samples, which were inferior to optimized polyspheres with a BJH adsorption of 234.603Å and a BJH desorption of 210.545Å. Pore size can influence drug release within the context of improper crosslinking. Figure 6.8 of Chapter 6.3.6 corroborates cumulative effects of poor crosslinker and large pores illustrated by the burst release in the dissolution profile for the control sample. Whilst the volume of pores is low for both formulations, the larger pores in evidence for the control sample, provide an expeditious means of polysphere erosion when exposed to a pH of 6.8 concurrently with the weaker crosslinking noted in molecular modeling of Chapter 6.3.5. For the purposes of the multiparticulates in this study, pore sizes greater that 300Å, were identified as potentiating factors for burst release identified in Figure 6.8 of Chapter 6.3.6. By limiting the pore size to under 240Å, the burst effect was significantly diminished for the optimized formulation (Figure 6.8 of Chapter 6.3.6). This study confirmed that formulations are obligated to have a limited pore size below 240Å such that pore size is a negligible factor in modulating drug release profiles as the influence of pore size on controlled release can be seen as prominent.

Since EC did not interact or bond with the PMMA latex (shown in Chapter 6.3.1 FTIR analysis), the few pores identified, can be attributed to uneven allocation of this cellulose derivative. This is an ideal situation as the system relies on a rate modulated drug release, with an ideal formulation having a low volume of pores relative to the surface area as evaluated and described in this study. This particular low distribution of pores is due to the crosslinking process and good formulation technique.

Control batches, with a surface area of 3.5910m^2/g and 3.8777m^2/g for adsorption and desorption isotherms respectively, revealed an adsorption isotherm of 0.028310m^2/g and desorption isotherm of 0.020460m^2/g. Similarly optimized multiparticulates indicated an adsorption isotherm of 0.020460m^2/g and a desorption isotherm of 0.020411m^2/g for a surface area with an adsorption isotherm indicating 3.4890m^2/g and desorption isotherm of 3.8777m^2/g. Relative to the surface area determined, both batches showed a low volume of pores for adsorption and desorption isotherms despite the formulation variance.

6.3.4 Chemometric and molecular modelling deducing the mechanism of crosslinking for the formation polyspheres and the drug release pattern thereof

Ionic bonding and weak intra and inter-ionic physical force interactions located on sites within and around the PMMA latex pockets determined the matrix resilience of the resultant polyspheres (Figure 6.5a and Figure 6.5b). Ionic interactions of crosslinked PMMA latex strands depended most on the ionization energies of the crosslinkers (i.e. $AlCl_3$, $BaCl_2$ and $MgCl_2$), hydration enthalpies over time and the thermodynamic stability of molecules accumulated at PMMA latex subunits.

The PMMA latex subunits exhibited a desirable selectivity for crosslinking ions due to its structural orientation and the ability to provide a pocket for crosslinkers to assemble in a thermodynamically stable form resulting in a latex-like intermediate phase. The adjacent carboxylate groups provided a thermodynamic barrier for the release of INH molecules. Ba^{2+} ions have larger atomic radii (1.35Å) as compared to Mg^{2+} (0.65Å) and Al^{3+} (0.5Å) ions and therefore restricted hydration in the PMMA latex pockets. Al^{3+} having the smallest atomic radii would have been expected to result into polyspheres with the best drug release (small ionic radius would have allowed the Al^{3+} ions to diffuse throughout the polysphere matrix and crosslink strongly on the PMMA latex surface) but on the contrary, its high degree of hydration resulted into a reduced effect, specifically a potential burst effect. Placement of a crosslinker between the PMMA latex subunits through double crosslinking process reduced the chain flexibility. The voids generated by the interaction of PMMA latex strands were firmly bound by the Ba^{2+} and Mg^{2+} crosslinkers. The physical interactions of inter- and intra-structural ions (Ba^{2+} and Mg^{2+}) with structural moieties present in clusters, resulted into reduced hydration of the latex-like PMMA matrix and therefore the best drug release patterns obtained particularly for Ba^{2+} crosslinked polyspheres due to the larger atomic radii and the more stable larger electrostatic energy output detailed in Chapter 6.3.5.

Furthermore, the irregular and heterogeneously scattered structure of PMMA latex subunits and their interaction with crosslinking ions were attributed to the physic-mechanical, hydrational and erosion differences of the resultant polyspheres.

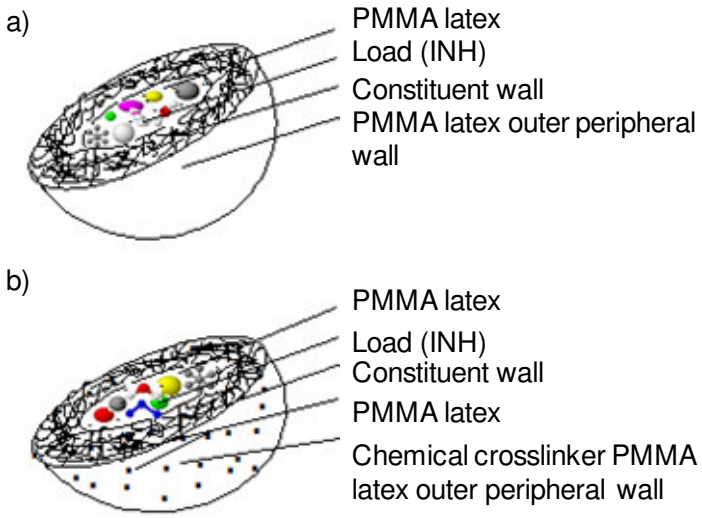


Figure 6.5 Polysphere formation process depicting: a) polymethacrylate latex with non-chemically crosslinked polymeric outer wall with load (isoniazid) in the polymethacrylate cavity; b) polymethacrylate latex with chemically crosslinked polymeric outer wall with load (isoniazid) in the polymethacrylate cavity

6.3.5 Molecular modelling of a novel multi-crosslinked Eudragit® L 100-55 based multiparticulate system

The environment surrounding the molecules of interest in molecular mechanics was defined in terms of a solvated system to prevent artefacts that arise from vacuum simulations and to reproduce bulk solvent properties well. Although the system could also be simulated in vacuum, but it may introduce artefacts in the molecular geometry caused due to surface charges of the charged molecules interacting with each other (as against interacting with the solvent in a solvated system), producing molecular conformations that are unlikely to be present in any other environment. The system was solvated by placing explicit water molecules, as 3 separate particles with fixed bond angles, in the simulation box with Eudragit® L 100-55 and the cations and the water molecules were treated as interacting particles like the molecules.

The association of the cations to the polymer was found to be dependent on the charge density and the size of the respective cation. In the calculated values for the various energies for the Eudragit® L 100-55 fragments caused by the interaction with cations are illustrated separately as van der Waals, electrostatic and H-bond energies in Table 6.4. It is evident from Table 6.4 and Figure 6.6 that the hydrophobic van der Waals energies are directly correlated to the size of the cation where Ba^{2+}, having the largest atomic radius, represented highest van der Waals energy followed by Mg^{2+} and Al^{3+}. The interaction energies of the Eudragit®-monocations appeared to be more influenced by the electrostatic energies of interaction. The Eudragit® L 100-55 molecule behaves like a cation in the presence of aqueous environment due to the prevalence of $–COO^-$ groups in its structure and tends to

interact with the cations in water solvated systems as depicted in Figure 6.6. The electrostatic interactions were calculated as Eudragit®-Mg^{2+} > Eudragit®-Ba^{2+} > Eudragit®-Al^{3+}. Thus Eudragit®-Al^{3+} (ΔE= -2041.68kcal/mol) and Eudragit®-Ba^{2+} (ΔE= -1806.77kcal/mol) are highly stabilized in comparison to Eudragit®-Mg^{2+} (ΔE= -624.64 kcal/mol) because of high charge densities and low intermolecular forces. These results corroborated with the assumption made in the *in vitro* drug release studies of Chapter 6.3.6 where it is postulated the Al^{3+} imparted a strong electrostatic ionic bond (high charge density) and a hydrophilic property (low van der Waals forces) on the multiparticulates. Spatially too, the Al^{3+} and Ba^{2+} ions are more closely packed in the conformational space of the periodic box (Figure 6.6). The hydrogen bonding interactions emerged to be insignificant with very small interaction values.

Although, Al^{3+} might provide superior crosslinking, the high hydration energy of the Al^{3+} cation (-4665kJ/mol) weakens the stability of the ionic bond to hydrolytic cleavage. Therefore, the polyspheres were doubly crosslinked with divalent cations, Mg^{2+} and Ba^{2+}, having low hydration energies of -1921kJ/mol and -1305kJ/mol, respectively. The cations were thus disposed alternatively, as shown in Figure 6.6, with the concentration of divalent ions being kept higher (5) as against trivalent ions (4) complementing the concentration used in crosslinking. After molecular mechanics simulations, Eudragit®-Al^{3+}-Ba^{2+} was observed to be stabilized by 102.252kcal/mol and Eudragit®-Al^{3+}-Mg^{2+} was destabilized by 213.13kcal/mol (Table 6.4). The high burst release in case of the control multiparticulates ($AlCl_3$-$MgCl_2$ crosslinked) may be due to the tendency of Eudragit®-Al^{3+}-Mg^{2+} system to attain energy minimized geometrical preferences thereby forming stabilized molecular conformers. Confirmation of Ba^{2+} as a valid and enhanced crosslinker was proven through this study.

Experimental and theoretical investigations on the crosslinking and cation interaction of different divalent and/or trivalent cations to Eudragit® L 100-55 polyspheres were in excellent agreement. The experimentally observable polymer-ion interaction behaviour could be predicted by the computational method. Furthermore, the calculations allowed for a prediction of the interaction mechanisms. This particular study allowed for a successful and in depth introspection of the interactions between the Eudragit® L 100-55 polymer and the relevant crosslinking primary and secondary crosslinkers, which constitute the novel pH responsive multiparticulate intended for the release of active within the small intestine of the GIT.

Table 6.4 Calculated energy parameters (kcal/mol) of the complexes between Eudragit® L 100-55 and divalent and/or trivalent cation

Structure	Energy (kcal/mol)				
	Total	**$\Delta E_{interaction}$**	**VDW**	**H bond**	**Elec**
Eudragit	-1470.834		13.1403	-4.47725	-1568.98
Eudragit - Al^{3+}	-3512.516	-2041.68	181.064	-5.09441	-3876.58
Eudragit - Ba^{2+}	-3277.600	-1806.77	145.114	-5.89739	-3758.47
Eudragit - Mg^{2+}	-2095.474	-624.64	348.451	-5.55139	-2356.45
Eudragit - Al^{3+}- Ba^{2+}	-1573.086	-102.252	72.2477	-3.15595	-1733.57
Eudragit - Al^{3+}- Mg^{2+}	-1239.704	231.13	-11.3466	-4.04261	-1314.09

$\Delta E_{interaction}$= E(Host:Guest) - E(Host) - E(Guest), Vdw: van der Waals energy and Elec: Electrostatic energy

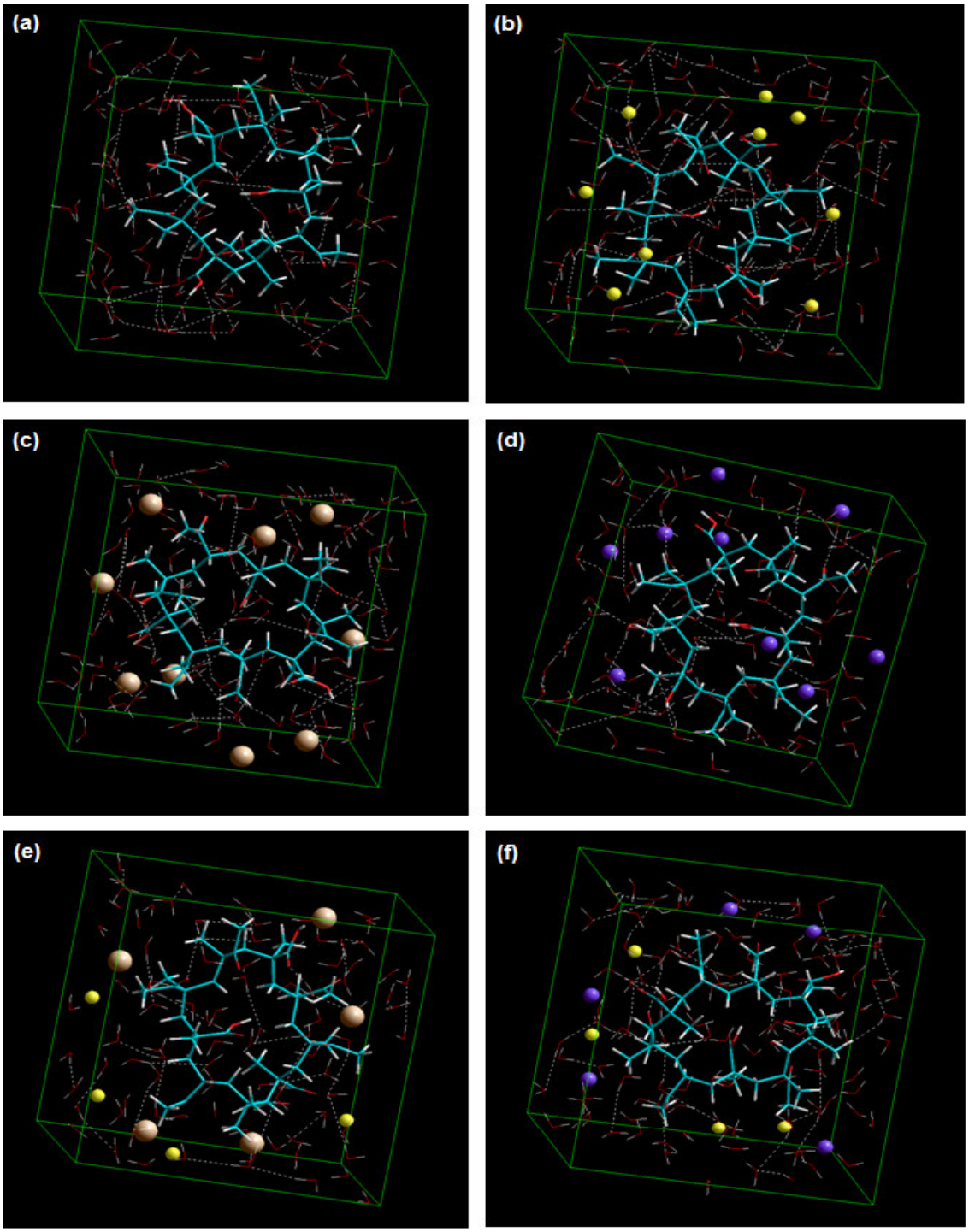


Figure 6.6 Visualization of geometrical preferences of Eudragit® E L100-55 molecule in complexation with divalent and trivalent cations after molecular simulation in a solvated system. Color codes: C (cyan), O (red), H (white), Al (yellow), Ba^{2+} (violet) and Mg^{2+} (brown)

6.3.6 *In vitro* drug release profiles for a novel Eudragit® E L100-55 based double crosslinked multiparticulate system for site-specific delivery of isoniazid to the small intestine

The results from drug release studies varied drastically due to type of crosslinker as can be seen in Figure 6.8. Both formulations utilized $AlCl_3$ for the initial crosslinking. As seen in

Chapter 6.3.1 Figure 6.3 for FTIR analysis, crosslinking using $AlCl_3$ does not disrupt the carboxylate band and is within the conventional band region. The Al^{3+} bonded carboxylate group is protected from immediate hydrolysis and hydration due to the ionic bond formed validated thorough high electrostatic energy (ΔE= -2041.68kcal/mol) derived in Chapter 6.3.5.

Pearson's HSAB scale describes Al^{3+} as a hard acid and thus the Al^{3+} imparted a strong electrostatic ionic bond and a hydrophilic property on the multiparticulate. The Hofmeister series similarly describes Al^{3+} as being the most susceptible ion for interacting with H_2O molecules and consequently weakening the stability of the ionic bond to hydrolytic cleavage (The Hofmeister series, 2009). Al^{3+} has an ionic radius of 0.5Å and is a trivalent ion. The trivalent ion can allow for a 3-dimensional bonding structure with the PMMA molecule, which when compared to the planar 2 dimensional bonding of divalent ions, allows for a more rigid bond formation (Winter, 2010). The small ionic radius can allow the Al^{3+} ions to diffuse throughout the polysphere matrix and not just crosslink at the surface of the formulation. Hydration of the Al^{3+} metal ion is relatively fast and a burst release of drug could be expected despite a saturated crosslinking process. It was for this reason that a secondary crosslinking electrolyte solution was incorporated for each solution. Ba^{2+} and Mg^{2+} are considered to be softer acids than Al^{3+} on Pearson's HSAB scale and interact less with H_2O when compared to Al^{3+}.

The control multiparticulates displayed a burst effect with 70% drug release within the first hour and thereafter a rapid release of the remaining 30%. Complete drug release occurred between 8-10 hours. The discrepancy between the control and optimized formulation is easily identified with the initial moderated 20% drug release. The consistent rate controlled release profile generated for the optimal formulation confirms the postulated MDT release for with an 80% correlation from Table 6.5.

Porosity evaluation, Chapter 6.3.3, implemented a large pore incongruity which influenced the respective formulation release profiles. Burst release was attributed to a combination of large pores (300Å for control samples), which propagated a faster matrix erosion and poor ionic crosslinking.

The crosslinking between the Eudragit® L 100-55 polymeric backbone and the respective cations have been fully documented in Chapters 6.3.5 and 6.3.4. Ionic radii of the cationic molecules play a highly influential role in intermolecular bonding. Barium with a larger an ionic radius of 1.35Å produces the highest van der Waals energy attraction in comparison to both magnesium (0.65Å) and aluminum (0.5Å). Electrostatic energies of interaction affected

the strength of bonding more so than the Van der Waals forces with barium displaying a predominant energy interaction over magnesium (Table 6.4, Chapter 6.3.5). Spatially too, the Al^{3+} and Ba^{2+} ions are more closely packed in the conformational space of the periodic box (Figure 6.6 of Chapter 6.3.5). Hence the crosslinking saturation was improved upon in comparison with the Mg^{2+} ions and the control sample which explains the burst release obtained for the control sample (Figure 6.8). A higher concentration of EC aided in achieving a more controlled release and prevented the burst effect for the optimal formulation.

Optimized multiparticulates were subjected to release testing within simulated gastric fluid (pH1.2) to ascertain the affinity of the formulation to prevent maximal release of INH within the stomach and consequently prevent the deleterious drug-drug interaction between INH and RIF. Figure 6.7 illustrates the efficacy of the system to retard INH release to a maximum 10% drug release within the gastric environment for a period of 2 hours (mimicking gastric transit time).

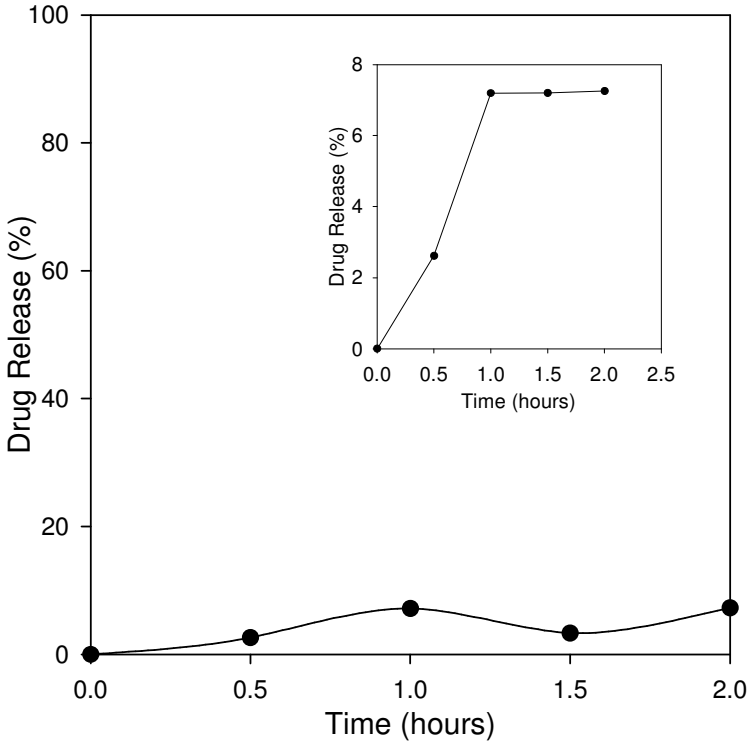


Figure 6.7 Limited isoniazid release from optimized multiparticulates within simulated gastric fluid at pH 1.2 (insert with full scale reference); where N= 3 and SD< 0.002 in all cases

Table 6.5 Correlation between predicted and experimental responses of mean dissolution and drug entrapment efficiency for the optimized multiparticulates

Responses	Predicted Values	Experimental Run Values	Desirability
DEE (%)	67.2216	71.4606	100%
MDT	74.4739	57.5162	80%

DEE (%)= drug entrapment efficiency and MDT= mean dissolution time

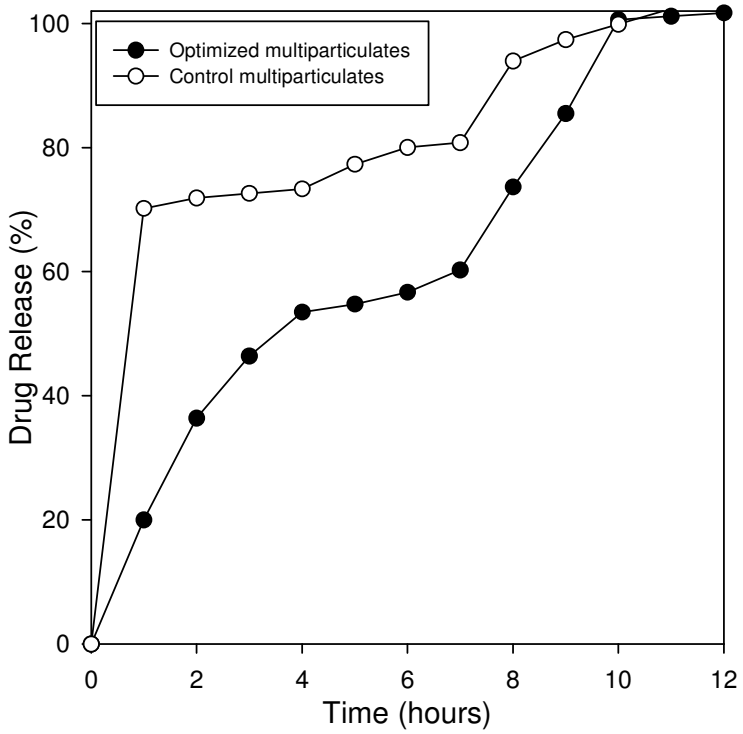


Figure 6.8 Percent drug release indicating the superior controlled drug release for an optimized multiparticulate system in relation to a control sample; where N= 3 and SD< 0.02 in all cases

6.4 Concluding Remarks

Controlled *in vitro* release of isoniazid was achieved for a 12 hour period for an optimized multiparticulate system. Segregated delivery of rifampicin and isoniazid was achieved in a rate controlled manner. Site-specific release of isoniazid with minimal quantities of drug releasing in the acidic pH of the stomach through simulated gastric fluid was achieved thus corroborating this concept. Optimized multiparticulates displayed enhanced intermolecular bonding, thoroughly investigated through chemometric and molecular modelling. The improvement on molecular bonding drastically affected both drug entrapment efficiencies and drug release profiles positively. A 71% drug entrapment was a large improvement of preliminary studies which barely entrapped adequate quantities of drug. Similarly, the lack of a major burst release of isoniazid in optimized multiparticulate profiles, can be attributed to this greater affinity of the Ba^{2+} cationic molecule to the Eudragit® L 100-55 polymeric carboxylic functional groups to produce electrostatic bonds. The primary Al^{3+} crosslinking interaction provided a dualistic strengthening of the polymeric backbone to regulate controlled release. Ethyl cellulose rather than negatively impact entrapment efficiencies, played a negligible role in drug entrapment but a significant one in moderating isoniazid release profiles. The optimized multiparticulate system achieved the objective of retarding drug isoniazid release within the simulated acidic pH of the stomach, whilst elucidating site-specific and controlled release for up to 12 hours within the simulated pH of the small intestine.

CHAPTER 7
THE *IN VIVO* INVESTIGATION INTO THE DUALISTIC DRUG BEHAVIOUR PATTERNS OF A COMBINATION OF RIFAMPICIN AND ISONIAZID LOADED ORAL SYSTEMS

7.1 Introduction

Selection of an animal model is an initial concern for *in vivo* studies. The animal's storage, eating and ablution patterns must be relative to a human. The size of an animal impacts sampling frequency. Smaller animals such as rats and mice are restricted in daily sampling intervals as compared to larger animals such as dogs, monkeys and pigs (Garrett and Hunt, 1977; Cryan *et al., 2007;* Schroeder *et al*., 2007). This is a crucial factor as more frequent sampling has a direct relationship with quantifiable controlled drug release data. The larger the data pool of sampling, the higher the accuracy of understanding drug release *in vivo*. The dosage quantity between species relies on the size of animals. Human dosage can be accurately correlated to larger animals such as pigs and dogs but the same dosage needs to be scaled down for a rat model (Sutton *et al*., 2006). From the larger animals listed, the dog and the monkey are considerably more expensive than the pig and pose more of an ethical dilemma. The pig model was selected over other models for *in vivo* analysis. The analogous features between the pig and the human include feeding patterns, digestive physiology, coronary artery distribution and the omnivorous nature (Brunet *et al*., 2006). The use of the pig as a model has been thoroughly exploited for drug delivery (Kumar *et al*., 1992; Dorkoosha *et al.,* 2002; Dorkoosha *et al.,* 2002) making it the ideal choice for *in vivo* studies.

The pig model is ideal for comparative *in vivo* analysis due to the physiological similarities between a human. Validity of the model chosen is seen by the near identical metabolism of pharmacological actives via common enzymatic metabolic pathways (cytochrome P450). The similarity between pig and human physiology extends to the total activity of cytochrome P450 which are comparable (Skaanild and Friis, 1997). Additionally, the slow gastric emptying time exemplifies a comparative model and the pig is considered an ideal animal for slow release formulations (Lennernäs H, 2007). Through continuous habituation, pigs are considered easy to handle, manipulate for blood sampling and to accommodate.

7.2 *In Vivo* Analytical Methodology for the Once Daily Multi-Unit System

7.2.1 Development of a blood sample retrieval protocol for the accurate analysis of plasma samples through the marginal ear vein

The initial phase of *in vivo* studies was focused on identifying an efficacious blood sampling protocol that was to be sustainable for the duration of the study. Due to the numerous studies being conducted in conjunction with this project, a carefully formulated timeline was implemented. To ensure reproducibility, 5 pigs were used at a time for the various projects undertaken and studies were conducted in a staggered fashion to allocate for wash out periods between the variant formulations drugs. Female white pigs were chosen for the study and upon arrival and averaged 30kg in mass.

To ensure expeditious and accurate blood sampling, habituation of the pigs was attempted which involved daily visitation of the pigs. During the course of habituation, pigs were fed an assortment of food such as raisins and sweet potatoes to build a relationship with the animal for easier handling, a strategy which proved effective. Pigs were anaesthetized with Anaket®, Dormicum® and Isofor® gas and were then monitored whilst under a constant sleep with oxygen. In an observational evaluation of the pig, the only visible veins were at the external surface of the ear. Consequently, catheterization at the marginal ear vein was attempted. The formulation samples for testing were administered via gastric intubation utilizing gastric tubing.

Prior to sampling, pigs began a 24 hour fast such that digested food would not impede results. Drawing blood samples proved to be an arduous task of luring the pig into a handling cage and keeping it occupied whilst drawing up blood from the marginal ear vein (Figure 7.1). Roughly 2mL of blood was drawn up from the conscious pig every 2 hours for a 0-12 hour interval and every 4 hours for the 16-24 hour time interval. Blood samples were stored in a heparinized tube and then centrifuged at 5000rpm for 10 minutes. The separated plasma was removed and stored in a -70℃ freezer until further analysis.

This particular protocol proved to be unsuccessful for many reasons. Blood sampling was not always successful as the marginal ear vein was sporadically blocked throughout the 24 hours testing period resulting in lost data at various time intervals. The marginal ear vein also ran the risk of rupturing, collapsing, bursting and hardening, all of which occurred frequently throughout the study. Trauma to the pig itself was undesirable through the work in the handling cage and the pain experienced through the physical act of blood sampling was extensive. The protocol was abandoned as unsatisfactory for accurate sampling.



Figure 7.1 Placement of the female white pig in a handling cage and blood sampling via the catheterized marginal ear vein

7.2.2 Development of a blood sample retrieval protocol for the accurate analysis of plasma samples through the insertion of a chronic catheter

A secondary strategy was to insert a permanent catheter through a surgery. A female white pig weighing 40-42kg was anaesthetised with Ketamine® (11mg/kg I.M.) and Midazolam®, (0.3mg/kg I.M.). Buprenorphine® (0.05mg/kg I.M.) and Carpofen® (4mg/kg I.M.) were administered for analgesia and inflammation. The pig was then intubated and anaesthesia was maintained with 2% Isoflurane® in 100% oxygen. Under aseptic conditions, a 7 french gauge double lumen 35cm catheter (CS-28702) (Arrow Deutschland GmdH, Erding, Germany) was surgically inserted into the left jugular vein. The jugular vein was exposed by an incision made dorsal to the jugular groove on the left lateral aspect of the neck.

Via blunt dissection, the vein was isolated and the catheter was inserted 10cm into the lumen of the vein. The lumen of the catheter was fastened to the wall of the vein using a purse suture technique. The remaining length of the catheter (25cm) was tunnelled subcutaneously, with the use of trocar, to an exit point cranial to the dorsal aspect of the scapula. The externalised injection ports of the catheter were sutured to the skin of the pig so as to limit excessive movement and bending. Blood was removed via the catheter and the catheter was flushed with heparin saline (1000i.u. of heparin in 1L of 0.9% saline). Thereafter the animal was allowed 10 days to recover from the surgical procedure. During this time, pigs were habituated to the process of blood sampling. Throughout the study, the catheter was flushed with heparinised saline 3 times a day.

A mixture of Dormicum® and Anaket® was injected directly into the jugular vein catheter. Once sedated, the pig was anaesthetised with 2% isoflurane in 100% oxygen. An intragastric tube was inserted into the stomach of the pig through which the testing samples were placed. To prevent accidental pulmonary insertion, wedging of samples on the oesophageal wall and regurgitation of the samples, all the formulations were washed down the tube with 10mL water. While under sedation, all wounds were checked and sutures were repaired. The pig was returned to its pen to recover under observation.

Blood samples were taken over a 24 hour period. A constant 2 hour interval was utilised for the first 12 hours, while samples were taken every 4 hours for the remaining 12 hours. The catheter was disinfected and an aseptic technique was utilised to prevent the introduction of foreign organisms. Before blood was sampled, the catheter was flushed with heparinised saline in order to clear any clots or remove old blood. Thereafter, blood was drawn and placed in a lithium heparin vial. To prevent accumulation of blood post sampling, the catheters were once again flushed with heparinised saline. Blood samples were centrifuged at 5000rpm for 10 minutes. The plasma supernatant layer was removed and frozen at -72℃ until analysis. Figure 7.2 illustrates an overview of the optimized sampling protocol for both the optimized ODMUS and the conventional dosage form (Rifinah®).

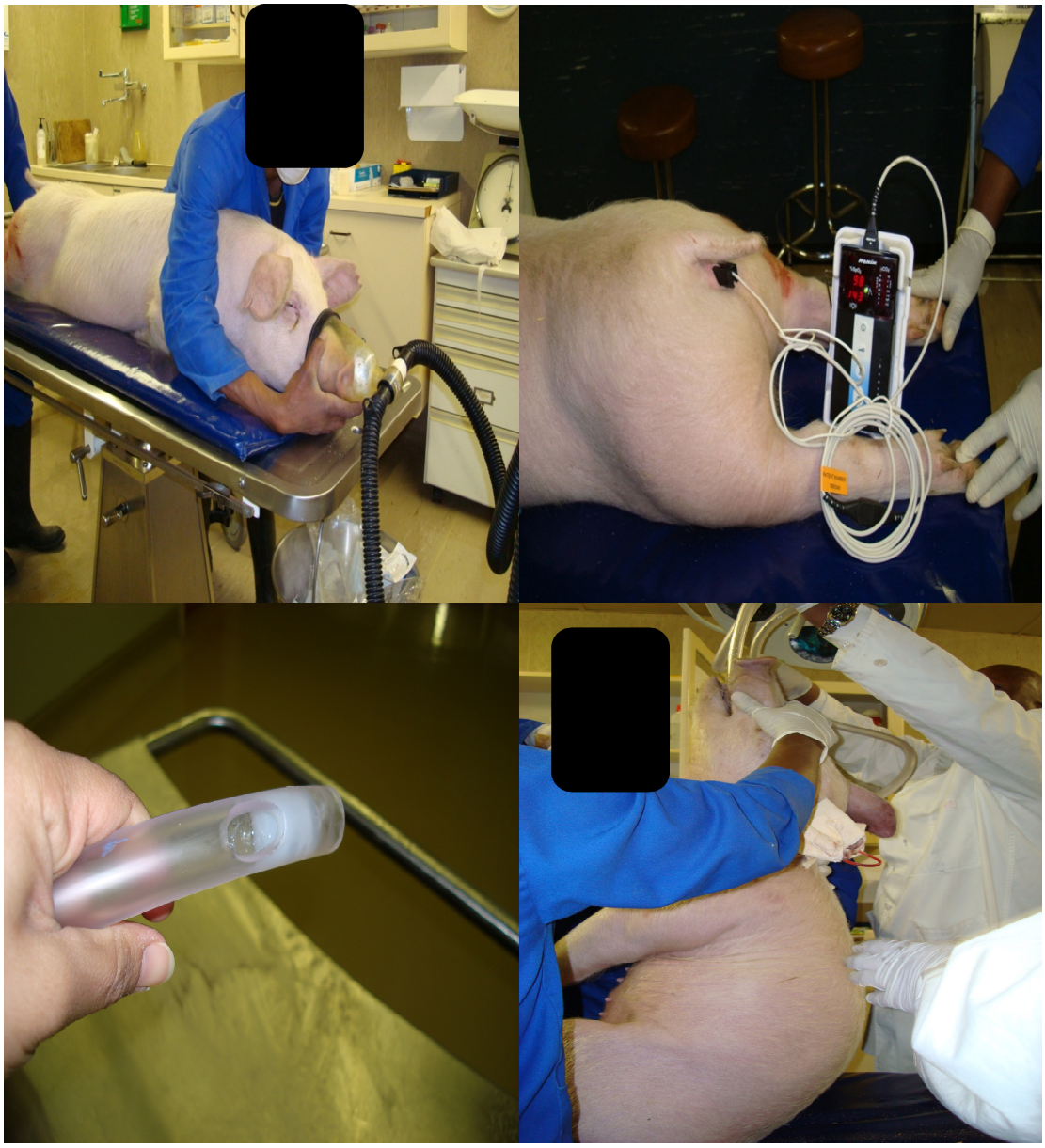


Figure 7.2 Dosing protocol employed to anaesthetize, monitor vitals, intubate and insert formulations

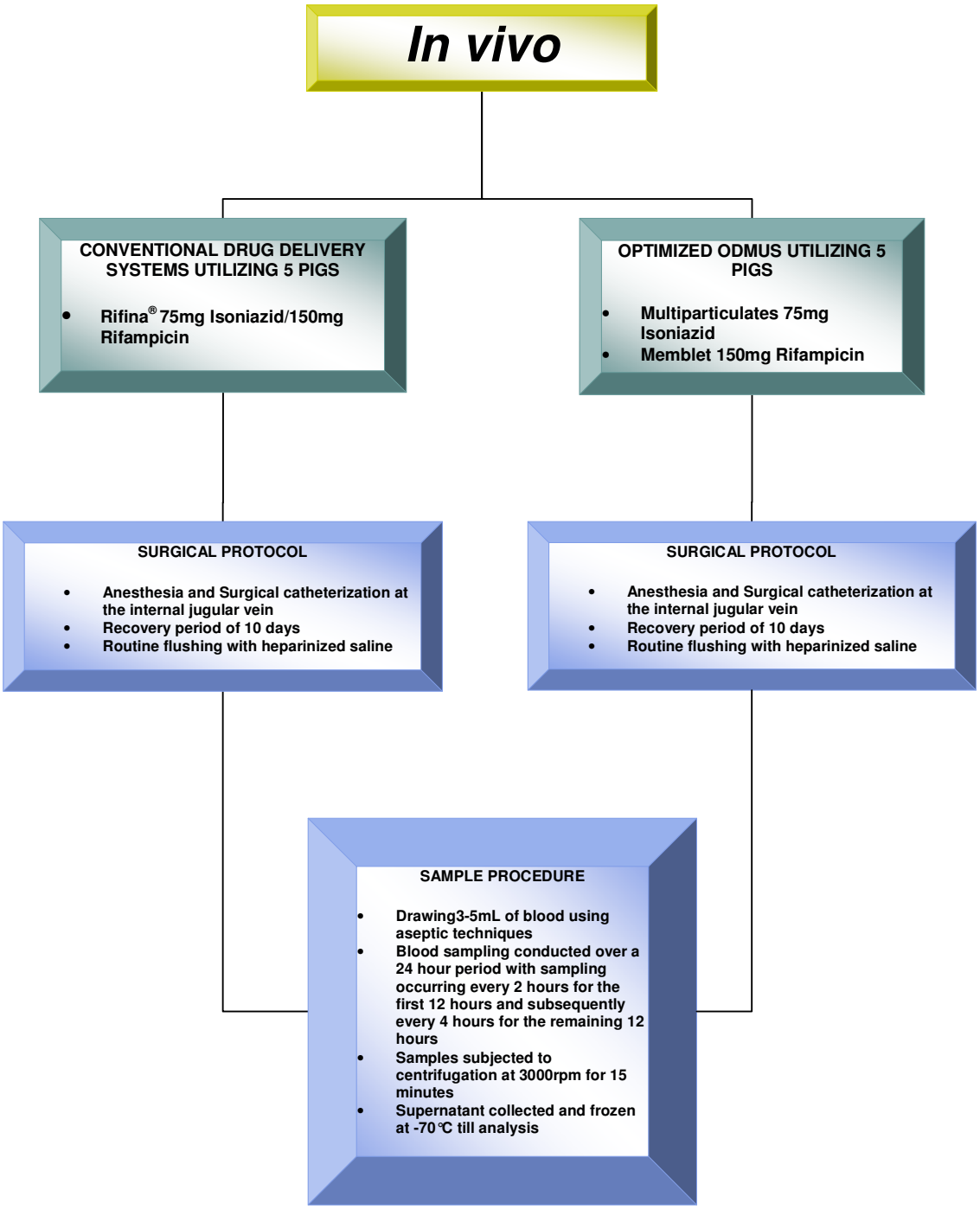


Figure 7.3 Schematic outline of the optimized blood sampling protocol for conventional and Once Daily Multi-Unit Systems

7.3 Materials and Methods

7.3.1 Materials

Solvents used for UPLC–MS/MS measurements were of UPLC grade, and all other reagents were of analytical grade. Oases HLB cartridges, for solid phase extraction, were provided by Waters (Milford, MA, USA). Double deionized UPLC grade water was obtained from a Milli-Q

system, (Milli-Q, Millipore, Johannesburg). Isoniazid (INH) (Sigma Aldrich.Inc St. Louis, Missouri USA), rifampicin (RIF) and the internal standards methylparaben (MP) for *in vitro testing* (Sigma Aldrich.Inc, St. Louis, Missouri USA) and furosemide (FUR) (Sigma Aldrich.Inc, St. Louis, Missouri USA) for *in vivo* testing were of analytical grade. A total of 5 female white pigs were used for study, each healthy and with an average weight of 35kg. Fresh blank plasma was routinely drawn and supplied from the catheterized pigs. Rifinah (Sanofi-aventis, pty.ltd, Midrand, South Africa).

7.3.2 Surgery and implantation of a permanent jugular catheter

Female white pigs, weighing on average 35kg, were anaesthetised with Ketamine® (11mg/kg I.M.) and Midazolam®, (0.3mg/kg I.M.). Buprenorphine® (0.05mg/kg I.M.) and Carpofen® (4mg/kg I.M.) were administered for analgesia and inflammation. Pigs were then intubated and anaesthesia was maintained with 2% Isoflurane® in 100% oxygen. Under aseptic conditions, a 7 french gauge double lumen 35cm catheter (CS-28702) (Arrow Deutschland GmdH, Erding, Germany) was surgically inserted into the left jugular vein. The jugular vein was exposed by an incision made dorsal to the jugular groove on the left lateral aspect of the neck.

Via blunt dissection, the vein was isolated and the catheter was inserted 10cm into the lumen of the vein. The lumen of the catheter was fastened to the wall of the vein using a purse suture technique. The remaining length of the catheter (25cm) was tunnelled subcutaneously, with the use of trocar to an exit point cranial to the dorsal aspect of the scapula. The externalised injection ports of the catheter were sutured to the skin of the pig so as to limit excessive movement and bending. Blood was removed via the catheter and the catheter was flushed with heparin saline (1000i.u. of heparin in 1L of 0.9% saline). Thereafter the animal was allowed 10 days to recover from the surgical procedure. During this time, pigs were habituated to the process of blood sampling. Routine flushing consisted of flushing the catheter with heparinised saline 3 times a day to prevent clotting of blood.

7.3.3 Administration of the once daily multi-unit system

A mixture of Dormicum® and Anaket® was injected directly into the jugular vein catheter. Once sedated, the pig was anaesthetised with 2% isoflurane in 100% oxygen. Both components of the ODMUS (spheres and memblet) were dosed via intubation utilizing a standard intra gastric tube. To prevent accidental pulmonary aspiration, wedging of samples on the oesophageal wall and regurgitation of the samples, all the formulations were washed down the tube with 10mL water. While under sedation, all wounds were checked and sutures were repaired. The pig was returned to its pen to recover under observation.

7.3.4 Blood sampling protocol for the once daily multi-unit system

Blood samples were taken over a 24 hour period at 2 hour intervals were for the first 12 hours, while samples were taken every 4 hours for the remaining 12 hours. The catheter was disinfected and an aseptic technique was used to prevent the introduction of foreign organisms. Before blood was sampled, the catheter was flushed with heparinised saline in order to clear any clots or remove old blood. Thereafter, blood was drawn and placed in a lithium heparin vial. The catheters were once again flushed with heparinised saline. Blood samples were centrifuged at 5000rpm for 10 minutes. The plasma supernatant layer was removed and frozen at -72℃ until analysis.

7.3.5 Ultra performance lipid chromatography for the *in vivo* determination of drug content

Ultra performance lipid chromatography is a widely used technique to utilizing a liquid mobile phase to separate compounds via peak identification. Through increases in pressure, samples are forced through a column. Furthermore, the UPLC is coupled with an Evaporative Light Scattering Detector which provides the qualitative and quantitative analysis of drug samples. According to the Van Deemter equation (Equation 7.1), the underlying principles of UPLC analysis is explained as an empirical formula which explains the relationship between linear flow rate and plate height or column efficiency. By utilizing particle sizes of below 2.5µm, efficiency is improved regardless of the flow rate. Since ultra performance liquid chromatography uses smaller particles, speed and peak capacity, a higher resolution peak can be determined in chromatographic analysis and determination of individual drug components (Swartz, 2005; Waters Chromatography Columns and Supplies Catalog, 2009).

$$H = A + \frac{B}{u} + C \times u \qquad \textit{(Equation 7.1)}$$

Where, A= Eddy-diffusion, B= longitudinal diffusion, C= mass transfer kinetics of the analyte between mobile and stationary phase and u = linear velocity.

As prerequisite data, a UPLC method is required to be produced for an *in vitro* assessment to function as the framework for plasma method determination. Dissolution testing of a conventional Rifinah® Tablet (75mg INH and 150mg RIF) was to be conducted and tested with an *in vitro* UPLC method and assessed against optimized release profiles generated in Chapters 5 and 6.

7.3.5.1 Preparation of calibration curves for the *in vitro* analysis of isoniazid and rifampicin from a conventional dosage form

Stock solutions of INH (0.083mg/mL) MP (1.0mg/mL) were dissolved in simulated gastric fluid of pH 1.2. Serial dilutions (5 dilutions) of INH were prepared for analytical evaluation of the calibration curve. 1.5mL of each dilution solution was mixed with 0.5mL of internal standard and passed through a 0.22µm Cameo Acetate membrane filter (Millipore Co., Bedford, MA, USA) within respective 2mL ANSI48 vials and subjected to analysis.

Similarly, stock solutions of RIF (0.1668mg/mL) MP (1.0mg/mL) were dissolved in simulated gastric fluid of pH 1.2. Serial dilutions (5 dilutions) of RIF were prepared for analytical evaluation of the calibration curve. 1.5mL of each dilution solution was mixed with 0.5mL of internal standard passed and through a 0.22µm Cameo Acetate membrane filter (Millipore Co., Bedford, MA, USA) within respective 2mL ANSI48 vials and subjected to analysis.

7.3.5.2 Development of a method for the concomitant *in vitro* analysis of isoniazid and rifampicin with subsequent analysis thereof

Drug release studies were conducted following the USP 33 Apparatus II (ERWEKA DT 700 GmbH Germany), in which Rifinah® Tablets were tested in duplicate and placed within the vessel under stainless steel ring meshes assembly to prevent the paddle inflicting physical/mechanical damage to the tablet and alter release profiles as well as to prevent erratic fluctuation due to unstable hydrodynamics (Pillay and Fassihi, 2000). Each vessel was filled with 900mL simulated gastric fluid (SGF) and heated to a temperature of 37°C prior to the addition of the multiparticulates and the stainless steel ring mesh assembly. The rotating paddle method was selected at a rotational speed of 50rpm and the machine was calibrated for a 90 minute run with samples taken at regular intervals. Sampling involved the drawing of 5mL of SGF from the dissolution vessel with subsequent refilling of removed buffer to maintain sink conditions. Samples were then subject to UPLC analysis.

Successful *in vivo* data is derived from a fundamental understanding of *in vitro* UPLC analysis. Prior to the construction of an *in vivo* method, an *in vitro* method was developed and used as the template of the plasma method derived.

Priming of the UPLC included a washing protocol of 2 cycles of 10 minutes each. A strong (90%$^{v}/_{v}$ acetonitrile and 10%$^{v}/_{v}$ water) and weak (90%$^{v}/_{v}$ water and 10% $^{v}/_{v}$ acetonitrile) wash were of analytical grade were used with the column temperature set at a constant 25°C.

Optimization of the *in vitro* UPLC method required a selection of either a gradient or isocratic method with varying quantities of mobile phases were selected to elute a detectable peak of

either drug component based on the affinity of the drug to that mobile phase. The 2 mobile phases selected were 100% acetonitrile and a 0.1% formic water mixture. The selection of a gradient method at a constant flow rate of 0.4mL/min is tabulated in Table 7.1.

Table 7.1 Method parameters for the simultaneous determination of isoniazid and rifampicin concentrations

Time (min)	Flow Rate (mL/min)	%A	%B
0	0.4	100	0
0.63	0.4	95	5
1.5	0.4	20	80
1.6	0.4	0	100
1.94	0.4	60	40
2.8	0.4	100	0

%A= 0.1% formic water and %B= pure acetonitrile

7.3.5.3 Plasma calibration curve development for the simultaneous evaluation of isoniazid and rifampicin concentrations

Stock solutions of INH (0.0002mg/µL), RIF (0.0002mg/µL) and internal standard FUR (0.0003mg/µL) were prepared. Blank plasma samples were removed from storage conditions (-70℃) and left to thaw at room temperature. For qualitative studies, the sample preparation method involved a combination of protein precipitation, freeze-liquid and solid-phase extraction (SPE) approaches. 0.5mL plasma and 125µL of serial diluted stock solutions (5 dilutions) of INH were placed in 10mL plastic centrifuge tubes. Samples were vortexed (Vortex genie 2, Bohemia, NY, USA) for 15 seconds to induce protein binding of the INH, similar to *in vivo* conditions. De-protenation was achieved using 3mL of acetonitrile and the sample was vigorously vortexed for 60 seconds. All serial dilutions were then centrifuged at 3000rpm for 15 minutes (Optima® LE-80K, Beckman, USA).

This liquid -liquid extraction method resulted in 3 immiscible layers (Figure 7.4) including an upper aqueous layer, a middle inorganic phase (acetonitrile) and a lower protein precipitate. Liquid supernatants (both aqueous and inorganic phases) were removed and placed into new sample tubes and were then frozen for 10 minutes in a -70℃ freezer. Thereafter samples were removed from the freezer and left to thaw. Due to density differences, the upper aqueous layer (containing water soluble INH) thawed out first and could be removed for solid phase extraction leaving behind the lower inorganic phase (containing RIF).

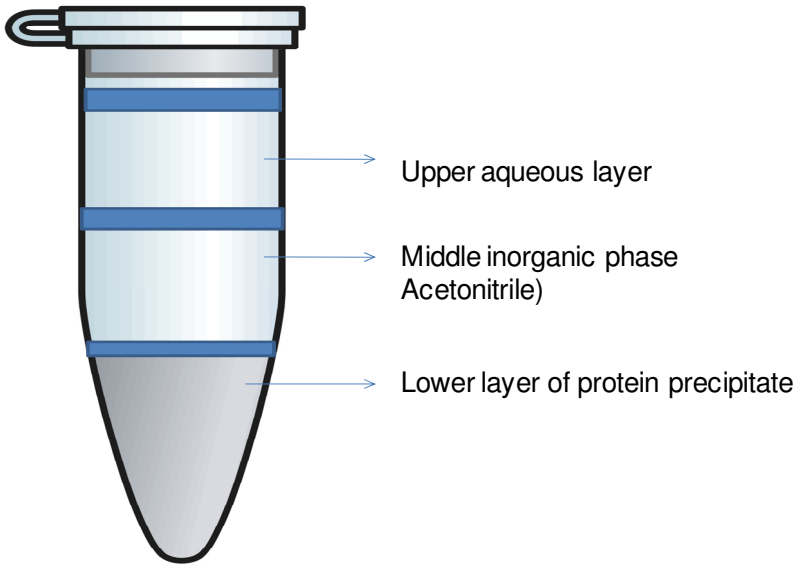


Figure 7.4 Formation of 3 immiscible layers via centrifugation of spiked plasma samples

The Generic Oasis® HLB Solid Phase Extraction (SPE) method was employed to determine the concentrations of methanol that would increase the elution purity of the analyte INH and thereby allow the determination of drug concentration within the samples. Oasis® HLB cartridges enabled with the Visiprep Vacuum Manifold and Standard Lid (Waters,) were conditioned with 1mL methanol and 1mL deionized water. The prepared INH loaded plasma standards were loaded onto the cartridges post-conditioning. Varying concentrations of methanol (10-100%) were used to elute INH loaded plasma samples which were then subjected to UPLC analysis to determine the most efficient methanol concentration for elution of INH spiked calibration standards. SPE confirmed that 30%$^{v}/_{v}$ methanol was evaluated as the most efficacious in producing the most distinctive peaks and determined as the viable elution standard for plasma analysis thereof.

Consequently, plasma calibration standards were loaded onto the HLB cartridges and eluted with 2mL of 30%$^{v}/_{v}$ methanol. These eluted aqueous samples and the organic phase remnant were combined in a sample tube and spiked with 125µL FUR (0.0003mg/µL). These mixed calibration sample tubes (INH, RIF and FURO) were passed through a 0.22µm Cameo Acetate membrane filter (Millipore Co., Bedford, MA, USA) and then expelled into 2mL ANSI 48 vials and subjected to analysis to construct suitable calibration curves for both INH and RIF.

Method parameters were altered in comparison to the *in vitro* testing as the plasma constituents (enzymes, proteins etc) affected the individual drug peaks. A new internal standard furosemide (FUR) was selected, as the MP peak was superimposed onto the RIF peak due to biological plasma interactions. Consequently, a noise degradation peak was in evidence at the elution times of both RIF and FUR, obscuring peak definition and sharpness

and affecting accuracy of data through an elevated baseline. Manipulation of method parameters (Table 7.2) produced a change to the chromatogram at 1.60 minutes and 2.25 minutes by inducing a flow of 100% formic water and 100% acetonitrile respectively. This manipulation successfully shifted the degradation peak to between 2.20 and 2.60 minutes as seen in Figure 7.9 of Chapter 7.4.3.

Table 7.2 Plasma method parameters for dual analysis of rifampicin and isoniazid

Time (min)	Flow Rate (mL/min)	%A	%B
0	0.4	100	0
0.63	0.4	100	0
1.5	0.4	20	80
1.6	0.4	0	100
2.25	0.4	100	0

%A= 0.1% formic water and %B= acetonitrile

7.3.5.4 Plasma sample analysis for the simultaneous evaluation of the once daily multi-unit system in a female white pig

Plasma samples of both the conventional Rifinah® and the ODMUS system were removed from storage conditions (-70℃) and left to thaw at room temperature. For qualitative studies, the sample preparation method involved protein precipitation, freeze-liquid and solid-phase extraction (SPE) approaches. 0.5mL plasma was added to 10mL plastic centrifuge tubes. An amount of 3mL acetonitrile was added to achieve full de-protenation and the sample was vigorously vortexed (Vortex genie 2, Bohemia, NY, USA) for 60 seconds. All plasma samples were then centrifuged at 3000rpm for 15 minutes (Optima® LE-80K, Beckman, USA).

The liquid-liquid extraction method described in Chapter 7.3.2.9 was adopted and resulted in 3 immiscible layers including the upper aqueous layer, a middle inorganic phase (acetonitrile) and a lower protein precipitate. Liquid supernatants (both aqueous and inorganic phases) were removed and placed into new sample tubes and were then frozen for 10 minutes in a -70℃ freezer. Thereafter samples were removed from the freezer and left to thaw. Due to density differences, the upper aqueous layer (containing water soluble INH) thawed out first and could be removed for solid phase extraction leaving behind the lower inorganic phase (containing RIF).

The aqueous extracted supernatant layers from both Rifinah® and ODMUS samples were loaded onto the HLB cartridges and eluted with 2mL of 30%$^{v}/_{v}$ methanol. These eluted aqueous samples and the organic phase remnant were combined in a sample tube and spiked with 125µL FUR (0.0003mg/µL). These mixed calibration sample tubes (INH, RIF and FURO) were passed through a 0.22µm Cameo Acetate membrane filter (Millipore Co.,

Bedford, MA, USA) and then expelled into 2mL ANSI 48 vials and subjected to analysis to generate drug release profiles for both Rifinah® and ODMUS samples.

7.4 Results and Discussion

7.4.1 Validation of a method for the concomitant *in vitro* analysis of isoniazid and rifampicin with subsequent analysis thereof

Dissolution samples were tested at 5, 30, 60 and 90 minutes. 5mL samples were drawn of which 1.5mL was expelled into a 2mL ANSI 48 vial. Additionally, 0.5mL of internal standard was included in each vial. Relative to i*n vitro* release profiles illustrated in Chapters 6.3.6 and 5.3.7, INH and RIF exhibit no control release patterns from the conventional Rifinah® tablet. Calibration curves developed for both INH and RIF (Figure 7.5a and Figure 7.5b) were used to generate the release profiles, displayed in Figure 7.6, within simulated gastric fluid. Within this simulated environment, dose dumping is evidently seen within the first 5 minutes. After half an hour of dissolution testing, the bulk of both INH and RIF are released. Within 90 minutes of conducting the dissolution test, complete dissolution of the Rifinah® tablet occurred. The optimized ODMUS system achieved vastly improved release profiles (Chapters 6.3.6 and 5.3.7). Furthermore, site-specific drug delivery was corroborated through segregated delivery of INH and RIF throughout specific gastrointestinal locations negating the deleterious drug-drug interactions that can occur. The conventional Rifinah® tablet fails to achieve the extended control release patterns of the ODMUS and does not ensure segregated delivery of INH and RIF. The lack of a delivery system as in the ODMUS clearly identifies Rifinah® to be inferior. A gradient method was selected such that an initial elution of the water soluble INH would occur at 0.621 minutes due to a higher formic water constitution (100%). Elution times of 1.907 and 2.065 minutes, successfully displayed 2 separate and distinct peaks of RIF and MP respectively. Figure 7.7 indicates the successful *in vitro* profile displaying INH, RIF and MP utilizing a single method. RIF metabolites are noted to elute prior to the RIF peak.

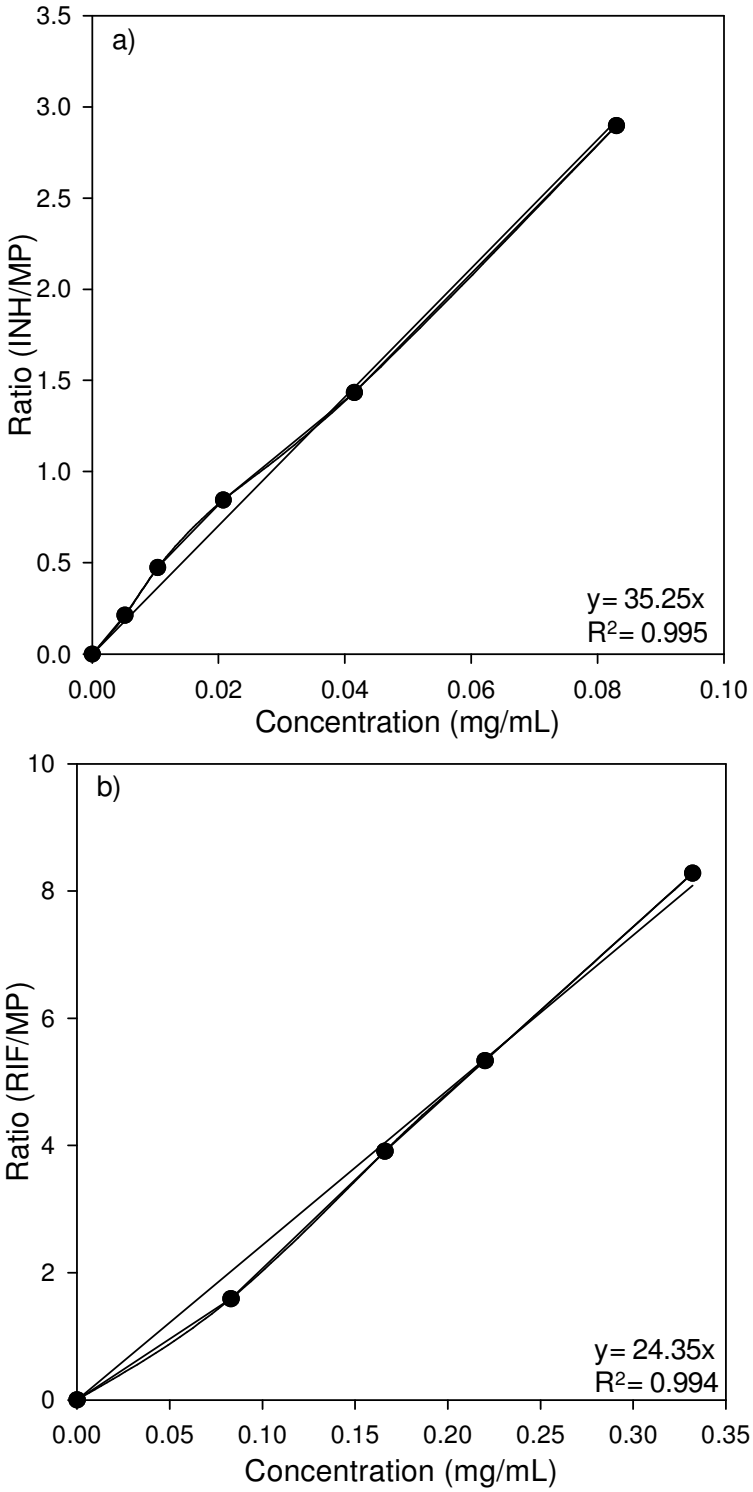


Figure 7.5 *In vitro* calibration curves for a) isoniazid and b) rifampicin to elucidate the conventional dosage form's (Rifinah®) drug release profiles

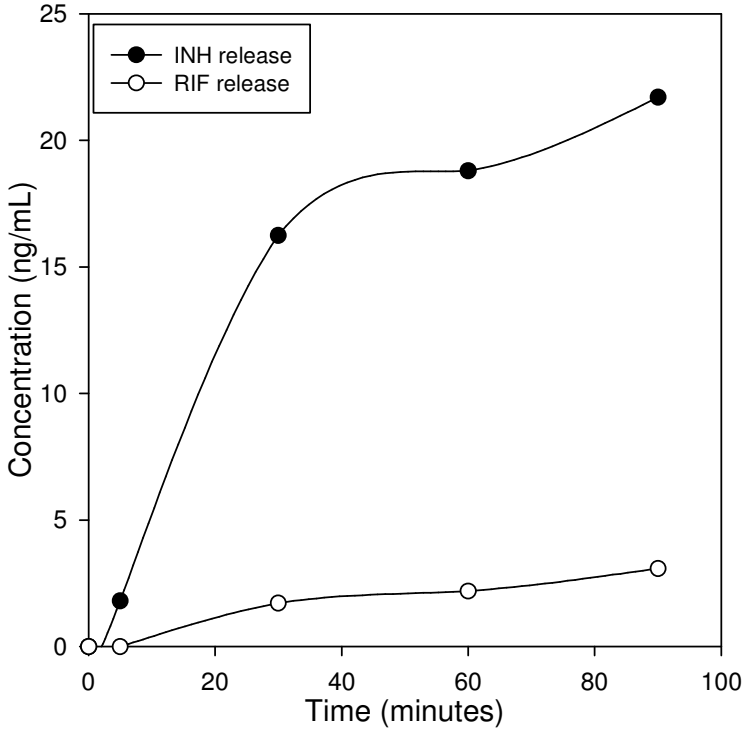


Figure 7.6 Determination of release patterns of isoniazid and rifampicin from the conventional Rifinah® tablet within simulated gastric fluid (pH 1.2); where N= 3 and SD< 0.04 in all cases

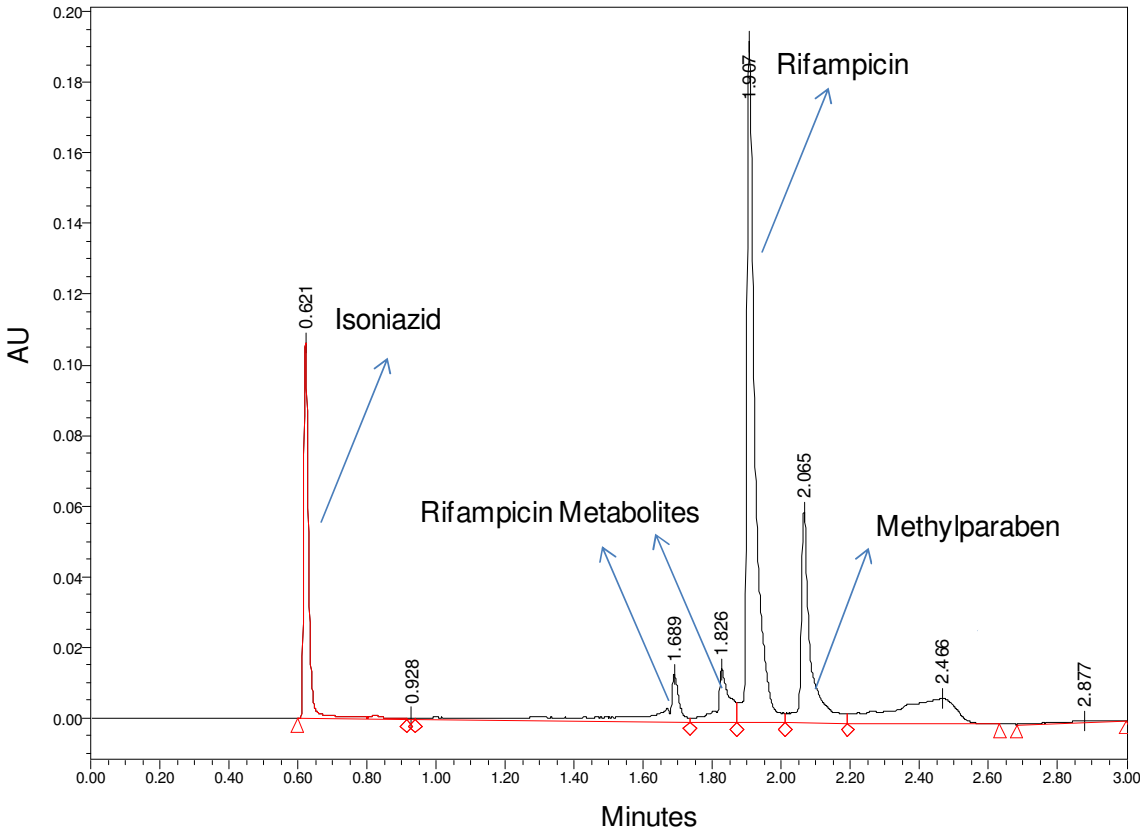
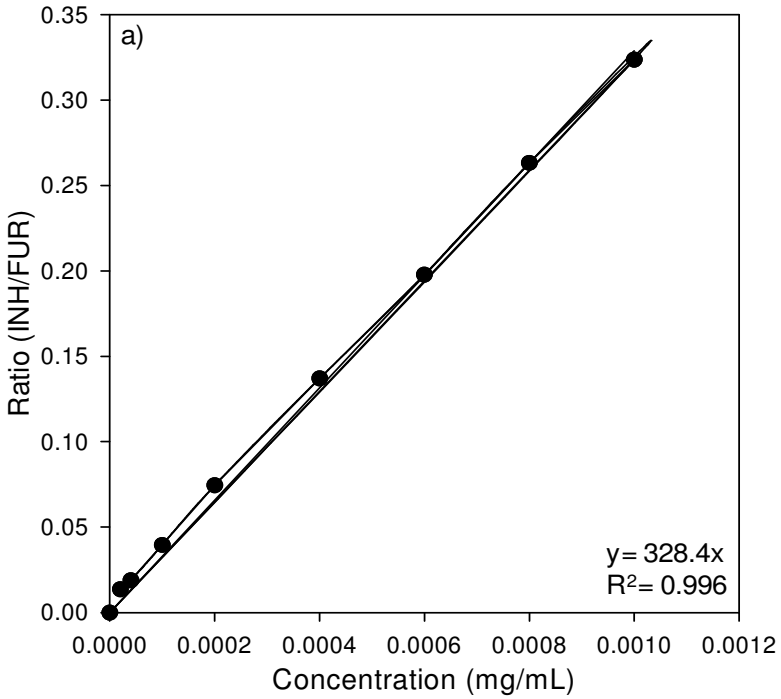


Figure 7.7 Ultra performance lipid chromatography chromatogram identifying isoniazid, rifampicin, methylparaben and the corresponding metabolites of rifampicin

7.4.2 Plasma calibration curves for the simultaneous evaluation of isoniazid and rifampicin concentrations



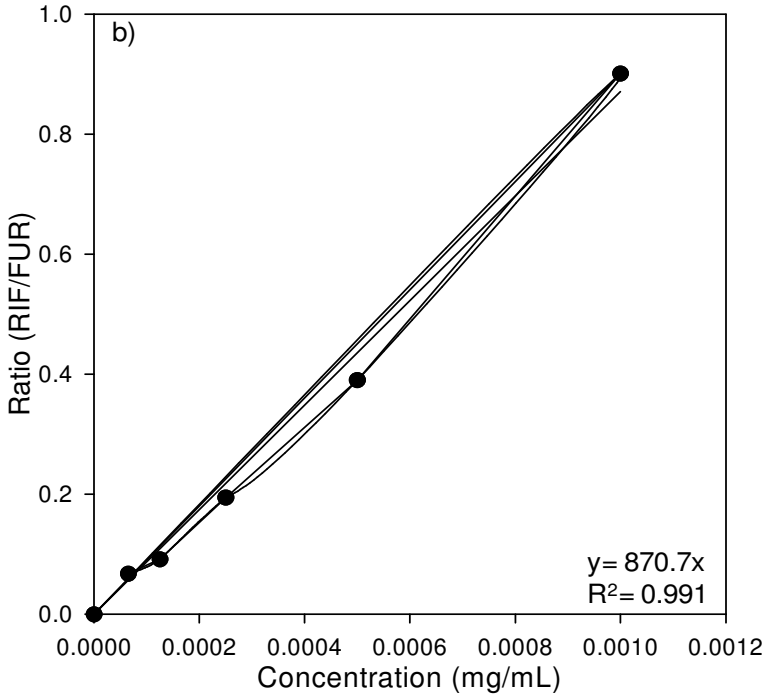


Figure 7.8 *In vivo* calibration curves for a) isoniazid and b) rifampicin

7.4.3 Plasma sample analysis for the evaluation of the once daily multi-unit system drug release in a female white pig

The purpose of *in vivo* drug content determination was to evaluate the variance of drug release between the ODMUS and conventional dosage form Rifinah®. *In vitro* release studies described in Chapters 6.3.6, 5.3.7 and 7.4.1 fully identify the large discrepancy that exists between the novel ODMUS and the Rifinah® tablet in a simulated environment. The combination of the memblet and the multiparticulate system successfully produced superior drug release profiles, site-specific drug distribution and segregation of actives within the gastrointestinal tract. However, whilst dissolution testing is a USP recognized methodology, it cannot emulate the dynamic and unique environment of the body. Through *in vivo* testing within the pig model, an accurate portrayal of how the body's physiological and anatomical design affects drug release of both the ODMUS and Rifinah® could be established.

Plasma UPLC method development was a critical first step in the determination of drug blood content. The template method derived from *in vitro* studies of Chapter 7.3.2.6 was moderated to accommodate the presence of blood constituents (enzymes, proteins etc) which biologically altered drug content. Method altercation proved essential due to the presence of a biological degradation product, absent with *in vitro* chromatograms. The undesirable phenomenon of superimposition of the degradation peak onto the FUR and RIF peaks was negated and is illustrated as being shifted to between 2.20 and 2.60 minutes in Figure 7.9. 3-Dimensional scrutiny was a valuable tool in isolating the range of absorption for each specific drug molecule and aided in separation of the drug degradation product (Figure 7.10).

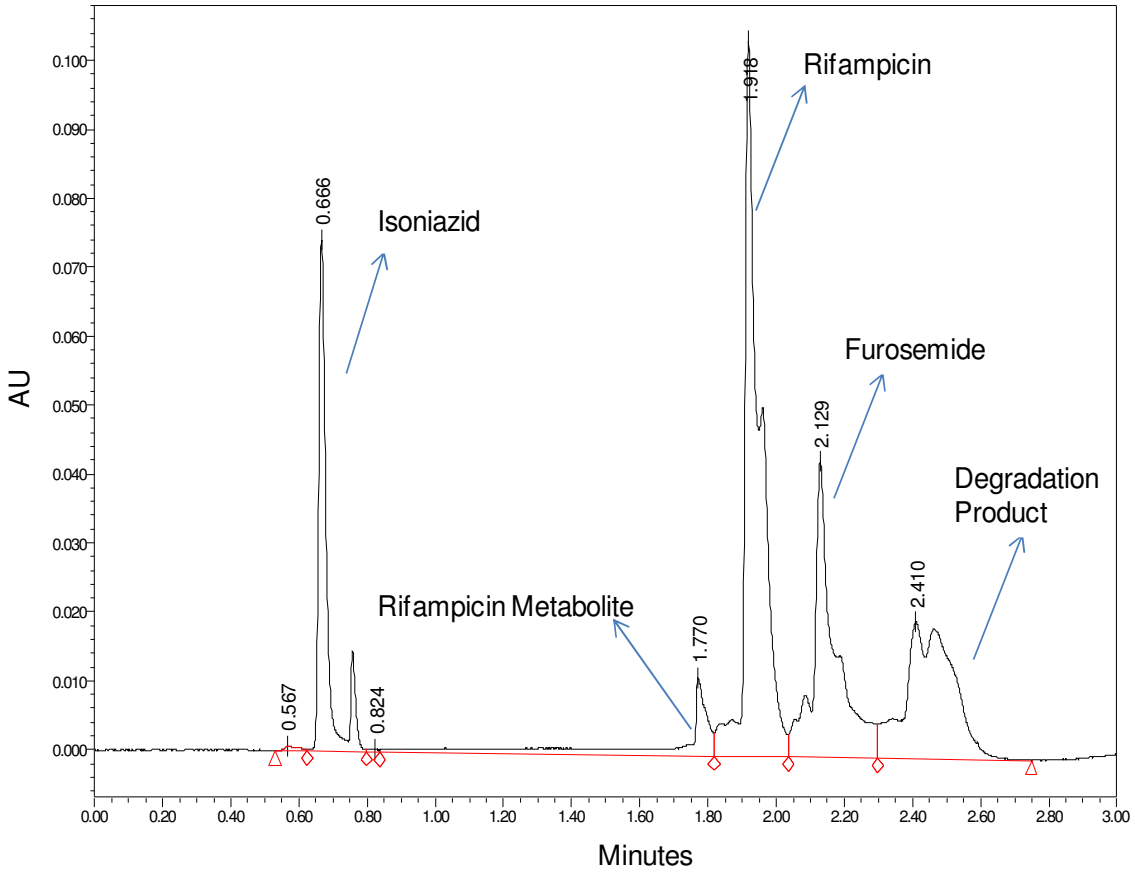


Figure 7.9 Ultra performance lipid chromatography method development for the concomitant plasma drug content evaluation of isoniazid and rifampicin with separation of the undesirable degradation product using blank plasma

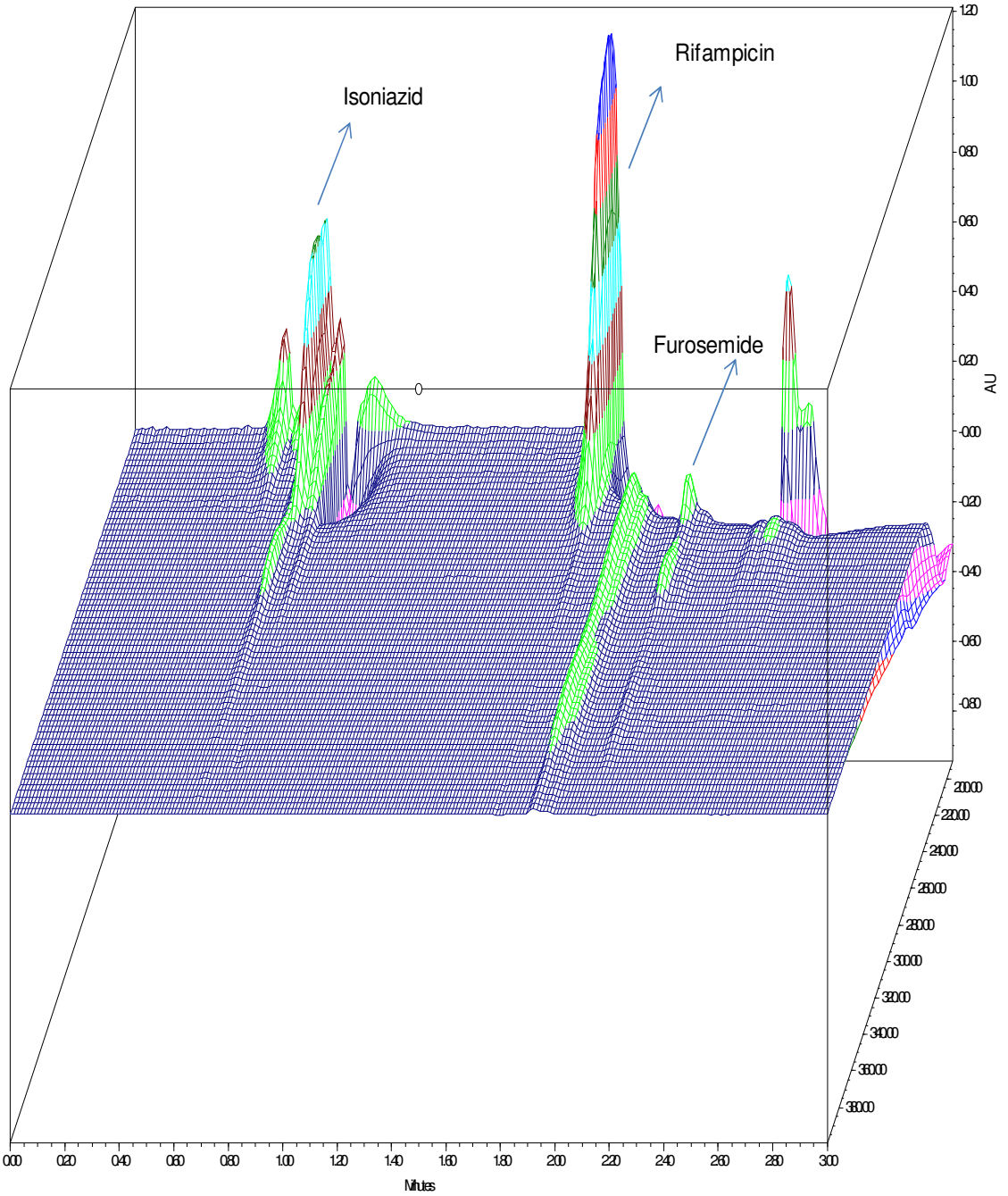


Figure 7.10 3-D modelling of a typical plasma chromatogram for isoniazid, rifampicin and furosemide indicating the respective range of absorption

Plasma levels of drug concentration for both conventional and the ODMUS are plotted in Figure 7.11 and Figure 7.12. Rifinah® tablets can be simply described as compressed INH and RIF powders. Release of both drugs is based on the dissolution and erosion upon immediate contact with gastric fluid. Within 2 hours of exposure to the gastric environment, a complete release of INH and RIF has occurred. In correspondence with the deleterious drug-drug interaction described in Chapter 2.3.3, the simultaneous delivery of INH and RIF within acidic stomach conditions provides the environment for formation of an insoluble complex. Blood drug content of both pharmacological actives showed considerable decreases in

relation to the optimized ODMUS formulation (C_{max}INH= 0.0138ng/mL and C_{max}RIF= 0.052ng/mL).

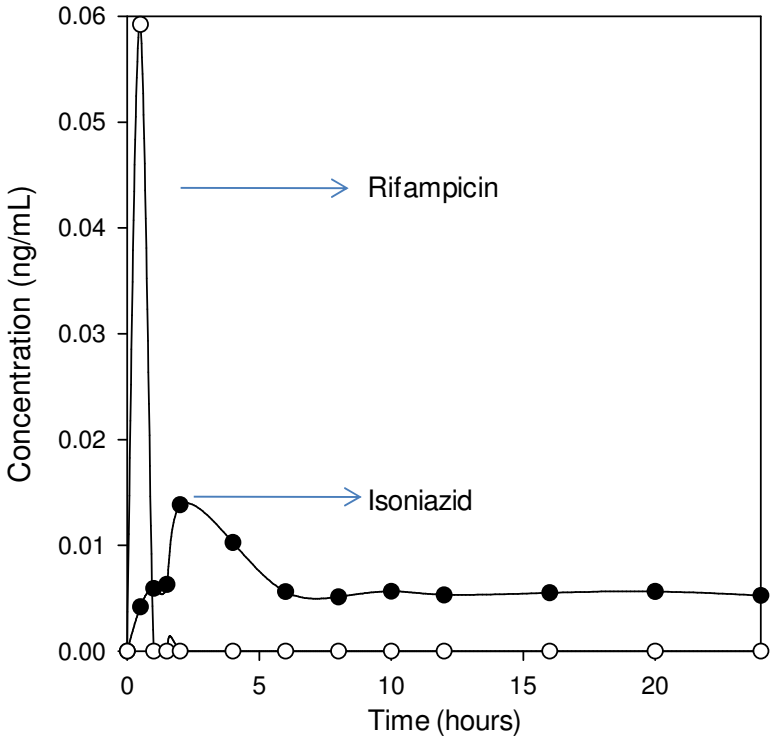


Figure 7.11 24 hour investigation into the divergence of drug blood content between isoniazid and rifampicin from a conventional dosage form; where N= 5 and SD < 0.1 in all cases

Significant improvement on release patterns and blood drug concentration is immediately noted in Figure 7.12. During the gastric retention period (0-4 hours), a complete release of RIF was achieved. Minimal INH levels were ascertained during these 4 hours, authenticating the acid resistant characteristic of the multiparticulates. Segregated, site-specific drug release, as per the objectives of this dissertation, was accomplished and reinforced with the notable increase in maximal blood drug content (C_{max}INH= 0.0368ng/mL and C_{max}RIF= 0.1052ng/mL) through avoidance of the deleterious interaction. Furthermore, an extended duration of release of INH is noted. A prolonged 10 hours of controlled release is illustrated which is a significant improvement on the conventional Rifinah® formulation (2 hours). No untoward, idiosyncratic toxic side effects were noted and the pigs remained healthy for the duration of the study validating the biocompatibility of the formulation.

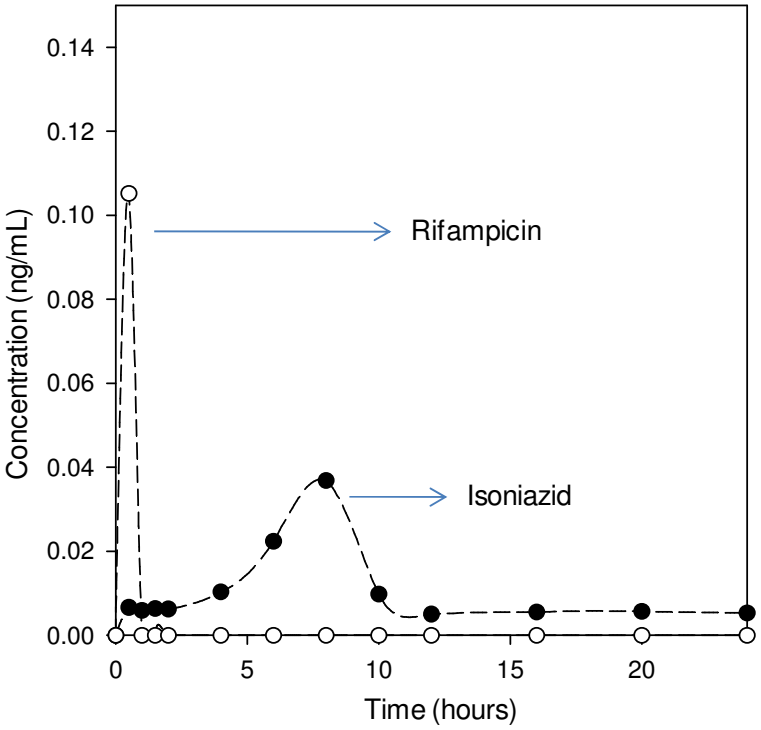


Figure 7.12 24 hour investigation into the divergence of drug blood content between isoniazid and rifampicin from the novel Once Daily Multi-Unit System; where N= 5 and SD< 0.33 in all cases

7.5 Concluding Remarks

This Chapter sought to address the behaviour of the ODMUS under *in vivo* conditions employing ultra performance lipid chromatography as an analysis tool.

Development of a suitable and efficacious *in vivo* model was theorized and implementation of the protocol was successfully achieved through the Pig model. Biocompatibility was determined as successful for this novel ODMUS.

The ODMUS system, through stringent UPLC method development and *in vivo* analysis, was determined to corroborate with data presented with *in vitro* testing. In addition, superiority of the system over the conventional Rifinah® formulation was made apparent. Segregated site-specific release of INH within the small intestine and RIF in the stomach was successfully executed. Noteworthy increases in blood drug concentration for both INH and RIF relative to the conventional system were indicative of counteraction of the deleterious interaction that occurs with simultaneous delivery of INH and RIF within an acidic environment.

In conclusion, the OMDUS was determined to be biocompatible and to display superior release patterns, to negate drug-drug interactions and to achieve segregated delivery of pharmacological actives in comparison to the conventional dosage form.

CHAPTER 8
CONCLUSIONS AND RECOMENDATIONS

8.1 Conclusions

Drug regimen therapy has been described as considerable problem over the years for both patient and practitioner (Lenert *et al*., 1989, Ormerod and Prescott, 1991; Jindani and Griffin, 2010). The compounding of factors side effects, high pill burden and the effort to take medication in a segregated fashion more than once a day, result in poor patient compliance ad drug therapeutic failure. Debilitating conditions such as tuberculosis and HIV are specifically notorious having close to unmanageable drug regimens especially within resource poor countries (De Cock and Wilkinson, 1995; Mehdi *et al.,* 2005; Vermund and Yamamoto, 2007).

Much emphasis has been placed on research and development to manage drug regimen therapies (Hernández *et al*., 2010; Renteria *et al*., 2010; Wong *et al*., 2010), but the allocated funding and skilled individuals to conduct such research is limited in South Africa. Pharmaceutical development is a benchmark to safer, more cost effective and efficacious drug regimen therapy.

Within a South African context, HIV and tuberculosis are seen as highly debilitating conditions, but it is the medication management that is seen as an equal challenge. The cost of treatment alone is a burden many South Africans cannot manage. It is fairly common through many drug regimen based conditions to see opportunistic infections occur and convolute and increase pharmacological actives complicating dosing and affecting cost. As a result, much treatment is left unattended.

This dissertation sought to highlight the research conducted on a similar complication within tuberculosis treatment with regards to the deleterious interaction occurring between isoniazid and rifampicin, 2 components essential for efficacious tuberculosis management.

The once daily multiple unit drug delivery system (ODMUS) provided a unique concept of manipulating Eudragit® molecules L 100-55 an E 100 to produce multiparticulate and memblet drug delivery systems respectively. The novelty of the system lies in the unique single process step for both formulations. The concomitant intake of the formulations would also ensure a controlled, segregated site-specific release of isoniazid and rifampicin to

negate the deleterious interaction that can occur between them and increase bioavailability of each active.

Extensive *in vitro* preliminary testing of each formulation was accomplished to produce an optimized design. Preliminary evaluation of dissolution and drug entrapment testing of the multiparticulate component established upper and lower limits for variant formulation parameters of crosslinker type, crosslinker and ethyl cellulose concentration. Similarly, the memblet variables were deduced through dissolution and differential scanning calorimetry to be crosslinker concentration, plasticizer content and surfactant contributions.

A total of 15 formulations for both the memblet and multiparticulate component of the ODMUS were proposed using a Box-Behnken factorial design and were accordingly synthesized. Responses testing for multiparticulates were MDT through dissolution testing and DEE through drug entrapment studies. T_g and MDT were responses tested through DSC and dissolution studies respectively for memblet optimization. Through these rigorous testing protocols, and optimized formulation was calculated for each component of the ODMUS.

A full testing protocol of the each optimized formulation was conducted to corroborate with the predicted data. Multiparticulate verification was successfully implemented through dissolution, FTIR, SEM, DEE, surface area and porosity analysis and chemometric modelling. These highly individualized tests were specifically chosen to understand the release mechanisms with relation to its internal structure and molecular interactions.

Memblet formulations underwent stringent rheological, thermal, mechanical and molecular characterization to ascertain the relevant nature of the memblet and the consequent release patterns.

This led to the development of an individualized *in vivo* protocol and the adoption of said protocol into a test procedure. The model adopted successfully indicated the segregated site-specific delivery of each isoniazid and rifampicin in a rate controlled manner with an improvement on bioavailability in relation to a concurrently tested conventional dosage form.

These delivery systems have been proven to be successful in managing a tuberculosis regimen, but the system itself is not exclusive to this conditions. Manipulation of variant polymers, surfactants and crosslinkers could very well alter the formulation to achieve even further release times and in a more controlled manner.

8.2 Recommendations

Multiparticulate and membranous technology must be thoroughly investigated as a combined delivery system such that the 2 technologies can be taken as a single dosage form. The benefits of such a combination of technologies have tremendous applications for drug regimen therapies with more emphasis placed on *in vivo* testing.

Multiparticulate formulations must have improved drug entrapment efficiency to limit the large quantity of multiparticulates required. Controlled release can also be extended up to 24 hours.

The memblet could potentially be manipulated into a gastro-floatable or adhesive system which could then be moderated to achieve an even longer release pattern for up to 8 hours. A modified desiccation strategy must be defined to reduce the drying time to less than a day without compromising optimized characteristics.

In vivo diagnostics must be furthered with expanded testing such as gamma scintigraphy and further improve *in vivo* assessment for future works.

REFERENCES

Abbaspour, M.R., Sadeghi, F. and Garekani, H.A., (2008). Design study of ibuprofen disintegrating sustained-release tablets compri*sing* coated pellets*. European Journal of Pharmaceutics and Biopharmaceutics, **68**,* 747-759.

Acosta, E.P. and Fletcher, C.V., (1995). Antiretroviral drug interactions, *International Journal of Antimicrobial Agents, **5***, 73-83.

AIDS treatment data network., (2006). Lamivudine/zidovudine (Combivir), Simple Facts Project. http://www.atdn.org/simple/combi.html [Accessed January 21, 2010].

Akihiro, F., Tatsuo, M., Tomohiro, S., Yoshikage, O. and Hideto, M., (2009). pH-responsive behavior of Hydrogel microspheres altered by layer-by-layer assembly of polyelectrolytes. *Colloids and Surfaces*, ***337***, 159-163.

Alex, R. and Bodmeier, R., (1990). Encapsulation of water-soluble drugs by a modified solvent evaporation method. I. Effect of process and formulation variables on drug entrapment. *Journal of Microencapsulation, **7***, 347-355.

Al-Zoubi, N., AlKhatib, H.S., Bustanji, Y., Aiedeh, K. and Malamataris, S., (2008). Sustained-release of buspirone HCl by co spray-drying with aqueous polymeric dispersions. *European Journal of Pharmaceutics and Biopharmaceutics, **69***, 735-742.

Audoin M., (2003). Enriching the knowledge about cellulose acetate. Presentation to the Coresta joint meeting, from 7-11 September 2003. Freiburg, Germany.

Aungst, B.J., (1999). P-glycoprotein, secretory transport and other barriers to the oral delivery of anti-HIV drugs. *Advanced Drug Delivery Reviews, **39***, 105-116.

Ausar, S.F., Bianco, D.I., Castagna, L.F., Alasino, R.V. and Beltramo, D.M., (2003). Interaction of a Cationic Acrylate Polymer with Caseins: Biphasic Effect of Eudragit® E100 on the Stability of Casein Micelles. *Journal of Agricultural and Food Chemistry, **51***, 4417-4423.

Aziz, M.A., Wright, A.M.P.H, De Muynck M.P.H and Laszlo A., (2004) Anti-tuberculosis drug resistance in the world. In Third global report. The WHO/IUATLD global project on drug resistance surveillance. World Health Organization, Geneva.

Babar, I.A. and Muhammad, A., (2002). Controlled-release naproxen using micronized ethyl cellulose by wet-granulation and solid-dispersion method. *Drug Development and Industrial Pharmacy,* ***28***, 129-134.

Bae, K.H., Mok, H. and Park, T.G., (2008). Synthesis, characterization, and intracellular delivery of reducible heparin nanogels for apoptotic cell death. *Biomaterials,* ***29***, 3376-3383.

Bangham, A.D., (1969). Membrane models with phospholipids. *Progress in Biophysics and Moecularl Biology,* ***18***, 29-95.

Bangsberg, D.R., Charlebois, E.D., Grant, R.M., Holodniy, M., Deeks, S.G. and Perry, S., (2003). High levels of adherence do not prevent accumulation of HIV drug resistance mutations. *AIDS,* ***17***, 1925-1932.

Bao, A., Phillips, W.T., Goins, B., Zheng, X., Sabour, S., Natarajan, M., Woolley, F.R., Zavaleta, C. and Otto, R.A., (2006). Potential use of drug carried-liposomes for cancer therapy via direct intratumoral injection, *International Journal of Pharmaceutics,****316***, 162-169.

Baraniuk, J., Ali, M., Brody, D., Maniscalco, J., Gaumond, E. and Fitzgerald, T., (1997). Glucocorticoids induce beta2-adrenergic receptor function in human nasal mucosa. *American Journal of Respiratory and Critical Care Medicine,* ***155***, 704-710

Battaglioli-DeNero, A.M., (2007). Strategies for improving patient adherence to therapy and long-term patient outcomes. *Journal of the Association of Nurses in AIDS care,* ***18***, 17-22.

Belland, D.S.H. and Wyne, K.L., (2006). Symposium on diabetes. *Postgraduate medicine,* ***119***, 8-14.

Blum, M.R., Liao, S.H.T., Good, S.S. and deMiranda, P., (1988). Pharmacokinetics and bioavailability of zidovudine in humans. *The American Journal of Medicine,* ***85***, 189-194.

Bodmeier, R. and Paeratakul, O., (1994). Suspensions and dispersible dosage forms of multiparticulates. In Multiparticulate Oral Drug Delivery. New York, Ghebre-Sellassie, volume 1.

Bodmeier, R., Wang, H. and Herrmann, J., (1994). Microencapsulation of chlorpheniramine maleate, a drug with intermediate solubility properties, by a non-aqueous solvent evaporation technique. *STP Pharma Sciences, **4***, 275-281

Boguszewski, C.L., Meister, L.H.F., Zaninelli, D.C.T. and Radominski, R.B., (2005). One year of GH replacement therapy with a fixed low-dose regimen improves body composition, bone mineral density and lipid profile of GH-deficient adults*. European Journal of Endocrinology, **152***, 67-75.

Bolton, S., (1997). Factorial designs. In: Pharmaceutical Statistics: Practical and Clinical Applications. New York, Marcel Dekker, volume 3.

Boulet, L.P., Gauvreau, G., Boulay, M.E., O'Byrne, P. and Cockcroft, D.W., (2007). The allergen bronchoprovocation model: an important tool for the investigation of new asthma anti-inflammatory therapies. *Allergy, **62***, 1101-1110.

Bourgeois, B.F.D., (2002). Reducing overtreatment. *Epilepsy Research, **52***, 53-60.

Bramer, S.L., Au, J.L.S. and Wientjes, M.G., (1993). Gastrointestinal and hepatic first-pass elimination of 2′,3′-dideoxyinosine in rats. *Journal of Pharmacology and Experimental Therapeutics, **265***, 731-738.

Brunet, B., Douceta, C., Venisseb, N., Haueta, T., Hébrardc, W., Papetb, Y., Maucoa, G. and Mura, P., (2009). Validation of Large White Pig as an animal model for the study of cannabinoids metabolism: Application to the study of THC distribution in tissues. *Forensic Science International,**161***, 169-174.

Cabañas, M.V., Peña, J., Román, J. and Vallet-Regí, M., (2009). Tailoring vancomycin release from β-TCP/agarose scaffolds. *European Journal of Pharmaceutical Sciences, **37***, 249-256.

Cao, N., Yang, X. and Fu, Y., (2009). Effects of various plasticizers on mechanical and water vapor barrier properties of gelatin films. *Food Hydrocolloids, **23***, 729-735.

Ceballos, B., Cirri, M., Maestrelli, F., Corti, G. and Mura, P., (2005). Influence of formulation and process variables on in vitro release of theophylline from directly-compressed Eudragit matrix tablets. *Farmaco, **60***, 913-918.

Celej,. M.S., Dassie, S.A., González, M., Bianconi, M.L. and Fidelio, G.D., (2006). Differential scanning calorimetry as a tool to estimate binding parameters in multiligand binding proteins. *Analytical Biochemistry,* ***350***, 277-284.

Chambin, O., Champion, D., Debray, C., Rochat-Gonthier, M.H., Le, Meste, M. and Pourcelot, Y., (2004). Effects of different cellulose derivatives on drug release mechanism studied at a preformulation stage. *Journal of Controlled Release,* ***95***, 01-108.

Chen, M.C., Tsai, H.W., Liu, C.T., Peng, S.F., Lai, W.Y., Chen, S.J., Chang, Y. and Sung, H.W.A., (2009). Nanoscale drug-entrapment strategy for Hydrogel-based systems for the delivery of poorly soluble drugs. *Biomaterials,* ***30***, 2102-2111.

Chun, K.W., Lee, J.B., Kim, S.H. and Park, T.G., (2005). Controlled release of plasmid DNA from photo-cross-linked pluronic hydrogel. *Biomaterials,* ***26***, 3319-3326.

Chung, C.W., Kim, H.W., Kim, Y.B. and Rhee, Y.H., (2003). Poly (ethylene glycol)-grafted poly(3-hydroxyundecenoate) networks for enhanced blood compatibility. International *Journal of Biological Macromolecules,* ***32***, 17-22.

Polyethylene glycol general properties., (2000). CELL CHEMICAL Company.. – [http://www.surfactant.co.kr/surfactants/peg.html] date accessed 12 January 2010.

Córdoba-Díaz, D., Córdoba-Díaz, M., Awad, S. and Córdoba-Borrego, M., (2001). Effect of pharmacotechnical design on the in vitro interaction of ketoconazole tablets with non-systemic antacids. *International Journal of Pharmaceutics,* ***226***, 61-68.

Corrigan, O.D., Healy, A.M. and Corrigan, O.I., (2006). Preparation and release of salbutamol from chitosan and chitosan co-spray dried compacts and multiparticulates. *European Journal of Pharmaceutics and Biopharmaceutics,* ***62***, 295-305.

Crevoisier, C., Zerr, P., Calvi-Gries, F. and Nilsen, T., (2003). Effects of food on the pharmacokinetics of levodopa in a dual-release formulation. *European Journal of Pharmaceutics and Biopharmaceutics,* ***55***, 71-76.

Crommelin, D., Bos, G. and Storm, G., (2002). Liposomes- Successful carrier systems for targeted drug delivery. The drug delivery companies Report Autumn/Winter 2002 © PharmaVentures.

Crowley, M.M., Schroeder, B., Fredersdorf, A., Obara, S., Talarico, M., Kucera, S. and McGinity, J.W., (2004). Physicochemical properties and mechanism of drug release from ethyl cellulose matrix tablets prepared by direct compression and hot-melt. *International Journal of Pharmaceutics, **269***, 509-522.

Cryan, A., Sivadas, N. and Garcia-Contreras, L., (2007). In vivo animal models for drug delivery across the lung mucosal barrier. *Advanced Drug Delivery Reviews, **59***, 1133-1151.

Cui, F., Wang, Y., Wang, J., Feng, L. and Ning, K., (2007). Preparation of redispersible dry emulsion using Eudragit E100 as both solid carrier and unique emulsifier. *Colloids and Surfaces A: Physicochem. Eng. Aspects, **307***, 137-141.

Currie, G.P., Lee, D.K.C. and Wilson, A.M., (2005). Effects of dual therapy with corticosteroids plus long acting β2-agonists in asthma. *Respiratory Medicine, **99***, 683-694.

Dashevsky, A. and Mohamad, A., (2006). Development of pulsatile multiparticulate drug delivery system coated with aqueous dispersion Aquacoat®. *International Journal of Pharmaceutics, **318***, 124-131.

De, Cock, K.M. and Wilkinson, D., (1995). Tuberculosis control in resource-poor countries: alternative approaches in the era of HIV. *The Lancet, **346***, 675-677.

De, Oliveira, H.P., Albuquerque, Jr, J.J.F., Nogueiras, C. and Rieumont, J., (2009). Physical chemistry behavior of enteric polymer in drug release systems. *International Journal of Pharmaceutics, **366***, 185-189.

De, Vasconcelos, C.L., Bezerril, P.M., dos, Santos, D.E.S., Dantas, T.N.C., Pereira, M.R. and Fonseca, J.L.C., (2006). Effect of Molecular Weight and Ionic Strength on the Formation of Polyelectrolyte Complexes Based on Poly(methacrylic acid) and Chitosan. *Biomacromolecules, **4***, 1245-1252.

Degussa Eudragit®., (2007). Manual for methacrylate polymers for pharmaceutical applictions. Degussa AG Pharma Polymers, Darmatadt, Germany.

Desaia, J., Alexandera, K. and Rigaa, A., (2006). Characterization of polymeric dispersions of dimenhydrinate in ethyl cellulose for controlled release. *International Journal of Pharmaceutics, **308***, 115-123.

Diamant, Z., Boot, D., Kamerling, I. and Bjermer, L., (2008). Methods used in clinical development of novel anti-asthma therapies. *Respiratory Medicine, **102***, 332-338.

Diamant, Z., Boot, J.D. and Virchow, J.C., (2007). Summing up 100 years of asthma. *Respiratory Medicine, **3***, 378-388.

Dongming, H., Heru, S. and Mathias, U., (2009). Photo-irradiation for preparation, modification and stimulation of polymeric membranes, *Progress in Polymer Science, **34***, 62-98.

Dorati. R., Genta, I., Colonna, C., Modena, T., Pavanetto, F., Perugini, P. and Conti, B., (2007). Investigation of the degradation behavior of poly(ethylene glycol-co-d,l-lactide) copolymer. *Polymer degradation and stability, **92***, 1660-1668.

Dorkoosh, F.A., Verhoef, J.C., Borchard, G., Rafiee-Tehrani, M., Verheijden, J.H.M. and Junginger, H.E., (2002). Intestinal absorption of human insulin in pigs using delivery systems based on superporous hydrogel polymers. *International Journal of Pharmaceutics, **247***, 47-55.

Dowdall, N., Evans, A., Figueroa, J., Ijaz, K. and Maloney, S., (2006). Tuberculosis and Air Travel: Guidelines for prevention and control. [http://whqlibdoc.who.int/hq/2006/WHO_HTM_TB_2006.363_eng.pdf] date accessed February 8 2010.

du, Toit, L.C., (2007). Formulation of an anti-tuberculosis drug delivery system. Dissertation, University of the Witwatersrand, Johannesburg, South Africa.

du, Toit, L.C., Pillay, V. and Danckwerts, M.P., (2006). Tuberculosis chemotherapy: current drug delivery approaches, *Respiratory Research*, doi:10.1186/1465-9921-7-118.

du, Toit, L.C., Pillay, V., Choonara, Y.E. and Iyuke, S.E., (2008). Formulation and evaluation of a salted-out isoniazid-loaded Nanosystem. *AAPS PharmSciTech, **9***, 174-181.

Dykeman, C.M., Wallace, R., Ferrell, P., Jasek, J. and Tortorice, P.V., (1996). Drug interactions: How they affect people living with HIV/AIDS. *Journal of the Association of Nurses in AIDS care, **7***, 67-69.

Flikkema, E., van Ekenstein A.G. and Brinke G.T., (1998). Temperature Modulated Calorimetry of Glassy Polymers and Polymer Blends. *Macromolecules, **31***, 892-898.

Edwards, S.F., (1994). The glass transition in polymers. *Polymer, **35***,. 3827-3830.

Eickelberg, O., Roth, M., Lorx, R., Bruce, V., Rüdiger, J. and Johnson, M., (1999). Ligand-independent activation of glucocorticoid receptor by β2-adrenergic receptor agonists in primary human lung fibroblasts and vascular smooth muscle cells. *The Journal of Biological Chemistry, **274***, 1005-1010.

Elgindy, N. and Samy, W., (2009). Evaluation of the mechanical properties and drug release of cross-linked Eudragit films containing metronidazole. *International Journal of Pharmaceutics, **376***, 1-6.

El-Malah, Y. and Nazzal, S., (2008). Novel use of Eudragit® NE 30D/Eudragit® L 30D-55 blends as functional coating materials in time-delayed drug release applications. *International Journal of Pharmaceutics, **357***, 219-227

Ensslin, S., Moll, K.P., Metz, H., Otz, M. and Mäder, K., (2009). Modulating pH-independent release from coated pellets: Effect of coating composition on solubilization processes and drug release. *European Journal of Pharmaceutics and Biopharmaceutics, **72***, 111-118.

Farah, C.S., Ashman, R. B. and Challacombe, S.J., (2000). Oral candidosis. *Clinics in Dermatology, **18***, 553-562.

Feldstein, M.M., Shandryuk, G.A. and Plate, N.A., (2000). Relation of glass transition temperature to the hydrogen-bonding degree and energy in poly(N-vinyl pyrrolidone) blends with hydroxyl-containing plasticizers. Part 1. Effects of hydroxyl group number in plasticizer molecule. *Polymer, **42***, 971-979.

Fini, A., Bergamante, V., Ceschel, G.C., Ronchi, C. and de, Moraes, C.A.F., (2008). Fast dispersible/slow releasing ibuprofen tablets. *European Journal of Pharmaceutics and Biopharmaceutics, **69***, 335-341.

Fleming, I., (1996). Frontier orbitals and organic chemical reactions. London, John Wiley and Sons Ltd, volume 1.

Fogarty, L., Roter, D., Larson, S., Burke, J., Gillepsie, J. and Levy, R., (2002). Patient adherence to HIV medication regimens: A review of published and abstract reports. *Patient Education and Counselling,* ***46***, 93-108.

Francis, S.J.K. and Matthew, H.W.T., (2000). Application of chitosan-based polysaccharide biomaterials in cartilage tissue engineering: A review, *Biomaterials,* ***21***, 2589-2598.

Friedland, G., Karim, S.A., Karim, Q.A., Lalloo, U., Jack, C., Gandhi, N. and Sadr, W.E., (2004). Utility of tuberculosis directly observed therapy programs as sites for access to and provision of antiretroviral therapy in resource-limited countries. *Clinical Infectious Diseases,* ***38***, 421-428.

Fujimori, J., Yoshihash,i Y., Yonemochi, E. and Terada, K., (2005). Application of Eudragit RS to thermo-sensitive drug delivery systems: II. Effect of temperature on drug permeability through membrane consisting of Eudragit RS/PEG 400 blend polymers. *Journal of Controlled Release,* ***102***, 49-57.

Fujimori, J., Yoshihashi, Y., Yonemochi, E. and Terada, K., (2005). Application of Eudragit RS to thermo-sensitive drug delivery systems: II. Effect of temperature on drug permeability through membrane consisting of Eudragit RS/PEG 400 blend polymers. *Journal of Controlled Release,* ***102***, 49-57.

Gal, A. and Nussinovitch, A., (2009). Plasticizers in the manufacture of novel skin-bioadhesive patches. *International Journal of Pharmaceutics,* ***370***, 103-109.

Garrett, E.R. and Hunt, C.A., (1977). Pharmacokinetics of delta-9-tetrahydrocannabinol in dogs, *Journal of Pharmaceutical Sciences,* ***66***, 395-407.

Schramm, G., (2004). A Practical Approach to Rheology and Rheometry. Thermo Electron (Karlsruhe), GmbH, Federal Republic of Germany, volume 2.

GINA science and executive committee Global Strategy for Asthma Management and Prevention., (2009). Global Initiative for Asthma (GINA) 2009. [http://www.ginasthma.org/Guidelineitem.asp??l1=2&l2=1&intId=1561] date accessed February 8 2010.

Glaessl, B., Siepmann, F., Tucker, I., Rades, T. and Siepmann, J., (2010). Deeper insight into the drug release mechanisms in Eudragit RL-based delivery systems. *International Journal of Pharmaceutics,* ***389***, 139-146.

Gleeson, T.D. and Decker, C.F., (2006). Treatment of Tuberculosis, *Disease-a-Month,* ***52***, 785-806.

Gleeson, T.D. and Decker, C.F., (2006). Treatment of Tuberculosis, *Disease-a-Month,* ***52***, 428-434.

Goddeeris, C., Willems, T., Houthoofd, K., Martens, J.A. and Van, den, Mooter, G., (2008). Dissolution enhancement of the anti-HIV drug UC 781 by formulation in a ternary solid dispersion with TPGS 1000 and Eudragit E100. *European Journal of Pharmaceutics and Biopharmaceutics,* ***70***, 861-868.

Gong, C.Y., Shi, S., Dong, P.W., Zheng, X.L., Fu, S.Z., Guo, G., Yang, J.L., Wei, Y.Q. and Qian, Z.Y., (2009). In vitro drug release behavior from a novel thermosensitive composite hydrogel based on Pluronic f127 and poly(ethylene glycol)-poly(ε-caprolactone)-poly(ethylene glycol) copolymer. *BMC Biotechnology*, doi: 10.1186/1472-6750-9-8.

Greenspan, D., (1994). Treatment of oropharyngeal candidiasis in HIV-positive patients. *Journal of the American Academy of Dermatology,* ***31***, S51-S55.

Greenspan, D., (1994). Treatment of oral candidiasis in HIV infection. *Oral Surgery, Oral Medicine, Oral Pathology,* ***78***, 211-215.

Gregoriadis, G., (1995). Engineering liposomes for drug delivery: progress and problems. *Trends in biotechnology,* ***13***, 527-535.

Gupta, A.K., Katz, H.I. and Shear, N.H., (1999). Drug interactions with itraconazole, fluconazole,and terbinafine and their management. *Journal of American Dermatology,* ***41***, 237-249.

Gupta, R.K. and Pillay, D., (2007). HIV resistance and the developing world. *International Journal of Antimicrobial Agents,* ***29***, 510-517.

Yanga, H.W., Tongb, W.P., Zhaoa, X., Zuoa, L and Wangc, J.Q., (2009). Identification of true glass transitions in an Al-based metallic glass using temperature modulated differential scanning calorimetry. *Journal of Alloys and Compounds*, ***473***, 347-350.

Haslam, J.L., Forbes, A.E., Rork, G.S., Pipkin, T.L., Slade, D.A. and Khossravi, D., (1998). Tableting of controlled release multiparticulates, the effect of millisphere size and protective overcoating. *International Journal of Pharmaceutics, **173***, 233-242.

Herbig, S.M., Cardinal, J.R., Korsmeyer, R.W. and Smith, K.L., (1995). Asymmetric-membrane tablet coatings for osmotic drug delivery. *Journal of Controlled Release, **35***, 127-136.

Herh, P., Tkachuk, J., Wu, S., Bernzen, M. and Rudolph, B., (1998). The rheology of pharmaceutical and cosmetic semisolids , Application Note, ATS Rheosystems Gerogetown Rd, Bordentown, NJ, USA.

Hernández, R.M., Orive, G., Murua, A. and Pedraz, J.L., (2010). Microcapsules and microcarriers for in situ cell delivery. *Advanced Drug Delivery Reviews, **62***, 711-730.

Hideaki, N., Nitar, N., Rangasamy, J., Tetsuya, F. and Hiroshi, T., (2008). Preparation of chitinous compound/gelatincomposite and their biological application. *Macromolecular Symposia, **264***, 8-12.

Hoepelman, I.M. and Dupont, B., (1996). Oral candidiasis: the clinical challenge of resistance and management. *International Journal of Antimicrobial Agents, **78***, 155-159.

Holappa, S., (2005). Complexation of Poly(ethylene oxide)-block-poly(methacrylic acid) in Aqueous Medium. Dissertation, University of Helsinki, Finland

Hossainy, S.F.A. and Hubbell, J.A., (1994). Molecular weight dependence of calcification of polyethylene glycol hydrogels, *Biomaterials, **15***, 921-925.

Huang, H., Wang, H., Sinz, M., Zoeckle,r M., Staudinger, J., Redinbo, M.R., Teotico, D.G., Locker, J., Kalpana, G.V. and Mani, S., (2007). Inhibition of drug metabolism by blocking the activation of nuclear receptors by ketoconazole. *Oncogene, **26***, 258-268.

Huang, Y. and Wang, C., (2006). Pulmonary delivery of insulin by liposomal carriers. *Journal of Controlled Release, **13***, 9-14.

Huynh, D.P., Nguyen, M.K., Pi, B.S., Kim, M.S., Chae, S.Y. and Lee, K.C., (2008). Functionalized injectable hydrogels for controlled insulin delivery. *Biomaterials,* ***29***, 2527-2534.

Hyland, M.E. and Elisabeth, St, hi., (2004). Asthma Treatment Needs: A Comparison of Patients' and Health Care Professionals' Perceptions. *Clinical Therapeutics,* ***26***, 2141-2152.

Inc. Morflex., (2004). The role of plasticizers as functional excipients in pharmaceutical dosage forms prepared by hot melt extrusion. Pharmaceutical Coatings Bulletin 102-6. - Morflex Inc. [http://www.morflex.com/pdf/Bul102.6.pdf] date accessed January 20 2010.

Jan, C. and Tseng, C., (2000). Mechanisms underlying ketoconazole induced Ca2+ mobilization in Madin-Darby canine kidney cells. *Biochemical Pharmacology,* ***59***, 947-951.

Jelliffe, R.W., Maire, P., Sattler, F., Gomis, P. and Tahani, B., (1994). Adaptive control of drug dosage regimens: Basic foundations, relevant issues, and clinical examples. *International Journal of Bio-Medical Computing,* ***36***, 1-23.

Jindani, A. and Griffin, G.E., (2010). Challenges to the development of new drugs and regimens for tuberculosis. *Tuberculosis,* ***90***, 168-170.

Kabanova, T.V., Zhdanova, E.R. and Moustafine, R.I., (2006) Characterization of Eudragit® E100/Carbomer 940P interpolyelectrolyte complexes using swellability measurements. *Journal of Controlled Release,* ***116***, 33-35.

Kaplan, W., (2010). Fixed-dose combination (FDC) drugs availability and use as a global public health necessity: intellectual property and other legal issues. World Health Organisation medicines, publications and documentation home. [http://apps.who.int/medicinedocs/en/d/Js6172e/11.html#Js6172e.11] date accessed February 8 2010.

Karasulu, H.Y., Hilmioglu, S., Metin, D.Y. and Guneri, T., (2004). Efficacy of a new ketoconazole bioadhesive vaginal tablet on Candida albicans. *Il Farmaco,* ***59***, 163-167.

Karlsson, P.C., Hughes, R., Rafter, J.J. and Bruce, W.R., (2005). Polyethylene glycol reduces inflammation and aberrant crypt foci in carcinogen-initiated rats. *Cancer Letters,* ***223***, 203-209.

Khandare, J. and Minko T., (2006). Polymer–drug conjugates: Progress in polymeric prodrugs. *Progress in Polymer Science, **31***, 359-397.

Khuller, G.K., Kapur, M. and Sharma, S., (2004). Liposome technology for drug delivery against mycobacterial infections. *Current Pharmaceutical Design, **10***, 3263-3274.

Kim, J., Kim, I.S., Cho, T.H., Lee, K.B., Hwang, S.J. and Tae, G., (2007). Bone regeneration using hyaluronic acid-based hydrogel with bone morphogenic protein-2 and human mesenchymal stem cells. *Biomaterials, **28***, 1830-1837.

Knupp, C.A., Shyu, W.C., Dolin, R., Valentine, F.T., McLaren, C., Martin, R.P., Pittman, K.A. and Barbhaiya, R.H., (1991). Pharmacokinetics of didanosine in patients with acquired immunodeficiency syndrome - related complex. *Clinical Pharmacology and Therapeutics, **49***, 523-535.

Knuth, K., Amiji, M. and Robinson, J.R., (1993). Hydrogel delivery systems for vaginal and oral applications : Formulation and biological considerations. *Advanced Drug Delivery Reviews, **11***, 137-167.

Kohri, N., Iwasa, K., Kurihara, J., Miyazaki, K. and Arita, T., (1989). Inter-subject variation in oral absorption of ketoprofen from controlled-release granules in rabbits. *International Journal of Pharmaceutics, 49*, 213-221.

Ko-Long, L., Huang, C., Cheng, J., Tsai, J., Lu, Y., Chang, H. and Jan, C., (2009). Ketoconazole-induced JNK phosphorylation and subsequent cell death via apoptosis in human osteosarcoma cells. *Toxicology in Vitro, **23***,1268-1276.

Kramer, J. and Blume, H., (1994). Biopharmaceutical aspects of multiparticulates. In Multiparticulate Oral Drug Delivery. Ghebre-Selassi volume 2

Kuethe, D.D., Augestein, D.C., Cresser, J.D. and Wise, D.L., (1992). Design of capsules that burst at predetermined times by dialysis. *Journal of Controlled Release,**18***, 159-164.

Kumar, S., Char, H., Patel, S., Piemontese, D., Malick, A.W., Iqbal, K., Neugroschel, E. and Behl, C.R., (1992). In vivo transdermal iontophoretic delivery of growth hormone releasing factor GRF (1–44) in hairless guinea pigs. *Journal of Controlled Release, **18***, 213-220.

Carpentier, L., Bustin, O. and Descamps, M., (2002). Temperature-modulated differential scanning calorimetry as a specific heat spectroscopy. *Journal of Physics: applied physics,* ***35***, 402–408.

Lamprecht, A., Torres, H.R., Schafer, U. and Lehr, C., (2000). Biodegradable microparticles as a two-drug controlled release formulation: a potential treatment of inflammatory bowel disease. *Journal of Controlled Release,* ***69***, 445-454.

Lasic, D.D., (1993). Liposomes: from physics to applications, Amsterdam, Elsevier. *Biophysical Journal,* ***67***, 1358-1362.

Lasic, D.D., (1998). Papahadjopoulos D Medical application of liposomes. *European Journal of Pharmaceutics and Biopharmaceutics,* ***54***, 358-359.

Laurent, C., Kouanfack, C., Koulla-Shiro, S., Nkoué, N., Bourgeois, A., Calmy, A., Lactuock, B., Nzeusseu, V., Mougnutou, R., Peytavin, G., Liégeois, F., Nerrienet, E., Tardy, M., Peeters, M., Andrieux-Meyer, I., Zekeng, L., Kazatchkine, M., Mpoudi-Ngolé, E and Delaporte, E., Effectiveness and safety of a generic fixed-dose combination of nevirapine, stavudine, and lamivudine in HIV-1-infected adults in Cameroon: open-label multicentre trial. *The Lancet,* ***364***, 29-34.

Lee, K.L. and Anema, S.G., (2009). The effect of the pH at cooking on the properties of processed cheese spreads containing whey proteins. *Food Chemistry,* ***115***, 1373-1380.

Lee, K.Y. and Mooney, D.J., (2001). Hydrogel for tissue engineering, *Chemical Reviews,* ***101***, 1869-1879.

Lee, K.Y. and Yuk, S.H., (2007). Polymeric protein delivery systems, *Progress in Polymer Science,* ***32***, 669-697.

Lee, S.K. and Anema, S.G., (2009). The effect of the pH at cooking on the properties of processed cheese spreads containing whey proteins. *Food Chemistry,* ***115***, 1373-1380.

Lenert, L., Sheiner, L. and Blaschke, T., (1989). Improving drug dosing in hospitalized patients: automated modeling of pharmacokinetics for individualization of drug dosage regimens. *Computer Methods and Programs in Biomedicine,* ***30***, 169-176.

Lennernäs, H., (2007). Animal data: The contributions of the Ussing Chamber and perfusion systems to predicting human oral drug delivery in vivo. *Advanced Drug Delivery Reviews,* ***59***, 1103-1120.

Lin, C. and Metters, A.T., (2006). Computational drug delivery of hydrogels in controlled release formulations: Network design and mathematical modeling. *Advanced Drug Delivery Reviews,* ***58***, 1379-1408.

Lin, C.C. and Metters, A.T., (2006). Hydrogels in controlled release formulations: network. *Advanced Drug Delivery Reviews,* ***58****,* 1379-1408.

Lin, H., Lin, S., Lin, Y., Ho, H., Lo, Y. and Sheu, M., (2008). Release characteristics and in vitro–in vivo correlation of pulsatile pattern for a pulsatile drug delivery system activated by membrane rupture via osmotic pressure and swelling. *European Journal of Pharmaceutics and Biopharmaceutics,* ***70***, 289-301.

Lin, Y. and Ho, H., (2003). Investigations on the drug releasing mechanism from an asymmetric membrane-coated capsule with an in situ formed delivery orifice. *Journal of Controlled Release,* ***89***, 57-69.

Liu, F.Y., Shao, Z., Kildsig, D.O. and Mitra, A.K., (1993). Pulmonary delivery of free and liposomal insulin. *Pharmaceutcial Research,* ***10***, 228-232.

Liu, Y., Huang, K., Peng, D., Ding, P. and Gui-Yin, Li., (2007). Preparation and characterization of glutaraldehyde crosslinked O-carboxymethylchitosan microspheres for controlled delivery of pazufloxacin mesilate. *International Journal of Biological Macromolecules,* ***41***, 87-93.

Ma, D. and McHugh, A.J., (2007). The interplay of phase inversion and membrane formation in the drug release characteristics of a membrane-based delivery system. *Journal of Membrane Science,* ***298***, 156-168.

Ma, L. and Liu, C., (2010). Preparation of chitosan microspheres by ionotropic gelation under a high voltage electrostatic field for protein delivery. *Colloids and Surfaces B: Biointerfaces,* ***75***, 448-453.

Ma N, Xu L, Wang Q, Zhang X, Zhang W, Li Y, Jin L and Li S Development and evaluation of new sustained-release floating microspheres. *International Journal of Pharmaceutics,* ***358***, 82-90.

Maertens, J.C., (2004). History of the development of azole derivatives. *Clinical Microbiology and Infection,* ***10***, 1-10.

Maes, C., Devaux, J., Legras, R. and McGrail, P.T., (1995). Glass transition temperature of crosslinked poly(ether sulfone)s. *Polymer,* ***36***, 3159-3164.

Mandal B.B , Kapoor S and Kundu S.C Silk fibroin/polyacrylamide semi-interpenetrating network hydrogels for controlled drug release. Biomaterials. - 2009. - Vol. 30. - pp. 2826-2836.

Manosuthi, W., Chaovavanich, A., Tansuphaswadikul, S., Prasithsirikul, W., Inthong, Y., Chottanapund, S., Sittibusaya, C., Moolasart, V., Termvises, P. and Sungkanuparph, S., (2007). Incidence and risk factors of major opportunistic infections after initiation of antiretroviral therapy among advanced HIV-infected patients in a resource-limited setting. *Journal of Infection,* ***55***, 464-469.

Mariappan, T.T., Singh, B. and Singh, S.A., (2000). validated reversed-phase (C18) HPLC method for simultaneous determination of rifampicin, isoniazidand pyrazinamide in USP dissolution medium and simulated gastric fluid. *Pharmacy Pharmacology Communications,* ***6***, 345-349.

Markus, W., Rudolpha, B., Kleina, S., Beckertb, E., Petereitb, H. and Dressman, J.B.A., (2001). new 5-aminosalicylic acid multi-unit dosage form for the therapy of ulcerative colitis. *European Journal of Pharmaceutics and Biopharmaceutics,* ***51***, 183-190.

Martinez, L., Nunn, L.B.P. and Raviglione, M., (2007). Tuberculosis and air travel; WHO guidance in the era of drug-resistant TB. *Travel medicine and infectious diseases,* ***6***, 177-181.

McConnell, E.L., Macfarlane, C.B. and Basit, A.W., (2009). An observational study on the influence of solvent composition on the architecture of drug-layered pellets. *International Journal of Pharmaceutics,* ***380***, 67-71.

McHugh, A.J., (2005). The role of polymer membrane formation in sustained release drug delivery systems. *Journal of Controlled Release,* ***109***, 211-221.

US Department of Health and Human Services Food and Drug Administration, Center for Drug Evaluation and Research (CDER) Food and Drug Administration., (2006). Guidance for Industry: Fixed Dose Combinations, Co-Packaged Drug Products, and Single-Entity Versions of Previously Approved Antiretrovirals for the Treatment of HIV. [www.fda.gov/oc/initiatives/hiv/hivguidance.html] date accessed January 20 2010.

Mirsaeidi S.M.M., Tabarsi, P., Khoshnood, K., Pooramiri, M.V., Rowhani-Rahbar, A., Mansoori, S.D., Masjedi, H., Zahirifardv, S., Mohammadi, F., Farnia, P., Masjedi, M.R. and Velayati, A.A., (2005). Treatment of multiple drug-resistant tuberculosis (MDR-TB) in Iran. *International Journal of Infectious Diseases,* ***9***, 317-322.

Meldrum, J., (2003). Nevirapine-Based Fixed-Dose Combination ARVs. The body: The complete HIV/AIDS resource. [http://www.thebody.com/content/art13379.html] date accessed February 8 2010.

Mestiri, M., Puisieux, F. and Benoit, J.P., (1993). Preparation and characterization of cisplatin-loaded polymethyl methacrylate microspheres. *International Journal of Pharmaceutics,* ***89***, 229-234.

Meyer, J.H., Dressman, J., Fink, A.S. and Amidon, G., (1985). Effect of size and density on gastric emptying of indigestible solids. *Gastroenterology,* ***89****,* 805-813.

Migliorat, C.A., Birman, E.G. and Cury, A.E., (2004). Oropharyngeal candidiasis in HIV-infected patients under treatment with protease inhibitors. *Oral Surgery, Oral Medicine, Oral Pathology, Oral Radiology, and Endodontology,* ***98***, 301-310.

Migliori, G.B., Raviglione, M.C., Schaberg,T., Davies, P.D.O., Zellweger, J.P., Grzemska, M., Mihaescu, T., Clancy, L. and Casali, L., (1999). Tuberculosis management in Europe. *European Respiratory Journal,* ***14***, 978-992.

University of Southern Mississippi., (2005). Differential Scanning Calorimetry. Polymer Science Learning Centre Department of Polymer Science. [http://pslc.ws/macrog//dsc.htm] date accessed March 19 2010.

Branco M.C. and Schneider J.P., (2009). Self-assembling materials for therapeutic delivery. *Acta Biomaterialia,* ***5***, 817-831.

Moody, D.E., Walsh, S.L., Rollins, D.E., Neff, J.A. and Huang, W., (2004). Ketoconazole, a cytochrome P450 3A4 inhibitor, markedly increases concentrations of levo-acetyl-alpha-methadol in opioid-naive individuals. *Clinical and Pharmacological Therapy,* ***76***, 154-166.

Moreno, F., Hardin, T.C., Rinaldi, M.G. and Graybill, J.R., (1993). Itraconazole didanosine excipient interaction [letter]. *The Journal of the American Medical Association,* ***269***, 1508.

Moustafine, R.I., Kemenova, V.A. and Van, den, Mooter, G., (2005). Characteristics of interpolyelectrolyte complexes of Eudragit E 100 with sodium alginate. *International Journal of Pharmaceutics,* ***294***, 113-120.

Mugavero, M.J. and Hicks, C.B., (2004). HIV resistance and the effectiveness of combination antiretroviral treatment. *Drug discovery today: therapeutic strategies,* ***1***, 529-535.

Muschert, S., Siepmann, F., Leclercq, B., Carlin, B. and Siepmann, J., (2009). Prediction of drug release from ethylcellulose coated pellets. *Journal of Controlled Release,* ***135,*** 71-79.

Nair, L.S. and Laurencin, C.T., (2006). Polymers as biomaterials for tissue engineering and controlled drug delivery. *Tissue Engineering,* ***47***, 47-90.

Nasser, S., Christie, P.E., Pfister, R., Sousa, A.R., Walls, A., Schmitz-Schumann, M. and Lee, T.H., (1996). Effect of endobronchial aspirin challenge on inflammatory cells in bronchial biopsy samples from aspirin-sensitive asthmatic subjects. *Thorax,* ***51***, 64-70.

National Asthma Education and Prevention Program (NAEPP) Coordinating Committee, (2010). Expert panel report 3 (EPR3). Guidelines for the diagnosis and management of Asthma. National Heart Lung and Blood Institute. [http://www.nhlbi.nih.gov/guidelines/asthma/asthgdln.htm] date accessed January 20 2010.

Nelson, H.S., (2001). Advair: Combination treatment with fluticasone propionate/salmeterol in the treatment of asthma. *The Journal of Allergy and Clinical Immunology,* ***107***, 397-416.

Nicca, D., Moody, K., Elzi, L. and Spirig, R., (2007). Comprehensive Clinical Adherence Interventions to Enable Antiretroviral Therapy: A Case Report. *Journal of the Association of Nurses in AIDS care,* ***18***, 44-53.

Nihant, N., Schugens, C., Grandfils, C., Jerome, R. and Teyssie, P., (1994). Polylactide microparticles prepared by double emulsion/evaporation technique. I. Effect of primary emulsion stability. *Pharmaceutical Research,* ***11***, 1479-1484.

Oosegi, T., Onishi, H. and Machida, Y., (2008). Gastrointestinal distribution and absorption behavior of Eudragit-coated chitosan–prednisolone conjugate microspheres in rats with TNBS-induced colitis. *International Journal of Pharmaceutics,* ***348***, 80-88.

Oosegi, T., Onishi, H. and Machida, Y., (2008). Novel preparation of enteric-coated chitosan-prednisolone conjugate microspheres and in vitro evaluation of their potential as a colonic delivery system. *European Journal of Pharmaceutics and Biopharmaceutics,* ***68***, 260-266.

Ormerod, L.P. and Prescott, R.J., (1991). Inter-relations between relapses, drug regimens and compliance with treatment in tuberculosis. *Respiratory Medicine,* ***85***, 239-242.

Out, H.J., Braat, D.D.M., Lintsen, B.M.E., Gurgan, T. Bukulmez, O., Gökmen, O., Keles, G., Caballero, P., González, J.M., Fábregues, F., Balasch, J. and Roulier, R., (2000). Increasing the daily dose of recombinant follicle stimulating hormone (Puregon®) does not compensate for the age-related decline in retrievable oocytes after ovarian stimulation. *Human Reproduction,* ***15***, 39-35.

Palmqvist, M., Ibsen, T., Mellen, A. and Lotvall, J., (1999). omparison of the relative efficacy of formoterol and salmeterol in asthmatic patients. *American Journal of Respiratory Critical Care Medicine,* ***190***, 244-249.

Panoyan, T., Quesnel, R. and Hildgen, P., (2003). Injectable nanospheres from a novel multiblock copolymer: cytocompatibility, degradation and in vitro release studies. *Journal of Microencapsulation,* ***20***, 745-758.

Park, S., Nho, Y. and Kim, H., (2004). Preparation of poly(polyethylene glycol methacrylate-co-acrylic acid) hydrogels by radiation and their physical properties. *Radiation Physics and Chemistry,* ***69***, 221-227.

Patil, J.S., Kamalapur, M.V., Marapur, S.C. and Kadam., (2010). d.v ionotropic gelation and polyelectrolyte complexation:the novel techniques to design hydrogel particulate sustained, modulated drug delivery system: a review. *Digest Journal of Nanomaterials and Biostructures,* ***5***, 241-248.

Patton, L.L., Bonito, A.J. and Shugars, D.A.A., (2001). systematic review of the effectiveness of antifungal drugs for the prevention and treatment of oropharyngeal candidiasis in HIV-positive patients. *Oral Surgery, Oral Medicine, Oral Pathology, Oral Radiology & Endodontics,* ***92***, 170-179.

Paul, S., Mary, C.K. and Niall, M.F.A., (2004). multiparticulate Bisoprolol formulation. Patent. 6,733,789.

Peppas, N.A., Bures, P., Leobandung, W. and Ichikawa, H., (2000). Hydrogels in pharmaceutical formulations. *European Journal of Pharmaceutics and Biopharmaceutics,* ***50***, 272-278.

Pepper, D.J., Meintjes, G.A., McIlleron, H. and Wilkinson, R.J., (2007). Combined therapy for tuberculosis and HIV-1: the challenge for drug discovery. *Drug Discovery Today,* ***12***, 980-989.

Pierce the protein people., (2008). Polyethylene Glycol (PEG)-containing Protein Reagents. Pierce the protein people. [http://www.piercenet.com/products/browse.cfm?fldID=12D97D8D-5056-8A76-4E95-9EA0D0B54BDB&WT.mc_id=go_Crosslinkers_PEG_pf&gclid=CMumxt6o6qECFVVo4wodo3JFIg] date accessed January 11 2010.

Pignatello, R., Bucolo, C., Ferrara, P., Maltese, A., Puleo, A. and Puglisi, G., (2002). Eudragit RS100® nanosuspensions for the ophthalmic controlled delivery of ibuprofen. *European Journal of Pharmaceutical Sciences,****16***, 1653-61.

Pillay, V. and Fassihi, R., (2000) A novel approach for constant rate delivery of highly soluble bioactives from a simple monolithic system. *Journal of Controlled Release,* ***67***, 67-78.

Pongjanyakul, T. and Rongthong, T., (2010) Enhanced entrapment efficiency and modulated drug release of alginate beads loaded with drug–clay intercalated complexes as microreservoirs. *Carbohydrate Polymers,* ***81***, 409-419.

Prabakaran, D, Singh P., Jaganathan, K.S. and Vyas. S.P., (2004). Osmotically regulated asymmetric capsular systems for simultaneous sustained delivery of anti-tubercular drugs. *Journal Of Controlled Release,* ***95***, 239-248.

Pund, S., Joshi, A., Vasu, K., Nivsarkar, M. and Shishoo, C., (2010). Multivariate optimization of formulation and process variables influencing physico-mechanical characteristics of site-specific release isoniazid pellets. *International Journal of Pharmaceutics,* ***388***, 64-72.

Qiu, B., Stefanos, S., Ma, J., Lalloo, A., Perry, B.A., Leibowitz, M.J., Sinko, P.J., and Stein, S., (2003). A hydrogel prepared by in situ crosslinking of a thiol-containing poly(ethylene glycol)-based copolymer: a new biomaterial for protein drug delivery. *Biomaterials,* ***24***, 11-18.

Quellen, S., (2003). Ingredients--Whats in the stuff we buy. [http://sci-toys.com/ingredients/polyethylene_glycol.html] date accessed March 1 2010.

Quinteros, D.A., Rigo, V.R., Kairuz, A.F.J., Olivera, M.E., Manzo, R.H. and Allemandi, D.A., (2008). Interaction between a cationic polymethacrylate (Eudragit E100) and anionic drugs. *European Journal of Pharmaceutical Sciences,* ***33***, 72-79.

Rad, M.E., Bifani, P., Martin, C., Kremer, K., Samper, S. and Rauzier, J., (2003), Mutations in putative mutator genes of Mycobacterium tuberculosis strains of the W-Beijing family. *Emerging Infectious Diseases,* ***9***, 838-845.

Radeva, T., (2001) In Physical Chemistry of polyelectrolytes, Marcel Dekker Inc, volume 99.

Rajagopal, K. and Schneider, J.P., (2004). Self-assembling peptides and proteins for nanotechnological applications. *Current Opinions in Structural Biology,* ***14***, 480-486.

Rattes, A.L.R. and Oliveira, W.P., (2007). Spray drying conditions and encapsulating composition effects on formation and properties of sodium diclofenac microparticles. *Powder Technology,* ***171***, 7-14.

Ray, S., Reaume, S.J. and Lalman, J.A., (2010). Developing a statistical model to predict hydrogen production by a mixed anaerobic mesophilic culture. *International Journal of Hydrogen Energy,* ***35***, 5332-5342.

Raya, S., Lalmanb, J.A. and Biswasc, N., (2009). Using the Box-Benkhen technique to statistically model phenol photocatalytic degradation by titanium dioxide nanoparticles. *Chemical Engineering Journal,* ***150***, 15-24.

Rege, P.R., Fegely, K.A., Scattergood, L.K. and Rajabi-Siahboomi, A.R., (2005). Predictability of Drug Release from Multiparticulate Systems Coated with an Aqueous Ethylcellulose Dispersion. Conference proceedings for Modified Release Technologies, Colorcon, 2005.

Renteria, S.S., Clemens, C.C. and Croyle, M.A., (2010). Development of a nasal adenovirus-based vaccine: Effect of concentration and formulation on adenovirus stability and infectious titer during actuation from two delivery devices. *Vaccine, **28***, 2137-2148.

Richter, A., Anton, S.E., Koch, P. and Dennett, S.L., (2003) The Impact of Reducing Dose Frequency on Health Outcomes. *Clinical therapeutics, **25***, 2307-2335.

Ruel-Gariepy, E. and Leroux, J.C., (2004). In situ-forming hydrogels – review of temperature-sensitive systems. *European Journal of Pharmaceutics and Biopharmaceutics, **58***, 409-426.

Xua, S.X., Lia, Y., and Fengb, Y.P., (2000). Some elements in specifc heat capacity measurement and. Thermochimica Acta. *Thermochimica Acta, **360***, 51-58.

Sadeghi, A.M.M., Dorkoosh, F.A., Avadi, M.R., Saadat, P., Rafiee-Tehrani, M. and Junginger, H.E., (2008). Preparation, characterization and antibacterial activities of chitosan, N-trimethyl chitosan (TMC) and N-diethylmethyl chitosan (DEMC) nanoparticles loaded with insulin using both the ionotropic gelation and polyelectrolyte complexation methods. *International Journal of Pharmaceutics, **355***, 299-306.

Sanders, M.J., (2003). Divide and conquer- A new approach to delivery of inhaled combination therapies. © PharmaVentures Ltd, The drug delivery companies report.

Sangalli, M.E., Maroni, A., Zema, L., Busetti, C., Giordano, F. and Gazzaniga, A., (2001). In vitro and in vivo evaluation of an oral system for time and/or site-specific drug delivery. *Journal of Controlled Release, **73***, 103-110.

Sangeorzan, J.A., Bradley, S.F., He, X., Zarin,s L.T., Ridenour, G.L., Tiballi, R.N. and Kauffman, C.A., (1994). Epidemiology of oral candidiasis in HIV-infected patients: Colonization, infection, treatment, and emergence of fluconazole resistance. *The American Journal of Medicine, **97***, 339-346.

Singh, S., Mariappan T.T., Shankar R., Sarda, N. and Singh, B., (2001). A critical review of the probable reasons for the poor variable bioavailability of rifampicin from from anti-tubercular fixed-dose combination (FDC) products, and the likely solutions to the problem. *International Journal of Pharmaceutics, **228**,* 5-17.

Sastry, S.V., Nyshadham, J.R. and Fix, J.A., (2000) Recent technological advances in oral drug delivery – a review. *Pharmaceutical Science & Technology Today, **3***, 138-145.

Schmidt, C. and Bodmeier, R.A., (2001). multiparticulate drug-delivery system based on pellets incorporated into congealable polyethylene glycol carrier materials. *International Journal of Pharmaceutics, **216***, 9-16.

Schroeder, I.Z., Franke, P., Schaefer, U.F. and Lehr, C., (2007). Delivery of ethinylestradiol from film forming polymeric solutions across human epidermis in vitro and in vivo in pigs. *Journal of Controlled Release, **118***, 196-203.

Schubert, M.L. and Peura, D.A., (2008). Control of Gastric Acid Secretion in Health and Disease. *Gastroenterology, **134***, 1842-1860.

Seifart, H.I., Parkin, D.P. and Donald, P.R., (1991). Stability of isoniazid, rifampicinand pyrazinamide in suspensions used for the treatment of tuberculosis in children. *The Pediatric Infectious Disease Journal, **10***, 827-831.

Shah, N.S., Wright, A., Bai, G., Barrera, L., Boulahbal, F., Martín-Casabona, Drobniewski, F., Gilpin, C., Havelková, M., Lepe, R., Lumb, R., Metchock, B., Portaels, F., Rodrigues, M.F., Rüsch-Gerdes, S., Van, Deun, A., Vincent, V., Laserson, K., Wells, C. and Cegielski, J.P., (2007). Worldwide emergence of extensively drug-resistant tuberculosis. *Emerging Infectious Diseases, **13**,* 380-387.

Shishoo, J.C., Shah, S.A., Rathod, I.S., Savale, S.S. and Vora, M.J., (2001). Impaired bioavailability of rifampicin in presence of isoniazid from fixed dose combination (FDC) formulation. *International Journal of Pharmaceutics, **228***, 53-67.

Siepmann, J. and Siepmann, F., (2008). Mathematical modelling of drug delivery. *International Journal of Pharmaceutics, **364***, 328-343.

Silicon far east., (2005). siliconfareast.com. [http://www.siliconfareast.com/tg.htm] date accessed Januray 29 2010.

Silverman, Jr, S., Gallo, W.J., McKnight, M.L., Mayer, P., deSanz, S. and Tan, M.M., (1996). Clinical characteristics and management responses in 85 HIV-infected patients with oral candidiasis. *Oral Surgery, Oral Medicine, Oral Pathology, Oral Radiology, and Endodontology,* ***82****,* 402-407.

Singh, B., Kumar, R. and Ahuja, N., (2004). Optimizing Drug Delivery Systems Using Systematic "Design of Experiments" Part I: Fundamental Aspects. *Critical Reviews in Therapeutic Drug Carrier Systems,* ***22***, 27-105.

Singh, S., Mariappan, T.T., Shankar, R., Sarda, N. and Singh, B.A., (2001). critical review of the probable reasons for the poor variable bioavailability of rifampicin from anti-tubercular fixed-dose combination (FDC) products and the likely solutions to the problem. *International Journal of Pharmaceutics,* ***228***, 5-17.

Sinko, J.P., Patel N.R. and Hu P., (1994). Site-specific oral absorption of didanosine: in situ characterization and correlation with extent of absorption in vivo. *International Journal of Pharmaceutics,* ***109***, 125-133.

Skaanild, M.T. and Friis, C., (1997). Characterization of the P450 system in Gottingen minipigs. *Pharmacology and Toxicology,* ***80***, 28-33.

Sriamornsak, P., Thirawong, N., Cheewatanakornkool, K., Burapapadh, K. and Sae-Ngow, W. Cryo-scanning electron microscopy (cryo-SEM) as a tool for studying the ultrastructure during bead formation by ionotropic gelation of calcium pectinate. *International Journal of Pharmaceutics,* ***352***, 115-122.

Stamatialis, D.F., Papenburg, B.J., Gironés, M., Saiful, S., Bettahalli, S.N.M., Schmitmeier, S. and Wessling, M., (2008). Medical applications of membranes: Drug delivery, artificial organs and tissue engineering. *Journal of Membrane Science,* ***308*** 1-34.

Streube,l A., Siepmann, J. and Bodmeier, R., (2002) Floating microparticles based on low density foam powder. *International Journal of Pharmaceutics.,* ***241***, 279-292.

Suarez, S., O'Hara, P., Kazantseva, M., Newcomer, C.E., Hopfer, R., McMurray, D.N. and Hickey, A.J., (2001). Airways delivery of rifampicin in microparticles for the treatment of tuberculosis. *Journal of Antimicrobial Chemotherapy,* ***48***, 431-434.

Sun, G. and Chu, C., (2006). Synthesis, characterization of biodegradable dextran–allyl isocyanate–ethylamine/polyethylene glycol–diacrylate hydrogels and their in vitro release of albumin. *Carbohydrate Polymers, **65***, 273-287.

Sutton, S.C., Evans, L.A., Fortner, J.H., McCarthy, J.M. and Sweeney, K., (2006). Dog colonoscopy model for predicting human colon absorption. *Pharmaceutical Research, **23***, 1554-1563.

Swartz, M.E., (2005). Ultra Performance Liquid Chromatography (UPLC): An Introduction. chromatographyonline [http://chromatographyonline.findanalytichem.com/lcgc/data/articlestandard//lcgc/242005/164646/article.pdf] date accessed July 13 2010.

Taburet, A.M. and Singlas, E., (1996). Drug interactions with antiviral drugs. *Clinical Pharmacokinetics, **30***, 385-401.

Temesgen, Z., Warnke, D. and Kasten, M.J., (2006). Current status of antiretroviral therapy. *Expert Opinion on Pharmacotherapy, **7***, 1541-1554.

Temtem, M., Pompeu, D., Jaraquemada, G., Cabrita, E.J., Casimiro, T. and Aguiar-Ricardo, A., (2009). Development of PMMA membranes functionalized with hydroxypropyl-β-cyclodextrins for controlled drug delivery using a supercritical CO2-assisted technology, *International Journal of Pharmaceutics*, ***376,*** 110-115.

The division of clinical pharmacology faculty of health sciences., (2005). In South African Medicines Formulary, University of Cape Town, J.C Gibbon, Cape Town Health and Medical Publishing Group, volume 7.

The Hofmeister series., (2009). martin.chaplin.btinternet. [http://www.martin.chaplin.btinternet.co.uk/hofmeist.html] date accessed October 19 2010.

The Malawi Paediatric Antiretroviral Treatment Group Antiretroviral therapy for children in the routine setting in Malawi., (2007). *Royal Society of Tropical Medicine and Hygiene, **101***, 511-516.

Thombre, A.G., Cardinal, J.R., DeNoto, A.R. and Gibbes, D.C., (1999). Asymmetric membrane capsules for osmotic drug delivery. *Journa of Controlled Release, **57***, 65-73.

Tibotec HIV information and living with HIV medications., (2010) tibotec-hiv.com. Janssen-Pharmaceutica, NV. [http://www.tibotec-hiv.com/;jsessionid=ZDTUKGCMM4EP4CUCERDBXCQ] date accessed January 20 2010.

Townsend, A., Hunt, K. and Wyke, S., (2003). Managing multiple morbidity in mid-life: a qualitative study of attitudes to drug use. *British Medical Journal, **327***, 837-840.

TreatHIV.com., (2010). TRIZIVIR® (abacavir sulfate, lamivudine, and zidovudine). [http://www.treathiv.com/safety/trizivir.html] date accessed January 20 2010.

United Pharmacies., (2010). www.lifepharmacy.com. [http://www.life-pharmacy.com/hiv/product_triomune.html] date accessed January 20 2010.

Usercom 11., (1998). Mettler Toledo Mettler Toledo Usercom 11. [http://us.mt.com/us/en/home/supportive_content/usercom.TA_UserCom11.twoColEd.html] date accessed January 20 2010.

Usercom 7., (1998). Mettler Toledo Mettler Toledo Usercom 7. [http://us.mt.com/us/en/home/supportive_content/usercom.TA_UserCom7.twoColEd.html] date accessed January 20 2010.

Van, Dyke, R.B., (1995). Opportunistic infections in HIV-infected children. *Seminars in Pediatric Infectious Diseases, **6**,* 10-16.

Vermund, S.H. and Yamamoto, N., (2007). Co-infection with human immunodeficiency virus and tuberculosis in Asia. *Tuberculosis, **87***, S18-S25.

Videx., (2010). Videx Highlights of Prescribing Information. packageinserts.bms.com, VIDEX EC. [http://packageinserts.bms.com/pi/pi_videx.pdf] date accessed January 20 2010.

Waters Chromatography Columns and Supplies Catalog., (2009). Massachusetts, USA.

Webb, P.A. and Orr, C., (1997). In Analytical methods in fine particle technology. Micromeritics Instrument Corporation, Norcross, volume 1.

Weidner, J., (2001). System for time and/or site-specific oral drug delivery. *Drug Discovery Today, **6***, 1028-1029.

West, J.L. and Hubbell, J.A., (1995). Comparison of covalently and physically crosslinked polyethylene glycol-based hydrogels for the prevention of postoperative adhesions in a rat model. *Biomaterials,* ***16***, 1153-156.

Wiliams, D.H. and Fleming, I., (1997). Spectroscopic methods in organic chemistry. London, The McGraw-Hill Companies, volume 1.

Wilson, H.J.G. and Wood, G.C., (1958). Drug delivery to the proximal colon. *The Journal of Pharmacy and Pharmacology,* ***37***, 874-877.

Winter, M., (2010). The University of Sheffield and WebElements Ltd, UK WebElements: the periodic table on the WWW. webelements.com [http://www.webelements.com/] date accessed January 20 2010.

Wong, D.W.S., Gastineau, F.A., Gregorski, K.S., Tillin, S.J. and Pavlath, A.E., (1992). Chitosan–lipid films: Microstructure and surface energy. *Journal of Agricultural and Food Chemistry,* ***40***, 540-554.

Wong, H.L., Chattopadhyay, N., Wu, X.Y. and Bendayan, R., (2010). Nanotechnology applications for improved delivery of antiretroviral drugs to the brain . *Advanced Drug Delivery Reviews,* ***62***, 503-517.

World Health Organisation Wordl Health Organisation Tuberculosis Fact Sheet., (2010). Wold Health Organisation [http://www.who.int/mediacentre/factsheets/fs104/en/index.html] date accessed January 20 2010.

World Health Organization Communicable Diseases Cluster., (1999). Fixed-dose combination tablets for the treatment of tuberculosis. The World Health Oganisation. Report from Geneva.

World Health Organization Didanosine Guidelines., (2005). Final text for inclusion in The International Pharmacopoeia. Validation guidelines [http://www.essentialdrugs.org/files/IntPh_Didanosine.pdf] date accessed January 20 2010.

Ike, Y., Seshimo, Y. and Kojima S., (2007). Complex heat capacity of non-Debye process in glassy glucose and fructose. *Fluid Phase Equilibria,* ***256***, 123–126.

Zalipsky, S., (1995). Chemistry of polyethylene glycol conjugates with biologically active molecules. *Advanced Drug Delivery Reviews, **16***, 157-182.

Zhang, H., Alsarra, I.A. and Neau, S.H., (2002). An in vitro evaluation of a chitosan-containing multiparticulate system for macromolecule delivery to the colon. *International Journal of Pharmaceutics, **239***, 197-205.

Zhu, Z., (2006). Development of self assembled polyelectrolyte membranes for pervaporation applications. Thesis. University of Waterloo.

Zintchenko, A., Rother, G. and Dautzenberg, H., (2003). Structural Analysis in Interpolyelectrolyte Complex Formation of Sodium Poly(styrenesulfonate) and Diallyldimethylammonium Chloride–Acrylamide Copolymers by Viscometry. *Langmuir, **13***, 2905-2910.

APPENDICES

Appendix A: Review Paper

Int. J. Biotechnology, Vol. X, No. Y, xxxx 1
Copyright © 200x Inderscience Enterprises Ltd.

Rationalising fixed dose combinations for tuberculosis and acquired immunodeficiency syndrome therapy

Shivaan Cooppan, Viness Pillay*,
Yahya E. Choonara, Lisa C. du Toit and
Valence M.K. Ndesendo

Department of Pharmacy and Pharmacology,
University of the Witwatersrand,
7 York Road, Parktown 2193, Johannesburg, South Africa
E-mail:
E-mail: viness.pillay@wits.ac.za
E-mail:
E-mail:
E-mail:
*Corresponding author

Abstract: Poorly managed healthcare can be directly attributed to extensive drug regimens. Numerous chronic illnesses and epidemics such as HIV/AIDS and tuberculosis require elaborate drug regimens for efficacious therapeutic outcomes. Various drug delivery systems have been developed to simplify their regimental drug therapy. However, more effective and innovative drug delivery technologies are required to increase patient compliance and provide controlled drug delivery. This review article attempts to provide a concise incursion into the use of fixed dose combinations as a strategy for drug delivery and describes the opportunities and challenges for the treatment of conditions that require chronic suppressive regimental drug therapy.

Keywords: Fixed dose drug combinations; tuberculosis; human immunodeficiency virus; HIV; asthma; polymeric drug delivery; multiparticulates; liposomes; drug efficacy; targeted drug delivery; drug resistance.

Reference to this paper should be made as follows: Cooppan, S., Pillay, V., Choonara, Y.E., du Toit, L.C. and Ndesendo, V.M.K. (xxxx) 'Rationalising fixed dose combinations for tuberculosis and acquired immunodeficiency syndrome therapy', *Int. J. Biotechnology*, Vol. X, No. Y, pp.000–000.

Appendix B: Patent Application for the ODMUS

Patent application title: HETEROGENEOUSLY CONFIGURED MULTIPARTICULATE GASTROINTESTINAL DRUG DELIVERY SYSTEM

Inventors: Viness Pillay Yahya Essop Choonara Lisa Claire Du Toit Michael Paul Danckwerts Shivaan Cooppan
Agents: HAMILTON, BROOK, SMITH & REYNOLDS, P.C.
Assignees:
Origin: CONCORD, MA US
IPC8 Class: AA61K31496FI
USPC Class: 51425411
Publication date: 07/15/2010
Patent application number: 20100179170

Abstract:

This invention relates to a heterogeneously configured multiparticulate drug delivery system for gastrointestinal delivery of at least one or a combination of active pharmaceutical compositions. The system comprises a multiplicity of enterosoluble or gastrosoluble multiparticulates loaded with the active pharmaceutical composition or compositions for the site-specific delivery of said active pharmaceutical composition or compositions to a specific region in the gastrointestinal tract of a human or animal body. The system can be supplied as reconstitutable granules which are reconstituted immediately before oral administration.

Read more: http://www.faqs.org/patents/app/20100179170#ixzz0ySGWZrug

Appendix C: Animal Ethics Screening Committee Approval Letter

AESC 3

UNIVERSITY OF THE WITWATERSRAND, JOHANNESBURG

STRICTLY CONFIDENTIAL

ANIMAL ETHICS SCREENING COMMITTEE (AESC)

CLEARANCE CERTIFICATE NO. 2007/56/04

APPLICANT: Professor V Pillay

SCHOOL: Pharmacy and Pharmacology
DEPARTMENT:
LOCATION: Medical School

PROJECT TITLE: **An in vivo assessment of novel biocompatible polymeric drug delivery system in pigs**

Number and Species

30 male/female pigs

Conditions:

i. The applicant must negotiate with CAS on the logistics and times
ii. Should blood sampling be done by the applicant or co-workers, they must prove that they are capable of performing this.

Approval was given for to the use of animals for the project described above at an AESC meeting held on 20070626. This approval remains valid until 20090626

The use of these animals is subject to AESC guidelines for the use and care of animals, is limited to the procedures described in the application form and to the following additional conditions:

Signed: _____ Date: 12/07/07
(Chairperson, AESC)

I am satisfied that the persons listed in this application are competent to perform the procedures therein, in terms of Section 23 (1) (c) of the Veterinary and Para-Veterinary Professions Act (19 of 1982)

Signed: _____ Date: 13/07/07
(Registered Veterinarian)

cc: Supervisor: #
Director: CAS

Works 2000/Iain0015/AESCCert.wps

Appendix D: Central Animal Services Clearance Letter



CENTRAL ANIMAL SERVICES

Tel: 011717-1312

Fax: 011 643-4318

DEAR ANIMAL USERS

It is with great satisfaction that we can relay to users, the positive outcome of their respective *in vivo* research. Central Animal Service acquired a batch of 30 pigs for *in vivo* research with the Department of Pharmacy and Pharmacology, for disease screening.

An ongoing animal surveillance program pre and post studies continued on a daily basis to assess the health and well being of the animals. We are confident to say that any unforeseen or fatal circumstance due to researchers or the research material itself had occurred. All pigs maintained an acceptable health status during and post studies.

Kind regards

Dr Leith Meyer (Director of the Central Animal Services) and the CAS team

……